MITIGATION OF CARBON DIOXIDE FROM SYNTHETIC FLUE GAS USING INDIGENOUS MICROALGAE

Submitted in fulfilment of the requirements

of the degree of

Doctor of Philosophy: Biotechnology

In the Faculty of Applied Sciences at

The Durban University of Technology

Virthie Bhola

2017

Supervisor: Professor Faizal Bux

Co-supervisor: Professor Feroz Mahomed Swalaha

MITIGATION OF CARBON DIOXIDE FROM SYNTHETIC FLUE GAS USING INDIGENOUS MICROALGAE

VIRTHIE BHOLA

I hereby declare that this thesis, submitted for Doctor of Philosophy in Biotechnology at the Durban University of Technology represents my own work. It has not been submitted before for any diploma/degree or examination at any other Technikon/University. Where use is made of any author's work, it has been duly acknowledged.

Virthie Kemraj Bhola

30/03/2017

Date

2017

Reference Declaration in Respect of a Doctor of Philosophy Thesis

I, **Virthie Bhola** (full name of student), **Professor Faizal Bux**, and **Professor Feroz Mahomed Swalaha** (full name of supervisors) do hereby declare that in respect of the following thesis:

Mitigation of carbon dioxide from synthetic flue gas using indigenous microalgae

1. As far as we know and can ascertain:
   (a) no other similar dissertation/thesis exists;
   (b) the only similar dissertation/thesis(s) that exist(s) is/are referenced in this thesis

2. All references as detailed in the thesis are complete in terms of all personal communications engaged in and published works consulted

[redacted]
Signature of Student

30/03/2017
Date

[redacted]
Signature of Supervisor

30/03/2017
Date

[redacted]
Signature of Co-supervisor

30-03-2017
Date

APPROVAL

We hereby approve the final submission of the following thesis:

Mitigation of carbon dioxide from synthetic flue gas using indigenous microalgae

[redacted]

Professor F. Bux
Supervisor
Doctoral Degree in Technology: Biotechnology
Durban University of Technology (DUT)

[redacted]

Professor F. M. Swalaha
Co-supervisor
Doctoral Degree in Technology: Biotechnology
Durban University of Technology (DUT)

This 30th day of March, 2017, at the Durban University of Technology.

ABSTRACT

Fossil carbon dioxide emissions can be biologically fixed which could lead to the development of technologies that are both economically and environmentally friendly. Carbon dioxide, which is the basis for the formation of complex sugars by green plants and microalgae through photosynthesis, has been shown to significantly increase the growth rates of certain microalgal species. Microalgae possess a greater capacity to fix CO_2 compared to terrestrial plants. Selection of appropriate microalgal strains is based on the CO_2 fixation and tolerance capability, both of which are a function of biomass productivity. Microalgal biomass could thus represent a natural sink for carbon. Furthermore, such systems could minimise capital and operating costs, complexity, and energy required to transport CO_2 to other places.

Prior to the development of an effective CO_2 mitigation process, an essential step should be to identify the most CO_2-tolerant indigenous strains. The first phase of this study therefore focused on the isolation, identification and screening of carboxyphilic microalgal strains (indigenous to the KwaZulu-Natal province in South Africa). In order to identify a high carbon-sequestering microalgal strain, the physiological effect of different concentrations of carbon sources on microalgae growth was investigated. Five indigenous strains (I-1, I-2, I-3, I-4 and I-5) and a reference strain (I-0: *Coccolithus pelagicus* 913/3) were subjected to CO_2 concentrations of 0.03 - 15% and $NaHCO_3$ of 0.05 - 2 g/1. The logistic model was applied for data fitting, as well as for estimation of the maximum growth rate (μ_{max}) and the biomass carrying capacity (B_{max}). Amongst the five indigenous strains, I-3 was similar to the reference strain with regards to biomass production values. The B_{max} of I-3 significantly increased from 0.214 to 0.828 g/l when the CO_2 concentration was increased from 0.03 to 15% ($r = 0.955$, $p = 0.012$). Additionally, the B_{max} of I-3 increased with increasing $NaHCO_3$ concentrations ($r = 0.885$, $p = 0.046$) and was recorded at 0.153 g/l (at 0.05 g/l) and 0.774 g/l (at 2 g/l). Relative electron transport rate (rETR) and maximum quantum yield (F_v/F_m) were also applied to assess the impact of elevated carbon sources on the microalgal cells at the physiological level. Isolate I-3 displayed the highest rETR confirming its tolerance to higher quantities of carbon. Additionally, the decline in F_v/F_m with increasing carbon was similar for strains I-3 and the reference strain (I-0). Based on partial 28S ribosomal DNA gene sequencing, strain I-3 was found to be homologous to the ribosomal genes of *Chlorella* sp.

The influence of abiotic parameters (light intensity and light:dark cycles) and varying nutrient concentrations on the growth of the highly CO_2 tolerant *Chlorella* sp. was thereafter investigated. It was found that an increase in light intensity from 40 to 175 umol m^2 s^{-1} resulted in an enhancement of B_{max} from 0.594 to 1.762 g/l, respectively ($r = 0.9921$, $p = 0.0079$). Furthermore, the highest B_{max} of 2.514 g/l was detected at a light:dark cycle of 16:8. Media components were optimised using fractional factorial experiments which eventually culminated in a central composite optimisation experiment. An eight-factor resolution IV fractional factorial had a biomass production of 2.99 g/l. The largest positive responses (favourable effects on biomass production) were observed for individual factors X_2 ($NaNO_3$), X_3 (NaH_2PO_4) and X_6 (Fe-EDTA). Thereafter, a three-factor ($NaNO_3$, NaH_2PO_4 and Fe-EDTA) central composite experimental design predicted a maximum biomass production of 3.051 g/l, which was 134.65% higher when compared to cultivation using the original ASW medium (1.290 g/l).

A pilot scale flat panel photobioreactor was designed and constructed to demonstrate the process viability of utilising a synthetic flue gas mixture for the growth of microalgae. The novelty of this aspect of the study lies in the fact that a very high CO_2 concentration (30%) formed part of the synthetic flue gas mixture. Overall, results demonstrated that the *Chlorella* sp. was able to grow well in a closed flat panel reactor under conditions of flue gas aeration. Biomass yield, however, was greatly dependent on culture conditions and the mode of flue gas supply. In comparison to the other batch runs, run B yielded the highest biomass value (3.415 g/l) and CO_2 uptake rate (0.7971 g/day). During this run, not only was the *Chlorella* strain grown under optimised nutrient and environmental conditions, but the culture was also intermittently exposed to the flue gas mixture. Results from this study demonstrate that flue gas from industrial sources could be directly introduced to the indigenous *Chlorella* strain to potentially produce algal biomass while efficiently capturing and utilising CO_2 from the flue gas.

DEDICATION

For my dad, **Mr Kemraj Bhola**

For your endless love, support and encouragement. All of my achievements I owe to your unwavering devotion.

ACKNOWLEDGMENTS

I would like to acknowledge the following:

- God Almighty without whom none of this would have been possible.
- My dad, Mr Kemraj Bhola, for his steadfast strength, wisdom and faith.
- My amazing husband, Mr Rakesh Bhana, for his help with multiple aspects of this thesis, for his moral support and for always believing in me. Without your constant support and encouragement this would not have been possible.
- My brother, Mr Kamith Bhola, for been my constant pillar of strength and for always been someone I could depend on.
- Prof F. M. Swalaha, for his devoted efforts in assisting me throughout my research and for all his guidance and encouragement in overcoming the various obstacles encountered during my study. I cannot thank you enough for the time you have dedicated to assist me.
- Prof F. Bux, for his advice, assistance and encouragement during the course of this research project. His commitment to research excellence ensured that my project conformed to the highest standards.
- Mrs Trisha Mogany, for her dependable friendship and ever obliging advice and assistance. I cannot thank you enough for your patience, support and understanding.
- Dr S. Kumari, for her valuable contribution towards the successful submission of my research article as well as supervision with molecular aspects of my study.
- Dr M. Nasr, for his insightful knowledge and experience, especially towards the submission of research publications.

- Dr K. Ramluckan, for assistance with gas chromatography studies and always going the extra mile to ensure that all my academic endeavours were successful.

- Miss Karen Reddy, a friend I could always rely on for her encouragement and support.

- Mr Ismail Rawat, for his invaluable efforts and aid throughout my research project.

- Staff and students at the Institute for Water and Wastewater Technology, Durban University of Technology for their analytical support and guidance.

- The National Research Foundation and Durban University of Technology for funding.

PREFACE

Aspects of the work covered in the following thesis can be found in the following publications:

Int. J. Environ. Sci. Technol. (2014) 11:2103–2118
DOI 10.1007/s13762-013-0487-6

REVIEW

Overview of the potential of microalgae for CO_2 sequestration

V. Bhola · F. Swalaha · R. Ranjith Kumar · M. Singh · F. Bux

Received: 15 October 2012 / Revised: 22 November 2013 / Accepted: 14 December 2013 / Published online: 9 January 2014

Abstract An economic and environmentally friendly approach of overcoming the problem of fossil CO_2 emissions would be to reuse it through fixation into biomass. Carbon dioxide (CO_2), which is the basis for the formation of complex sugars by green plants and microalgae through photosynthesis, has been shown to significantly increase the growth rates of certain microalgal species. Microalgae possess a greater capacity to fix CO_2 compared to C_4 plants. Selection of appropriate microalgal strains is based on the CO_2 fixation and tolerance capability together with lipid potential, both of which are a function of biomass productivity. Microalgae can be propagated in open raceway ponds or closed photobioreactors. Biological CO_2 fixation also depends on the tolerance of selected strains to high temperatures and the amount of CO_2 present in flue gas, together with SO_x and NO_x. Potential uses of microalgal biomass after sequestration could include biodiesel production, fodder for livestock, production of colorants and vitamins. This review summarizes commonly employed microalgal species as well as the physiological pathway involved in the biochemistry of CO_2 fixation. It also presents an outlook on microalgal propagation systems for CO_2 sequestration as well as a summary on the life cycle analysis of the process.

Keywords CO_2 sequestration · Flue gas · Life cycle analysis · Microalgae · Photosynthesis

V. Bhola · F. Swalaha · R. Ranjith Kumar · F. Bux (✉)
Institute for Water and Wastewater Technology, Durban University of Technology, Durban, South Africa
e-mail: faizalb@dut.ac.za

M. Singh
College of Engineering, University of Georgia, Athens, GA 30602, USA

Introduction

The impending threat of global climate change has amplified. This has been mainly attributed to greenhouse gas (GHG) emissions of which carbon dioxide (CO_2) contributes up to 68 % of total emissions (Brennan and Owende 2010; Ho et al. 2011; Kumar et al. 2011). This is partly due to the high-energy usage and the dependence on coal for electricity generation (Kumar et al. 2011). According to a report by the Carbon Dioxide Information Analysis Center (CDIAC), CO_2 emissions worldwide have increased from 3 metric tons in 1,751 to 8,230 metric tons in 2006. Further increases in emissions are projected to permanently alter future climates as well as cause significant dents to the economy. Therefore, it is imperative to develop an appropriate technology to reduce the emissions and accumulation of CO_2. CO_2 sequestration strategies implemented globally can be divided into physical and biological techniques (Khoo et al. 2011). However, due to numerous challenges associated with physical methods, there is a need to develop other suitable technologies. Biological CO_2 fixation appears to be the only economical and environmentally viable technology of the future (Ho et al. 2011; Kumar et al. 2011). This presents an attractive development option as plants and other photosynthetic organisms naturally capture and use CO_2 as part of their photosynthetic process. Terrestrial plants are able to sequester vast amounts of CO_2 from the atmosphere. However, when compared to terrestrial plants, microalgae and cyanobacteria have faster growth rates, and their CO_2-fixation efficiency is also between 10 and 50 times higher (Costa et al. 2000; Langley et al. 2012). The biological mitigation of CO_2 using microalgae could therefore offer several advantages. No additional CO_2 is created, while nutrient utilization is achieved in a continuous fashion

Eur. J. Phycol. (2016), 1–12

Physiological responses of carbon-sequestering microalgae to elevated carbon regimes

VIRTHIE KEMRAJ BHOLA[1], FEROZ MAHOMED SWALAHA[2], MAHMOUD NASR[1], SHEENA KUMARI[1] AND FAIZAL BUX[1]

[1]*Institute for Water and Wastewater Technology, Durban University of Technology, Durban 4001, South Africa*
[2]*Department of Biotechnology and Food Technology, Durban University of Technology, Durban 4001, South Africa*

(Received 28 September 2015; revised 28 January 2016; accepted 18 February 2016)

In order to identify a high carbon-sequestering microalgal strain, the physiological effect of different concentrations of carbon sources on microalgae growth was investigated. Five indigenous strains (I-1, I-2, I-3, I-4 and I-5) and a reference strain (I-0: *Coccolithus pelagicus* 913/3) were subjected to CO_2 concentrations of 0.03–15% and $NaHCO_3$ of 0.05–2 g CO_2 l^{-1}. The logistic model was applied for data fitting, as well as for estimation of the maximum growth rate (μ_{max}) and the biomass carrying capacity (B_{max}). Amongst the five indigenous strains, I-3 was similar to the reference strain with regards to biomass production values. The B_{max} of I-3 significantly increased from 214 to 828 mg l^{-1} when CO_2 concentration was increased from 0.03 to 15% ($r = 0.955$, $P = 0.012$). Additionally, the B_{max} of I-3 increased with increasing $NaHCO_3$ ($r = 0.885$, $P = 0.046$) and was recorded at 153 mg l^{-1} (at 0.05 g CO_2 l^{-1}) and 774 mg l^{-1} at (2 g CO_2 l^{-1}). Relative electron transport rate (rETR) and maximum quantum yield (F_v/F_m) were also applied to assess the impact of elevated carbon sources on the microalgal cells at the physiological level. Isolate I-3 displayed the highest rETR confirming its tolerance to higher quantities of carbon. Additionally, the decline in F_v/F_m with increasing carbon was similar for strains I-3 and the reference strain. Based on partial 28s ribosomal RNA gene sequencing, strain I-3 was homologous to the ribosomal genes of *Chlorella* sp.

Key words: CO_2 fixation, CO_2 tolerance, logistic model, microalgal isolation, $NaHCO_3$, $NaHCO_3$ tolerance, physiological stress

INTRODUCTION

Carbon dioxide (CO_2) emissions play an important role in global climate regulation by changing the earth's radiation budget, temperature, meteorology and hydrology (Feng *et al.*, 2008). The main sources of CO_2 emissions are combustion of fossil fuels, such as coal, natural gas and oil, for energy and transportation (Al-Hothaly *et al.*, 2015). Emissions of CO_2 have dramatically increased within the last 50 years and continue to increase by almost 3% each year (Pires *et al.*, 2012). The normal CO_2 content in air is assumed to be approximately 0.03% (e.g. Chinnasamy *et al.*, 2009). However, Kumar & Das (2012) reported a CO_2 concentration in air of nearly 391 ppmv (0.0391% by volume) based on research carried out at the Manua Loa Observatory (Hawaii, USA) in 2011 and that this concentration is rapidly increasing worldwide at a rate of ~2 ppmv per year (2×10^{-4} % by volume). Thus remediation strategies are urgently required.

Carbon dioxide sequestration strategies can be broadly classified into physical and biological protocols (Anjos *et al.*, 2013). Physical sequestration protocols are associated with several challenges, including high costs and space requirements as well as CO_2 leakage (Yue & Chen, 2005). In this context, biological CO_2 sequestration has been reported as a promising alternative solution for CO_2 fixation (Yang & Gao, 2003). Since CO_2 is essential for the formation of complex sugars by green plants through photosynthesis, it can be used to significantly enhance growth rates of certain microalgal species. Biological mitigation of CO_2 using autotrophic microalgal cultivation offers several advantages, such as the production of biofuels and other secondary metabolites (Watanabe *et al.*, 1992). Microalgal strains are able to fix CO_2 gases present in the atmosphere or from industrial flue and flaring practices. Microalgal species are able to take up CO_2 in the form of soluble carbonates ($NaHCO_3$ and Na_2CO_3). Those microalgal strains that display tolerance to high concentrations of these carbonates could serve in an effective screening method for high CO_2 tolerant strains (Wang *et al.*, 2008).

Prior to the development of an effective CO_2 mitigation process, an essential step should be to identify the most CO_2-tolerant indigenous strains (Khan *et al.*, 2009). Researchers have reported that very few

Correspondence to: Faizal Bux. Email: faizalb@dut.ac.za

ISSN 0967-0262 (print)/ISSN 1469-4433 (online)/16/000001-12 © 2016 British Phycological Society
http://dx.doi.org/10.1080/09670262.2016.1193902

Environmental Technology, 2013
Vol. 34, Nos. 13–14, 1765–1775, http://dx.doi.org/10.1080/09593330.2013.826287

Taylor & Francis
Taylor & Francis Group

Improving the feasibility of producing biofuels from microalgae using wastewater

I. Rawat, V. Bhola, R. Ranjith Kumar and F. Bux*

Institute for Water and Wastewater Technology, Durban University of Technology, P.O. Box 1334, Durban 4000, South Africa

(*Received 9 April 2013; accepted 6 July 2013*)

Biofuels have received much attention recently owing to energy consumption and environmental concerns. Despite many of the technologies being technically feasible, the processes are often too costly to be commercially viable. The major stumbling block to full-scale production of algal biofuels is the cost of upstream and downstream processes and environmental impacts such as water footprint and indirect greenhouse gas emissions from chemical nutrient production. The technoeconomics of biofuels production from microalgae is currently unfeasible due to the cost of inputs and productivities achieved. The use of a biorefinery approach sees the production costs reduced greatly due to utilization of waste streams for cultivation and the generation of several potential energy sources and value-added products while offering environmental protection. The use of wastewater as a production media, coupled with CO_2 sequestration from flue gas greatly reduces the microalgal cultivation costs. Conversion of residual biomass and by-products, such as glycerol, for fuel production using an integrated approach potentially holds the key to near future commercial implementation of biofuels production.

Keywords: biofuels; microalgae; wastewater; biorefinery

Introduction

The steady increase in the price of crude oil and growing concerns surrounding the increase in anthropogenic greenhouse gases (GHGs) and climate change have signalled a need to diversify energy production. Biofuels have received much attention as they are renewable and sustainable. Suitable alternatives to transportation fuels from renewable feedstocks in the near future are paramount to mitigating climate change. The production of crop-based biofuels, such as biodiesel, is unlikely to meet the production capacity required for liquid fuels using traditional feedstocks (soybeans, rapeseed/canola, palm, various greases and used cooking oils).[1–3] Research initiatives have established that microalgae have great potential as feedstocks for renewable fuels owing to their faster growth rates and higher CO_2 fixation efficiency when compared with terrestrial plants.[1–5] Commercial biofuels production using microalgal biomass has been hampered by the unfavourable process technoeconomics.[6,7]

In addition to serving as a biofuels feedstock, microalgae offer the potential for wastewater treatment. Discharge of wastewater with excessive amounts of nitrogen (N) and phosphorus (P) due to improper or incomplete treatment leads to eutrophication, and thereby damage to ecosystems.[8] Existing chemical- and physical-based technologies for nutrient removal utilize a considerable amount of energy and chemical additives. The high energy demand and cost associated with treatment of wastewaters remain ongoing challenges for industries and municipalities.[6,7]

Microalgae-based treatment has the added benefits of resource recovery and recycling. Microalgae cultivated in wastewater as a feedstock for biofuels production can be achieved in the near future.[9] Microalgal biomass production coupled with wastewater treatment could prove beneficial for both wastewater treatment as well as biomass production for biofuels. Wastewater usage can offset utilization of unsustainable amounts of freshwater and the costs associated with commercial fertilizers that are ordinarily used for microalgae production, and reduced energy consumption from wastewater treatment can offset microalgae production costs.[6] The availability of land for microalgal biomass production in the vicinity of wastewater treatment plants comes strongly into perspective if wastewater is to be used as a substrate for cultivation. Fortier and Sturm [10] found that it is feasible to commercially produce microalgal biofuels in Kansas USA due to the availability, within 1 mile, of most wastewater treatment plants. They have further suggested that nutrients and not land is the limiting factor to microalgal cultivation. Studies of this nature are required to determine the feasibility in other regions.

The biorefinery concept is an emerging field whereby an integrated approach to the production of multiple fuels/products from a single feedstock or its by-products is undertaken.[11,12] A biorefinery approach is key for an economically competitive process of fuel production. Microalgae biorefineries provide a promising technology that mediates between biodiesel production, economic feasibility (bio-based by-products provide additional

*Corresponding author. Email: faizalb@dut.ac.za

ASPECTS OF THE WORK COVERED IN THE FOLLOWING THESIS CAN ALSO BE FOUND IN THE FOLLOWING PUBLISHED BOOK CHAPTER:

Volume 7 of the series Developments in Applied Phycology pp 147-154

Date: 22 December 2015

Carbon Dioxide Sequestration by Microalgae: Biorefinery Approach for Clean Energy and Environment

Abhishek Guldhe ✉ , Virthie Bhola, Ismail Rawat, Faizal Bux

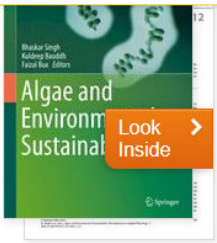

Abstract

Environmental implications and climate change due to greenhouse gas emissions have raised concerns about the sequestration of CO_2. Photosynthetic microalgae have shown excellent potential as a precursor for renewable biofuels, commercial bioproducts, and animal or aquaculture feed. Utilization of CO_2 for cultivation of microalgae is a sustainable and environmentally friendly approach for biological CO_2 sequestration. There are engineering constraints and challenges to make the overall process economically feasible which needs to be addressed. Integrating this biological CO_2 sequestration approach in a microalgal biorefinery with utilization of wastewater is a green approach for clean energy and environment.

THIS RESEARCH WAS PRESENTED AT THE FOLLOWING CONFERENCES:

- Virthie Bhola; Feroz Mahomed Swalaha and Faizal Bux (2016). Physiological responses of carbon sequestering microalgae to elevated carbon regimes. South African Society for Microbiology (SASM): Environmental/ Agricultural Biotechnology session. 18 January 2016. Coastlands Hotel, Umhlanga, Durban (oral presentation).

- Virthie Bhola; Feroz Mahomed Swalaha and Faizal Bux (2016). Evaluation of elevated carbon concentrations on indigenous carboxyphilic microalgae. Municipal Institute of Learning (MILE): eThekwini-University Research Symposium. 5 April 2016. International Convention Centre (ICC), Durban (poster presentation).

CONTENTS

ABSTRACT i
DEDICATION iii
ACKNOWLEDGMENTS iv
PREFACE vi
LIST OF FIGURES xv
LIST OF TABLES xviii
CHAPTER ONE: GENERAL INTRODUCTION AND OBJECTIVES OF STUDY 1
1.1 INTRODUCTION 1
1.2 AIM AND OBJECTIONS 7
1.2.1 Aim: 7
1.2.2 Objectives: 7
CHAPTER TWO: LITERATURE REVIEW 8
2.1 INTRODUCTION 8
2.2 GLOBAL WARMING 9
2.3 CARBON DIOXIDE SEQUESTRATION TECHNIQUES 10
2.4 RESEARCH INITIATIVES FOR THE BIOLOGICAL MITIGATION OF CO_2 11
2.5 MICROALGAE: AN INSTRUMENT FOR CARBON SEQUESTRATION 13
2.5.1 Biomass Production 15
2.6 STRATEGIES FOR ISOLATING HIGHLY CO_2 TOLERANT MICROALGAL STRAINS 17
2.7 PHYSICOCHEMICAL REQUIREMENTS FOR EFFECTIVE CO_2 CAPTURE AND 19
BIOMASS PRODUCTION 19
2.7.1 Growth Medium 19
2.7.2 Light Requirement 20
2.8 PROPAGATION SYSTEMS 21
2.9 SOLUBILITY AND SPECIATION OF CO_2 25
2.10 MICROALGAL SPECIES EMPLOYED FOR CARBON BIO-MITIGATION 28
2.11 PHYSIOLOGICAL PATHWAY INVOLVED IN THE BIOCHEMISTRY OF CO_2 FIXATION 34
2.12 INFLUENCE OF FLUE GAS COMPOSITION ON MICROALGAL CULTIVATION 40
2.13 CHALLENGES AND ECONOMICS ASSOCIATED WITH MICROALGAL CO_2 SEQUESTRATION 43
2.14 VALUABLE END-PRODUCTS 49
2.15 CONCLUSION 52
2.16 RATIONALE FOR STUDY 53
CHAPTER THREE: ISOLATION, SCREENING AND PHYSIOLOGICAL RESPONSES OF CARBON-SEQUESTERING MICROALGAE TO ELEVATED CARBON REGIMES 54
3.1 INTRODUCTION 54

3.2 MATERIALS AND METHODS 56
3.2.1 Sampling and Preliminary Screening 56
3.2.2 Reference Strain 57
3.2.3. Isolation 57
3.2.4 Experimental Set-up 58
3.2.5 Fluorescence Measurements 59
3.2.6 Strain Identification 60
3.2.7 Growth Profile and Logistic Model 61
3.2.7.1 Biomass (dry cell weight) 61
3.2.7.2 Logistic model 62
3.2.8 CO_2 Uptake Rate 62
3.3 RESULTS AND DISCUSSION 63
3.3.1 Sampling and Preliminary Screening 63
3.3.2 Growth of Strains under Different CO_2 Concentrations 66
3.3.3 Growth of Strains under Varying $NaHCO_3$ Concentrations 73
3.3.4 Relative Electron Transport Rate (rETR) at the Different CO_2 Concentrations 80
3.3.5 Relative Electron Transport Rate (rETR) at the Various $NaHCO_3$ Levels 82
3.3.6 Maximum Quantum Yield of the Most Tolerant Strain 85
3.3.7 Identification of the Most Tolerant Strain 87
CHAPTER FOUR: OPTIMISATION OF ABIOTIC CULTURE CONDITIONS FOR INCREASED BIOMASS PRODUCTION 89
4.1 INTRODUCTION 89
4.2 MATERIALS AND METHODS 90
4.2.1 Microalgal Strain and Isolation 90
4.2.2 Analytical Methods for Growth Determination 90
4.2.2.1 Light scattering (turbidity) 90
4.2.2.2 Biomass (dry cell weight) 91
4.2.2.3 Logistic model 91
4.2.3 Experimental Set-up 92
4.2.3.1 Effect of light intensity and photoperiods on the growth of the *Chlorella* strain I-3. 92
4.3 RESULTS AND DISCUSSION: 92
CHAPTER FIVE: OPTIMISATION OF NUTRIENT COMPOSITION FOR INCREASED BIOMASS PRODUCTION USING THE ONE-FACTOR-AT-A-TIME-APPROACH AND DESIGN OF EXPERIMENTS 98
5.1 INTRODUCTION 98
5.2 MATERIALS AND METHODS 99
5.2.1 Screening of Media for Cultivation of the *Chlorella* strain I-3 99

5.2.2 Preliminary Study: One-Factor-at-a-Time Approach to Determine Effects of Medium Components on Biomass Production 100
5.2.3 Statistical Experimental Designs 100
5.2.3.1 Fractional factorial design (FFD) 101
5.2.3.2 Central composite design (CCD) 103
5.2.4 Confirmatory Experiment to Determine Validity of Prediction 105
5.2.5 Statistical Analysis 106
5.2.6 Model Validation 106
5.2.7 Model Fit 107
5.2.8 Analysis of Variance (ANOVA) 107
5.2.9 Diagnostics 108
5.2.10 Graphs 108
5.3 RESULTS AND DISCUSSION 109
5.3.1 Selection of Nutrient Medium 109
5.3.2 Preliminary Study: One-Factor-at-a-Time Approach to Determine Effects of Medium Components on Biomass Production 111
5.3.3 Fractional Factorial Design 125
5.3.4 Central Composite Design 134
5.3.5 Validation Experiment 141
CHAPTER SIX: UTILISATION OF FLUE GAS FOR CULTIVATION OF THE SELECTED *CHLORELLA* SP. IN A PHOTOBIOREACTOR 143
6.1 INTRODUCTION 143
6.2 MATERIALS AND METHODS 145
6.2.1 Microalgal Strain, Growth Medium and Culture Conditions 145
6.2.2 The Photobioreactor System 145
6.2.2.1 The flat panel photobioreactor experimental system 145
6.2.2.2 Reactor operation 147
6.2.3 Biochemical Composition Determination 148
6.2.3.1 Carbohydrate analysis (phenol-sulfuric acid method) 148
6.2.3.2 Protein analysis 149
6.2.3.3 Lipid analysis 150
6.2.4 Analytical Methods 150
6.2.4.1 Growth profile and the logistic model 150
6.2.5 Statistical Analysis 151
6.2.6 CO_2 Uptake Rate 151
6.2.7 Gas Chromatography 152
6.2.8 Fluorescence Measurements 153
6.2.9 Morphological Observation by Scanning Electron Microscopy (SEM) 153

6.3 RESULTS AND DISCUSSION 154
6.3.1 The Photobioreactor System 154
6.3.2 Microalgae Growth Profile Using Synthetic Flue Gas 157
6.3.3 CO_2 Uptake Rate 163
6.3.4 Fluorescence Measurements 164
6.3.5 Biochemical Composition 169
6.3.6 Morphological Observation by SEM 172
CHAPTER SEVEN: CONCLUSION AND RECOMMENDATIONS 174
7.1 CONCLUSIONS 174
7.2 RECOMMENDATIONS 176
REFERENCES 177
APPENDICES 218
Appendix A: Data obtained for Tukey's post hoc test (Chapter Three) 218
Appendix B: Recipe for ASW media (Watanabe *et al*., 1992; Watanabe *et al*., 2000) 223
Appendix C: Recipe for BG11 media (Watanabe *et al*., 2000) 225
Appendix D: Recipe for NSW (natural seawater) media (Watanabe *et al*., 2000) 226
Appendix E: Recipe for L1 media (Guillard and Hargraves, 1993) 227
Appendix F: Recipe for ATCC 1142 media (Allen and Arnon, 1955) 229
Appendix G: Recipe for f/2 media (Guillard and Ryther, 1962) 230
Appendix H: Recipe for f/2 + Si media (Guillard, 1975) 231
Appendix I: Data obtained for Tukey's post hoc test (Chapter Six) 233

LIST OF FIGURES

Figure 1: An illustration of the relationship between microalgal CO_2 sequestration and biomass production……...……...……...……17

Figure 2: Aerial schematic of an open raceway pond showing feed and harvest points……22

Figure 3: Schematic representation of an airlift photobioreactor for flue gas sequestration.....25

Figure 4: Microalgal photosynthesis: modified from Zeng *et al*., 2011…….……...34

Figure 5: Images of the nine algal strains viewed under the light microscope at 1000x magnification……..……...…….....65

Figure 6: Effect of CO_2 concentrations (%) on the growth of the reference (I-0) and five (I-1 to I-5) indigenous microalgal strains. Shaded squares (blue) = 0.03% CO_2 (control), triangles (green) = 0.5% CO_2, inverted shaded triangles (yellow) = 5% CO_2, circles = (orange) 10% CO_2, shaded circles (red) = 15% CO_2 67

Figure 7: CO_2 uptake rate of the microalgal strains at varying CO_2 levels (%)……...….72

Figure 8: Effect of $NaHCO_3$ (0.05 - 2 g/l) on the growth of the reference and five indigenous strains. Shaded squares (blue) = 0.05 g/l (control), triangles (green) = 0.2 g/l, inverted shaded triangles (yellow) = 0.6 g/l, circles (orange) = 1 g/l, shaded circles (red) = 2 g/l……...74

Figure 9: CO_2 uptake rate of microalgal strains at varying $NaHCO_3$ concentrations (g/l)…....79

Figure 10: Maximum relative electron transport rate ($rETR_{max}$) at different CO_2 concentrations (0.03 - 15%). Shaded squares (blue) = 0.03% CO_2 (control), triangles (green) = 0.5% CO_2, inverted shaded triangles (yellow) = 5% CO_2, circles = (orange) 10% CO_2, shaded circles (red) = 15% CO_2 …….…....81

Figure 11: Maximum relative electron transport rate ($rETR_{max}$) at different $NaHCO_3$ (0.05 - 2 g/l) concentrations. Shaded squares (blue) = 0.05 g/l (control), triangles (green) = 0.2 g/l, inverted shaded triangles (yellow) = 0.6 g/l, circles (orange) = 1 g/l, shaded circles (red) = 2 g/l …….83

Figure 12: The difference in the maximum quantum yield of PSII (*Fv/Fm*) for I-0 and I-3 at different (a) CO_2 and (b) $NaHCO_3$ concentrations …….....……..85

Figure 13: Evolutionary history inferred using the Neighbour-Joining method……...…....87

Figure 14: The effect of varying light intensities (40, 80, 125, 175 and 200 umol m^{-2} s^{-1}) on the biomass production of the *Chlorella* sp. …….....94

Figure 15: The effect of varying photoperiods (8:16, 12:12, 16:8 and 24:0) on the biomass production of the *Chlorella* sp……..…….....97

Figure 16: Growth profiles of the *Chlorella* sp. on each nutrient medium investigated over 21 days……..……..……111

Figure 17: Time-course profiles of cell growth acquired growing in varying concentrations of $Na_2SiO_3.9H_2O$ (in g/l) with all other factors constant……..…..…...112

Figure 18: Effects of varying $NaNO_3$ concentrations (in g/l) on the growth of the *Chlorella* sp. over a 22 day duration…….……...……...114

Figure 19: Growth of the *Chlorella* sp. in response to different NaH_2PO_4 concentrations (in g/l) over a 22 day period……....…...……..116

Figure 20: Effects of varying NaCl concentrations (in g/l) on the growth of the *Chlorella* sp. over a 22 day duration…….……...……...118

Figure 21: Time-course profiles of cell growth acquired under varying concentrations of trace metals (in ml/l)……...…….……..121

Figure 22: Growth of the *Chlorella* sp. in response to different Fe-EDTA concentrations (in ml/l) over a 22 day period…….122

Figure 23: Effects of varying anhydrous salt concentrations (in ml/l) on the growth of the *Chlorella* sp. over a 22 day duration……..……..…….123

Figure 24: Effects of varying hydrous salt concentrations (in ml/l) on the growth of the *Chlorella* sp. over a 22 day duration……....…….125

Figure 25: The half-normal probability plot for biomass produced by the *Chlorella* sp…..…128

Figure 26: Box-Cox plot for FFD0821 indicating the position of lambda……...129

Figure 27: Pareto chart indicating the magnitudes of positive (orange) and negative (blue) effects on biomass production of the *Chlorella* sp. in the eight-factor design……..……132

Figure 28: Contour plot of biomass production by *Chlorella* sp. showing the effects of two factors, $NaNO_3$ and NaH_2PO_4…….……..……...138

Figure 29: Contour plot of biomass production by *Chlorella* sp. showing the effects of two factors, $NaNO_3$ and Fe-EDTA……...139

Figure 30: Contour plot of biomass production by *Chlorella* sp. showing the effects of two factors, NaH_2PO_4 and Fe-EDTA……...140

Figure 31: Cube plot illustrating the interactions between X_2: $NaNO_3$, X_3: NaH_2PO_4 and X_6: Fe-EDTA……...141

Figure 32: Biomass obtained when *Chlorella* sp. was grown in un-optimised and optimised ASW medium……142

Figure 33: Schematic diagram depicting the photobioreactor lid……...155

Figure 34: Schematic diagram depicting flat panel photobioreactor system…….....156

Figure 35: Growth profiles of the selected *Chlorella* sp. (A) cultured in a flat panel reactor aerated continuously with flue gas under optimised conditions of light intensity, photoperiod and nutrients, (B) grown under optimised conditions of light intensity, photoperiod and nutrients and periodic exposure to the flue gas mixture, (C) control run: periodic exposure to the flue gas mixture under un-optimised conditions of light intensity, photoperiod and nutrients…….159

Figure 36: CO_2 uptake rate of the *Chlorella* sp. during the different photobioreactor runs …164

Figure 37: Maximum relative electron transport (rETR) at the different runs within the photobioreactor……..166

Figure 38: Relationship between rETR and biomass production during the different photobioreactor runs……..168

Figure 39: Relationship between CO_2 uptake rate and biomass production during the different photobioreactor runs……..169

Figure 40: Scanning electron microscopic images of *Chlorella* sp. on day 16 of cultivation: (a) no flue gas aeration (b) grown under optimised conditions of light intensity, photoperiod and nutrients and intermittently exposed to the flue gas mixture, (c) control run: periodic exposure to the flue gas mixture under un-optimised conditions of light intensity, photoperiod and nutrients, (d) aerated continuously with flue gas under optimised conditions of light intensity, photoperiod and nutrients…….172

LIST OF TABLES

Table 1: Important characteristics of the five major algae groups……..…15

Table 2: Advantages of using microalgae as opposed to terrestrial plants for CO_2 biofixation…….....29

Table 3: Commonly employed microalgal species used for CO_2 sequestration under varying cultivation modes…….……...……33

Table 4: Approximate annual global CO_2 flue gas emissions per industrial sector……..…....42

Table 5: Feasible downstream applications of various microalgae species…….…...……...51

Table 6: Samples collected in KwaZulu-Natal (South Africa)……...…..…..64

Table 7: Summary of pure microalgal strains isolated from samples……....…65

Table 8: Logistic model parameters of the microalgal strains at different CO_2 concentrations (0.03 - 15%)……..……..…….69

Table 9: Logistic model parameters of the microalgal strains at different quantities of $NaHCO_3$ (0.05 - 2 g/l)……..……..…….75

Table 10: Estimated logistic model parameters (μ_{max} and B_{max}) at different light intensities and light:dark cycles……...……..……...……..93

Table 11: Independent variables and concentration levels in the fractional factorial experiment indicating low, high and center points ……..…....102

Table 12: Experimental design of FFD0821 with five center points, showing the coded values of the variables and randomised order used to determine the effect of ASW medium components on the biomass production of the isolated *Chlorella* sp ……...103

Table 13: Independent variables and the concentration levels studied in the optimisation design ……..……...……...103

Table 14: Experimental design of a three factor central composite experiment showing coded factor levels with standard order to determine effect of the variables on biomass production ……...105

Table 15: Fractional factorial experimental design for FFD0821 with the coded values of the variables tested showing actual, predicted and residual values……..…..…....127

Table 16: Analysis of variance for the eight factor factorial model……...…..133

Table 17: Central composite experimental design showing the actual and predicted biomass values……..……..…….135

Table 18: Analysis of variance for the central composite model……...…..137

Table 19: The optimised solution from the model, generated for the three factors to maximise biomass production of the *Chlorella* sp…….…...….....142

Table 20: Estimated logistic model parameters (μ_{max} and B_{max}) at the different runs within the photobioreactor…….……163

Table 21: Carbohydrate, protein and lipid production of *Chlorella* sp. during flue gas exposure at different runs…….....…….....171

Table 22: Data obtained for Tukey's post hoc test for the different strains when grown at 15% CO_2…….……...……218

Table 23: Data obtained for Tukey's post hoc test for the different strains when grown at 10% CO_2…….…...……218

Table 24: Data obtained for Tukey's post hoc test for the different strains when grown at 5% CO_2……...…..……219

Table 25: Data obtained for Tukey's post hoc test for the different strains when grown at 0.5% CO_2……..…..……219

Table 26: Data obtained for Tukey's post hoc test for the different strains when grown at 0.03% CO_2……..……..……220

Table 27: Data obtained for Tukey's post hoc test for the different strains when grown at 2 g/l $NaHCO_3$……..……..……220

Table 28: Data obtained for Tukey's post hoc test for the different strains when grown at 1 g/l $NaHCO_3$……221

Table 29: Data obtained for Tukey's post hoc test for the different strains when grown at 0.6 g/l $NaHCO_3$…….……..……221

Table 30: Data obtained for Tukey's post hoc test for the different strains when grown at 0.2 g/l $NaHCO_3$……..…...……...222

Table 31: Data obtained for Tukey's post hoc test for the different strains when grown at 0.05 g/l $NaHCO_3$…….……...……...222

Table 32: Data obtained for Tukey's post hoc test for the different photobioreactor runs…..233

CHAPTER ONE: GENERAL INTRODUCTION AND OBJECTIVES OF STUDY

1.1 INTRODUCTION

A well-balanced ecosystem is one in which carbon deposition in soil and the oceans, carbon release from geological and biological sources as well as the carbon capture from photosynthesis are all in equilibrium (Sayre, 2010). However, since the beginning of the industrial age, humans discovered fossil fuels and ultimately developed various applications for its use, unsuspectingly releasing large quantities of greenhouse gases (GHG) into the atmosphere without realising the grave consequences of their actions (Mohan *et al*., 2016). In recent years alarming increases in GHG emissions globally have amplified the impending threat of global climate change (Brennan and Owende, 2010; Ho *et al*., 2011; Kumar *et al*., 2011-b). Escalations in GHG emissions can be mainly attributed to the rise in anthropogenic activities such as deforestation, burning of fossil fuels and energy generation and usage (Kumar *et al*., 2011-b). At present, more than 80% of the global energy produced is generated through combustion of fossil fuels. Direct carbon combustion for energy production releases more than 24 gigatons of carbon dioxide (CO_2) annually into the atmosphere.

As a result, CO_2, a major greenhouse gas has rose unceasingly since pre-industrial revolution to date and currently contributes ±52% in total global warming and climate change (Cheah *et al*., 2015; Kumar *et al*., 2014; Singh and Ahluwalia, 2013). The CO_2 theory states that the amount of CO_2 in the atmosphere directly controls temperature due to the fact that CO_2 molecules in the air absorb infrared radiation. Carbon dioxide present in the atmosphere is virtually transparent to the visible radiation that delivers the sun's energy to the earth. The earth however, reradiates much of the energy in the invisible infrared region of the spectrum. This radiation is most intense at wavelengths very close to the principal absorption band (13 to 17 microns) of the CO_2 spectrum. At a sufficiently high concentration of CO_2, the weaker absorption bands become effective,

leading to a greater amount of infrared radiation been absorbed. However, the high CO_2 concentration forms a thick blanket preventing the escape of infrared radiation into space, which leads to the trapped radiation warming up the atmosphere. This phenomena is referred to as the greenhouse effect (Hansen *et al*., 1981).

Furthermore, steel plants, electric power plants and cement manufacturing companies are also major contributors of CO_2 emissions worldwide, as CO_2 is the primary emission of flue gases which are released continuously from these plants (Li *et al*., 2015; Radmann *et al*., 2012). Flue gas is a collection of several noxious gases including nitrogen (N_2), CO_2, nitrogen oxides (NO_x), sulphur dioxide (SO_x) as well as particulate matter (Kumar *et al*., 2014; Li *et al*., 2015). The composition and concentration of flue gases vary depending on the source of its generation (Kumar *et al*., 2014; Li *et al*., 2015).

According to a report by the International Energy Agency, approximately 28.8 Gt of CO_2 emissions were recorded in 2007 (Mohan *et al*., 2016). If drastic measures are not taken immediately to limit emissions, this amount is likely to increase to 40.3 Gt by the year 2030 and to 50 Gt by 2050 (Mohan *et al*., 2016). These increases in emissions are projected to permanently alter future climates which would have catastrophic implications on nature as well as mankind (Khoo *et al*., 2011). The urgency of these crises have led scientists, politicians and environmentalists to agree that crucial steps should be implemented to reduce the emissions and accumulation of CO_2 (Mohan *et al*., 2016).

An example of a crucial step taken was implementation of the Kyoto protocol which was a popular international accord that was established by the United Nations in an effort to reduce CO_2 emissions by 5.2% based on emissions recorded in 1990. This protocol was ratified by more

than 170 countries (Cheah *et al*., 2015; Gutierrez *et al*., 2008; Ho *et al*., 2011; Mohan *et al*., 2016; Pires *et al*., 2012). In 2010, the United Nations further suggested the introduction of a carbon credit system with a projected unit price of US $270/ton (Ho *et al*., 2011). Thereafter, in 2010, the Copenhagen accord was drawn up, whereby it was agreed that US $100 billion will be provided to aid in GHG mitigation by 2020 (Ho *et al*., 2011). This accord not only aimed to decrease CO_2 emissions but also intended to lessen climate change (Rogelj *et al*., 2010). Numerous other research and development efforts are currently under way to reduce and limit the amount of CO_2 entering the atmosphere (de Morais and Costa, 2007; Ho *et al*., 2011). However, selecting the most appropriate technology has sparked much debate globally.

Carbon dioxide sequestration strategies implemented globally thus far can broadly be divided into physical and biological techniques (Khoo *et al*., 2011). Physical strategies basically involve CO_2 capture and storage (CCS). This CCS methodology occurs in three steps: (1) CO_2 capture, (2) CO_2 transportation and (3) CO_2 storage (Pires *et al*., 2012). Carbon dioxide capture is usually performed at facilities that discharge large amounts of CO_2 into the atmosphere daily (such as cement manufacturing facilities and power plants). Methods of capture include: (a) adsorption, (b) gas separation membranes, (c) absorption and (d) cryogenic distillation (Kanniche and Bouallou, 2007; Thiruvenkatachari *et al*., 2009). Following capture, the subsequent CO_2 rich gas mixture is compressed to a supercritical fluid or liquid to aid in transportation (by ship or pipelines) to places of storage. Storage options often comprise injection into deep oceanic or geological trenches as well as mineralisation (Pires *et al*., 2012). In essence, CCS techniques are able to minimise the disastrous effects of CO_2 increases on the Earth's climate system by capturing it and injecting it into deep reservoirs where it can be contained for thousands of years (Pires *et al*., 2012). However, such procedures are short-term solutions as there are numerous challenges associated with physical techniques, such as high costs and space requirements as

well as CO_2 leakage over time. Therefore, there is a need to develop other more sustainable technologies.

Biological CO_2 fixation (whereby CO_2 is biologically converted to organic matters) appears to be the only economical and environmentally viable technology for the future (Ho *et al*., 2011; Kumar *et al*., 2011-b). This presents an attractive development option as plants and other photosynthetic organisms naturally capture and use CO_2 as part of their photosynthetic process. Even though terrestrial plants are able to sequester vast amounts of CO_2 from the atmosphere, they are expected to contribute a minor 3 - 6% reduction in global CO_2 emissions (Ho *et al*., 2011). When compared to terrestrial plants, microalgae (primitive, unicellular, microscopic organisms) have faster growth rates (with biomass volumes that double within 24 h), and their CO_2-fixation efficiency is also between 10 and 50 times higher (Costa *et al*., 2000; Langley *et al*., 2012). This can be attributed to several reasons. As opposed to terrestrial plants, microalgae possess a higher photosynthetic efficiency owing to their greater ability to capture and utilise light, converting it to usable chemical energy. Therefore, during ideal growth conditions, microalgae direct most of this chemical energy into cell division (6 - 12 hour cycle), resulting in rapid biomass accumulation. Furthermore, unlike plants, microalgae do not partition large amounts of biomass for supportive structures such as roots and stems. In contrast to terrestrial crops, microalgal biomass can be harvested at any time of the year. With respect to most terrestrial crops, only a small portion of the total biomass (corn cob, soybean seed) is harvested seasonally.

Additionally, microalgae are also able to endure high concentrations of CO_2, and this inherent ability makes them very advantageous in utilising CO_2 from flue gases of power plants. Furthermore, these organisms show much promise for the production of value-added products

(cosmetics, biofilters, fertilisers, biomolecules) and biofuels (biodiesel, biohydrogen, bioethanol), as they are rich in minerals, vitamins, oils and fatty acid methyl esters (Del Campo *et al*., 2007; Khan *et al*., 2009; Mutanda *et al*., 2011; Spolaore *et al*., 2006). Therefore, the biological mitigation of CO_2 using microalgae could offer several advantages: no additional CO_2 will be created, while nutrient utilisation can be achieved continuously leading to the production of biofuels and other scientifically and commercially important products (Kumar *et al*., 2011-a). Hence, microalgal-mediated CO_2 fixation coupled with useful by-products could present a promising alternative to existing CO_2 mitigation strategies (Lam *et al*., 2012; Wang *et al*., 2008).

To develop the most effective microalgal CO_2 mitigation process, it is necessary to select fast-growing, indigenous microalgal species with high CO_2 fixation efficiency (Huang *et al*., 2010; Khan *et al*., 2009). After isolating a strain of interest, the next step to follow would be the appropriate cultivation of the organism. Artificial cultivation of microalgae should reproduce and enhance the optimum natural growth conditions (Brennan and Owende, 2010; Vasumathi *et al*., 2012). For CO_2 sequestration studies involving microalgae, both open (raceway ponds) as well as closed systems (photobioreactors) can be used (Brennan and Owende, 2010; Chisti, 2008; Kumar *et al*., 2011-a; Molina *et al*., 2001; Suh and Lee, 2003). Owing to the fact that raceway ponds are cost-effective, they are the most commonly used artificial growth systems. However, due to significant CO_2 losses to the atmosphere (algal cells unable to sequester CO_2 adequately due to very low residence time of the sparged gas in the culture), microbial contaminants and low photosynthetic efficiency and productivity; the design and development of enclosed photobioreactors (PBRs) has become popular for microalgal CO_2 sequestration studies (Borowitzka, 1999; Brennan and Owende, 2010; Chisti, 2007; Kumar *et al*., 2011-a). Closed systems provide regulated and well-controlled cultivation. Higher biomass productivities may

also be achieved as these systems utilise CO_2 much more efficiently and contamination can also be easily prevented (Borowitzka, 1999; Chisti, 2007; Ho *et al*., 2011; Ugwu *et al*., 2008).

Each type of photobioreactor has its own distinct set of advantages and disadvantages in terms of potential efficiency of light utilisation, effective mass transfer of oxygen (O_2) and CO_2, ease of cleaning, as well as scalability (Molina *et al*., 2001). Of the many closed systems employed, flat panel reactors are some of the most promising since they are easy to use, have a high surface area to volume ratio (S/V ratio) for effective illumination and have open gas disengagement systems (Kumar *et al*., 2011-a). It can therefore be hypothesised that the manipulation of conditions within a flat panel reactor will increase biomass concentrations and hence be appropriate for use as a technology for CO_2 mitigation.

This research project was divided into three major stages. The first stage focused on the isolation, identification and screening of carboxyphilic microalgal strains that are indigenous to the KwaZulu-Natal province in South Africa. The second stage involved optimisation of environmental and nutritional parameters for increased biomass production of the selected strain using a one-factor-at-a-time-approach (OFAT) and design of experiments (DOE). The third and final stage entailed designing and optimisation of a closed reactor for cultivation of the chosen microalgal strain under flue gas aeration.

1.2 AIM AND OBJECTIONS

1.2.1 Aim:

To develop and optimise a microalgal CO_2 sequestration system for the treatment of flue gases using an enclosed bioreactor.

1.2.2 Objectives:

- Screening and identification of indigenous microalgae with high CO_2 assimilation rates.
- Determination of the physiological responses of selected strains to increasing concentrations of CO_2 and $NaHCO_3$.
- Optimisation of media and abiotic culturing conditions for the selected strain using statistical screening and optimisation techniques.
- Design and operation of a photobioreactor for the evaluation of the CO_2 sequestration potential using synthetic flue gas.

CHAPTER TWO: LITERATURE REVIEW

2.1 INTRODUCTION

The impending threat of global climate change has amplified. This has been mainly attributed to GHG emissions of which CO_2 contributes up to 68% of total emissions (Brennan and Owende, 2010; Ho *et al*., 2011; Kumar *et al*., 2011). This is partly due to the high-energy usage and the dependence on coal for electricity generation (Kumar *et al.*, 2011). According to a report by the Carbon Dioxide Information Analysis Center (CDIAC), CO_2 emissions worldwide have increased from 3 metric tons in 1751 to 8,230 metric tons in 2006. Further increases in emissions are projected to permanently alter future climates as well as cause significant dents to the economy. Therefore, it is imperative to develop an appropriate technology to reduce the emissions and accumulation of CO_2. Carbon dioxide sequestration strategies implemented globally can be divided into physical and biological techniques (Khoo *et al*., 2011). However, due to numerous challenges associated with physical methods, there is a need to develop other suitable technologies. Biological CO_2 fixation appears to be the only economical and environmentally viable technology of the future (Ho *et al*., 2011; Kumar *et al*., 2011). This presents an attractive development option as plants and other photosynthetic organisms naturally capture and use CO_2 as part of their photosynthetic process. Terrestrial plants are able to sequester vast amounts of CO_2 from the atmosphere. However, when compared to terrestrial plants, microalgae and cyanobacteria have faster growth rates, and their CO_2- fixation efficiency is also between 10 and 50 times higher (Costa *et al*., 2000; Langley *et al*., 2012). The biological mitigation of CO_2 using microalgae could therefore offer several advantages. No additional CO_2 is created, while nutrient utilization is achieved in a continuous fashion leading to the production of biofuels and other secondary metabolites. Therefore, microalgal-mediated CO_2 fixation coupled with biofuel production, and wastewater treatment could present a promising alternative

to existing CO_2 mitigation strategies (Lam *et al*., 2012; Wang *et al*., 2008). This chapter focuses on commonly used microalgal species as well as the physiological pathway involved in the biochemistry of CO_2 fixation. It also presents an outlook on microalgal propagation systems for CO_2 sequestration as well as a summary on the life cycle analysis of the process.

2.2 GLOBAL WARMING

Global climate change has been mainly attributed to GHG emissions of which CO_2 contributes up to 68% of total emissions (Brennan and Owende, 2010; Ho *et al*., 2011; Kumar *et al*., 2011-b). South Africa by far is one of the largest emitters of GHGs and amongst the top 20 most carbon intensive countries in the world (Murugesan *et al.*, 2008). This is partly due to increasing energy demand and the dependence on coal for electricity generation (Kumar *et al*., 2011-b; Murugesan *et al.*, 2008). Coal still remains the predominant source of electricity production in most countries as it is a relatively cheap fossil fuel. In 2013, 29.9% of the world's primary energy needs were met by coal as well as 41% of global electricity production (Jacob *et al*., 2015). The reserves/production ratio (R/P) is a technique that is used to ascertain the size of reserves (fossil fuel resources) available for years to come. The R/P value represents the number of years that current reserves would last if their rate of use did not change. Investigations into proven coal reserves in 2013 revealed that when compared to other fossil fuels, coal proved to have the highest R/P ratio of 113. Oil had an R/P ratio of 53.3 and natural gas a ratio of 55.1 (Jacob *et al*., 2015). Owing to the fact that coal is the cheapest and most abundant fossil fuel supply in non-OECD (Organization for Economic Cooperation and Development) countries, it will probably be utilised as a primary source of power generation for years to come. Developed OECD states also possess large indigenous coal reserves that will possibly be used to generate electricity at the cheapest cost (Jacob *et al*., 2015).

A 4.9% increase in CO_2 emissions owing to coal combustion was noted in 2011 compared to 2010. In 2012, 40% of global CO_2 emissions were due to coal combustion, with 28% of these emissions from coal-fired power plants (Jacob *et al*., 2015). It has been estimated by The International Energy Agency that CO_2 emissions related to global energy will reach a staggering 38 billion tons per annum in 2030. This is 70% more than the levels recorded in 2002, with developing countries expected to contribute two-thirds to this increase (IEA, 2002). Further increases in emissions are projected to permanently alter future climates which would have disastrous effects on nature and humankind (Chung *et al*., 2011).

2.3 CARBON DIOXIDE SEQUESTRATION TECHNIQUES

Concerns over carbon emissions and global warming have sparked much interest in limiting the amount of CO_2 entering the atmosphere as well as methods of sequestering carbon (Chung *et al*., 2011; Farrelly *et al*., 2013). However, there has been much debate on selection of the most appropriate technology. Carbon dioxide mitigation strategies applied worldwide can be divided into physical and biological techniques. Physical-based methodologies often entail three steps: capture, transportation and storage. Carbon dioxide is collected from a fixed source, for instance, from power plants or cement manufacturing facilities. Following capture, the gas mixture is converted to a supercritical fluid. This aids in transportation by pipeline or ship to a place of storage. Storage options often involve injection into deep oceanic or geological trenches and mineralisation (Khoo *et al*., 2011; Pires *et al*., 2012). These currently employed disposal methods are considered unsustainable as they are expensive, require large amounts of space, are energy intensive and eventually lead to CO_2 leakage over time (Stewart and Hessami, 2005). However, even with the aforementioned drawbacks, this still remains a popular technology. It enables societies to maintain their existing carbon-based infrastructure while aiming to reduce the effects of CO_2 on global warming (Pires *et al*., 2012).

Another option would be to utilise the collected CO_2. For example, precipitated calcium carbonate (PCC), which is manufactured by controlling the reaction of CO_2 with lime, can be used as a substitute for titanium dioxide or kaolin in the manufacture of paper products. Carbon dioxide could also be employed in the manufacture of paint, plastic, solvent and packaging. However, these industries would consume relatively minute quantities of CO_2, as compared to the large amounts released annually into the atmosphere (Stewart and Hessami, 2005).

Biofixation of CO_2 using microalgae could offer a sustainable alleviation technology without the aforementioned shortcomings (Stewart and Hessami, 2005). Although terrestrial plants are responsible for fixing around 500 billion tons of CO_2 per annum, they are expected to play a minor role (3 - 6%) in the overall reduction of atmospheric CO_2 (Skjanes *et al.,* 2007). Microalgae and cyanobacteria have come to the forefront of research as they offer greater potential owing to their rapid growth rates, higher CO_2-fixation ability and tolerance to extreme environments (Ho *et al*., 2011). Sydney *et al*. (2010) stated that carbon uptake is often dependent on the metabolic activity of microalgae. Studies have suggested that microalgae exposed to increased levels of CO_2 respond better (on a biomass basis), when compared to microalgae exposed to ambient air only. Microalgae are capable of generating roughly 280 tons of dry biomass per ha per year by utilising 9% of the freely available solar energy. During this process, approximately 513 tons of CO_2 can be sequestered (Sydney *et al*., 2010).

2.4 RESEARCH INITIATIVES FOR THE BIOLOGICAL MITIGATION OF CO_2

Microalgae have been studied for several decades as a feedstock for renewable energy in an attempt to reduce global warming. These organisms are able to use concentrated amounts of CO_2, present in power plant flue gases as well as from other sources. Therefore, they represent a powerful GHG mitigation strategy. During the mid-1970s, the US Department of Energy (DOE)

began encouraging research pertaining to microalgal wastewater treatment (Benemann *et al*., 1977). The recovered microalgal biomass was subjected to anaerobic digestion which yielded methane gas. The 'Aquatic Species Program' (US) funded by the office of fuels development started out as a project investigating the possibilities of using microalgae to sequester CO_2 emissions from coal power plants (Sheehan *et al*., 1998). The project screened microalgae that could produce high amounts of oils as well as grow under adverse environmental conditions (extreme temperature, pH and salinity). This program was able to develop a culture collection system as well as support a pilot-scale project consisting of two raceway ponds in New Mexico. It was proposed that sufficient resources would be available in the southwest region of the USA for large-scale microalgae processes capable of capturing several hundred million tons of CO_2 annually (Benemann and Oswald, 1996). However, by the end of this program, it was concluded that in order for such a process to be economically feasible, favourable sites that yielded productivities near the theoretical maximum would be required (Benemann and Oswald, 1996; Sheehan *et al*., 1998).

During the 1990s in Japan, a major research and development (R&D) program totalling over $250 million was carried out. The assignment focused on microalgae biofixation of CO_2 as well as GHG abatement using closed PBRs. However, owing to the high costs associated with PBRs (which still pose a problem today), the Japanese R&D initiative did not continue. The use of PBRs was then confined to inoculum production only (Lipinsky, 1992; Nakajima and Ueda, 2000).

The US DOE-NETL promoted microalgae R&D using closed PBRs. Other international participants of R&D pertaining to microalgae CO_2 abatement included the following: Arizona Public Services, ENEL Produzione Ricerca, EniTecnologie, ExxonMobil and Rio Tinto. Due to

the initiative of these governmental and private industries, the International Network on Microalgae Biofixation of CO_2 and GHG Abatement was formed in 2000 in an effort to bring together the limited technical expertise in this field (Pedroni *et al*., 2001).

Past research initiatives suggest that practical CO_2 utilisation using microalgae still requires innovative scientific and technological breakthroughs to render this a feasible technology. Unless coupled with other technologies or co-processes, investments into microalgae R&D are unlikely to make a considerable contribution to solving the CO_2 problem globally. The use of microalgae can be classified as a direct CO_2 mitigation technology. Direct strategies usually encompass much higher economic projections, amounting to billions of dollars, as opposed to indirect approaches. Therefore, for this technology to be a success, future R&D should focus on achieving higher biomass productivities using indigenous strains, culture stability over long periods of time when exposed to high concentrations of CO_2, economical reactor designs and potential for useful by-products. The economics of microalgal CO_2 utilisation may be improved by integrating this procedure with other co-processes. Potential co-processes include wastewater treatment, production of useful metabolites, as well as biofuels, animal feed and biofertiliser manufacturing. These would greatly aid in the economics of the entire process as well as contribute to GHG abatement by not producing additional fossil fuel that is generally required for product formation (Ho *et al.*, 2011).

2.5 MICROALGAE: AN INSTRUMENT FOR CARBON SEQUESTRATION

Microalgae which are primitive, unicellular, microscopic (2 - 200 μm) organisms that can also be classified as thallophytes, have an important ecological role (Brennan and Owende, 2010; Greenwell *et al*., 2010; Khan *et al*., 2009; Mutanda *et al*., 2011). Besides the fact that they can serve as food and feed sources for people and animals as primary producers, they are also the

principal producers of O_2 on Earth (Khan *et al*., 2009). Microalgae are categorised based on their basic cellular structure, pigmentation and life cycle. These organisms can be grouped into five main categories (Chlorophyceae, Rhodophyceae, Phaeophyceae, Cyanophyceae and Bacillariophyceae), whose characteristics are summarised in Table 1. Microalgae can be autotrophic or heterotrophic, and in some cases even both. Autotrophic microalgae require inorganic compounds, salts and an appropriate light source for growth, whereas heterotrophic microalgae utilise external sources of organic compounds as well as nutrients, which are used as energy sources. Due to novel genetic and ultra-structural information constantly emerging, the evolutionary history and taxonomy of microalgae is complex (Brennan and Owende, 2010; Mutanda *et al*., 2011). Microalgae can also be classified into two prokaryotic divisions and nine eukaryotic divisions (Khan *et al*., 2009; Mutanda *et al*., 2011). These organisms show much promise for the production of value-added products and biofuels, as they are rich in minerals, vitamins, oils and fatty acid methyl esters (Del Campo *et al*., 2007; Khan *et al*., 2009; Mutanda *et al*., 2011; Spolaore *et al*., 2006). Microalgae are able to grow at high concentrations of CO_2, and this inherent ability makes them very advantageous in utilising CO_2 from industrial emissions. They are fast growers with biomass volumes that double within 24 h. At a flow rate of 0.3 l/min of air with 4% CO_2 concentration, most microalgal strains are able to achieve a carbon-fixation rate of roughly 14.6 g C m^{-2}/day (Farrelly *et al*., 2013). Due to their rapid growth rates and high CO_2 bioconversion, microalgae represent a promising agent for carbon sequestration (Cheah *et al*., 2015).

Table 1: Important characteristics of the five major algae groups (Cheah *et al*., 2015)

Algae group	Common name	Characteristics
Chlorophyceae	Green algae	(i) Estimated 6000-8000 species (ii) 90% live in freshwater rather than marine (iii) Ranging from tiny unicellular and colonial organisms to large macroscopic weeds (iv) In monophyletic group as the terrestrial plants
Rhodophyceae	Red algae	(i) Estimated 4000-5000 species (ii) 90% live in marine environments (iii) Ranging from unicellular to macroscopic algae often found on rocky shores (iv) In monophyletic group as the terrestrial plants
Phaeophyceae	Brown algae	(i) Estimated 1500-2000 species (ii) Almost all live in marine environments (iii) Ranging from giant kelps to smaller intertidal seaweeds (iv) Grow in rocky intertidal zone
Cyanophyceae	Blue-green algae	(i) Prokaryotic cell (ii) Present in almost all feasible habitats (iii) CO_2 and nitrogen fixers since billions of years ago
Bacillariophyceae	Diatoms	(i) 12,000 known species (ii) Single celled and microscopic in size (iii) Grow in seas, lakes and moist soils (silicon dioxide or silicon)

2.5.1 Biomass Production

Research involving microalgal CO_2 bio-sequestration is largely dependent on biomass production (Figure 1). The monitoring of biomass production is regarded as the most significant indicator during CO_2 sequestration studies. Successful CO_2 bioconversion for biomass production is dependent on the selected microalgal strain (Cheah *et al*., 2015). An ideal species is one that possesses tolerance to elevated CO_2 concentrations, has the ability to endure toxic pollutant concentrations, nutrient limitations as well as pH stress. The most promising and robust microalgae species for carbon sequestration include *Scenedesmus* sp., *Botryococcus* sp., *Chlorella* sp. and *Nannochloropsis* sp. (Cheah *et al*., 2015; Singh and Ahluwalia, 2013). When

compared to *Cyanophytes* and *Chrysophyte* sp., *Chlorella* sp. was identified as possessing higher biomass production values during carbon sequestration studies (Cheah *et al*., 2015).

In 1995, Maeda *et al*., established that *Chlorella* sp. T-1 was resistant to high temperatures (35°C) and CO_2 concentrations (15%). They also observed that this strain was able to grow under conditions of actual flue gas aeration. This particular strain therefore proved ideal for biological fixation of CO_2 as it was not only resistant to high temperatures and CO_2 concentrations but also to SO_X, NO_X, chlorine, fluorine and dust. In another study, Kao *et al*. (2014) cultivated *Chlorella* sp. MTF-15 with flue gas from a power plant, containing approximately 24% CO_2 and low concentrations of SO_X (15 - 20 ppm) and NO_X (25 - 30 ppm). They were able to conclude that this robust microalga was able to efficiently utilise the industrial wastes present in the flue gas, producing a maximum biomass concentration of 1.872 g/l and a growth rate of 0.342 d^{-1}.

Nevertheless, it must be noted that the high performance of a microalgal strain can only be achieved after optimisation of the growth medium and environmental conditions (such as CO_2 concentration, photobioreactor design as well as light intensity and duration) (Cheah *et al*., 2015). Variations in any of the environmental conditions would affect bio-fixation efficiency and hence biomass production.

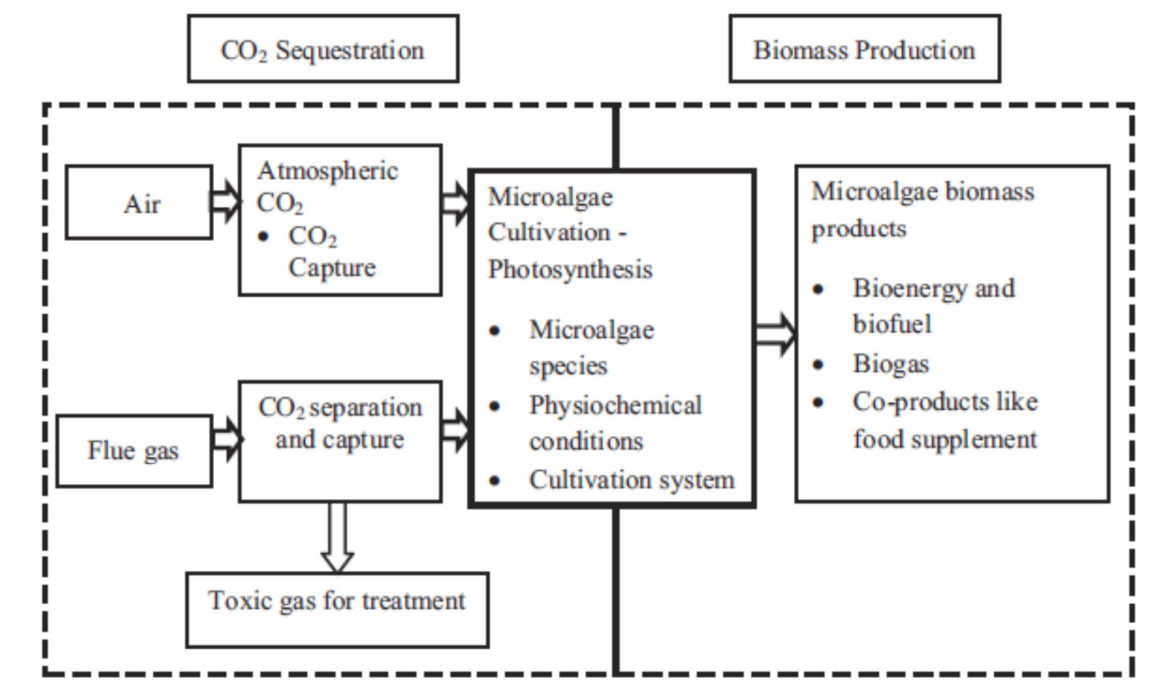

Figure 1: An illustration of the relationship between microalgal CO_2 sequestration and biomass production (Cheah *et al*., 2015).

2.6 STRATEGIES FOR ISOLATING HIGHLY CO_2 TOLERANT MICROALGAL STRAINS

For effective CO_2 sequestration using microalgae, the crucial step would be to search for, collect and identify hyper-CO_2-tolerant strains (Huang *et al*., 2010; Khan *et al*., 2009). Sampling for these microalgal strains is largely influenced by environmental factors as well as the aquatic system (Mutanda *et al*., 2011). Brackish aquatic environments appear to be ideal areas to sample for superior carbon sequesters as they are rich in dissolved CO_2, O_2 and dissolved salts. Also, most CO_2 sources, such as power plants, are located along coastal areas. Proper sampling techniques need to be in place in order to ensure success, as damaged or dead cells often lead to failure to cultivate microalgal strains. Temporal and spatial collection is often employed to offset any mishaps that may occur at the sampling site. The success of any microalgal mass culture

ultimately depends on fast-growing, productive strains that are adapted to the local climatic conditions (Mutanda *et al*., 2011).

It is imperative that certain factors are measured on-site so that these conditions can be simulated when culturing the specimens under laboratory conditions. Over the years, microalgal collection and selection processes have been well established. Sampling equipment should include a knife, mesh net, scooping jar, vessels for sample collection, scalpels, light meter, GPS, salinity meter and a multi-probe system (measuring pH, temperature, turbidity, conductivity and light intensity) (Mutanda *et al*., 2011). No definite sampling procedure has been recognised in literature. Researchers are encouraged to follow simple and cheap techniques when collecting microalgal samples (Mutanda *et al*., 2011).

Once samples are brought back to laboratories, microalgae are usually identified by means of microscope-based techniques. For species-level identification, conventional light microscopy has been extended to include fluorescence microscopy, phase-contrast microscopy, transmission electron microscopy (TEM) and scanning electron microscopy (SEM). Conventional microscope techniques, however, could often prove misleading in precise microalgal identification as many cell types lack morphological markers. Microalgae are also known to alter cell size and shape during their life cycle (Godhe *et al*., 2001; Mutanda *et al*., 2011). A proper identification is impossible as most microalgae fail to survive fixation or in some cases shrink, lose pigmentation and flagella. Microalgal identification from field samples using microscopy is also time-consuming and requires significant experience in technical and taxonomic skills. Molecular-based techniques developed in recent years have led to rapid and precise monitoring, identification and quantification of microalgal species. Commonly analysed DNA regions for phylogenetic purposes include mitochondrial genes, ribosomal RNA genes (rRNA), internal

transcribed sequences (ITS), plastid genes (rbcL) and microsatellite DNA sequences. Therefore, molecular-based techniques using species-specific molecular probes offer a powerful technology for rapid screening and identification of microalgal species when compared to conventional identification techniques (Mutanda *et al*., 2011).

2.7 PHYSICOCHEMICAL REQUIREMENTS FOR EFFECTIVE CO_2 CAPTURE AND BIOMASS PRODUCTION

After selecting a microalgal strain, the step to follow is appropriate cultivation of the organism. Artificial cultivation of microalgae ought to reproduce and enhance the optimum natural growth conditions (Brennan and Owende, 2010; Vasumathi *et al*., 2012). A successful microalgal cultivation system is one that is optimised and tightly controlled. Nutrients, light and CO_2 are essential requirements for microalgal growth (Zeng *et al*., 2011).

2.7.1 Growth Medium

An appropriate growth medium is one that provides sufficient nutrients to support microalgal growth. Carbon, nitrogen, phosphorus, and sulphur are the most important elements constituting microalgal cells. Other inorganic salts such as iron, magnesium and trace elements are essential but required in lesser amounts (Rebolloso-Fuentes *et al*., 2001; Zeng *et al*., 2011). For effective microalgal cultivation and CO_2 fixation a balanced growth medium is essential (Wang *et al*., 2008). Nutrient media formulations differ depending on the target product accumulation by microalgae. Lipids for biodiesel production are often the most desired, followed closely by proteins and some fatty acids for high value health care products (Zeng *et al*., 2011).

Optimal nutritional requirements can be determined by conventional or statistical methods. Conventional medium optimisation is achieved by the OFAT approach; whereby a single factor

is varied while keeping all others at a constant specific level. However, the OFAT approach can be tedious and time consuming. Furthermore, it does not take in account the interactions among all the factors involved. This can be attributed to the fact that it does not identify true optimal conditions as it does not take into consideration the interactive effects among the variables (Dobrev *et al.*, 2007; Mehta *et al.*, 2012; Silveira *et al.*, 2007).

In order to overcome the above-mentioned limitations, statistical approaches such as fractional factorial design (FFD) and response surface methodology (RSM) experiments can be applied to optimise media to improve biomass production. Fractional factorials are one of the most widely used screening experiments which can be applied to identify the important factors with the greatest effect. The final step is RSM which involves an experimental design such as central composite design (CCD) to fit a second-order polynomial by a least squares technique. It is used to evaluate the relationship between a response value and a set of design variables. More importantly, the purpose is to find the optimum conditions to maximise or minimise a given response. For one numeric variable, CCD has 5 levels ($-\alpha$, -1, 0, $+1$, $+\alpha$). An equation is used to describe the test variables, and describe the combined effect of all the test variables in the response (Burrows *et al*., 2008; Mehta *et al.*, 2012).

2.7.2 Light Requirement

Light is one of the most important requirements for microalgal growth as it provides the main source of energy. Even though microalgal cells require relatively lower light intensities compared to higher plants, microaglal metabolic rates can be enhanced with increasing light intensities (Zeng *et al*., 2011). For instance, *Chlorella* and *Scenedesmus* sp. often exhibit a saturating light intensity of $\pm$ 2 x 10^5 umol m^{-2} s^{-1} (Kumar *et al*., 2011-a). Some microalgal species are capable of growing successfully at both high light as well as low light intensities (Zeng *et al.*, 2011). For

example, *Chlorogleopsis* sp. displays high light adaptability, growing successfully under both low light (3.69 x 10^4 umol m^{-2} s^{-1}) and high light intensities (2.461 x 10^5 umol m^{-2} s^{-1}), with the optimum light intensity being ± 2 x 10^5 umol m^{-2} s^{-1}. During low light conditions microalgal species often switch from phototrophic to heterotrophic growth, while others grow mixotrophically. Genetic modifications that alter the size of the chlorophyll antennae can be investigated to modify the optimum light intensity for microalgal growth. This strategy could be used to increase microalgal biomass production when cultivated in indoor PBRs with flue gas CO_2 supplementation under periodic light provision (Zeng *et al*., 2011).

2.8 PROPAGATION SYSTEMS

Two systems that have been extensively proposed are based on open pond and closed PBR technologies (Brennan and Owende, 2010; Chisti, 2008; Molina *et al*., 2001; Suh and Lee, 2003). However, there is ongoing debate pertaining to which of the open pond or closed PBR would be a better system for CO_2 sequestration. Raceway ponds are the most commonly used artificial growth systems because they are cost-effective, but significant CO_2 losses to the atmosphere occur. Open systems are also known to utilise CO_2 much less efficiently than PBRs (Borowitzka, 1999; Brennan and Owende, 2010; Chisti, 2007).

Open ponds are typically constructed of a closed-loop, oval-shaped recirculation channels, generally between 0.2 and 0.5 m deep (Figure 2) (Brennan and Owende, 2010; Chisti, 2007). Mixing and circulation, which is required to stabilise microalgal growth and productivity, is maintained within the pond by a paddlewheel (Borowitzka, 1999; Brennan and Owende, 2010; Chisti, 2007). The paddlewheel is a continuous operation that prevents sedimentation. Flow can be guided around bends by baffles placed in the flow channel (Chisti, 2007). Open systems are built in concrete or compacted earth, and are usually lined with white plastic (Borowitzka, 1999;

Brennan and Owende, 2010; Chisti, 2007; Ugwu *et al*., 2008). For continuous production, microalgal media and nutrients are introduced in front of the paddlewheel and circulated through the loop to the harvest extraction point. Medium is harvested behind the paddlewheel, on the completion of the circulation loop (Chisti, 2007). In raceways, temperature fluctuates seasonally and cooling is solely achieved by evaporation. Considerable loss of water due to evaporation can occur. Due to significant losses to the atmosphere, raceway ponds are known to use CO_2 much less efficiently than PBRs (Chisti, 2007). Microalgae present in open ponds usually obtain their CO_2 requirements from dissolved surface air, but submerged aerators have been known to be installed to enhance CO_2 supply (Brennan and Owende, 2010).

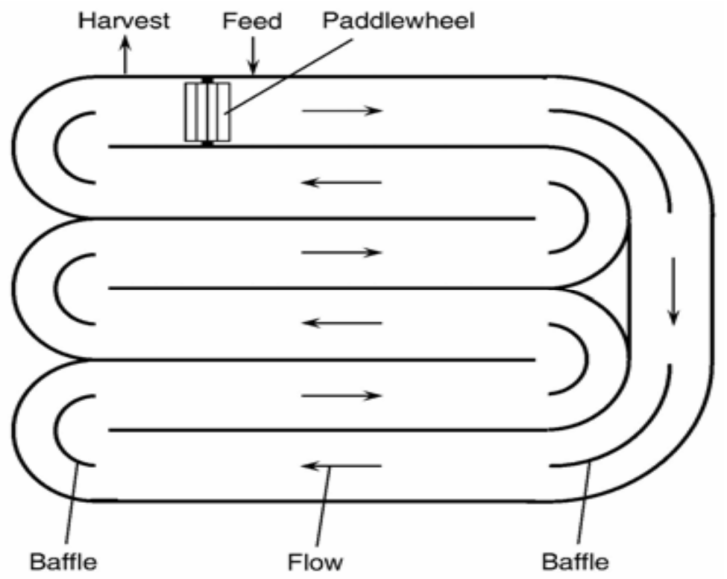

Figure 2: Aerial schematic of an open raceway pond showing feed and harvest points (Chisti, 2007).

Microalgal production using closed PBR technology has been implemented to overcome some of the key problems associated with the described open pond production systems. A major

advantage of PBRs when compared to open raceway systems is that they permit cultivation of axenic microalgal cultures for prolonged durations with lower risk of contamination (Brennan and Owende, 2010). Harvesting costs may also be significantly reduced owing to the higher cell mass productivities attained, and CO_2 is also utilised more effectively (Brennan and Owende, 2010; Chisti, 2007; Vasumathi *et al*., 2012). Despite the fact that a great deal of work has already been done to develop PBRs for microalgal cultures and effective CO_2 utilisation, more effort is still required to improve PBR technologies. Photobioreactor design and development is perhaps one of the first major steps that should be undertaken for efficient mass cultivation of microalgae for carbon mitigation (Ugwu *et al*., 2008). Light distribution and higher biomass productivities are more efficient in PBRs that have larger optical cross-sectional areas. Photobioreactors having specially designed light systems have been investigated for the effective CO_2 sequestration and biomass production (Lee, 2001). In 2003, Suh and Lee designed and operated an internally illuminated airlift PBR which was employed to study the light distribution in an attempt to maximise the photosynthetic efficiency and hence carbon uptake of a *Synechococcus* sp. A flat-plate PBR was constructed by Zijffers *et al*. (2010) in which sunlight was focused on the top of the reactor by dual-axis positioning of lenses. Solar radiation was captured by vertical plastic light guides and then distributed into the PBR. This design allowed for a more uniform distribution of light throughout the reactor and hence, more effective light utilisation (Kumar *et al*., 2011-a; Zijffers *et al*., 2010).

Volumetric gas transfer coefficient is another important characteristic that should be considered when designing reactors. Gas transfer and cell growth rates vary in different regions of liquid flow. Liquid flow within reactors is often divided into three regions: bubble flow, transitional flow and a heterogeneous zone. These zones are often dependent on gas velocity. The bubble flow region is an area in which gas hold-up, interfacial area as well as the volumetric gas transfer

coefficient is proportional to the gas superficial velocity. Increases in the gas transfer coefficient promote cell growth rate. However, toward the end of the transition zone, a reduction in growth rate can be observed. The drop in specific growth rate could be attributed to shear stress (Kumar *et al*., 2011-a). In 2002, Zhang *et al*. conducted a series of experiments to comparatively analyse gas transfer in different PBRs at various CO_2 percentages. They were able to conclude that the gas transfer coefficient increases with a decrease in the CO_2 concentration from the inlet gas stream.

A study by Borkenstein *et al*. (2011) investigated the cultivation of C. *emersonii* for 30 days using both flue gas and pure CO_2 in 5.5 l airlift PBRs. The experimental setup is shown in Figure 3. Results showed that the *Chlorella* sp. supplied with CO_2 containing flue gas produced a biomass yield of 2.00 g/l; when cultivated with pure CO_2, it yielded 2.06 g/l biomass. There was no significant difference in biomass yields. When supplied with flue gas, C. *emersonii* was able to grow as successfully as when supplied with pure CO_2. It can be concluded that the concentrations of the components within the flue gas together with the size and proximity of the culture vessel and characteristics of the microalgal species are imperative in developing an effective CO_2 remediation technology.

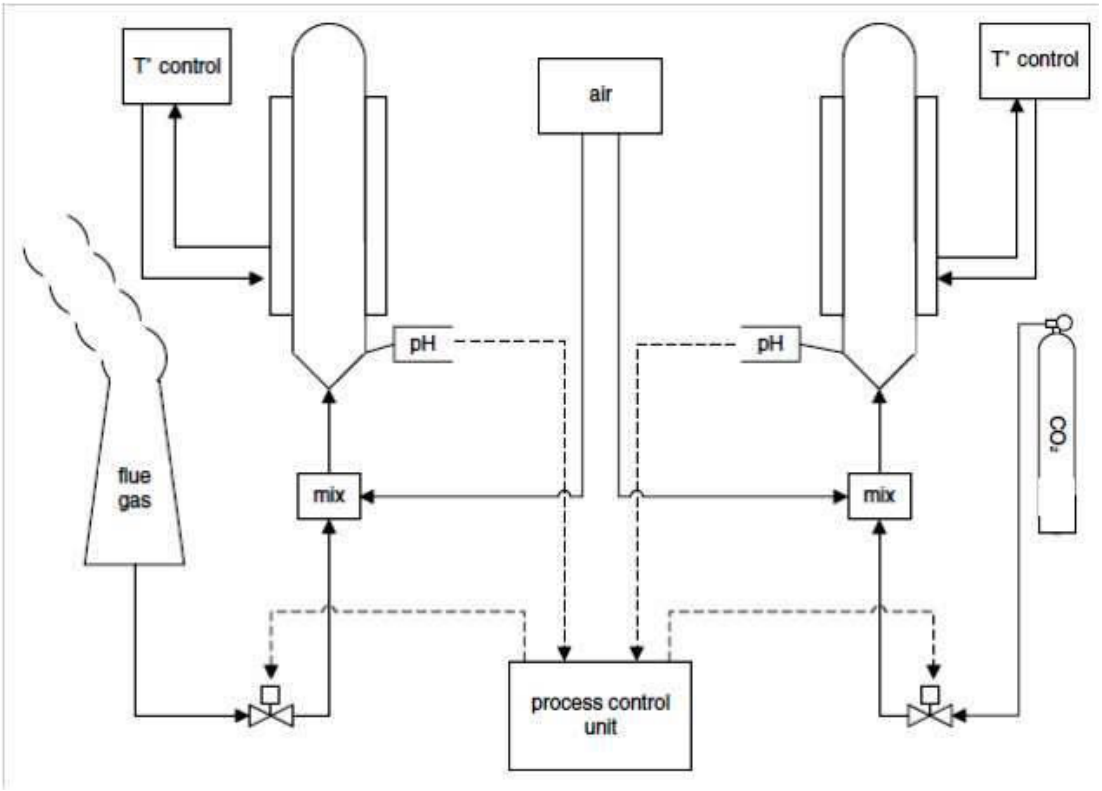

Figure 3: Schematic representation of an airlift photobioreactor for flue gas sequestration (Borkenstein *et al*., 2011).

2.9 SOLUBILITY AND SPECIATION OF CO_2

Carbon dioxide does dissolve in an aqueos medium, however the system is somewhat complex. The solubility and speciation of CO_2 in the medium is dependent on pH, temperature and nutrient concentration. Henry's law states that CO_2 dissolves in water to an extent determined by its partial pressure (PCO_2), temperature, as well as the interaction of dissolved CO_2 with other solutes in the water (Carroll and Mather, 1992). Carbon dioxide solubility is known to increase with increasing pressures and decrease with increasing temperatures. Due to the thermodynamics of the reaction, CO_2 becomes more soluble at lower temperatures. Solubility of CO_2 in freshwater is also significantly higher as opposed to solubility in salt water (Carroll and Mather, 1992). This

is owing to the fact that NaCl promotes a salting out effect on the CO_2 solubility in water, thereby decreasing its CO_2 solubility in sea water when compared with freshwater. The salting out effect is dependent on many factors, such as: salt concentration, temperature, the ions charge as well as on the radius static dielectric constant of the solvent. Interactions between the ions and the solute are partially shielded by formation of the hydration shell and this in turn influences the solvation energy and ultimately the gas solubility (Carvalho *et al*., 2015).

The two-film theory states that mass transfer of CO_2 to the cell phase from the gas phase transpires through sequential stages, but is mostly defined by the gas-liquid stage (Hende *et al*., 2012). Carbon dioxide mass transfer rate (N_{CO2}) can be expressed using the following equation:

$$N_{CO_2} = k_L \alpha \left(C_{CO_2 L} * - C_{CO_2 L} \right)$$

(Eq. 1)

Where:

k_L represents the liquid-phase mass transfer coefficient; α the specific area available for mass transfer; C_{CO2L}^* is the CO_2 concentration available in the liquor that is responsible for equilibrating its actual partial pressure on the gas side; while C_{CO2L} is the actual CO_2 concentration in the liquor (Hende *et al*., 2012; Markle, 1977).

Various methods that involve increasing k_L and/or α have been suggested for enhancing the N_{CO2}. Some commonly employed techniques involve air-lift bubble columns, stirring, microporous hollow-fibre membranes, as well as gas injection and gas recirculation methods (Hende *et al*., 2012). When compared to O_2, the gas-liquid transfer of CO_2 from flue gases is considerably faster. This can be attributed to the relatively high solubility of CO_2 (1.496 g/CO_2/l in water at 25°C and 1 atm: this is over 100 times greater than that of O_2). Carbon dioxide solubility is

largely dependent on temperature, pH and salt concentrations (Liu and Liu, 2011). Carbon dioxide reacts through a set of chemical equilibria when it dissolves in an aqueous medium.

The main pathway at a pH lower than 8 is direct hydration (with pK at 25 °C; 1 atm) (Hende *et al*., 2012; Housecroft and Sharpe, 2005). In this reaction the hydration of CO_2 is slow (Reaction 4), while the dissociation of carbonic acid is so rapid that H_2CO_3, HCO_3^- and CO_3^{2-} are in equilibrium (Hende *et al*., 2012).

$CO_{2(g)} > CO_{2(aq)}$ $(pK = 1.468)$……..Reaction 1

$CO_{2(aq)} + H_2O > H_2CO_3^*$ $(pK = 2.840)$……..Reaction 2

$H_2CO_3^* > HCO_{3(aq)}^- + H^+$ $(pK = 6.352)$…….Reaction 3

$HCO_{3(aq)}^- > CO_{3(aq)}^{2-} + H^+$ $(pK = 10.329)$……..Reaction 4

(Eq. 2)

At pH levels above 10, the main pathway involves the attack of hydroxide ions (Hende *et al*., 2012; Housecroft and Sharpe, 2005).

From the information presented above it can be deduced that the solubility of CO_2 in an aqueous medium is largely dependent on temperature and pH. A pH range of 6 - 9 would be optimal for microalgal cultivation with CO_2 aeration. A pH value lower than 6 would lead to a slower rate of CO_2 dissolution, whereas pH values higher than 9 would result in an accumulation of carbonate.

2.10 MICROALGAL SPECIES EMPLOYED FOR CARBON BIO-MITIGATION

Ambient CO_2 levels are generally low (approximately 0.036%) when compared to industrial areas, which release large amounts of flue gases into the atmosphere. Carbon dioxide concentrations present in flue gases vary from industry to industry, but are normally within the range of 3 - 30%. Microalgae are able to fix CO_2 from a range of sources, such as the atmosphere, industrial exhaust gases (flue and flaring gas) as well as in the form of soluble carbonates ($NaHCO_3$ and Na_2CO_3) (Wang *et al*., 2008).

Carbon dioxide is an essential nutrient for all photosynthetic life forms. Terrestrial plants naturally capture and utilise CO_2 from the atmosphere. Microalgae, however, possess a greater capacity to fix CO_2 (Kumar *et al*., 2011-b). This can be attributed to their photosynthetic apparatus and chlorophyll being present within a single microalgal cell permitting rapid biomass generation. Listed below in Table 2 are some advantages of using microalgae over higher plants for CO_2 sequestration.

In the context of propagation, atmospheric CO_2 (0.036%) is most often not sufficient to support microalgal growth as microalgae requires an enriched point source of carbon. Due to this, biofixation of CO_2 from power plants and other point sources using microalgae has emerged as a likely alternative to combat the growing concerns of global warming due to CO_2 emissions (Ho *et al*., 2011; Kumar *et al*., 2011-a and b).

Table 2: Advantages of using microalgae as opposed to terrestrial plants for CO_2 biofixation

Factors	Microalgae	Terrestrial plants	References
Resilience to adverse climatic conditions	High	Low	Mata *et al*., 2010
Conventional agricultural food production	No competition	Direct competition	Demirbas and Demirbas, 2011; Radakovits *et al*., 2010
Photon conversion efficiencies	High (8 - 10%)	Low (0.5%)	Aresta *et al*., 2005; Sharma *et al*., 2011
CO_2 fixation efficiency	High	Low	Kumar *et al*., 2011-b
Growth rate	Rapid	Slow	Greenwell *et al*., 2010; Mata *et al*., 2010
Production and harvesting	All year round	Seasonal	Kumar *et al*., 2011-b
Acid deposition	None	Fair	Sharma *et al*., 2011
Scale-up	Easy	Difficult	Clarens *et al*., 2010
Carbon rich biomass	High	Low	Chisti, 2007
Cultivation costs	Low	High	Kumar *et al*., 2011-b
Direct CO_2 sequestration from power plants	High	Low	Ho *et al*., 2011

An increase in the maximum growth rate of microalgal species due to higher CO_2 concentrations has been investigated by many researchers (Cheng *et al*., 2006; Ho *et al*., 2011; Kumar *et al*., 2011-b; Lopez *et al*., 2010-a; Ono and Cuello, 2006). Microalgal-CO_2 fixation occurs via photoautotrophic growth. Therefore, the CO_2-fixation potential of microalgal species should positively correlate with their light utilisation efficiency and cell growth rate. Increases in temperature (> 20°C) can cause significant reduction in CO_2 solubility, which eventually leads to a decline in the photosynthetic efficiency.

Strains often favoured are those that can directly utilise CO_2 from industrial flue gas, those that grow well under natural day-night cycles, strains with high productivities that are easy to harvest and most importantly those that produce biomass that can be used in the production of desirable co-products. Unfortunately, it is rare for a single microalgal strain to possess all these attributes. Most often, a highly productive strain functions poorly in dense mass culture, while a robust strain could have low growth rates (Farrelly *et al*., 2013). In recent years, there has been talk of genetically manipulating microalgal strains to enhance their properties pertaining to carbon mitigation and mass culture (Farrelly *et al*., 2013). Over the years, research has largely focused on single effective carbon sequesterers and efforts to upscale these strains for mass culture. However, it would appear that a more effective approach would be to isolate strains from nature that thrive in mass culture, and subsequently manipulate these strains to grow in dense culture while altering their physiology to increase their productivity and ease of harvesting (Farrelly *et al*., 2013). Microalgae and cyanobacterial species routinely used for CO_2 mitigation include *Anabaena* sp., *Botryococcus braunii*, *Chlamydomonas reinhardtii*, *Chlorella* sp., *Chlorocuccum littorale*, *Scenedesmus* sp., and *Spirulina* sp. (Chen *et al*., 2010; Chiang *et al*., 2011; de Morais and Costa, 2007; Ho *et al*., 2011; Ota *et al*., 2009; Packer, 2009). Table 3 represents commonly employed carbon sequesters cultivated in different bioreactors.

Green microalgae that are effective carbon sequesters generally belong to the genera *Chlorococcum*, *Chlorella*, *Scenedesmus* and *Euglena*. In 1970, Seckbach and Libby isolated species from the aforementioned genera that were able to survive after exposure to pure (100%) CO_2. Experiments on the *Scenedesmus* sp. revealed that this strain thrived under 100% CO_2 concentration and cell concentration increased for up to 30 days, reaching 3.65 g/l. This was a considerable increase in cell concentration, when compared to the 1.19 g/l obtained under atmospheric CO_2 conditions (0.036%). *Chloroccum littorale* represents a fast-growing species

that is able to tolerate high CO_2 concentrations. In another experiment, Seckbach and Libby (1970) demonstrated that C. *caldarium* could tolerate 10 atm of CO_2 but not 50 atm of CO_2. They were able to conclude that growth was inhibited due to the effect of high CO_2 concentrations and not due to the high pressure. These species, however, are known to have low growth rates, and therefore, productivity and CO_2 recovery were found to be low (Satoh *et al*., 2001).

A *Chlorella* Tx 71105 strain was supplied with pure CO_2 at a rate of 3.3 mL min^{-1} over a 28-day period. During the first six days, the effluent gas contained more than 96% O_2. On the 12th day of cultivation, a spike in temperature from 37 to 39°C was observed. On the 13^{th} day, a 32% CO_2 concentration was noted in the effluent gas. The gas flow was then turned off for 3.5 h. Upon re-addition of CO_2, the effluent gas then contained 97.8% O_2. During the last six days, no alterations were made to the experiment, and over this period, it was noted that the effluent gas contained 18% CO_2. When this strain was cultured under 41, 71 and 100% CO_2, the mean biomass concentration recorded was 3.15, 2.71 and 2.49 g/l/day, respectively. These cell concentrations are reasonably similar to those obtained with other *Chlorella* species (Table 3) (Geckler *et al*., 1962).

Zhao *et al*. (2011) did a comparative study of the growth and CO_2 biofixation of a *Chlorella* sp. under closed and open cultivation modes. Findings showed that closed cultivation substantially enhanced microalgal performance with regard to growth and carbon biofixation. Specific growth rate and CO_2-fixation rate during closed cultivation were observed to be 1.78 and 5.39 times higher that of open cultivation, respectively. Closed systems also allow for effective gas bubble motion, which plays a vital role in reducing dissolved O_2 build-up. Under the proper cultivation mode, *Chlorella* sp. exhibited greater potential as an effective carbon sequester.

A study by Kurano *et al*. (1995) showed that *C. littorale* was able to reach a maximum cell concentration of 4.9 g/l at a 20% CO_2 concentration. When exposed to CO_2 concentrations of more than 20%, a short lag phase was observed prior to active photosynthesis. It must be noted that the performance of microalgal strains does not solely depend on CO_2 concentrations, but also on culture and experimental conditions, such as culture medium, temperature, light intensity as well as reactor design. Variation in any of these conditions could have an effect on the CO_2-fixation efficiency of the strains (Ho *et al*., 2011).

Table 3: Commonly employed microalgal species used for CO_2 sequestration under varying cultivation modes

Strain	Propagation system	Temperature (°C)	pH	Light intensity	Supplied CO_2 (%)	Growth rate (g/l/day)	CO_2 fixation rate (g/l/day)	CO_2 fixation efficiency (%)	Ref[d]
Chlorella sp.	Open pond	30	10	30[a1]	10	-	-	46	1
Chlorella sp.	PBR	26	-	-	2	1.21	0.261	58	2
Chlorella kessleri	Conical flask PBR	30	-	-	0.038	0.090	-	-	3
Chlorella vulgaris	Tubular PBR	25	-	-	0.036	0.4	0.075	-	4
Chlorococcum littorale	Flat-plate reactor	25	6.1.7.2	2000[a1]	5	-	200.4[b1]	-	5
Dunaliella tertiolecta	Bubble column reactor	25	7.2±0.2	3500[a2]	5	-	0.271	-	6
Dunaliella sp.	PBR	3	-	-	27	0.17	0.313	-	7
Botryococcus braunii	Bubble column reactor	25	7.2±0.2	3500[a2]	5	-	0.497	-	6
Scendesmus obliquus	Tubular PBR	30	-	-	6	0.10	-	28.08	8
Scendesmus obliquus	Tubular PBR	30	-	-	12	0.14	-	13.56	8
Nannochlorophsis oculata	PBR	26	-	-	15	0.372	0.393[b2]	15	9
Haematococcus pluvialis	Tubular PBR	16-18	-	-	0.036	0.076	0.143	-	10
Aphanothece m. Nageli	Air-lift Reactor	25	6.8	150[a1]	15	-	14.5	-	11
Aphanothece m. Nageli	Bubble column reactor	35	-	11.000[a2]	15	-	2.621	-	12
Thermosynechococcus sp.	Bubble column reactor	55	-	10.000±350[a2]	10	2.7	-	-	13
Spirulina sp.	Tubular PBR	30	-	-	12	0.33	-	45.61	7
Spirulina platensis	Open pond	30	10	30[a1]	10	-	-	39	1
Anabaena sp.	Bubble column reactor	27	8.5	900[a3]	0.036	-	1.45	-	14
Chlorogleopsis sp.	PBR	50	-	-	5	-	20.45[b3]	-	15
Synechococcus sp.	Air-lift reactor	30	6.8	8000[a2]	5	-	0.6	-	16

[a1] µmol m^{-2} s^{-1}

[a2] lux

[a3] µ$Em^{-2}s^{-1}$

[b1] g $m^{-2}d^{-1}$

[b2] g/h

[b3] mgC/l/d

[d] Ref : 1-(Ramanan *et al*., 2010); 2-(Chiu *et al*., 2008); 3-(de Morais and Costa, 2007); 4-(Scragg *et al*., 2002); 5-(Hu *et al*., 1998); 6-(Sydney *et al*., 2010); 7-(Wang *et al*., 2008); 8-(de Morais and Costa, 2007); 9-(Chiu *et al*., 2009); 10-(Huntley and Redalje, 2007); 11-(Jacob-Lopes *et al*., 2009); 12-(Jacob-Lopes *et al*., 2008); 13-(Hsueh *et al*., 2009);14-(Lopez *et al*., 2010-a); 15-(Ono and Cuello, 2007); 16-(Heasman *et al*., 2000).

2.11 PHYSIOLOGICAL PATHWAY INVOLVED IN THE BIOCHEMISTRY OF CO_2 FIXATION

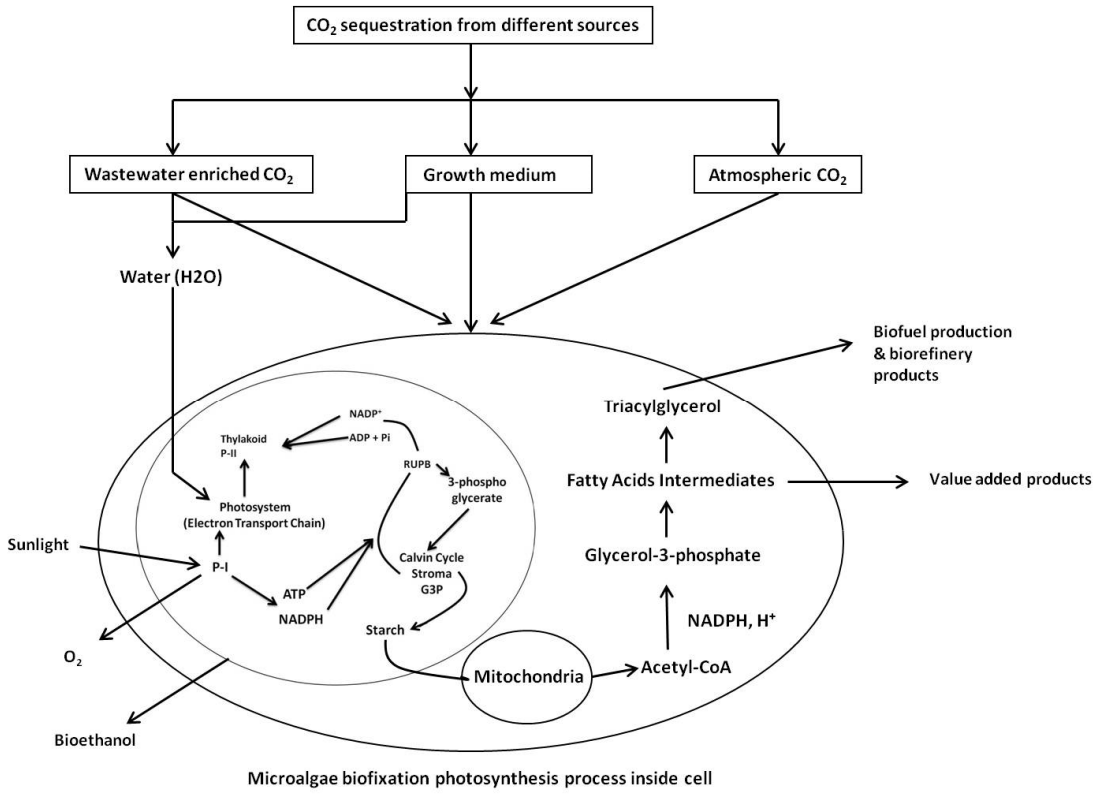

Figure 4: Microalgal photosynthesis: modified from Zeng *et al*., 2011.

Photosynthesis (Figure 4) within microalgae cells occurs in two stages. The first stage involves light-dependent or light reactions that only take place when cells are illuminated. This step exploits light energy to form the energy-storage molecules adenosine triphosphate (ATP) and nicotinamide adenine dinucleotide phosphate (NADPH). Carbon-fixation or dark reactions that form the second stage of photosynthesis transpire both in the presence and in the absence of light. Energy-storage products generated during light reactions are used at this step to capture and reduce CO_2 (Calvin, 1989).

Photosystem I (PSI) and photosystem II (PSII) are major photoactive complexes responsible for transferring sunlight into the electron transport chain via the excited chlorophyll dimer (Calvin, 1989; Ho *et al*., 2011; Iverson, 2006). Photosynthesis begins in the PSII complex. Once a chlorophyll molecule at the core of the PSII complex attains ample excitation energy, an electron is transferred to the primary electron acceptor molecule. This process is often termed photo-induced charge separation. Electrons are then transported across the membrane through an electron transport chain. Photosystem I accepts the electrons transferred from PSII and transports them via the P700 dimer of chlorophyll, which is oxidised from light-excited antenna chlorophyll to strongly reducing ferredoxin and NADPH (Cerveny *et al*., 2009; Ho *et al*., 2011). Energy harvested via the light reaction can be stored by the formation of ATP during photophosphorylation (Yang *et al*., 2000). Research has concluded that 1.3 ATP molecules are formed per pair of electrons moving through the photosynthetic electron transport chain (Yang *et al*., 2000). Nicotinamide adenine dinucleotide phosphate that is the main reducing agent in chloroplasts is responsible for supplying electrons to fuel other reactions. Due to its formation, a deficit of electrons exist in the chlorophyll of PSI. These electrons are replaced from the electron transport chain by plastocyanin (Yang *et al*., 2000).

Carbon-fixation reactions (dark reactions) involve the Calvin cycle (Calvin, 1989; Iverson, 2006; Yang *et al*., 2000). During the Calvin cycle, CO_2 is converted into carbohydrates with the aid of ATP by the carboxylase activity of the enzyme RuBisCO (Ribulose 1, 5-bisphosphate carboxylase/ oxygenase). Ribulose 1, 5-bisphosphate carboxylase/oxygenase that has low affinity for CO_2 also carries out oxygenase activity and produces glycolate 2-phosphate as an end product. This end product is of no use to the cell and its synthesis consumes considerable amounts of cellular energy. It is also responsible for releasing previously fixed CO_2 by the

carboxylase activity of RuBisCO. The oxygenase activity of RuBisCO can hinder around 50% of biomass formation (Giordano *et al*., 2005; Kumar *et al*., 2011-b).

As mentioned previously, light supply (light intensity and duration) is a key variable that greatly impacts the photosynthetic activity and hence growth kinetics of microalgae. Culture systems are illuminated by sunlight, artificial light or a combination of both. Light/dark cycle durations also play a significant role in microalgal growth (Pires *et al*., 2012). Grobbelaar *et al*. (1996) used a *Scenedesmus obliquus* strain to demonstrate that photosynthetic rates increase exponentially with increasing light/dark frequencies. Research suggests that microalgal cells associate a low light/dark cycle with low light conditions and vice versa. It was also observed during this study that the microalgal cells became increasingly more proficient in the overall exploitation of light energy during a longer dark phase relative to light phase. However, it must be noted that a relatively longer dark phase did not necessarily achieve higher photosynthetic rates nor did the microalgal cells acclimatise to a precise light/dark cycle. High photon flux densities over a long duration of time eventually led to damage to protein D1 in PSII. Damage to protein D1 led to poor trapping of photons. This then causes an overall reduction in the photosynthetic activity. During the dark phase, the photo-induced damage can be repaired by the algae. Airlift and flat panel reactors are extremely beneficial in this regard, allowing cells to experience adequate amounts of shading in which time they are able to repair damage to PSII. Within airlift reactors, light flux decreases exponentially with the distance from the irradiated surface. As a result of this, cells near the irradiation source are exposed to a high photon density when compared to cells at the centre. These cells at the centre receive less light owing to shading. Photosynthesis can be measured as rates of carbon accumulation or O_2 evolution. Either measurement can be converted into the other using the photosynthetic quotient (Pires *et al*., 2012).

The influence of photoperiods on the rates of CO_2 sequestration was also studied by Jacob-Lopes *et al*. (2010) using a cyanobacterial strain in both BGN medium and refinery wastewater. A linear decrease in biomass productivity was observed during a longer dark period in BGN medium. A photosynthetic quotient of 0.74 was achieved using refinery wastewater as the growth medium. This essentially means that 1 g of CO_2 consumed corresponds to the release of 0.74 g of O_2. From this study, it can be concluded that the gas-exchange pattern within a system is greatly influenced by the intermittent light cycle. During dark periods, microalgal cells consume organic carbon through heterotrophic metabolism and release CO_2 in the process. Microalgal growth can, therefore, be enhanced through sequential changing in the light intensity. Furthermore, it is imperative that irradiance be regulated according to the culture density. Low culture densities exposed to high light intensities would lead to photoinhibition of cells; and at high culture densities, light penetration becomes the limiting factor. Studies have also suggested that growth under red light (600 - 700 nm) enhanced PSII relative to PSI, whereas blue light (400 - 500 nm) could induce PSI. These findings suggest that blue and red light are more suitable than others for both microalgal cell growth and CO_2 mitigation (Ravelonandro *et al*., 2008; You and Barnett, 2004).

Microalgae possess a unique, inherent ability of accumulating large quantities of inorganic carbon in their cytoplasm. These concentrations are usually several orders of magnitude higher when compared to that on the outside. This system is called a CO_2-concentrating mechanism (CCM). Carbonic anhydrase (CA) is an important metalloenzyme present on the surface of microalgal cells that participates in the CCM. This enzyme is of fundamental importance as it is responsible for the delivery of CO_2/HCO_3 across cellular membranes by the following reversible reaction (Kupriyanova *et al*., 2017):

$$CO_2 + H_2O \leftrightarrow H^+ + HCO_3^-$$ (Eq. 3)

Owing to the fact that CA is one of the fastest enzymes, it allows for multiple acceleration inter-conversions of CO_2/HCO_3. The catalysis reaction involves two stages. During the first stage the metal hydroxide derivative (which is a strong nucleophile) present in the active site of the enzyme attacks a CO_2 molecule converting it to HCO_3^-. This step allows the bicarbonate ion to become associated with Me^{2+} (Eq. 4) (Kupriyanova *et al*., 2017). Thereafter, the bicarbonate ion is replaced with a water molecule and released into solution. This leads to the generation of an inactive acid form of the enzyme, together with water bound to Me^{2+}.

$$E - Me^{2+} - OH^- + CO_2 \leftrightarrow E - Me^{2+} - HCO_3^- \leftrightarrow E - Me^{2+} - H_2O + HCO_3^-$$ (Eq. 4)

The second stage involves ionisation of the water bound Me^{2+} and transfer of a proton from the active site to the external buffer which results in regeneration of the active basic form of the enzyme.

$$E - Me^{2+} - H_2O \leftrightarrow E - Me^{2+} - OH^- + H^+$$ (Eq. 5)

The CCM maintains a high concentration of CO_2 molecules near Rubisco. Inorganic carbon uptake systems assist this mechanism by generating an intracellular pool of bicarbonate, which is then rapidly converted into CO_2 by CA near the active site of Rubisco. The CCM only requires the presence of one CA (Kupriyanova *et al*., 2017).

Carbon dioxide concentration is an important factor for photosynthesis. Too high a concentration would increase the CO_2 mass transfer mechanism from the gas mixture to the medium, resulting in a pH drop. This sudden reduction in pH hinders the growth of most microalgal species. Flue gases typically contain very high concentrations of CO_2 (sometimes even greater than 30%). It should also be noted that another key inhibitor of microalgal growth is the O_2 produced during photosynthesis. It is imperative that this gas be removed routinely and not be allowed to accumulate within the system (Pires *et al*., 2012).

Numerous studies have been documented on improving the CO_2-fixation rate via the Calvin cycle, PEP carboxylase and/or through synthetic pathways (Gimpel *et al*., 2013; Rosgaard *et al*., 2012). These efforts have met with varying degrees of success. They can broadly be classified into these categories: engineering of RuBisCO for increased catalysis rates of carboxylation and reduction of the oxygenation reaction, enhancing the activation state of RuBisCO, enhancing the regeneration phase of the Calvin cycle and CO_2 enrichment around RuBisCO in an effort to inhibit the oxygenase reaction. Findings from most of these studies indicate that the challenge lies in the activity of RuBisCO for carbon flux through the Calvin cycle when CO_2 is not supplemented in the medium, or under conditions of high temperature/light. *Chlamydomonas reinhardtii* strains are RuBisCO deficient and are able to complete their life cycle heterotrophically. This makes them ideal candidates for engineering of RuBisCO. *Chlamydomonas* sp. containing varying amounts of RuBisCO have been engineered for the effective utilisation of energy, carbon and nitrogen. This has been achieved using the nuclear genome of a MRL1-deficient strain and expressing the rbcl mRNA maturation factor MRL1 at different levels. When compared to the wild type, results for the deficient strain showed that RuBisCo could maintain phototrophic growth even when it was lowered up to 15%. These findings suggest that based on the culture conditions (light intensity

or CO_2 concentration), an inducible promoter for MRL1 could effectively be applied to modify RuBisCo mediated CO_2 accumulation (Gimpel *et al*., 2013; Rosgaard *et al*., 2012).

2.12 INFLUENCE OF FLUE GAS COMPOSITION ON MICROALGAL CULTIVATION

The ability of microalgae to utilise CO_2 from flue gas and thereby mitigate the amount of carbon discharged into the atmosphere is an attractive idea. However, there are several major challenges that need to be addressed before this idea can be implemented:

When compared to atmospheric air, CO_2 is an effective supplement to stimulate microalgal growth. However, at high concentrations of CO_2 (> 5%), microalgal growth can be suppressed. This is often attributed to acidification of the cellular content which eventually hinders growth (Lee and Lee, 2003). A study by Watanabe *et al*. (1992) showed that strains that grew well at CO_2 concentrations between 5 and 10% had drastic decreases in their growth rate above CO_2 concentrations of 20%. At elevated CO_2 concentrations, pH can drop down to 5 or even lower due to the formation of high amounts of bicarbonate buffer. This environmental stress causes a biological reduction in the capacity of microalgal cells to sequester CO_2. Slight decreases in pH due to increased CO_2 concentrations usually have a minor impact on microalgal growth. Strong pH changes, however, could inhibit all growth (Kumar *et al*., 2011-b). Considering that flue gas usually contains between 3 and 30% CO_2, it is imperative to identify strains capable of growing under very high CO_2 concentrations. Screening studies have yielded strains that grow well in CO_2 concentrations between 30 and 70% (Hanagata *et al*., 1992; Iwasaki *et al*., 1996; Sung *et al*., 1999). Findings by Olaizola (2003) indicate that microalgal growth may even be sustained at a 100% CO_2 concentration by controlling changes in pH and only releasing CO_2 to the microalgae on demand.

Flue gases are often made up of CO_2, water vapour, NO_x, SO_x and heavy metals such as nickel, vanadium and mercury (Packer, 2009). Carbon dioxide is a major component of industrial flue gases. Table 4 shows the approximate global CO_2 flue gas emissions per industrial sector. The use of flue gas to culture microalgae is advantageous in that a carbon-free nutrient medium could be used as the carbon requirement will be provided for by CO_2. Pre-treatment costs could be minimimed by direct utilisation of flue gas; however, this would depend on the presence and quantities of the aforementioned components (Benemann, 1993; Ono and Cuello, 2007). Some researchers argue that the presence of NO_x in flue gases pose little or no problem to microalgal growth, while the difficulty arises in the presence of SO_x, which decreases the pH due to the formation of sulphurous acid (Kumar *et al*., 2011-a and b; Maeda *et al*., 1995; Packer, 2009). Others, however, further argue that some strains are not inhibited by CO_2 with < 50 ppm SO_x, but can be inhibited by CO_2 when NO_x are also present (Ho *et al*., 2011; Lee *et al*., 2002; Negoro *et al*., 1993). Therefore, denitrification and desulphurisation along with cooling and dedusting represent scrubbing options that may be necessary for pretreatment of flue gases. It should also be noted that nickel concentrations above 1 and 0.1 ppm of vanadium decrease microalgal productivity while mercury can be remediated by certain microalgal species (Hende *et al*., 2012; Packer, 2009). A few tolerant microalgae exist: *Dunaliella tertiolecta* (Nagase *et al*., 1998), *Tetraselmis* sp. (Matsumoto *et al*., 1995), *Chlorella* sp.T-1 and *Chlorella* sp. HA-1 (Maeda *et al*., 1995) are capable of growing at NO_x concentrations of up to 300 ppm. In these cases, excess NO is absorbed by the cultivation medium and transformed to NO_2, which is then further utilised as a nitrogen source by the microalgae. Therefore, it must be noted that the tolerance of microalgae to NO_x and SO_x varies depending on the species. By buffering the medium, pH drops could be prevented leading to little or no changes in growth rates (Hende *et al*., 2012; Kumar *et al*., 2011-b).

Table 4: Approximate annual global CO_2 flue gas emissions per industrial sector (Kuramochi *et al*., 2012)

Industrial sector	Worldwide CO_2 emissions (Gt/year)
Iron and steel manufacturing	2.3
Petroleum refineries	1.0
Cement production	2.0
Chemical and petrochemical	1.3

Thermal stability is another essential characteristic required by microalgal strains involved in CO_2 sequestration. Flue gas temperatures are extremely high (around 120°C) and could have an adverse effect on cells when introduced to the system (Kumar *et al*., 2011-b; Ono and Cuello, 2007). Therefore, the feasibility of sequestering CO_2 from flue gas would either depend on using thermophilic microalgal species or installing a heat-exchange system. Over the years, numerous species capable of tolerating temperatures up to 60°C have been identified. Miyairi (1995) studied the effects of various CO_2 concentrations at different temperatures on the growth of the cyanobacteria *Synechococcus* elongates. The study revealed that a drop in pH at 52°C with 60% CO_2 was comparable to a drop in pH at 25°C with 20% CO_2. These findings suggest that the temperature-dependent solubility of CO_2 gives an advantage to the thermophilic microalgae, enabling them to endure a higher concentration of CO_2. As temperature increases so too does the ratio of O_2 to CO_2 solubility. This leads to considerable O_2 fixation by the oxygenase activity of RuBisCO. Increases in temperature also lead to a decrease in RuBisCOs affinity for CO_2 (Kumar *et al*., 2011-b).

Light is one of the principal requirements for photosynthesis. The relationship between light and photosynthesis can be illustrated using the photosynthesis-irradiance response (P-I) curve, which has three distinctive regions: light-limited photosynthesis, light-saturated photosynthesis

and photoinhibition (Ralph and Gademann, 2003). For effective CO_2 fixation leading to biomass production, optimum light intensity is required. Light becomes the limiting factor for microalgal cultivation when it is below the optimum, while exposure of cells to a high light intensity over long periods of time leads to photoinhibition. Photoinhibition is due to damage to the repair mechanism of PSII, which leads to the inactivation of other systems (electron carriers, oxygen evolving systems and the related D1/D2 proteins). Light intensity is dependent on wavelength, cell concentration and the penetrating distance of light as well as the geometry of the system (Kumar *et al*., 2011-a, b and c).

2.13 CHALLENGES AND ECONOMICS ASSOCIATED WITH MICROALGAL CO_2 SEQUESTRATION

There are numerous hurdles that need to be overcome before microalgae can be employed to significantly reduce CO_2 emissions at a commercial level. Strain selection and design of the culturing system are key factors in maximising CO_2 mitigation rates. Even though open systems are much more cost-effective compared to closed PBRs, it is difficult to maintain culture purity in such systems. Closed systems are efficient vessels for sustaining axenic cultures as well as minimising CO_2 losses to the atmosphere. However, cleaning and sterilising of large-scale PBRs is difficult, and this then poses a problem in the production of high value-added products. Land availability for set-up of propagation vessels also becomes a problem in developing countries. For example, Kadam (2001) demonstrated that 1,000 ha of land area will be required for the construction of open ponds to mitigate CO_2 emissions from a 50-MW power plant. Carbon-fixation rates for microalgal cultures differ under varying operational conditions. Preliminary ideas of these values are required so as to estimate space requirements for reactor implementation for effective CO_2 fixation. A Portuguese cement industry annually produces ± 450 kt of CO_2. If two types of reactors (open ponds and light-diffusing optical fibre reactors)

are considered for the effective sequestration of CO_2 emitted from this industry, the estimated space required would be very different. Studies showed that under natural day/night cycles, a 4,000 m^3 pond could sequester up to 2.2 kt of CO_2 per year. If ponds were to be scaled up to a height of 30 cm (to prevent dark zones), open ponds occupying an area of 2.72 X 10^6 m^2 would be required to sequester almost all the CO_2 from this cement company. Carbon dioxide-fixation rates for light-diffusing optical fibre reactors were reported to be 4.44 g L^{-1} d^{-1}. Therefore, a reactor height of 1 m and a culturing area of 2.78 X 10^5 m^2 would be needed to effectively sequester CO_2 from this cement plant (Pires *et al*., 2012; Stewart and Hessami, 2005).

Geographical considerations must also be taken into account: fluctuations in temperature and solar irradiation over the seasons. Tropical areas are often considered most suitable for microalgal cultivation. To maximise the overall economic and environmental efficiency of microalgal CO_2 sequestration, culturing systems should be located as close as possible to the point source. Furthermore, a comprehensive plan should be compiled for the large-scale production of microalgae. This scheme should encompass modeling and LCA of the overall process. Failure in doing so could render many algal production systems unsustainable. It should also be noted that potential leaks from large-scale algal systems could cause ecological damage by eutrophication (Farrelly *et al*., 2013; Pires *et al*., 2012).

Bio-mitigation of carbon at large scale may entail the cultivation of non-transgenic as well as transgenic microalgae. Even under the best of conditions, minor releases of microalgae into the surrounding environment is bound to occur. While natural disasters would lead to massive releases. Very little has been discussed in literature pertaining to minor or massive spills, especially those involving large amounts of non-transgenic microalgae. Possible risks from non-transgenic strains should be taken seriously as the introduction of many non-native species

to terrestrial and aquatic environments could have far reaching ecological effects. In recent years, public awareness on the possible risks of commercial production of algae (especially non-transgenic algae) has increased. There have been suggestions that detailed scientific risk analysis reports for each strain be compiled, prior to large-scale cultivation (Gressel *et al*., 2013).

Biomass recovery poses a challenge in microalgal biomass production processes. This phase generally requires one or more solid-liquid separation steps and usually accounts for 20 - 30% of the total costs of production (Brennan and Owende, 2010; Wang *et al*., 2008). Common harvesting practices include flocculation, filtration, flotation and centrifugal sedimentation. Some of these procedures can be highly energy intensive. Selecting an appropriate harvesting technology during microalgal cultivation is crucial for the economically feasible production of microalgal biomass (Brennan and Owende, 2010).

The choice of harvesting technique is dependent on microalgal characteristics such as size, density and the value of the target products (Brennan and Owende, 2010; Packer, 2009). According to Brennan and Owende (2010), microalgal harvesting is a two-stage process, involving bulk harvesting and thickening. Bulk harvesting aims to separate biomass from the bulk suspension. Thickening is generally a more energy-intensive step as it involves concentrating the slurry through techniques such as centrifugation, filtration and ultrasonic aggregation (Packer, 2009).

Flocculation is a popular technique as it is simple and cost-effective to apply. This harvesting mode uses multivalent cations to overcome the overall negative charge present on the surface of microalgae. Multivalent metal salts (ferric chloride, aluminum sulfate and ferric sulfate) and

polymers (polyelectrolyte and chitosan) are usually effective flocculants. An ideal flocculant is one that can be applied at low concentrations, is inexpensive, non-toxic, and further downstream processing is not adversely affected by its use. For effective microalgal harvesting, flocculation is often combined with floatation. This simple technique allows microalgae to float on the surface of the medium which can then be easily removed as scum (Packer, 2009). Dissolved air flotation (DAF) is a costly process that uses fine bubbles, which are injected under high pressure into the water column and then rise to the surface (Packer, 2009). Most microalgae can be easily harvested from suspension by centrifugation. However, while centrifugal recovery is quick and easy, it is highly energy intensive (Ho *et al*., 2011). For low-value products (biofuels or animal feed), gravity sedimentation enhanced via flocculation is probably the most appropriate method (Ho *et al*., 2011).

Life cycle analysis (LCA) is a methodological environmental technique used for evaluating the input-output inventory of a product system throughout its entire life cycle. This process encompasses acquisition of raw material, production, use and ultimate disposal (from cradle to grave) (Tsoutsos *et al*., 2010). Such an assessment helps detect problem-shifting during life cycle stages (lower energy utilisation during use, attained at a much higher manufacturing energy consumption cost), transfer from one medium to another (lower air emissions, but increased solid waste), identification of technological innovation opportunities as well as projection of the environmental performance based on a selected functional unit of the product (Gnansounou *et al*., 2009; Tsoutsos *et al*., 2010). Energy balance, an essential factor within a microalgal system, is usually calculated by evaluating energy inputs required at each LCA stage, against the total required inputs of the embodied energy related to the specific product/idea of interest. Energy balance may be influenced at each or any life cycle phase. It is thus imperative that each stage be closely monitored so as to prevent any mishaps that could

have far-reaching implications on the rest of the chain (Gnansounou *et al*., 2009; Tsoutsos *et al*., 2010). Life cycle analysis essentially covers cultivation, harvesting, lipid extraction and finally product formation. Wastewater emissions as well as waste (solids or wastewater) treatment is generally not covered in a LCA study (Khoo *et al*., 2011).

In theory, an efficient GHG capture mechanism would entail the capture of CO_2 flue gas from power stations and its subsequent utilisation in promoting the growth of microalgae for biofuel production (Khoo *et al*., 2011). However, according to Campbell *et al*. (2011), such a theory is only marginally correct. They propose that permissible carbon credits do not arise from captured flue gas due to the fact that the algae-derived fuel will ultimately be burnt and returned to the atmosphere. Carbon credits arise from the replacement of the fossil fuel that would have been used if the biofuel had not become accessible. Additional carbon credits may become available if the spent microalgal biomass went into the generation of electricity. Hence, the biomass would displace any coal, gas or other materials that would have originally been used for energy production (Campbell *et al*., 2011). It is necessary to therefore carry out comprehensive life cycle calculations of the processing energy required to create the biofuel. These calculations would allow one to quantify GHG emissions at each stage of the process, enabling the researcher to establish whether the process does in fact emit less CO_2 than the use of fossil fuels and if this is the case to quantify the associated GHG savings (Gnansounou *et al*., 2009; Khoo *et al*., 2011). Different microalgal propagation systems can only be compared if they perform the same function. After selection of a shared function, a unit is chosen that will enable one to compare the systems on the same quantitative basis. All energy and mass flows within the operating system will then be standardised to this functional unit (Kadam, 2001). When assessing the CO_2 balance of a system, it is necessary to take into account the total discharge from fossil energy versus the CO_2 uptake of the microalgae during cultivation

(Khoo *et al*., 2011). Alabi *et al*. (2009) did a detailed cost analysis on different algal production systems. Findings from this study revealed that capital investment required per litre volume for each production facility was as follows: US$52 L^{-1} for raceway ponds, US$2 L^{-1} for fermenters and US$111 L^{-1} for PBRs. Production costs (which included labour and running costs) for a kg of dried algal biomass showed that PBRs were the most expensive system to operate (US$7.32 kg^{-1}), followed by raceway ponds (US$2.66 kg^{-1}). Surprisingly, fermenters proved the least expensive, at a cost of US$1.54 kg^{-1}. Another cost analysis study by Molina-Grima *et al*. (2003) illustrated that it would cost US$32.16 to produce a kg of microalgal biomass (dry) in a standard PBR. This study further served to highlight the high costs associated with closed systems.

Carbon dioxide sequestration costs depend largely on microalgal productivity, carbon content of selected strains and overall process efficiency. Stewart and Hessami (2005) investigated the carbon uptake rate of *Synechocystis aquatilis* and found that this strain was able to uptake carbon at a rate of 1.5 g/l/day. It was then proposed that under natural light conditions, this strain could mitigate up to 2.2 kT CO_2/4,000 m^3 pond/yr. In a separate study, Kadam (2001) demonstrated that a 1,000-ha open raceway pond could mitigate 210,000 T/yrCO_2 of the 414,000 T/yrCO_2 generated by a 50-MW power plant. This suggests that a 50% reduction in CO_2 from the flue gas emissions could be achieved. Carbon sequestration strategies routinely implemented in the USA entail the injection of carbon in saline aquifers and amine scrubbing of CO_2 from flue gases. Carbon burial in saline aquifers is far cheaper (US$40 t^{-1} CO_2) as opposed to amine scrubbing (US$150 t^{-1} CO_2). The combined costs of these two processes, however, are still significantly lower when compared to carbon mitigation using microalgal open ponds (US793t^{-1}$ CO_2). However, mitigation costs using algae could be reduced if

recovered biomass was utilised in the production of valuable by-products (Farrelly *et al*., 2013; Pires *et al*., 2012).

2.14 VALUABLE END-PRODUCTS

Following carbon sequestration, the microalgal biomass has considerable potential in the cosmetic, food, pharmaceutical and biofuel industries (Ho *et al*., 2011). Due to their valuable blend of vitamins, carbohydrates and proteins, microalgae are able to provide good overall nutrition to animals. Table 5 shows some microalgal species that have been successfully employed for commercial applications. In addition to the applications listed in Table 5, microalgal biomass is known to store substantial amounts of energy which can be converted to methane, butanol, ethanol and hydrogen (Wang *et al*., 2008). In 2006, Ono and Cuello, investigated a sustainable microalgal-CO_2 mitigation model for commercial application. From their study, they were able to conclude that in order for a process to be feasible, it should not only fix CO_2 efficiently, but also be able to transform the biomass to various valuable by-products.

For example, in recent years studies have shown that *Scenedesmus* sp. is not only a promising candidate for CO_2-fixation but also represents a high lipid producer (de Morais and Costa, 2007; Ho *et al*., 2010). Many microalgal species display suitable fatty acid profiles that permit biodiesel production with high oxidation stability. Research has revealed that *Scenedesmus* sp. has the ability to convert ± 15 - 25% atmospheric CO_2 into biodiesel. The remaining biomass can be exploited for the production of lutein and other essential pigments (Ho *et al*., 2011).
Not only are most microalgae high lipid producers, but they also represent good protein sources owing to their amino acid pattern and content (Pires *et al*., 2012; Spolaore *et al*., 2006).

Microalgal cells have proved capable of synthesising all amino acids. This inherent ability could be beneficial in providing essential amino acids to animals as well as humans.

Microalgal biomass are also rich in ω-3 fatty acids. These fatty acids can be purified to produce a high value food supplement. Microalgae usually possess two functional sources of ω-3 fatty acids: decosahexaenoic acid (DHA) and eicosapentanoic acid (EPA). Eicosapentanoic acid has many benefits to human health. It displays considerable anti-inflammatory effects, which allows it to be successfully used in the prevention of arthritis as well as in alleviating the painful symptoms. Eicosapentanoic acid can also contribute to cardiovascular health (lowering cholesterol). Furthermore, EPA can be used in the treatment of schizophrenia and depression as it also exhibits effective neuro-protective properties (Pires *et al*., 2012; Spolaore *et al*., 2006).

Table 5: Feasible downstream applications of various microalgae species (adapted from Ho *et al*., 2011)

Microalgal species	End products	References
Chlorella	1. Health-promoting molecules	Gouveia *et al*., 1996
	2. Food additives	Borowitzka, 1999
	3. Animal nutrition	Spolaore *et al*., 2006
	4. Cosmetics	Wang *et al*., 2010
	5. Biofuels	Chen *et al*., 2010
Dunaliella salina	1. β-carotene	Metting, 1996
	2. Food supplements	Spolaore *et al*., 2006
	3. Cosmetics	Spolaore *et al*., 2006
Botryococcus braunii	1. Biodiesel	Chen *et al*., 2010
		Chisti, 2007
Spirulina platensis	1. Pharmaceuticals	Raja *et al*., 2008
	2. Phycobiliproteins	Spolaore *et al*., 2006
	3. Human nutrition	Belay *et al*., 1993
Haematococcus pluvialis	1. Astaxanthin	Spolaore *et al*., 2006
	2. Food additives	Spolaore *et al*., 2006
	3. Pharmaceuticals	Spolaore *et al*., 2006
Arthrospira	1. Carotene	Spolaore *et al*., 2006
	2. Cosmetics	Viskari and Colyer, 2003
	3. Phycobiliproteins	
Nannochloropsis	1. Eicosapentaenoic acid (EPA)	Zittelli *et al*., 1999
	2. Biodiesel	Chen *et al*., 2010
		Chisti, 2007

2.15 CONCLUSION

The use of microalgae for the purpose of CO_2 sequestration is a unique environmental technology. Microalgae are promising candidates for CO_2 mitigation, which aids in combating GHG-related environmental impacts and has the added benefit of producing renewable biomass. In comparison with terrestrial plants, microalgae are capable of fixing CO_2 at a rate several times higher than plants owing to their high photosynthetic efficiencies. Additionally, selected microalgal strains can assimilate CO_2 from industrial flue gas within various ranges of concentrations from ambient (0.036% v/v) to extremely high (100% v/v). Carbon dioxide fixation from industrial flue gas coupled with nutrient recycling from wastewater makes algae ideal organisms for the production of useful by-products. Several algal strains capable of growing in and consuming high CO_2 concentrations from flue gas streams have been isolated and propagated; however, they are just a fraction of the vast majority of total algal species that have yet to be isolated and exploited for this purpose. For effective CO_2 sequestration, an in-depth knowledge of flue gas composition and biology of microalgal cells would be required. Furthermore, strategic engineering decisions should be taken into consideration to realize effective microalgal CO_2 sequestration systems. Microalgal cultivation requires the development of suitable reactors with features such as high S/V ratio, mixing, mass transfer, scalability and ease of operation. Technical viability of algal CO_2 sequestration has already been demonstrated in a few systems; however, the major challenges are the strategic and holistic development of technologies that will improve economic feasibility of algal CO_2 sequestration and make this a viable industrial approach to GHG remediation.

2.16 RATIONALE FOR STUDY

To develop the most effective CO_2 emission mitigation process, it is necessary to select fast-growing, indigenous microalgal species with high CO_2 fixation efficiency. To date, very little information is available regarding the influence of high CO_2 levels (> 20%) produced by industry on the growth and CO_2 biofixation rate of indigenous microalgae as well as the physiological responses of microalgae at varying concentrations of carbon. This project explored the capabilities of high CO_2 tolerant microalgae to sequester CO_2 from flue gases with the ultimate goal of using microalgae to remediate GHG. Potential uses of the microalgal biomass after sequestration studies could involve various options (biorefinery approach), and therefore the biomass was evaluated (carbohydrate, protein and lipid percentages) for the potential production of other value added products.

CHAPTER THREE: ISOLATION, SCREENING AND PHYSIOLOGICAL RESPONSES OF CARBON-SEQUESTERING MICROALGAE TO ELEVATED CARBON REGIMES

3.1 INTRODUCTION

Carbon dioxide emissions play an important role in global climate regulation by changing the Earth's radiation budget, temperature, meteorology and hydrology (Feng *et al*., 2008). The main sources of CO_2 emissions are combustion of fossil fuels, such as coal, natural gas and oil, for energy and transportation (Al-Hothaly *et al*., 2015). Emissions of CO_2 have dramatically increased within the last 50 years and continue to increase by almost 3% each year (Pires *et al*., 2012). The normal CO_2 content in air is assumed to be approximately 0.036% (Chinnasamy *et al*., 2009). However, Kumar and Das (2012) reported a CO_2 concentration in air of nearly 391 ppmv (0.0391% by volume) based on research carried out at the Manua Loa Observatory (Hawaii, US) in 2011. This concentration is rapidly increasing worldwide at a rate of ~2 ppmv per year (2×10^{-4} % by volume). Thus, remediation strategies are urgently required for the mitigation of this GHG.

Carbon dioxide sequestration strategies can be broadly classified into physical and biological protocols (Anjos *et al*., 2013). Physical sequestration protocols are associated with several challenges, including high costs and space requirements as well as CO_2 leakage (Yue and Chen, 2005). In this context, biological CO_2 sequestration has been reported as a promising alternative solution for CO_2 fixation (Yang and Gao, 2003). Since CO_2 is essential for the formation of complex sugars by green plants through photosynthesis, it can be used to significantly enhance growth rates of certain microalgal species. Biological mitigation of CO_2 using autotrophic microalgal cultivation offers several advantages, such as the beneficial production of biofuels

and other secondary metabolites (Watanabe *et al*., 1992). Microalgal strains are able to fix CO_2 gases present in the atmosphere or from industrial flue and flaring practices. Microalgal species are able to take up CO_2 in the form of soluble carbonates ($NaHCO_3$ and Na_2CO_3). Tolerance to high concentrations of these carbonates could serve as an effective screening method for high CO_2 tolerant strains (Wang *et al*., 2008).

Prior to the development of an effective CO_2 mitigation process, an essential step should be to screen for and choose the most CO_2-tolerant indigenous strains (Khan *et al*., 2009). Researchers have reported that very few species of microalgae are capable of tolerating high levels of CO_2 (Ho *et al*., 2011; Sydney *et al*., 2010; Wang *et al*., 2008). The carbon uptake in microalgae is largely dependent on its metabolic potential, which is in turn reliant on photosynthesis. Pulse amplitude modulated (PAM) fluorometry has been considered one of the most common non-invasive and rapid techniques to determine the photosynthetic performance in microalgae (Baker, 2008). Additionally, PAM fluorometry has been used extensively to ascertain the physiological stress of phytoplankton caused by temperature, salinity, nutrients and irradiance (Baker, 2008). Relative electron transport rate (rETR) is a PAM parameter used for describing the photosynthetic performance of microalgae by fluorescently measuring the rate of linear electron transport through PSII (Juneau *et al*., 2005). However, the application of PAM fluorometry to monitor stress in microalgae when exposed to various levels of carbon sources has not been well established in the microalgal biotechnology field. The maximum quantum efficiency (F_v/F_m) can be used to estimate nutrient limitation or stress, where 'healthy' phytoplankton has F_v/F_m values of 0.6 - 0.7 (Kromkamp and Peene, 1999). Additionally, the F_v/F_m value tends to decrease in nutrient-stressed cultures allowing for the detection of non CO_2-tolerant strains (Eggert *et al*., 2007).

To develop the most effective CO_2 emission mitigation process, it is necessary to select fast-growing, indigenous microalgal species with high CO_2 fixation efficiency. Furthermore, there is currently very little information available regarding the influence of high carbon levels on the growth and CO_2 biofixation rate of indigenous microalgae. This chapter therefore focused on the isolation, identification and screening of microalgal strains (indigenous to the KwaZulu-Natal province in South Africa) by cultivation under a range of CO_2 and $NaHCO_3$ concentrations and ultimate selection for the highest CO_2 tolerant organism. The logistic model was used to accurately describe the microalgal performance during exposure to CO_2 concentrations of 0.03 - 15% and $NaHCO_3$ of 0.05 - 2 g/l. This model was chosen for explaining the growth curve as it does not use substrate term for explaining the entire growth profile of the microorganisms. It was therefore applied for data fitting, as well as for estimation of the maximum growth rate (μ_{max}) and the biomass carrying capacity (B_{max}). Furthermore, assessment of the photosynthetic performance was undertaken using relative rETR and quantum yield techniques.

3.2 MATERIALS AND METHODS

3.2.1 Sampling and Preliminary Screening

Water samples were collected from various aquatic environments close to high CO_2-producing industries, with the aim of isolating microalgae that had already been acclimatised to high levels of CO_2. Grab samples were collected in sterile 500 ml Schott bottles and transported to the laboratory within 24 h for further analysis. Debris and unwanted microorganisms were removed from the water samples by filtration through 100 μm filters (Whatman filters, Kent, United Kingdom) into sterile 500 ml vessels.

3.2.2 Reference Strain

Coccolithus pelagicus 913/3 was purchased from the Culture Collection of Algae and Protozoa (CCAP), Scottish Marine Institute, UK. This marine alga was chosen as a reference strain since it grows at elevated CO_2 concentrations (≥ 20%) (Moheimani *et al*., 2012).

3.2.3. Isolation

Standard plating methods were used to separate algal populations in order to isolate single microalgal species. One millilitre of each water sample was spread-plated onto Artificial Sea Water (ASW) media (Appendix B) agar plates (Watanabe *et al*., 1992; Watanabe *et al*., 2000). Artificial Sea Water media was used as the samples were obtained from high saline environments. Not only is ASW a nutrient rich medium, but it is also a medium with a high salt concentration (27.960 g/l NaCl). Cultures were incubated at 100 umol m^{-2} s^{-1}, with a light/dark-cycle of 16:8 h at a temperature of 25±1°C. Thereafter, grown algae cultures were streaked using sterile technique onto additional sets of ASW plates and incubated. The streak plating method was performed repeatedly until single colonies were obtained. Single colonies were selected based on colour and size before sub-culturing onto new agar plates containing ampicillin (50 μg ml^{-1}) to inhibit bacterial growth. This process was repeated several times until bacteria and fungi-free microalgal colonies were obtained. The axenic cultures obtained were maintained as stock cultures. These stock cultures were maintained by re-plating each onto new nutrient media at least once a month, or more frequently depending on the nature of each isolated strain.

3.2.4 Experimental Set-up

The isolated strains were grown under different CO_2 and $NaHCO_3$ concentrations in order to ascertain their carbon utilisation tolerance. Carbon dioxide concentrations were selected based on previous studies reported in literature (de Morais and Costa, 2007; Ho *et al*., 2011; Kumar and Das, 2012; Pires *et al*., 2012; Sydney *et al*., 2010; Wang *et al*., 2008). The microalgal strains were grown in 250 ml of ASW medium in gas-tight 500 ml incubation vessels. A 10% v/v mid-log, exponentially growing culture (from a predetermined growth curve) was used as seed inoculum. Based on preliminary research by Chinnasamy *et al*. (2009) the CO_2 content in air was assumed to be approximately 0.03%. The headspace atmosphere was repeatedly flushed with graded concentrations of CO_2 (0.03, 0.5, 5, 10 and 15%) which was filtered through a 0.45 μm filter into the individual incubation vessels daily using commercial grade CO_2 (99.97% v/v with less than 10 μl l^{-1} CO) as described by Chinnasamy *et al*. (2009). The flow rate required to achieve the desired CO_2 levels were calculated using the ideal gas law. Thereafter, a rotameter was employed to manipulate the flow rate as required.

The respective head space CO_2 concentrations were verified using gas chromatography (GC). The GC system (Agilent 7820) used was equipped with a thermal conductivity detector and contained a GS-Gaspro (30 m x 0.32 mm I.D) packed column. Nitrogen was used as the carrier gas. The operational conditions were as follows: injector temperature of 120°C, oven temperature of 80°C and detector temperature of 250°C. Areas obtained after GC analysis was compared with reference curves to determine CO_2 concentrations (Basu *et al*., 2013).

The isolated strains were also grown in predetermined amounts of $NaHCO_3$ that was dissolved into the appropriate cultivation medium to achieve 0.05, 0.2, 0.6, 1, 2 g/l of total CO_2

(equivalent). The initial pH of the cultivation medium was adjusted to 7 and maintained throughout the experiment using a buffering agent, 2-(N-morpholino) ethanesulfonic acid (MES). A 10% v/v mid-log exponentially growing culture (from a predetermined growth curve) was used as seed inoculum.

3.2.5 Fluorescence Measurements

Effects of CO_2 and $NaHCO_3$ concentrations on the physiology of the isolated microalgal strains were determined using non-invasive fluorescence measurements. A Dual-PAM 100 Chlorophyll Fluorometer (Heinz Walz Gmbh, Effeltrich, Germany) was used for the fluorescence measurements of PSI and PSII. Photon irradiance (400 to 700 nm) incident on the sample surface was measured using a PAR micro-sensor (Spherical MicroQuantum Sensor US-SqS/W, Waltz) connected to the PAM fluorometer control unit. The Dual-PAM software v 1.19 was used to record and analyse all data.

Relative electron transport rate was calculated by the Dual PAM software using the formula (Eq. 6) (Ramanna *et al*., 2014; White *et al*., 2011).

$$rETR = \frac{F'_q}{F'_m} \times PPFD \qquad \text{(Eq. 6)}$$

Where: F'_q is a representation of the PSII operating efficiency and can be calculated from Eq. 7; F'_m is the maximum fluorescence in a light adapted sample; *PPFD* is the photoactive photon flux density.

$$F'_q = F'_m - F'$$

(Eq. 7)

Where: F' is the dark fluorescence yield.

The quantum efficiency of PSII charge separation (F_v/F_m) was estimated by:

$$F_v \Big/ F_m = \frac{F_m - F_0}{F_m}$$

(Eq. 8)

Where: F_m and F_0 are the maximum and minimum fluorescence yields, respectively, of a 30 min dark adapted sample, respectively (Genty *et al*., 1989).

3.2.6 Strain Identification

Genomic DNA of a strain was extracted using the ZR Fungal/Bacterial DNA MiniPrep™ kit (Sigma-Aldrich*)*. The Nanodrop (ND-1000) Spectrophotometer was used to determine the purity and concentration of extracted genomic DNA. One microliter of genomic DNA was measured using absorbance ratios 260/230 and 260/280 nm.

Thereafter, the extracted DNA was subjected to polymerase chain reaction (PCR) in order to amplify the DNA sequence for further analyses. The reaction mixture consisted of DreamTaq Green 2X master mix, 50 pM of each primer (18S C-2 b, 5‘ATTGGAGGGCAAGTCTGGT3’ /18S D-2 b, 5‘ACTAAGAACGGCCATGCAC3’) and 10 ng of genomic DNA (Lenaers *et al*., 1989). Polymerase chain reaction was performed using the Veriti TM 96-well Thermal Cycler (Applied Biosystems) under the following conditions: 95ºC for 1 min followed by 45 cycles of

95ºC for 30 s; 50ºC for 30 s; then 72ºC for 2 min, and a final extension step at 72ºC for 10 min (4 hold). All amplified PCR products were visualised using agarose gel electrophoresis. Products were run on a 1% (w/v) agarose gel stained with ethidium bromide at 80V for 60 min and thereafter viewed using a gel documentation system (Vacutec). In order to approximate the size of amplicons produced, 100bp and 1kb gene rulers were used.

Sequencing of PCR amplified 18S ribosomal DNA (18SrRNA) was done at a commercial lab, Inqaba Biotechnical Industries, Pty Ltd, South Africa. Sequences were edited using FinchTV (Geospiza) and were then compared to the National Centre for Biotechnology Information (NCBI) database (http://www.ncbi.nlm.nih.gov/blast/Blast.cgi) using the Basic Local Alignment Search Tool (BLAST) to determine phylogenetic affiliations. The sequence was then edited using Bioedit aligned (CLUSTAL_X).

A phylogenetic tree was constructed from the alignment using Mega 5.1 beta 2 and bootstrap analysis was performed using 1000 replicates by the neighbour-joining (NJ) method (Saitou and Nei, 1987). The evolutionary distances were computed using the Maximum Composite Likelihood method (Kumar *et al*., 2004) and are in the units of the number of base substitutions per site. Evolutionary analyses were conducted in Mega 5.1 beta 2 (Tamura *et al*., 2011).

3.2.7 Growth Profile and Logistic Model

3.2.7.1 Biomass (dry cell weight)

Biomass concentration was measured as DCW as it is one of the most direct and cost effective means to estimate biomass production. Dry cell weight was estimated using the traditional technique involving sampling, separation, drying and weighing. A 50 ml sample was

centrifuged (Heraeus multifuge centrifuge 4KR, USA) at 1509 x g for 15 min at 4°C. The supernatant was discarded and the pellet was washed with 0.05 M HCl and distilled water to remove non-biological adhering materials such as mineral precipitates, and dried at 60°C for 24 h. The watch glasses were cooled in desiccators, and thereafter weighed. Growth kinetics was determined using spectrophotometeric data and biomass yields.

3.2.7.2 Logistic model

A plot of biomass (B) vs time (t) gives a sigmoid variation of biomass as a function of time, displaying lag, exponential and stationary phase of the culture (Kumar and Das, 2012). The growth profile can be explained by the logistic equation as formulated in Eq. 9. The growth kinetic values were determined by creating M-file for a genetic algorithm in MATLAB. The validation procedure was carried out using the correlation coefficient (r^2).

$$\frac{dB}{dt} = \mu_{\max} B\left(1 - \frac{B}{B_{\max}}\right) \qquad \text{(Eq. 9)}$$

Where:

B is the dry cell mass (g/l), B_{max} is the maximum dry cell mass (g/l) and μ_{max} is the apparent specific growth rate (d^{-1}).

3.2.8 CO_2 Uptake Rate

The CO_2 uptake rate (Q_{CO2}) in g/day was estimated for the first 19 days of cultivation by using the biomass productivity, the carbon content and the molar masses of CO_2 and carbon (Slade and Bauen, 2013):

$$Q_{CO_2} = \frac{(X_1 - X_2)}{(t_1 - t_2)} \times X_c \times \frac{M_{CO_2}}{M_c} \times V$$

(Eq. 10)

Where:

X = cell concentration (g/l)

t = time (days)

X_C = the average mass fraction of carbon

M_{CO2} = 44 g/mol

M_C = 12 g/mol

V = working volume of incubation vessel (250 ml)

3.3 RESULTS AND DISCUSSION

3.3.1 Sampling and Preliminary Screening

A total of 12 water samples including fresh, marine and brackish water bodies in KwaZulu-Natal, South Africa were collected and used for isolation (Table 6). A total of nine axenic microalgal cultures (I-01 - I-09) were obtained which were further purified and screened for their CO_2 tolerance potential (Table 7). To isolate CO_2-tolerant strains, the culture broth was frequently aerated with 5% CO_2. The time required for purifying these strains varied greatly as it was both species and strain-dependent and took approximately several weeks to months to produce axenic cultures as this was largely dependent on the microalgal cell growth rate (He *et al.*, 2012). The antibiotic ampicillin was added to the growth medium to prevent bacterial growth. It was noted that the marine strains grew much slower when compared to the freshwater

isolates. Freshwater microalgal strains formed visible colonies on the agar plates within 5 - 10 days, whereas the marine strains took at least 15 - 20 days to produce colonies. Images of the microalgal strains are shown in Figure 5.

Table 6: Samples collected in KwaZulu-Natal (South Africa)

Sample No	Location	GPS co-ordinates	Water body type	Salinity (g/l)	Sample description	Growth
001	Amanzimtoti	-30.057783, 30.882646	River Mouth	44	Turbid/brown	Yes
002	Amanzimtoti	-30.056564, 30.877507	River	32	Turbid/green	Yes
003	Amazimtoti	-30.047705, 30.891905	Beach	35	Turbid/green	Yes
004	Bluff	-29.959967, 30.964915	River	28	Dark green murky	Yes
005	Durban	-29.865269, 31.017518	Beach	36	Turbid/brown	No
006	Hibberdene	-30.584597, 30.569854	River	29	Turbid/brown	Yes
007	Isipingo Beach	-29.993774, 30.948485	River	33	Dark green murky	Yes
008	La Mercy	-29.647115, 31.091580	River	33	Dark green murky	No
009	Merebank	-29.969253, 30.978479	River Mouth	41	Turbid/green	Yes
010	NPC Simuma	-30.674966, 30.347469	Stream	27	Turbid/brown	No
011	Umkomaas	-30.201427, 30.802529	River Mouth	31	Turbid/green	Yes
012	Umlazi	-30.002614, 30.874393	River	30	Turbid/green	No

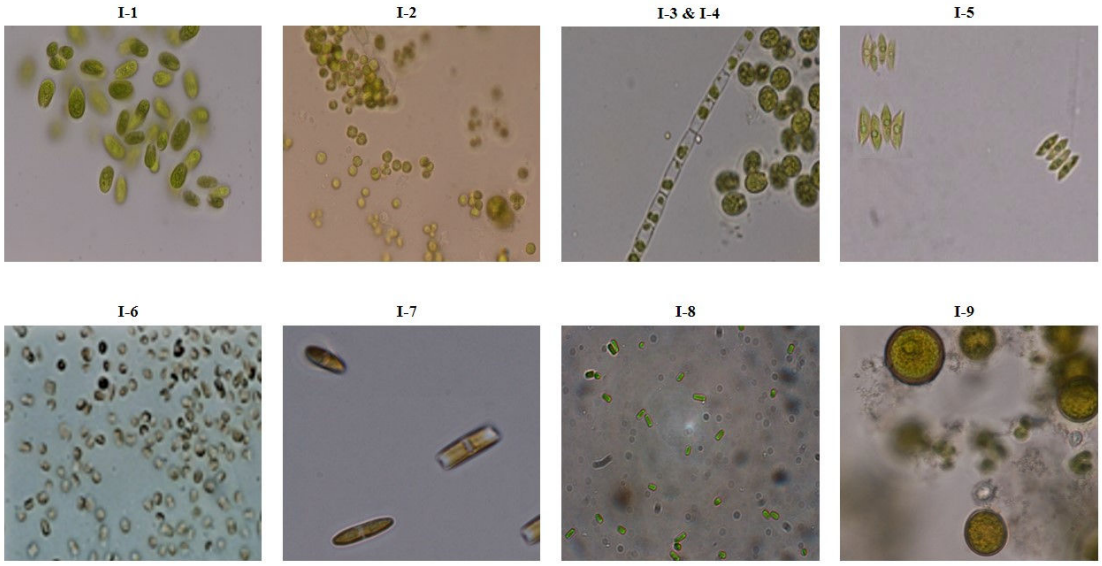

Figure 5: Images of the nine algal strains viewed under the light microscope at 1000x magnification.

Table 7: Summary of pure microalgal strains isolated from samples

Isolate	Sample no	Class	Description	Identification	CO_2 uptake rate (g/day) when grown at 5% CO_2
I-1	002	Chlorophyceae	Green, spherical	*Scotiellopsis* sp.	0.0057
I-2	004	Chlorophyceae	Green, spherical	*Chlorella* sp.	0.0060
I-3	003	Chlorophyceae	Green, spherical	*Chlorella sp.*	0.0110
I-4	003	Chlorophyceae	Green, filaments	*Klebsormidium* sp.	0.0071
I-5	007	Chlorophyceae	Green, colonial, found in clusters of four cells	*Scenedesmus* sp.	0.0043
I-6	006	Bacillariophyta	Brown, small cells, central sternum present	*Eolimna* sp.	0.0021
I-7	001	Bacillariophyta	Brown, boat-shaped	*Navicula* sp.	0.0026
I-8	009	Chlorophyceae	Bright green, elongated/rod shaped cells	*Stichococcus sp.*	0.0034
I-9	011	Chlorophyceae	Green, big spherical cells	*Chlorococcum* sp.	0.0039

3.3.2 Growth of Strains under Different CO_2 Concentrations

Photoautotrophic microorganisms appear to be promising candidates for the mitigation of CO_2 emissions. The five isolates (out of the nine strains) that exhibited the highest CO_2 uptake potential was sleceted for further studies. The indigenous microalgal cultures were exposed to incremental CO_2 and $NaHCO_3$ concentrations to ascertain an optimum range for microalgal productivity. Each isolated microalgal strain was exposed to incremental CO_2 concentrations between 0.03 and 15% over 21 days of cultivation. The biomass quantities of most strains increased with an increase in contact time and completed the growth phase during nine days (Figure 6). Thereafter, the biomass growth exhibited a different trend based on CO_2 levels in the culture media. The r^2-value of the logistic model equation was high, which indicates a good agreement between experimental data and the model simulation (Table 8).

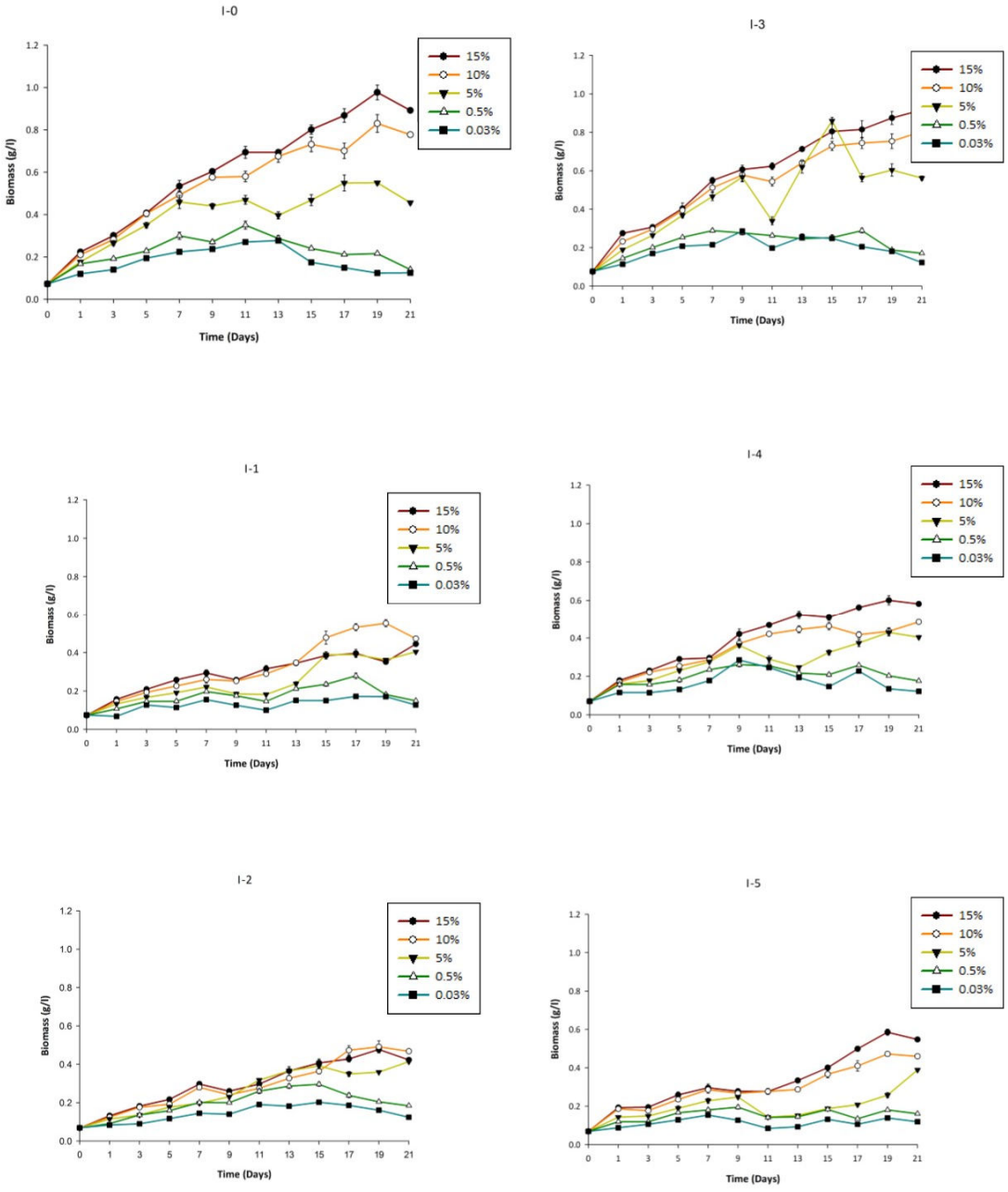

Figure 6: Effect of CO_2 concentrations (%) on the growth of the reference (I-0) and five (I-1 to I-5) indigenous microalgal strains. Shaded squares (blue) = 0.03% CO_2 (control), triangles (green) = 0.5% CO_2, inverted shaded triangles (yellow) = 5% CO_2, circles = (orange) 10% CO_2, shaded circles (red) = 15% CO_2.

Based on the findings by Lam and Lee (2013), a CO_2 concentration of 5 - 10% was considered an optimum range for microalgal productivity. Due to its poor solubility in water (approximately 1.450 mg/l at 25°C and 1 atm), CO_2 can be released back to the atmosphere before it has a chance to dissolve and be utilised by the microalgae (Lam and Lee, 2013). In 2012, Pires *et al*. reported that toxicity occurring at high CO_2 concentrations can be attributed to the reduced pH of the culture medium or by direct inhibition. However, in our study, the negative impact of a pH decrease was diminished by the buffering action of MES.

In a study, Kumar and Das (2012) investigated the feasibility of bioCO_2 sequestration using *Chlorella sorokiniana*. The study found that 5% CO_2 was the most suitable concentration for the growth of this organism, achieving μ_{max} and B_{max} of 0.45 d^{-1} and 4.440 mg/l respectively. Furthermore, Ryu *et al*. (2009) found that the B_{max} of *Chlorella* increased from 1.780 to 2.020 mg l^{-1} (nearly 12%) by increasing the CO_2 level in air from 2 to 5%, respectively. In 2015, Pradhan *et al*. investigated the bio-sequestration of CO_2 in a 1.8 L flat plate photobio-bubble-reactor using the microalgae *Rhizoclonium hieroglyphicum* JUCHE2. Results from their study revealed that the maximum specific growth rate (μ_{max} = 0.996 d^{-1}) was obtained at a high CO_2 concentration of 15% and a light intensity of 398.71 µmol photons m^{-2} s^{-1}. Solovchenko *et al*. (2015) studied the acclimation, growth, and photosynthetic performance of a *Desmodesmus* sp. 3Dp86E-1 at an elevated CO_2 level of 20%. It was observed that during the first six days of cultivation, *Desmodesmus* sp. cultures exposed to the elevated CO_2 concentration produced biomass (in terms of culture dry mass, DM per unit volume) nearly two times faster than cultures cultivated at atmospheric CO_2 levels. A decline in growth rates of *Desmodesmus* sp. cultures exposed to the elevated CO_2 concentration (20%) was noted from the 7^{th} day of cultivation. This suggested the start of the stationary phase of growth, however, this was not observed for the cultures exposed to ambient CO_2 levels.

Pearson's correlation coefficient (*r*) was applied during this study to assess the relationship between cultivation time and biomass growth. As shown in Figure 6, at a CO_2 concentration of 0.03%, the biomass of the reference strain (I-0) increased from 0.073 to 0.237 g/l with an increase in contact time until day 9 ($r = 0.977$, $p = 0.0008$), after which it declined to 0.125 g/l by d 21 ($r = -0.876$, $p = 0.0097$). However, at 15% CO_2, strain I-0 was still growing even after 9 days of cultivation ($r = 0.937$, $p = 0.0018$).

Table 8: Logistic model parameters of the microalgal strains at different CO_2 concentrations (0.03 - 15%)

CO_2 (%)	**Isolates**	**μ_{max} (d^{-1})**	**B_{max} (g/l)**	**r^2**
0.03 (control)	I-0	0.67	0.197	0.627
	I-1	0.292	0.149	0.784
	I-2	0.281	0.174	0.873
	I-3	0.701	0.214	0.755
	I-4	0.476	0.190	0.64
	I-5	0.73	0.121	0.654
0.5	I-0	0.975	0.248	0.706
	I-1	0.382	0.202	0.764
	I-2	0.372	0.243	0.891
	I-3	0.94	0.247	0.833
	I-4	0.672	0.224	0.837
	I-5	0.638	0.166	0.824
5	I-0	0.608	0.478	0.954
	I-1	0.163	0.481	0.924
	I-2	0.248	0.406	0.98
	I-3	0.453	0.607	0.863
	I-4	0.394	0.358	0.893
	I-5	0.557	0.228	0.618

10	I-0	0.415	0.737	0.974
	I-1	0.212	0.573	0.958
	I-2	0.209	0.518	0.966
	I-3	0.418	0.725	0.967
	I-4	0.378	0.451	0.975
	I-5	0.237	0.452	0.928
15	I-0	0.385	0.864	0.973
	I-1	0.358	0.379	0.935
	I-2	0.272	0.444	0.966
	I-3	0.392	0.828	0.968
	I-4	0.334	0.573	0.981
	I-5	0.201	0.620	0.942

The logistic model was used to identify μ_{max} and B_{max} of the microalgal biomass during different concentrations of CO_2 (Table 8). The correlation between simulated results from the logistic equation and the actual data was determined by the r^2-value (Table 8). The reference strain I-0 recorded the highest μ_{max} of 0.98 d^{-1} with the assimilation of 0.5% CO_2. However, the μ_{max} declined to 0.39 d^{-1} with further increase in CO_2 concentration to 15% (r = - 0.925, p = 0.075). The B_{max} significantly increased from 0.2 to 0.86 g/l when CO_2 concentration was increased from 0.03 to 15% (r = 0.990, p = 0.001).

Values of μ_{max} and B_{max} varied greatly among the indigenous strains. The μ_{max} of strains I-2 and I-4 showed peak values of 0.37 d^{-1} and 0.67 d^{-1}, respectively at 0.5% CO_2, and then exhibited a slight decline with an increase in CO_2 concentration to 15% (r = - 0.612, p = 0.388 for I-2 and r = - 0.852, p = 0.148 for I-4). The μ_{max} of strain I-5 dropped considerably from 0.73 to 0.20 d^{-1} with an increase in CO_2 concentration from 0.03 to 15%, respectively (r = - 0.964, p = 0.008). Also, μ_{max} of strain I-1 showed a minimum value of 0.16 d^{-1} at 5% CO_2, and then

slightly increased during higher CO_2 concentrations and reached 0.36 d^{-1} at 15% CO_2 (r = 0.961, p = 0.178). This indicates that growth of the microalgae was largely dependent on the strain as well as the cultivation conditions.

Amongst the five indigenous strains, I-3 had similar biomass production values to the reference strain. As listed in Table 8, the B_{max} of strain I-3 was higher than other strains, even at raised concentrations of CO_2. For example, at 15% CO_2, B_{max} of strain I-3 (0.83 g/l) was 2.2, 1.9, 1.4 and 1.3 fold higher than that of I-1, I-2, I-4 and I-5, respectively. In contrast, Chen and Gao (2003) observed that enriched CO_2 concentrations (800 µatm) under laboratory conditions did not stimulate the growth of *Skeletonema costatum*. However, in another study involving a mesocosm set-up, growth was enhanced at an elevated CO_2 concentration of 750 µatm (Kim *et al*., 2006). In other studies it was observed that elevated CO_2 levels under laboratory conditions did enhance the growth of diatoms (King *et al*., 2011; Low-DÉCarie *et al*., 2011; Wu *et al*., 2010). These controversial results suggest that different microalgal species display diverse physiological and growth responses during experimental conditions. This could explain the lower μ_{max} and B_{max} values for the other indigenous strains at raised CO_2 concentrations when compared to the indigenous strain I-3.

The statistical significance in biomass production values among the strains at each CO_2 concentration was determined by applying the Tukeys post hoc test (Appendix A). This test revealed that at all CO_2 concentrations there was no significant difference ($p > 0.05$) in biomass production values of I-0 (reference strain) and I-3. At low CO_2 concentrations (0.03 - 5%) strains I-2, I-3 and I-4 produced comparable biomass yields to the reference strain (I-0) ($p > 0.05$). However at high CO_2 concentrations (10 and 15%), I-3 was the only strain that produced similar biomass values to the reference strain (I-0) ($p > 0.05$), implying that I-3 was the only

indigenous strain capable of growing at elevated CO_2 concentrations. It was also noted that the reference strain (I-0) yielded significantly higher ($p < 0.05$) biomass values at all CO_2 concentrations when compared to the indigenous strains I-1 and I-5.

Carbon dioxide uptake rates of the microalgal strains at varying CO_2 levels (%) are depicted in Figure 7. At low CO_2 concentrations of 0.03 - 0.5% all six microalgal strains displayed similar uptake rates with no significant difference ($p > 0.05$). The highest uptake rate (0.0175 g/day) was observed for strain I-0 at 15% CO_2. This rate was closely followed by strain I-3, which had a rate of (0.0154 g/day) at 15% CO_2. At the highest CO_2 concentration (15%), strain I-1 had the lowest CO_2 uptake rate of 0.0054 g/day.

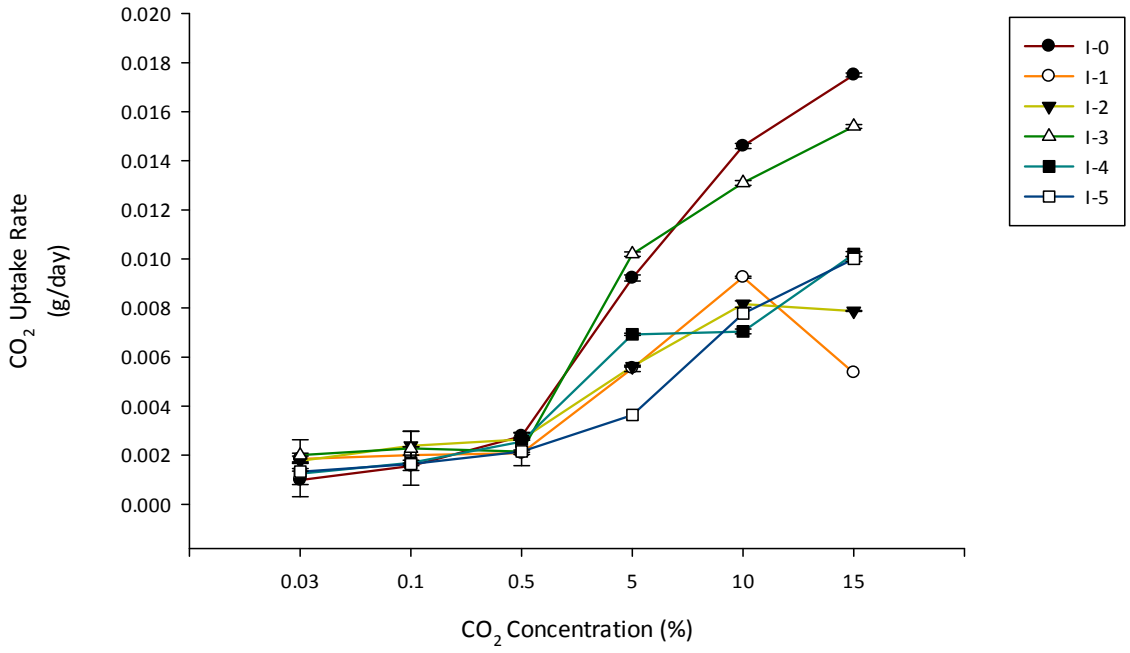

Figure 7: CO_2 uptake rate of the microalgal strains at varying CO_2 levels (%).

3.3.3 Growth of Strains under Varying $NaHCO_3$ Concentrations

The five indigenous strains were grown with incremental additions of $NaHCO_3$ (0.05, 0.2, 0.6, 1 and 2 g/l). Under a low $NaHCO_3$ concentration of 0.05 g/l (Figure 8), the biomass of I-0 increased with contact time and reached 0.094 g/l after 9 days ($r = 0.993$, $p < 0.001$). After a further increase in contact time to 21 days, the microalgal biomass showed a slight enhancement to 0.12 g/l ($r = 0.851$, $p = 0.015$). However, the biomass significantly increased from 0.075 to 0.894 g/l during the cultivation period (21 days) ($r = 0.983$, $p < 0.0001$), when subjected to a higher $NaHCO_3$ concentration of 2 g/l.

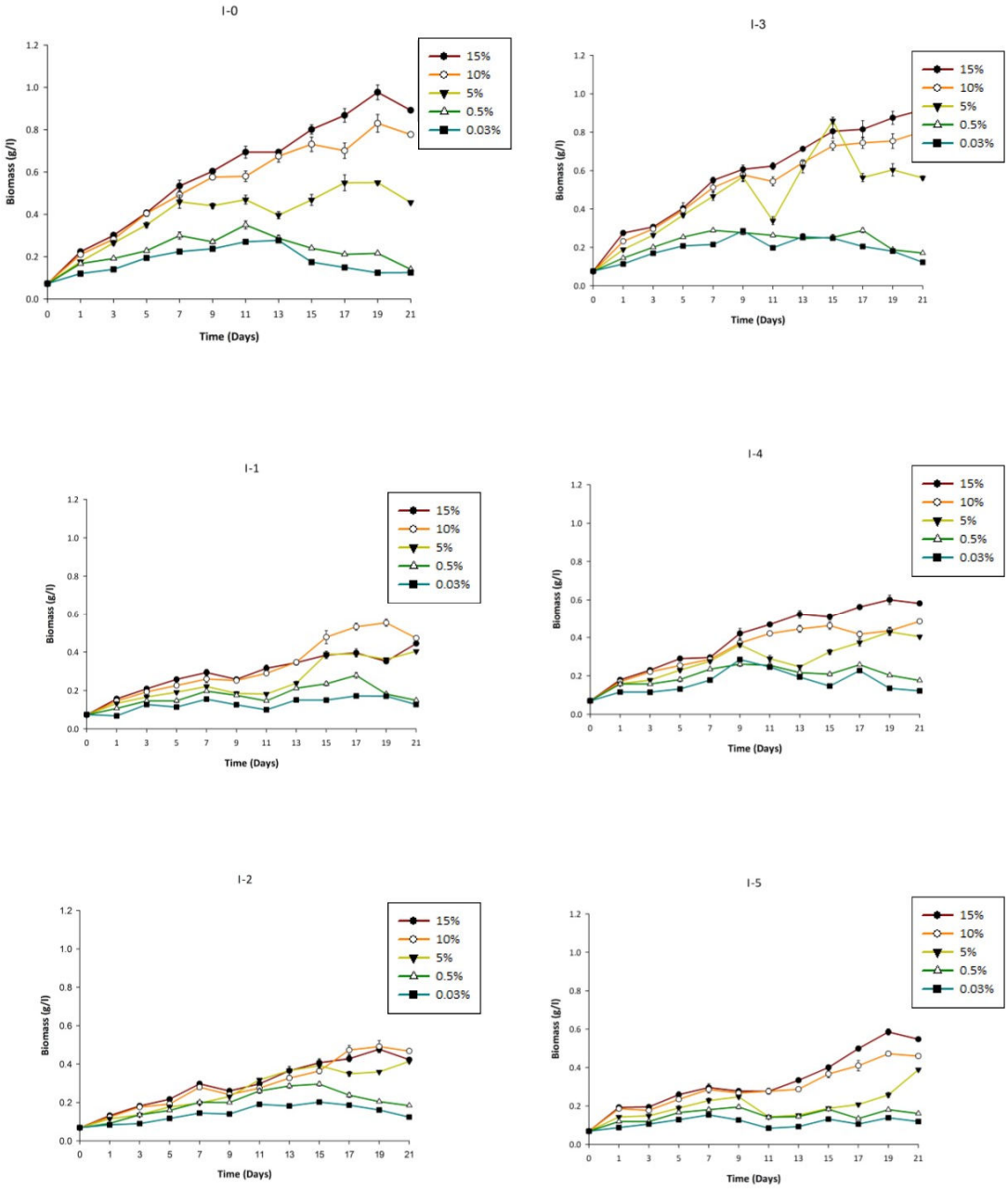

Figure 8: Effect of $NaHCO_3$ (0.05 - 2 g/l) on the growth of the reference and five indigenous strains. Shaded squares (blue) = 0.05 g/l (control), triangles (green) = 0.2 g/l, inverted shaded triangles (yellow) = 0.6 g/l, circles (orange) = 1 g/l, shaded circles (red) = 2 g/l.

Table 9: Logistic model parameters of the microalgal strains at different concentrations of $NaHCO_3$ (0.05 - 2 g/l)

$NaHCO_3$ (g/l)	**Isolates**	μ_{max} **(d^{-1})**	B_{max} **(g/l)**	r^2
0.05 (control)	I-0	0.07	0.154	0.975
	I-1	0.136	0.097	0.836
	I-2	0.19	0.088	0.84
	I-3	0.099	0.153	0.989
	I-4	0.207	0.088	0.877
	I-5	0.343	0.080	0.725
0.2	I-0	0.225	0.162	0.943
	I-1	0.146	0.145	0.952
	I-2	0.101	0.191	0.972
	I-3	0.17	0.222	0.993
	I-4	0.117	0.125	0.918
	I-5	0.289	0.11	0.777
0.6	I-0	0.232	0.536	0.987
	I-1	0.294	0.259	0.945
	I-2	0.221	0.366	0.977
	I-3	0.332	0.506	0.978
	I-4	0.27	0.419	0.992
	I-5	0.265	0.268	0.936
1	I-0	0.298	0.644	0.979
	I-1	0.369	0.336	0.938
	I-2	0.259	0.475	0.955
	I-3	0.416	0.759	0.966
	I-4	0.314	0.545	0.984
	I-5	0.304	0.341	0.91
2	I-0	0.356	0.836	0.975
	I-1	0.403	0.340	0.947
	I-2	0.237	0.497	0.964
	I-3	0.408	0.774	0.969

I-4	0.323	0.543	0.985
I-5	0.314	0.344	0.914

The logistic model was applied to describe the microalgal growth (Table 9). The μ_{max} of strain I-0 increased with an increase in $NaHCO_3$ concentration and reached 0.36 d^{-1} at 2 g/l ($r = 0.862$, $p = 0.061$). When supplied with $NaHCO_3$ concentrations up to 1 g/l, the other indigenous strains showed an increase in growth performance. However, when these strains were supplied with 2 g/l $NaHCO_3$, no significant difference in growth rate was exhibited. For example, μ_{max} of strain I-4 increased from 0.12 to 0.31 d^{-1} ($r = 0.953$, $p = 0.196$), as well as B_{max} elevated from 0.125 to 0.545 g/l ($r = 0.974$, $p = 0.145$) with an increase in $NaHCO_3$ concentration from 0.2 to 1 g/l, respectively. However, a further increase in $NaHCO_3$ concentration to 2 g/l did not enhance the growth performance, where μ_{max} and B_{max} remained steady at 0.32 d^{-1} and 0.543 g/l, respectively.

It should be noted that at each $NaHCO_3$ concentration, either the reference strain (I-0) or the indigenous strain I-3, yielded the highest biomass. For example, at high concentrations of $NaHCO_3$ (2 g/l) strains I-0 and I-3 achieved the highest B_{max} of 0.836 and 0.774 g/l, respectively (Table 9). This revealed that strain I-3 was successfully adapted to the cultivation conditions of the experiments. Other strains showed lower B_{max} values (between 0.34 and 0.54 g/l) when cultivated with a concentration of 2 g/l $NaHCO_3$, implying extreme stress when compared with the reference strain I-0.

According to the findings from this study, addition of $NaHCO_3$ (0.6 - 1 g/l) was found to improve the photosynthetic activity of the studied microalgal cultures, enabling them to reproduce at a faster rate, hence achieving a higher biomass yield within a shorter cultivation

time. The lower biomass concentrations detected at $NaHCO_3$ concentrations of 0.05 - 0.2 g/l implied that this range limits photosynthesis and subsequently microalgal growth.

The statistical significance in biomass production values among the strains at each $NaHCO_3$ concentration was determined by applying the Tukey's post hoc test (Appendix A). This test revealed that at a high $NaHCO_3$ concentration (2 g/l) there was no significant difference ($p > 0.05$) in biomass production values of I-0 (reference strain) and I-3.

$NaHCO_3$ can easily dissolve in water to form different carbon species (H_2CO_3 at pH 4.5 or HCO_3^- at pH 8.5 or CO_3^{-2} at pH higher than 8.5), which can be utilised by microalgae (Devgoswami *et al*., 2011). Lower biomass yield of some isolates can be attributed to the low diffusion of bicarbonate ions across their cell membranes.

Lam and Lee, 2013 conducted an experiment to study the effect of using $NaHCO_3$ as a resource to grow *Chlorella vulgaris*. They found that the microalgae yield was enhanced from 0.043 to 0.112 d^{-1} when $NaHCO_3$ increased from 0.05 to 0.3 (g/l). Results from their study showed that at 0.3 g/l $NaHCO_3$, the highest biomass yield achieved was 0.27 g/l at a pH of 4 and 0.089 g/l at a cultivation pH of 8.5.

When comparing CO_2 and $NaHCO_3$ as carbon sources, the latter induced an overall slower microalgal growth rate and lower biomass production. For example, the highest B_{max} of strains I-1 and I-5, during CO_2 addition were 1.7 fold and 1.8 fold higher than during cultivation with $NaHCO_3$ (Tables 8 and 9). Additionally, the μ_{max} of I-3, I-4 and I-5 at the optimum CO_2 concentration (5 - 10%) was higher compared to cultivation with $NaHCO_3$ concentration of 0.6 - 1 g/l.

Although many microalgae are able to utilise different sources of organic carbon for growth, CO_2 still remains the main source of carbon for the majority under illuminated conditions (Chinnasamy *et al*., 2009). This could be attributed to the fact that it is often difficult for bicarbonate ions to diffuse across cell membranes (Yue and Chen, 2005). The enzyme CA, present on the surface of microalgae cells, converts the bicarbonate ions to CO_2 which is subsequently transported into the cell for assimilation (Anjos *et al*., 2013). This additional step in the carbon concentrating pathway could possibly reduce the photosynthetic activity of microalgae, causing them to reproduce at a slower rate (Chinnasamy *et al*., 2009).

It was found that at each CO_2 or $NaHCO_3$ concentration, either the reference strain (I-0) or the indigenous strain I-3, yielded the highest biomass. Additionally, the μ_{max} and B_{max} of strain I-3 were higher than other strains, even at elevated concentrations of carbon sources. Strain I-3 displayed remarkable tolerance to high levels of carbon (15% CO_2) under un-optimised cultivation conditions. Therefore, further optimisation of physicochemical parameters (media components and light) could possibly lead to higher CO_2 uptake rates in this strain. In a study by Gibbin and Davy (2014), *Aiptasia* sp. displayed increased densities when compared to the control group at high and intermediate levels of CO_2 exposure. Moderate increases were initially observed during intermediate CO_2 concentrations (5 - 15%), however by the end of the experiment densities were 32% higher relative to the control group. A greater cell density was noted during exposure to high CO_2 concentrations, leading to an 81% increase by the end of experimentation (Gibbin and Davy, 2014).

Carbon dioxide uptake rates of the microalgal strains at varying $NaHCO_3$ levels (g/l) are depicted in Figure 9. At low $NaHCO_3$ concentrations of 0.05 - 0.2 g/l all 6 microalgal strains displayed similar uptake rates with no significant difference ($p > 0.05$). A similar observation

for uptake rates was noted for the CO_2 study. The highest uptake rate (0.0161 g/day) was observed for strain I-0 at 2 g/l $NaHCO_3$. This rate was closely followed by strain I-3, which had a rate of 0.0155 g/day at 2 g/l $NaHCO_3$. At the highest CO_2 concentration (2 g/l), strain I-1 had the lowest CO_2 uptake rate of 0.0051 g/day. At the highest $NaHCO_3$ concentration (2 g/l), strain I-0 had a 2.2 fold increase in uptake rate when compared to strain I-1.

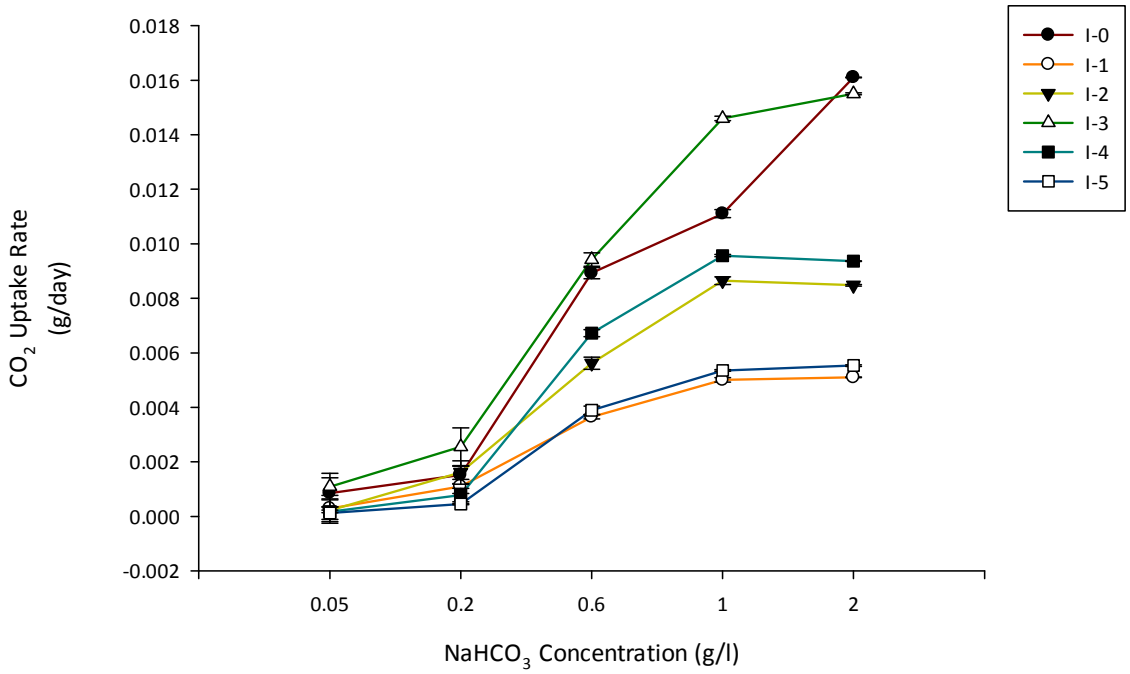

Figure 9: CO_2 uptake rate of microalgal strains at varying $NaHCO_3$ concentrations (g/l).

3.3.4 Relative Electron Transport Rate (rETR) at the Different CO_2 Concentrations

In general, the isolates showed an increase in rETR at all CO_2 concentrations over the first nine days of cultivation (Figure 10). This could be attributed to a successful acclimatisation of the microalgal strains to the new environment. Following that, the rETR attained a steady state between days nine to fifteen before decreasing. At $CO_2 > 10\%$ it was observed that the rETR diminished earlier for some strains. For example, on day 18, the rETR of strain I-2 declined to 0 at a CO_2 concentration range of 10 - 15%, while a value of 10.58 was recorded when subjected to 5% CO_2. A decline in rETR to a value of 0 implies that this strain is quickly approaching or has already entered the death phase (Ramanna *et al*., 2014). Other strains, such as I-1, showed a decline in rETR values after day 15, indicating physiological stress.

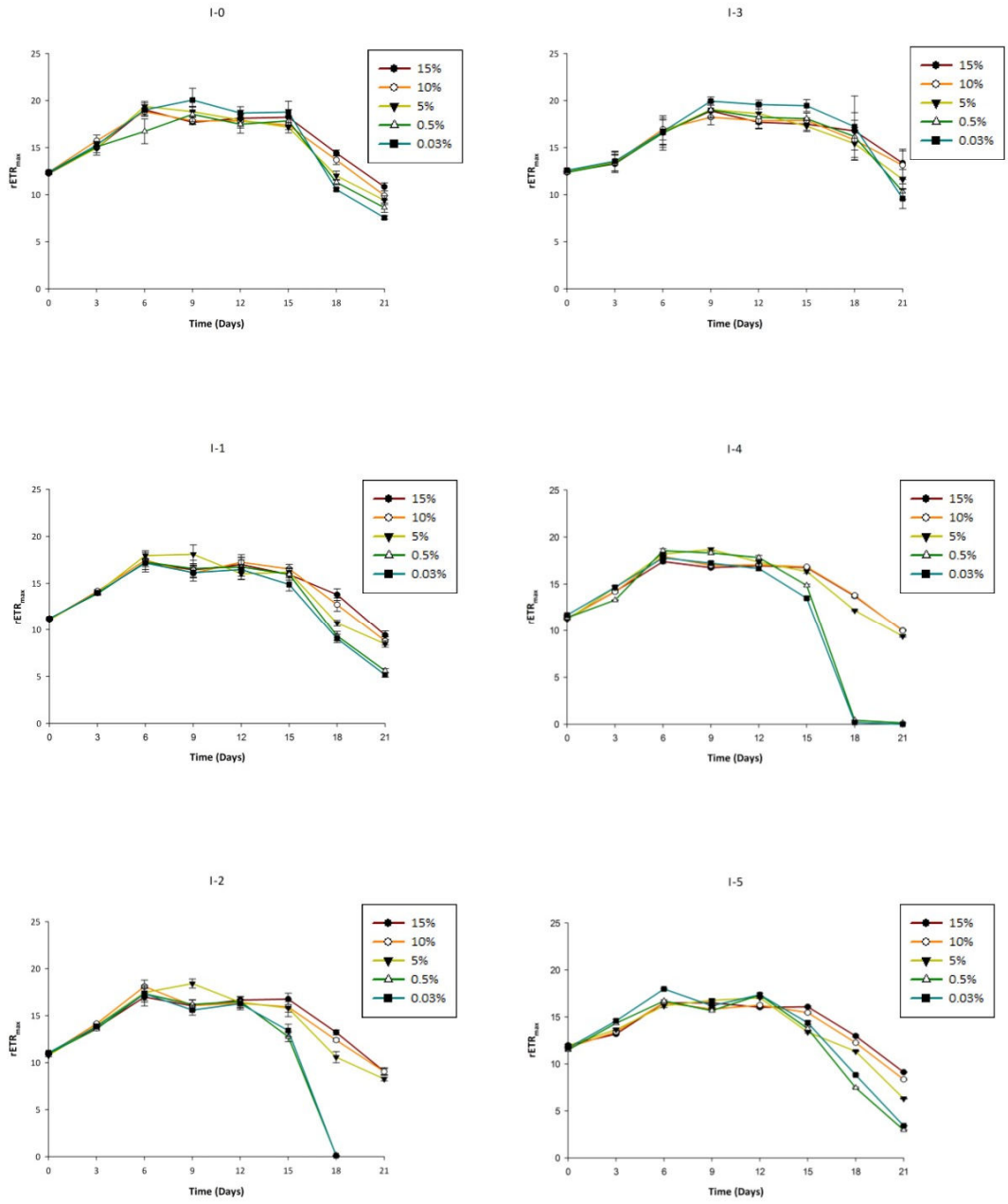

Figure 10: Maximum relative electron transport ($rETR_{max}$) at different CO_2 concentration (0.03 - 15%). Shaded squares (blue) = 0.03% CO_2 (control), triangles (green) = 0.5% CO_2, inverted shaded triangles (yellow) = 5% CO_2, circles = (orange) 10% CO_2, shaded circles (red) = 15% CO_2.

The reference strain I-0 and strain I-3 displayed the highest $rETR_{max}$ during 15% CO_2, equivalent to values of 20.07 and 18.10, respectively (Figure 10). These results were in accordance with the highest B_{max} recorded (Table 8) during 15% CO_2, demonstrating a lower degree of stress at higher CO_2 concentrations. Some strains displayed varying behaviour. For example, $rETR_{max}$ of I-1 and I-2 peaked at 5% CO_2 with values of 18.10 and 18.42, respectively, after which it declined (r = - 0.911, p = 0.271 for I-1 and r = - 0.862, p = 0.338 for I-2) with a further increase in CO_2 concentration to 15%. For strain I-5, the $rETR_{max}$ increased significantly until a CO_2 concentration of 15% (r = 0.993, p < 0.001), indicating favourable environmental conditions at a higher CO_2 concentration.

3.3.5 Relative Electron Transport Rate (rETR) at the Various $NaHCO_3$ Levels

When the strains were subjected to different $NaHCO_3$ concentrations, they exhibited similar trends in rETR values as those observed during CO_2 exposure (Figure 11). The isolates showed an increase in rETR at all $NaHCO_3$ concentrations within the first 9 days of cultivation, and then remained steady or decreased thereafter. For example, at 0.05 g/l $NaHCO_3$, rETR of strain I-0 increased from 11.79 to 17.55 (at day 9) (r = 0.904, p = 0.096). However, rETR declined to 10.21 with further increase in contact time to 21 days (r = - 0.884, p = 0.047). Strains I-2 and I-4 entered the death phase on day 18 at a $NaHCO_3$ concentration of 1 - 2 g/l.

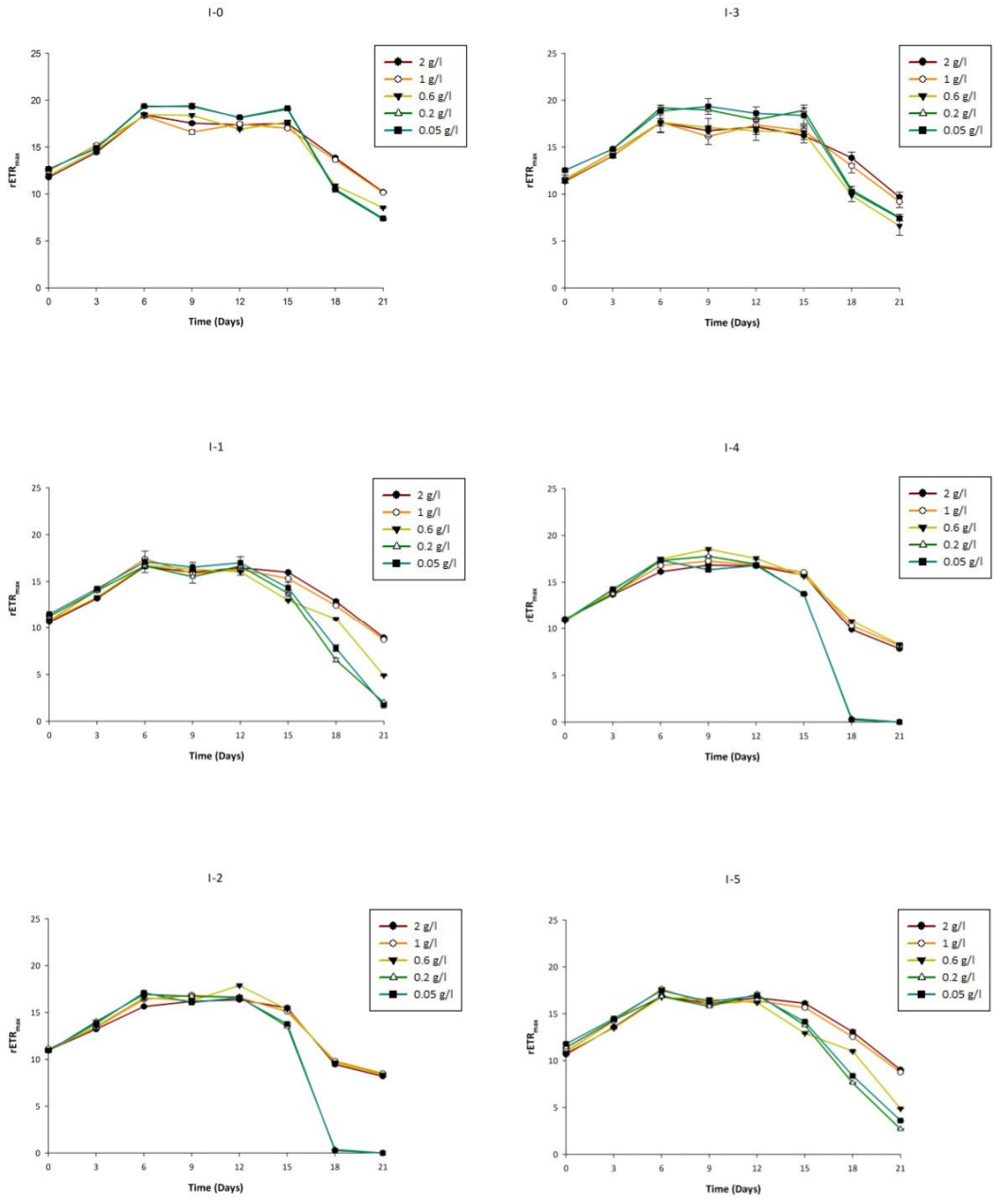

Figure 11: Maximum relative electron transport ($rETR_{max}$) at different $NaHCO_3$ (0.05 - 2 g/l) concentrations. Shaded squares (blue) = 0.05 g/l (control), triangles (green) = 0.2 g/l, inverted shaded triangles (yellow) = 0.6 g/l, circles (orange) = 1 g/l, shaded circles (red) = 2 g/l.

The $rETR_{max}$ of 18.45 for the reference strain (I-0) was recorded at 0.05 g/l, which elevated to 19.42 (r = 0.855, p = 0.145) when $NaHCO_3$ concentration increased to 1 g/l. When compared to cultivation at ambient conditions, strain I-3 showed an 8.8% enhancement in $rETR_{max}$ during cultivation with 1 g/l $NaHCO_3$. This is possibly due to the increased availability of essential elements required for cellular maintenance (White *et al*., 2013). The $rETR_{max}$ of strain I-4 significantly improved from 16.85 to 18.55 with increasing $NaHCO_3$ concentration to 0.6 g/l (r = 0.990, p = 0.013), and thereafter declined to 17.38 with a further increase in $NaHCO_3$ concentration to 2 g/l (r = - 0.918, p = 0.260). A similar trend was observed for I-2. However, $rETR_{max}$ of strain I-5 gradually increased after 0.6 g/l (r = 0.987, p = 0.104), which was possibly due to a greater stress tolerance of the cells.

The PAM results suggested that the photosynthetic apparatus of I-3 was not under much stress at elevated carbon levels, compared to other isolated cultures including the reference strain. Although, rETR of strain I-3 tended to decline, the biomass increased until day 21 of cultivation. This indicates that this strain is capable of being cultured even under conditions of physiological stress. Stress is generally defined as a deviation from nominal conditions for as long as homeostasis permits (Power, 1998). Stressful conditions can include excess or low availability of nutrients, high or low light intensity, high temperature and high salinity (Li *et al*., 2008). In 2014, Gibbin and Davy showed that *Aiptasia* sp. displayed significant increases in photo-physiological parameters with the addition of CO_2. The increased response appeared to be proportional to the amount of CO_2 added and was noticed within 2 - 3 weeks of CO_2 addition (Gibbin and Davy, 2014). In another study, Sutherland *et al*., 2015, used high rate algal mesocosms to study the effects of CO_2 addition along a pH gradient on the growth of wastewater microalgae. They observed that CO_2 augmentation enhanced the rate of $rETR_{max}$

as well as photosynthesis by up to 256%. Increases in photosynthetic rates of the wastewater microalgae led to substantial increases in biomass yields.

3.3.6 Maximum Quantum Yield of the Most Tolerant Strain

(a) (b)

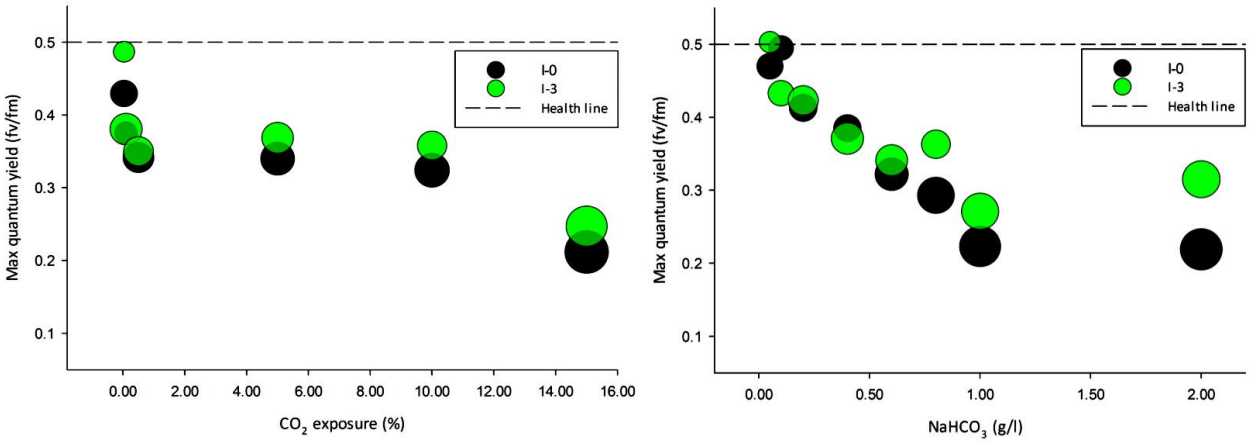

Figure 12: The difference in the maximum quantum yield of PSII (F_v/F_m) for I-0 and I-3 at different (a) CO_2 and (b) $NaHCO_3$ concentrations (a larger bubble represents a greater decrease in the F_v/F_m ratios. Healthy strains have F_v/F_m ratios > 0.5).

Due to the large amount of data generated from the PAM studies, only the reference strain and the isolate I-3 were represented graphically in the F_v/F_m analysis of PSII. Although the microalgal strains displayed high initial F_v/F_m, these readings slowly decreased during the course of the experiment (Figure 12) At CO_2 percentages of 10 and 15%, the F_v/F_m for the reference strain declined by 54.12 and 69.36%, respectively, while I-3 declined by 47.81 and 64.86%, respectively by the end of the experiments (Figure 12). The reference strain (I-0) showed a 42.48, 67.06 and 67.84% decline in F_v/F_m values by the end of experiments during exposure to $NaHCO_3$ concentrations of 0.2, 1 and 2 g/l, respectively. A similar pattern was

noted for I-3. The considerable decline in maximum quantum efficiency suggests that the microalgal strains had neared or entered the death phase (Ramanna *et al*., 2014).

In addition to rETR measurements, stress in microalgae can also be monitored by a decrease in the F_v/F_m. Microalgal cultures having F_v/F_m ratios > 0.5 are in 'good health' (Ramanna *et al*., 2014). Low F_v/F_m (< 0.5) is generally linked with physiological stress, often brought about by the limitations in a carbon source ($NaHCO_3/CO_2$) and other essential nutrients (White *et al*., 2013). During the start of experimentation, the recorded F_v/F_m values at varying CO_2 and $NaHCO_3$ concentrations were > 0.65. Since these values were higher than 0.5, they were regarded as an acceptable physiological acclimation of the microalgal isolates to their environmental conditions (Logothetis *et al*., 2004).

The size of the bubbles in Figure 12 represents the difference in F_v/F_m readings from the start of cultivation to the end. A larger bubble signifies a greater decrease in the maximum quantum efficiency and 'bad health'. At the end of experimentation, although the bubbles of strain I-3 were below the health line, their sizes were smaller than the reference culture. This suggests that the physiology of I-3 was under less stress compared with the reference strain. In 2011, White *et al*. found that $rETR_{max}$ of the control was 45, which declined to 11, 20 and 17 for media lacking nitrates, iron and phosphates, respectively. Additionally, Ramanna *et al*., 2014, found that the highest rETR value reached by cultures growing in 1.5 g/l urea was 15.23 on day 6. They noted that the rETR decreases as the urea concentration increases, which was probably due to nutrient toxicity (Ramanna *et al*., 2014).

3.3.7 Identification of the Most Tolerant Strain

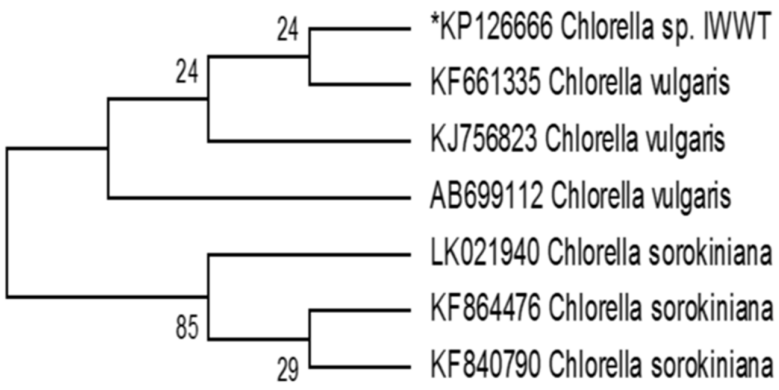

Figure 13: Evolutionary history inferred using the Neighbour-Joining method.

The indigenous strain I-3, which displayed the greatest CO_2 sequestration potential in this study, was identified using ribosomal DNA sequencing and analysis. BLAST searches of the Gen-Bank databases revealed that the obtained sequences were homologous to the ribosomal genes of *C. vulgaris* and C. *sorokiniana* with 99% similarity (Figure 13). The phylogentic tree using the NJ method indicated that the sequence falls into the *Chlorella* cluster (Figure 13). The sequence obtained was deposited in National Center for Biotechnology Information (NCBI) with the accession number KP126666.

Recent studies conducted on *Chlorella* spp. (Anjos *et al*., 2013; Ho *et al*., 2011; Ono and Cuello, 2007) suggest that these species are very promising candidates for the assimilation of CO_2. In 2011, Ho *et al*. reported that *Chlorella* spp. are able to achieve CO_2 consumption rates between 0.73 and 1.79 g L^{-1} d^{-1}. Additionally, Keffer and Kleinheinz, 2002 indicated that *Chlorella* spp. were extremely resilient microorganisms since they were unaffected by the presence of volatile organic compounds in the air stream during CO_2 sequestration.

Increased biomass in the presence of higher CO_2 concentrations might add to the economic utility of this strain in field applications. For example, Yun *et al*., 1997 cultivated *C. vulgaris* in wastewater discharged by a steel-manufacturing plant. This wastewater was selected as the cultivation medium to provide the microalgae with nutrients as well as CO_2. The study achieved CO_2 fixation and ammonia removal of 26.0 g m^3 h^{-1} and 0.92 g m^3 h^{-1}, respectively (Yun *et al*., 1997). Moreover, species with high CO_2 fixation (such as *Chlorella sorokiniana* and *C. vulgaris*) have the ability to minimise the significant costs of flue gas treatment (Ono and Cuello, 2007). The indigenous isolate (I-3) demonstrated a CO_2 fixation rate of 77.0 g m^3 h^{-1} at high CO_2 concentrations and therefore, could be used as a strain of choice for potential scale-up as it shows much promise of been a high CO_2 sequesterer.

CHAPTER FOUR: OPTIMISATION OF ABIOTIC CULTURE CONDITIONS FOR INCREASED BIOMASS PRODUCTION

4.1 INTRODUCTION

Optimal production of *Chlorella* biomass depends on many factors. Abiotic parameters such as light and photoperiods are amongst the most important factors (Dautania and Singh, 2012). These factors affect the growth of *Chlorella* and the composition of the biomass produced by causing changes in metabolism (Raeesossadati *et al*., 2014). Light is the energy source during the photoautotrophic growth phase, where organisms use light energy to convert CO_2 to organic compounds (Long *et al*., 1994). Light intensity, duration and quality are responsible for enhancement of biomass concentrations and overall growth rates, since they influence photosynthesis and the cellular composition of algae (Raeesossadati *et al*., 2014).

The use of conventional methods, advanced modelling and statistical tools can aid in optimising growth conditions. For example, the logistic model is a good choice for explaining the growth curve as it does not require a substrate term for explaining the entire growth profile. The logistic model is used to fit the growth data, leading to a lag phase, an initial exponential growth rate and stationary cell concentration (Schanz and Zahler, 1981).

The present chapter focuses on evaluating different abiotic conditions on the growth of the selected CO_2 tolerant *Chlorella* sp. Although numerous studies have been documented on *Chlorella* sp. pertaining to light intensity and photoperiod, the optimal value varies greatly among *Chlorella* spp. The range of light intensities and photoperiods chosen for this experiment was based on studies from literature (Chang and Yang, 2003; Cheirsilp and Torpee, 2012; Dautania and Singh, 2012; Ho *et al.*, 2011). Furthermore, since this was an indigenous

strain (not purchased from a culture collection) that had adapted to the local climatic conditions, it was imperative that the optimal light intensity and photoperiod be determined for maximum biomass yield.

4.2 MATERIALS AND METHODS

4.2.1 Microalgal Strain and Isolation

A microalgal strain (*Chlorella* strain I-3) was originally isolated from a turbid, saline environment in KwaZulu-Natal, South Africa. The strain was grown and maintained in the best suited medium, ASW, according to Goldman and McCarthy, (1978). Moreover, during culture growth and maintenance the inoculums were adapted to elevated levels of CO_2 (up to 15% CO_2) as discussed in the previous chapter.

4.2.2 Analytical Methods for Growth Determination

4.2.2.1 Light scattering (turbidity)

The microalgal density was determined by absorbance measurements at 686 nm using a Spectrophotometer (SpectroquantR Pharo 300, Merck USA) (Li *et al*., 2008). A wavelength spectrum (400 - 700 nm) was performed to determine the absorbance maxima (λmax) of the microalgal culture. The wavelength spectrum revealed that absorbance should be measured at 686 nm for the selected microalgal strain. Spectrophotometric determinations of biomass were periodically verified by DCW measurements. Correlation between the dry weights of microalgae was taken to measure the growth rate of the *Chlorella* strain I-3.

4.2.2.2 Biomass (dry cell weight)

Biomass concentration was measured as DCW as it is one of the most direct and cost effective means to estimate biomass production. Dry cell weight was estimated using the traditional technique involving sampling, separation, drying and weighing. A 50 ml sample was centrifuged (Heraeus multifuge centrifuge 4KR, USA) at 1509 x g for 15 min at 4^{o}C. The supernatant was discarded and the pellet was washed with 0.05 M HCl and distilled water to remove non-biological adhering materials such as mineral precipitates, and dried at 60^{o}C for 24 h. The watch glasses were cooled in desiccators, and thereafter weighed. Growth kinetics was determined using spectrophotometeric data and biomass yields.

4.2.2.3 Logistic model

A plot of biomass (B) vs time (t) gives a sigmoid variation of biomass as a function of time, displaying lag, exponential and stationary phases of the culture (Kumar and Das, 2012). As the population approaches stationary phase, the rate of growth slows, finally reaching zero (no net growth) at carrying capacity. The logistic model (Eq. 9) was applied to represent the general growth process of the microalgae.

$$\frac{dB}{dt} = \mu_{max} B \left(1 - \frac{B}{B_{max}}\right) \qquad \text{(Eq. 9)}$$

Where: dB/dt is the net rate of increase; B is the biomass of the organism (g/l) at arbitrary time t; μ_{max} is the maximum specific growth rate constant (d^{-1}); B_{max} is the carrying capacity (at the quasi-stationary phase in g/l).

The values of μ_{max} and B_{max} were estimated using a genetic algorithm by creating MATLAB code (M-files). This approach was used rather than other statistical methods due to its simplicity. The validation procedure was carried out using the efficient of determination (r^2-value) between the simulated and the experimental values.

4.2.3 Experimental Set-up

4.2.3.1 Effect of light intensity and photoperiods on the growth of the *Chlorella* strain I-3.

A culture (v/v) of the selected *Chlorella* sp. in the exponential growth phase was inoculated into 250 ml Erlenmeyer flasks containing 200 ml sterilized ASW medium. The cultures were grown according to the previously described section. To study the effects of different light intensities, the cultures were exposed to 40, 80, 125, 175 and 200 μmol m^{-2} s^{-1}. The desired light intensity was obtained by varying the number and distance of Sylvania Gro Lux t12" T5 8W fluorescent tubes (Osram Sylvania, Germany) from the inoculated flasks. Gro-Lux light provides blue and red light in the proportions needed for photosynthesis. Light intensity was measured using a digital lux meter (Major Tech, South Africa). The effects of different photoperiods on the growth of the *Chlorella* sp. were studied by exposing the culture to different light:dark periods (hours) (8:16, 12:12, 16:8 and 24:0).

4.3 RESULTS AND DISCUSSION:

Light intensity is an important environmental parameter that affects microalgal cultivation. Different light intensities of 40, 80, 125, 175 and 200 μmol m^{-2} s^{-1} were tested to study their effect on the growth of the *Chlorella* sp. Other environmental conditions such as light:dark period and temperature were kept constant at 16:8 and 25°C, respectively.

Table 10: Estimated logistic model parameters (μ_{max} and B_{max}) at different light intensities and light:dark cycles

	μ_{max} (d^{-1})	B_{max} (g/l)	r^2
Light intensity (µmol m^{-2} s^{-1})			
40	0.308	0.594	0.977
80	0.308	0.797	0.981
125	0.271	1.298	0.991
175	0.295	1.762	0.986
200	0.268	1.481	0.988
Light:dark cycles			
8:16	0.282	2.058	0.985
12:12	0.283	1.333	0.985
16:8	0.282	2.514	0.998
24:0	0.340	0.652	0.989

Sylvania Gro Lux t12" T5 8W fluorescent tubes (Osram Sylvania, Germany) were used as Gro lux light provides blue and red light in adequate proportions required for photosynthesis. Studies have demonstrated that growth under red light (600 - 700 nm) induces PSII relative to PSI. While exposure to blue light (400 - 500 nm) enhances PSI (Ho *et al*., 2011; Ravelonandro *et al*., 2008; You and Barnett, 2004). Therefore, fluorescent tubes that are able to provide both blue and red wavelengths are more suitable than others for microalgal cell growth and CO_2 mitigation as PSI and II require photon energy associated with both these wavelengths (Ho *et al.*, 2011). Sylvania Gro lux radiates energy in the far-red (700 - 800 nm), red (600 - 700 nm) as well as blue (400 - 500 nm) regions of the spectrum. The use of these tubes produces results comparable to the combined use of cool white fluorescent and incandescent lamps. Hence, by using this single fluorescent source, the need for the colour of incandescent lamps is eliminated and temperatures can be better controlled.

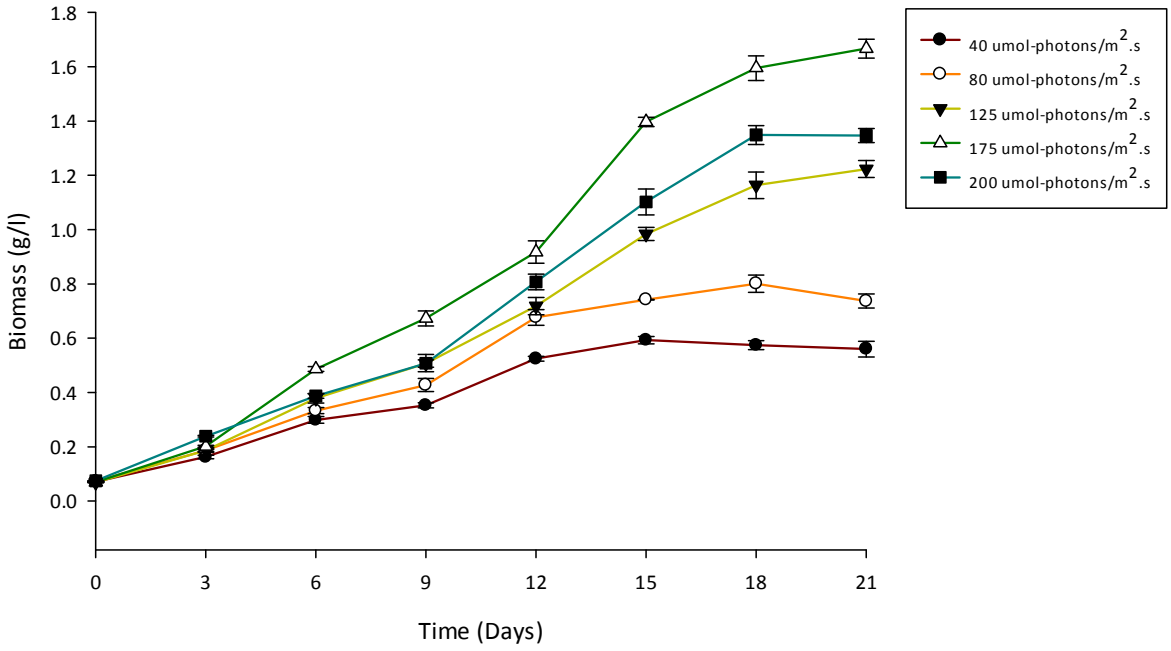

Figure 14: The effect of varying light intensities (40, 80, 125, 175 and 200 µmol m^{-2} s^{-1}) on the biomass production of the *Chlorella* strain I-3. Each value is the mean value of three trials. Error bars indicate standard deviations.

The logistic model was proposed for describing the microalgal growth profile. As listed in Table 10, the logistic model tracked the experimental data in good agreement with an efficient of determination (r^2) of 0.977 - 0.991. This high r^2-value indicated that the logistic model was highly suitable for explaining the microalgal growth with minimal error. Furthermore, the Pearson's correlation coefficient was used to measure the strength of the linear relationship between light intensity and B_{max}. Pearson's *r*-value can range from -1 (perfect negative linear relationship) to 1 (perfect positive linear relationship). U_{max} and B_{max} are not expected to correlate positively as U_{max} represents the specific growth rate which is related to concentrations of limiting nutrients, whereas B_{max} is a value that depicts the maximum biomass produced

during the length of time that the U_{max} was able to maintain. A correlation between the length of U_{max} to the B_{max} value can be positive, however one cannot specifically relate U_{max} to B_{max}.

It was found that, an increase in light intensity from 40 to 175 µmol m^{-2} s^{-1} resulted in an enhancement of B_{max} from 0.594 to 1.762 g/l, respectively (r = -0.9921, p = 0.0079). However, a further increase in light intensity to 200 µmol m^{-2} s^{-1} did not improve the growth and B_{max} dropped to 1.481 g/L. Accordingly, the highest B_{max} from the logistic model (1.762 g/l) was detected at a light intensity of 175 µmol m^{-2} s^{-1} (Figure 14). The simulated B_{max} of 1.762 g/l was close to the experimental maximum biomass concentration (1.67 g/l) (Figure 14) obtained at 175 µmol m^{-2} s^{-1}. This value was 3.0, 2.2, 1.4 and 1.2 fold higher than B_{max} at 40, 80, 125 and 200 µmol m^{-2} s^{-1}, respectively. However, no significant variation ($p > 0.05$) was observed in the μ_{max} for this experiment, where it ranged between 0.268 and 0.308 d^{-1}. Accordingly, in this study, the optimum light intensity of 175 µmol m^{-2} s^{-1} was selected based on B_{max} values.

B_{max} is the maximum microalgal biomass concentration that can be supported at particular experimental conditions without any significant negative impact on the microalgal population. It was observed that the B_{max} of the *Chlorella* sp. increased when the light intensity was raised to 175 µmol m^{-2} s^{-1} (Table 10). A further increase in light intensity did not encourage the growth of this strain, and a slight decrease in B_{max} was noticed. This indicates that the photosynthetic system eventually reaches a saturation point whereby any further increases in light intensity will either result in no benefit or may cause a decline in biomass productivity. Thus, to support maximum biomass production, it is imperative that the microalgal cells do not receive insufficient or excess amounts of light.

The intensity of light is an important parameter affecting microalgal growth. However, an increase in light intensity above the optimal range has been known to cause photoinhibition and photooxidative damage to the culture (Dautania and Singh, 2012). Every microalga has a unique requirement for light intensity. For example, in a study by Chang and Yang (2003), *Chlorella* sp. NTU-H25 displayed high growth rates at light intensities between 589 - 912 µmol m^{-2} s^{-1}. However, the growth rate of this *Chlorella* strain declined during exposure to lower light intensities of 190 - 293 µmol m^{-2} s^{-1}. Additionally, the effect of light intensity on the growth of a marine *Chlorella* sp. was investigated by Cheirsilp and Torpee (2012). Results from their study showed that the growth of the *Chlorella* sp. increased when the light intensity was increased from 28 - 112 µmol m^{-2} s^{-1}. However, any further increases in light intensity higher than 112 µmol m^{-2} s^{-1} did not promote growth of this microalgal strain.

In the next experiment, the *Chlorella* sp. was cultivated at different light:dark cycles of 8:16, 12:12, 16:8 and 24:0. Light intensity and temperature were maintained at constant values of µmol m^{-2} s^{-1} and 25°C, respectively. The effect of light:dark periods on the biomass production is summarised in Table 10. The logistic model was found to give reasonably good fit with all the experimental results (r^2: 0.985 - 0.998). At the optimum light:dark cycle of 16:8, logistic constants B_{max} and μ_{max} were 2.514 g/l and 0.282 d^{-1}, respectively. The highest B_{max} was 1.2, 1.9 and 3.9 times higher than those at light:dark cycles of 8:16, 12:12 and 24:0, respectively. However, there was no statistically significant difference ($p > 0.05$) between the μ_{max} when subjected to the different light:dark periods.

Our results showed that the optimum light:dark cycle was 16:8. At this photoperiod, the highest biomass yield (2.29 g/l) was recorded on day 21 (Figure 15). Light is essential for algal generation times however, excessive periods of light inhibit cell division (Dautania and Singh,

2012). Thus, B_{max} declined during a light:dark period of 24:0, producing the lowest biomass of 0.633 g/l on day 21 (Figure 15). This can be due to the fact that excess light can cause photooxidation reactions and/or formation of reactive O_2 species such as hydroxyl radicals, singlet oxygen, superoxide radicals and hydrogen peroxide (Kumar *et al*., 2012). In 2012, Dautania and Singh reported that when exposed to continuous light, the growth of *Anacystis nidulans* was greatly hindered owing to photoinhibition and photooxidation.

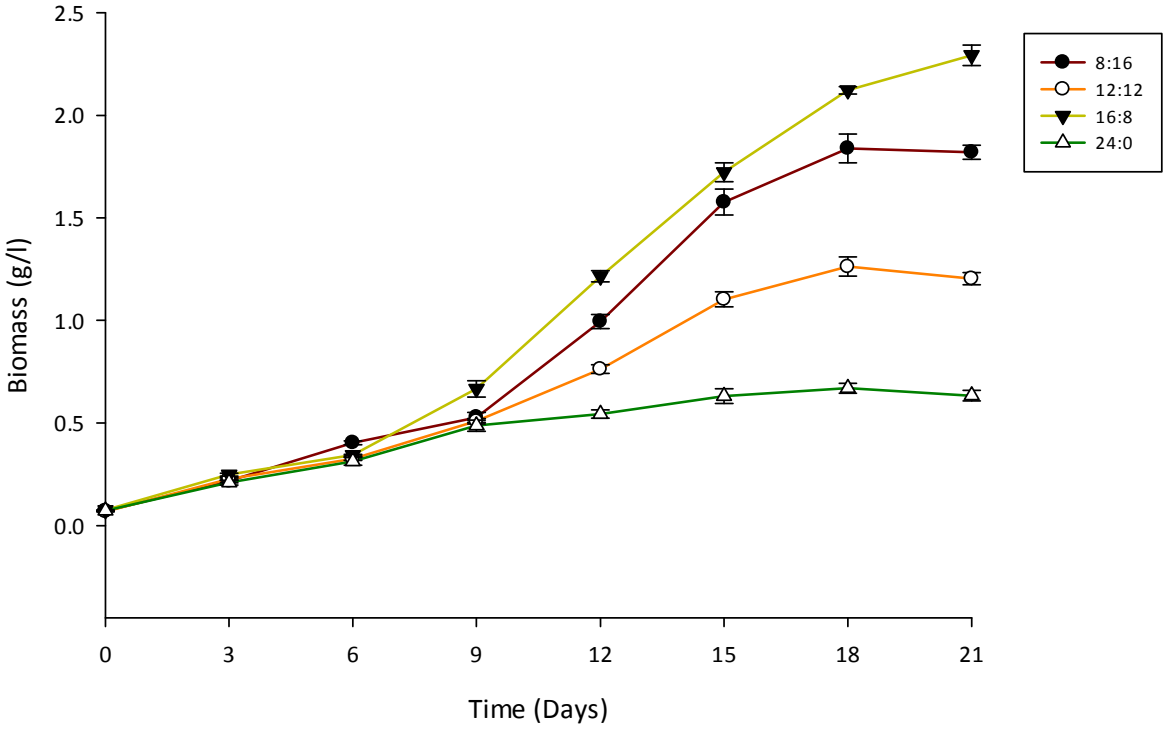

Figure 15: The effect of varying photoperiods (8:16, 12:12, 16:8 and 24:0) on the biomass production of the *Chlorella* strain I-3. Each value is the mean value of three trials. Error bars indicate standard deviations.

CHAPTER FIVE: OPTIMISATION OF NUTRIENT COMPOSITION FOR INCREASED BIOMASS PRODUCTION USING THE ONE-FACTOR-AT-A-TIME-APPROACH AND DESIGN OF EXPERIMENTS

5.1 INTRODUCTION

Researchers involved in CO_2 biofixation studies using microalgae aim to achieve high biomass yields which ultimately lead to high CO_2 fixation rates (Chang *et al*., 2016). To enhance microalgal biomass production, it is important that microalgae are grown under optimised abiotic parameters (light intensity and photoperiods) as well as nutrient conditions (medium composition) (Chang *et al*., 2016; George *et al*., 2014).

The optimal combination of major and minor nutrients are necessary to provide the minimum quantity of nutrients to support maximum growth (Crofcheck *et al*., 2012). Not only do nutrient deficiencies induce decreased microalgal cell growth rates, but they are also responsible for lower CO_2 fixation rates (Crofcheck *et al*., 2012). It is therefore imperative that the most appropriate nutrients and suitable quantities be selected for the strain of choice as this will directly influence biomass yield and eventual CO_2 uptake.

Over the years, numerous culture media with varying nutrient quantities have been formulated and used for isolation and cultivation of microalgae. Certain microalgal species can be cultivated in a simple mineral medium, whereas others require a more complex growth medium containing essential nutrients, vitamins and trace elements to sustain growth (Ernst *et al.*, 2005; Singh *et al.*, 2009). Major nutrients such as nitrate, phosphate, magnesium and potassium are essential for the formation of various structural and functional components of cells. Whereas, minor nutrients or trace elements (iron, copper, cobalt, manganese, zinc and molybdenum)

often act as cofactors for enzymes involved in various metabolic pathways (Ernst *et al.*, 2005; Singh *et al.*, 2009).

Conventional medium optimisation is achieved by OFAT; whereby a single factor is varied while keeping all others at a constant specific level (Singh *et al.*, 2009). Design of experiments is also a popular tool which has recently been applied for medium optimisation of microalgae. This entails a planned approach which determines the causes and effects on relationships including interactions of different nutrient combinations (Anderson and Whitcomb, 2005). Common DOE techniques use a limited number of experiments to screen between five and ten variables. This process allows for several medium components to be simultaneoulsy compared while their effects are analysed, which are then ranked based on observed properties or parameters.

Hence the objective of the present chapter was to evaluate the influence of different nutrients at varying concentrations on the growth of the *Chlorella* strain I-3 using OFAT and DOE techniques.

5.2 MATERIALS AND METHODS

5.2.1 Screening of Media for Cultivation of the *Chlorella* strain I-3

The selected *Chlorella* sp. was sub-cultured in seven different media: ASW (Watanabe *et al*., 1992; Watanabe *et al*., 2000) (Appendix B), Blue Green medium (BG11) (Watanabe *et al*., 2000) (Appendix C), Natural Seawater (NSW) (Watanabe *et al*., 2000) (Appendix D), L1 (Guillard and Hargraves, 1993) (Appendix E), Allen and Arnon Medium (Allen and Arnon, 1955) (ATCC 1142) (Appendix F), f/2 (Guillard and Ryther, 1962) (Appendix G) and f/2 + Si

(Guillard, 1975) (Appendix H). Growth medium was prepared and subsequently transferred into 250 ml *Erlenmeyer* flasks. Prior to inoculation, flasks containing media were sterilised by autoclaving at 121°C for 15 min and then allowed to cool. Thereafter, a 10% v/v pure culture of the *Chlorella* sp. (in the exponential growth phase) was inoculated into each medium. Flasks were exposed to an irradiance of 175 µmol m^{-2} s^{-1} using Sylvania Grolux 12" T5 8W fluorescent tubes (Osram Sylvania, Germany), a light dark-cycle of 16:8 h and a temperature of 25±1 °C on an orbital shaker at 90 rpm. Experimentation for each medium was carried out in triplicate.

5.2.2 Preliminary Study: One-Factor-at-a-Time Approach to Determine Effects of Medium Components on Biomass Production

Based on the results, the most appropriate medium for cultivation of the *Chlorella* sp. was ASW. An OFAT approach was applied to evaluate the effect of individual ASW medium components at varying concentrations on biomass production. Concentrations were varied based on the original suggested medium. The results from this study were used to establish the concentrations of medium components for the FFD.

5.2.3 Statistical Experimental Designs

Statistical experimental designs; involving (i) FFD and (ii) CCD were applied to screen and optimise the nutrient variables (ASW culture medium) that influence biomass production of the *Chlorella* sp. as one or more nutrients and its concentration levels may significantly affect the production (Jeong *et al*., 2008). Screening of factors was achieved using FFD in order to ascertain which factors had the greatest effect on biomass production. The selected factors were

then further optimised using RSM which comprised of a three-factor CCD. The statistical programme, Design Expert 8.0.7.1 Software (Stat-Ease Inc., Minneapolis, Minnesota, USA) was used in the experimental design, quadratic model building, and data analysis. This program produced a matrix of factors which allowed us to investigate the effect of each component on the biomass production in an effort to optimise the culture medium. Statistical analyses of results generated a mathematical model for each experiment. The FFD model was necessary to guide the direction in which concentrations of media components should be adjusted (Jeong *et al*., 2008; Suzuki *et al*., 2009).

5.2.3.1 Fractional factorial design (FFD)

Fractional factorial design is a popular statistical tool that can be used to screen significant factors in a growth medium (Jeong *et al*., 2008). Factors were selected on the basis of preliminary OFAT experiments. Eight nutrient factors at varying concentrations were studied, namely: $Na_2SiO_3.9H_2O$, $NaNO_3$, NaH_2PO_4, NaCl, trace metals, Fe-EDTA, anhydrous salts and hydrous salts. Five center points were chosen for the FFD. Center points are important as they estimate error within an experiment and also provide a quality check on the accuracy of the experiment. A resolution IV FFD was selected with $2^{8-4} = 16$ experiments and 5 center points, giving a total of 21 runs. Run order represents the random order of each run, while standard order sorts the experiment into 16 runs and 5 center points. A full factorial design was not used as this would have led to a remarkable large number of runs excluding center points ($2^8 = 256$). The experimental design showing concentration and levels of the variables utilised is given in Table 11. The experimental design is shown in Table 12. All required chemicals were purchased from Sigma-Aldrich® (South Africa).

Table 11: Independent variables and concentration levels in the fractional factorial experiment indicating low, high and center points

Symbol	Factor	Units	Coded Variable		
			-1	0	+1
X_1	$Na_2SiO_3.H_2O$	g/l	0.61	0.905	1.2
X_2	$NaNO_3$	g/l	0.3	0.45	0.6
X_3	NaH_2PO_4	g/l	0.04	0.065	0.09
X_4	NaCl	g/l	30	45	60
X_5	Trace metals	ml/l	0.15	0.325	0.5
X_6	Fe-EDTA	ml/l	0.15	0.325	0.5
X_7	Anhydrous salts	ml/l	33	49.5	66
X_8	Hydrous salts	ml/l	66.5	99.75	133

Table 12: Experimental design of FFD0821 with five center points, showing the coded values of the variables and randomised order used to determine the effect of ASW medium components on the biomass production of the isolated *Chlorella* sp.

Std row order	Randomised run order	Factors							
		X_1	X_2	X_3	X_4	X_5	X_6	X_7	X_8
1	6	-1	-1	-1	-1	-1	-1	-1	-1
2	11	1	-1	1	-1	-1	1	-1	1
3	12	-1	1	-1	-1	-1	1	1	1
4	13	1	1	1	-1	-1	-1	1	-1
5	4	-1	1	1	-1	1	1	-1	-1
6	18	1	1	-1	-1	1	-1	-1	1
7	9	-1	-1	1	-1	1	-1	1	1
8	14	1	-1	-1	-1	1	1	1	-1
9	20	-1	1	1	1	-1	-1	-1	1
10	17	1	1	-1	1	-1	1	-1	-1
11	16	-1	-1	1	1	-1	1	1	-1
12	5	1	-1	-1	1	-1	-1	1	1
13	1	-1	-1	-1	1	1	1	-1	1
14	3	1	-1	1	1	1	-1	-1	-1
15	7	-1	1	-1	1	1	-1	1	-1
16	8	1	1	1	1	1	1	1	1
17	2	0	0	0	0	0	0	0	0
18	21	0	0	0	0	0	0	0	0
19	15	0	0	0	0	0	0	0	0
20	10	0	0	0	0	0	0	0	0
21	19	0	0	0	0	0	0	0	0

5.2.3.2 Central composite design (CCD)

Table 13: Independent variables and the concentration levels studied in the optimisation design

Symbol	Factor	Units	Coded Variable				
			-α	**-1**	**0**	**+1**	**+α**
X_2	$NaNO_3$	g/l	0.39	0.60	0.90	1.20	1.40
X_3	NaH_2PO_4	g/l	0.04	0.06	0.08	0.09	0.10
X_6	Fe-EDTA	ml/l	0.41	0.50	0.63	0.75	0.83

Following OFAT and FFD experiments, a CCD was used to optimise the levels of variables with a significant influence on cell growth (biomass production). The biomass production of the *Chlorella* sp. can be written as a function of a response surface (Jeong *et al*., 2008). Response surface methodology based on CCD is a widely accepted method of optimisation. This mathematical and statistical technique allows one to assess the relationship between independent variables and to gauge the response in an effective experimental design (Tasharrofia *et al*., 2011). Central composite design is especially effective for analysis of problems wherein a response of interest is influenced by several significant variables and the ultimate objective is to optimise this response. Data acquired from a CCD is used to fit a polynomial. In order to fit response surfaces, this model consists of a 2^3 factorial design with six replicates at the center point, corner points of coded distance ±1, and axial points of a given distance (Pujari and Chandra, 2000). Axial points need to be of coded distance from the centre in order to achieve rotatability. Rotatability is when the variance has the same value on concentric spheres, adding stability to the variance (Burrows *et al*., 2008). The software calculates the coded distance 'α' for placement on the star points. For this study the programme calculated an α value of 1.682. For the CCD three variables were identified as significant: $NaNO_3$ (X_2), NaH_2PO_4 (X_3) and Fe-EDTA (X_6). The three nutrient components were varied by employing a total number of 20 experiments. Coded and actual values of the variables at the low, centre and high levels as well as two additional points at $\pm\alpha = 1.682$ are given in Table 13. The experimental design is shown in Table 14.

Table 14: Experimental design of a three factor central composite experiment showing coded factor levels with standard order to determine effect of the variables on biomass production

Std row order	Randomised run order	X_2	X_3	X_6
1	12	-1	-1	-1
2	10	+1	-1	-1
3	17	-1	+1	-1
4	9	+1	+1	-1
5	14	-1	-1	+1
6	1	+1	-1	+1
7	19	-1	+1	+1
8	11	+1	+1	+1
9	13	-1.682	0	0
10	7	+1.682	0	0
11	18	0	-1.682	0
12	15	0	+1.682	0
13	3	0	0	-1.682
14	6	0	0	+1.682
15	4	0	0	0
16	16	0	0	0
17	8	0	0	0
18	20	0	0	0
19	5	0	0	0
20	2	0	0	0

5.2.4 Confirmatory Experiment to Determine Validity of Prediction

A confirmatory experiment at different levels of the factors, as suggested by the numerical modeling to support data under optimised conditions was performed. Only one solution for the confirmatory experiment was generated by the programme. The confirmatory experiment was run in triplicate in 100 ml volumes in 250 ml Erlenmeyer flasks. As described previously, a 10% v/v *Chlorella* sp. inoculum within the exponential phase of growth was used. Media composition for the confirmatory experiment was as follows: 0.61 g/l $Na_2SiO_3.9H_2O$, 1.17 g/l

$NaNO_3$, 0.08 g/l NaH_2PO_4, 30 g/l NaCl, 0.15 ml/l trace metal stock solution, 0.53 ml/l Fe-EDTA stock solution, 33 ml/l anhydrous salt stock solution, and 66.5 ml/l hydrous salt stock solution.

5.2.5 Statistical Analysis

The design software package (Design Expert 8.0.7.1.) was utilised in the statistical analysis of data obtained from the FFD and CCD experiments. ANOVA was used to determine the significance of each term in the equations fitted as well as to estimate the goodness of fit in each case.

5.2.6 Model Validation

Each experiment was conducted according to the generated design and results were subsequently recorded. Thereafter, the data set was analysed. In order to determine if data responses can be described using a linear model or if data transformation was required, the ratio of the maximum to minimum response was evaluated. A linear relationship between response and parameters occurs when the maximum to minimum ratio is less than 10. A ratio greater than 10 implies that in order to determine the best fit of the response data to descriptive models an interactive transformation will be required. Usually, a natural log transformation of data or a square-root is sufficient to fit descriptive models (Box *et al.,* 2005).

5.2.7 Model Fit

After experimentation the design expert software was used to compute the 'sequential or extra sum of squares'. This software selected the highest order polynomial, where additional terms are significant. How well the model fits the data is determined by the predicted residual sum of squares (PRESS) statistic. In comparison to the other models under consideration, the PRESS for the chosen model as well as the standard deviation of the error in the design should be small. The determination coefficient (R^2) defines the goodness of fit of the model. The R^2 value is necessary to provide a measure of the variability in the actual response values that could be explained by the experimental factors and their interactions. An ideal case is when a R^2 value is 1 or very close to 1. This implies that 100% of the variation in the observed value can be explained by the model. The responses predicted by the model is referred to as predicted values. These values are obtained by substituting the coded factor levels into the coded model. Residual values are generated by comparing the actual and predicted responses.

5.2.8 Analysis of Variance (ANOVA)

Analysis of variance which is based on the F-test, is a statistical technique that evaluates the significance of the experimental results and assists in understanding the pattern of the mutual interactions between the variables (Somnath and Smita, 2010). It is required for assessment on the adequacy of the fitted model. The significance of each of the coefficients is determined by the *p*-values (Boddy and Smith, 2009).

5.2.9 Diagnostics

The half normal plot is useful for determining what is significant at a quick glance. This, however, should be verified by the ANOVA results. A half normal plot takes the absolute value of the data based on the positive half of the full normal curve, allowing for the normal distribution to fold over to the right of the zero value, thereby permitting the experimenter to view the magnitudes of both positive and negative effects on one axis. Absolute values are more precise for identification of significant outcomes. Curvature can be defined as the measure of the offset at the center point of actual versus predicted values from the model. If this is significant then a quadratic model may be fitted to the data from a response surface design.

5.2.10 Graphs

A pareto chart (acquired from the FFD), ranked effects of the variables according to the greatest effect on the final response. Thus the magnitude and direction of effects on outcomes was conveniently represented in a bar chart. Orange bars represented positive effects, while blue bars represented negative effects. Two different *t*-limits were plotted on this chart (Bonferroni corrected *t* and a standard *t*). Once effects were selected, those that lay above the Bonferroni limit were taken to be definitely significant. Effects that appeared above the *t*-value limit were possibly significant and those that were present below the *t*-value limit were unlikely to be significant (Montgomery, 2005).

In order to illustrate the main and interactive effects of the independent variables on the dependent ones for the CCD, the fitted polynomial equation was expressed in the form of

response surface plots. Analysis of the plots assisted in obtaining the optimal concentrations of the critical variables.

Effects of three factors at a time was represented using the cube plot. This plot predicted values from the coded model for the combinations of the low (-1) and high (+1) levels of any three factors that were selected. Cube plots are useful in determining the steepest ascent or descent of an optimisation experiment.

5.3 RESULTS AND DISCUSSION

5.3.1 Selection of Nutrient Medium

Seven different culture media (ASW, BG11, NSW, L1, ATCC 1142, F/2 and F/2 + Si) with varying chemical compositions were assessed in order to determine which medium was most effective in promoting growth (biomass production) of the *Chlorella* strain I-3.

Results obtained (Figure 16) showed that all the media investigated were able to support the growth of the microalgal strain, giving variable biomass results. Natural seawater was used as the control medium as the selected strain was isolated from a marine environment. Direct use of NSW for microalgal cultivation is rarely acceptable as microalgal yield is often too low without addition of further nutrients and trace metals. This was evident in the study: when cultured in ASW and BG11 media, the biomass concentration obtained was significantly higher ($p < 0.05$) when compared to the control (NSW). An enriched solution (such as ASW or BG11) is usually required for microalgae experimentation and culture maintenance. Enriching a solution refers to the addition of trace elements and macronutrients in order to produce a substantial biomass yield (Berges *et al*., 2001).

In comparison to all media tested, f/2 and f/2 + Si were found to be least effective in promoting growth of the *Chlorella* sp. (yielding 0.309 and 0.440 g/l biomass respectively on day 17). When cultured in BG11 medium, a biomass concentration of 1.276 g/l was obtained on day 17. The maximum biomass of 1.502 g/l was attained on day 17 when grown in ASW. In a study by Kulshreshtha and Singh (2013), *Dunaliella salina* (a unicellular, halophilic, green microalga) was grown using various inorganic media that varied in chemical compositions. It was observed that *D. salina* grew best in ASW when compared to the other media tested (De Walne's media, Johnson's media, AS-100 and Modified Bold's Basal media). They attributed their findings to the fact that ASW is a nutrient rich medium with adequate amounts of the necessary elements required to encourage and support microalgal growth (Kulshreshtha and Singh, 2013).

In the present study, cultivation of the *Chlorella* sp. in ASW produced a 17.69% increase in biomass on day 17 when compared to cultivation in BG11 and a 58.81% increase when compared to cultivation in NSW (Figure 16). Therefore, ASW was selected as a base medium for statistically optimising the biomass production of this microalgal strain, using OFAT, FFD and CCD as statistical tools. Artificial seawater is not only a nutrient rich medium, but also a medium with a high salt concentration (27.960 g/l NaCl). Since the selected *Chlorella* sp. was isolated from a marine environment, the high NaCl concentration of ASW medium could possibly have been one of the important factors that promoted growth of this microalga.

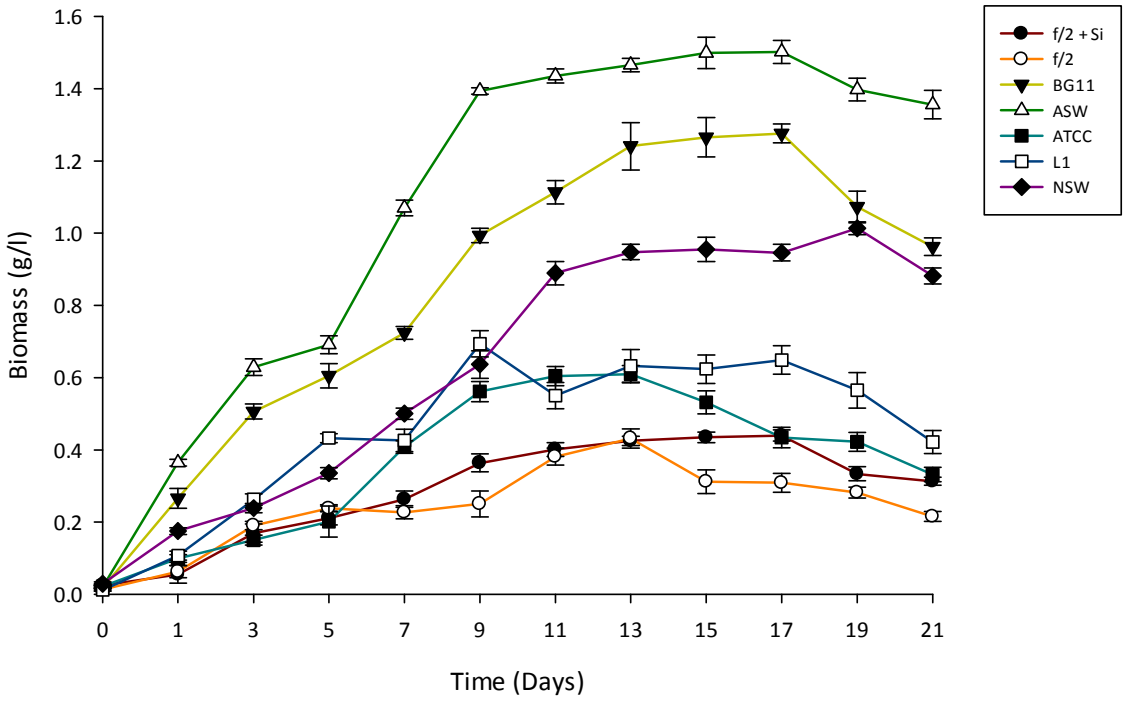

Figure 16: Growth profiles of the *Chlorella* sp. on each nutrient medium investigated over 21 days. Each value is the mean value of three trials. Error bars indicate standard deviations.

5.3.2 Preliminary Study: One-Factor-at-a-Time Approach to Determine Effects of Medium Components on Biomass Production

Although silica is usually only required for the growth of diatoms, it has been known to support the growth of other microalgal species (such as *Chlorella* and *Scenedesmus* spp.) (Ilavarasi *et al.*, 2011). Sodium metasilicate nonahydrate together with $NaHCO_3$ are responsible for maintaining the alkaline buffering within the medium (Ilavarasi *et al.*, 2011). From Figure 17 it can be seen that a gradual increase in $Na_2SiO_3.9H_2O$ concentration (0.304 - 0.912 g/l) encouraged the growth of the *Chlorella* sp. (Figure 17). The microalgae entered the stationary

phase of growth around day 12, and maintained this state up to day 20, thereafter leading to a decline in growth. A $Na_2SiO_3.9H_2O$ concentration of 0.912 g/l proved most effective in promoting growth of the microalga, generating a biomass concentration of 1.987 g/l on day 20 (Figure 17). This was a 5.78% increase in growth when compared to growth at the lowest $Na_2SiO_3.9H_2O$ concentration of 0.304 g/l.

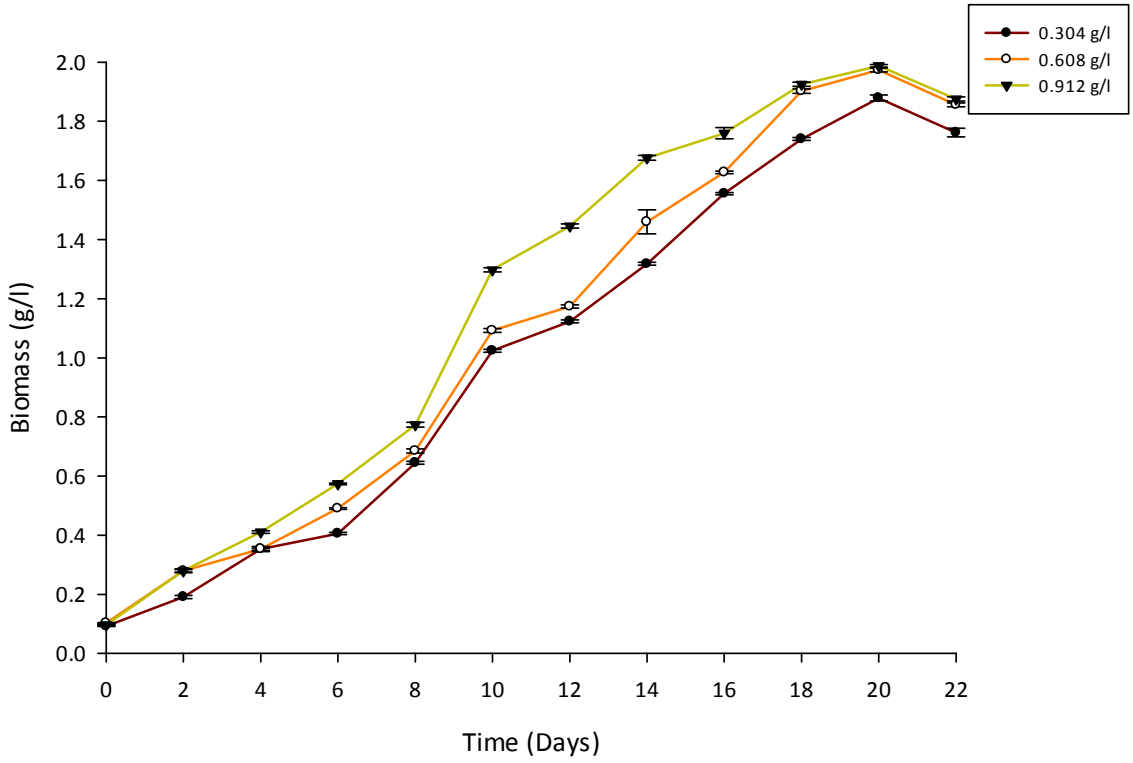

Figure 17: Time-course profiles of cell growth acquired growing in varying concentrations of $Na_2SiO_3.9H_2O$ (in g/l) with all other factors constant. Each value is the mean value of three trials. Error bars indicate standard deviations.

A sufficient concentration of $NaNO_3$ is imperative for microalgal cultivation as nitrate has a central role in protein synthesis, cell physiology and growth. Therefore, increases in $NaNO_3$

concentrations are known to enhance the growth rate of microalgal cultures (Changdong and Azevedo, 2005; Martin-Jezequel *et al*., 2000; Sorensen *et al*., 1996). This was evident in the present study: the gradual increase in $NaNO_3$ concentrations supported a steady increase in cell growth.

A steady increase in growth at the different $NaNO_3$ concentrations (0.150; 0.299 and 0.448 g/l) were observed from days 1 to 20 (Figure 18), thereafter a considerable reduction in microalgal growth occurred between days 20 and 22. A steady decline in cellular reproduction rate ensues when vital nutrients such as N become depleted or limited in the medium (Fields *et al*., 2014). During the exponential and linear phases of growth (days 4-10), $NaNO_3$ concentrations of 0.150 and 0.448 g/l generated comparable biomass values. However, it was noticed that during the stationary phase of growth (days 10-20), 0.448 g/l $NaNO_3$ produced considerably higher biomass yields when compared to cultivation at 0.150 g/l $NaNO_3$.

The highest $NaNO_3$ concentration of 0.448 g/l facilitated maximum growth, enabling the microalga to reach a biomass value of 2.057 g/l on day 20. This was a 9.56% increase in growth (day 20) when compared to the lowest $NaNO_3$ concentration (0.150 g/l). The lowest $NaNO_3$ concentration yielded a biomass value of 1.877 g/l on day 20, while the intermediate $NaNO_3$ concentration (0.299 g/l) resulted in 1.977 g/l biomass been produced.

Nitrate deficiency severely affected all basic metabolic pathways of microalgae as nitrate is a vital constituent for protein synthesis. This ultimately could lead to a reduction in photosynthetic rates which could in turn impede growth and biomass production as shown by Singh *et al*. (2015). This could explain why the lowest biomass value was recorded when the

Chlorella sp. was cultivated at the lowest $NaNO_3$ concentration of 0.150 g/l. This implies that a low nitrate concentration of 0.150 g/l was not sufficient to support growth of the strain under investigation.

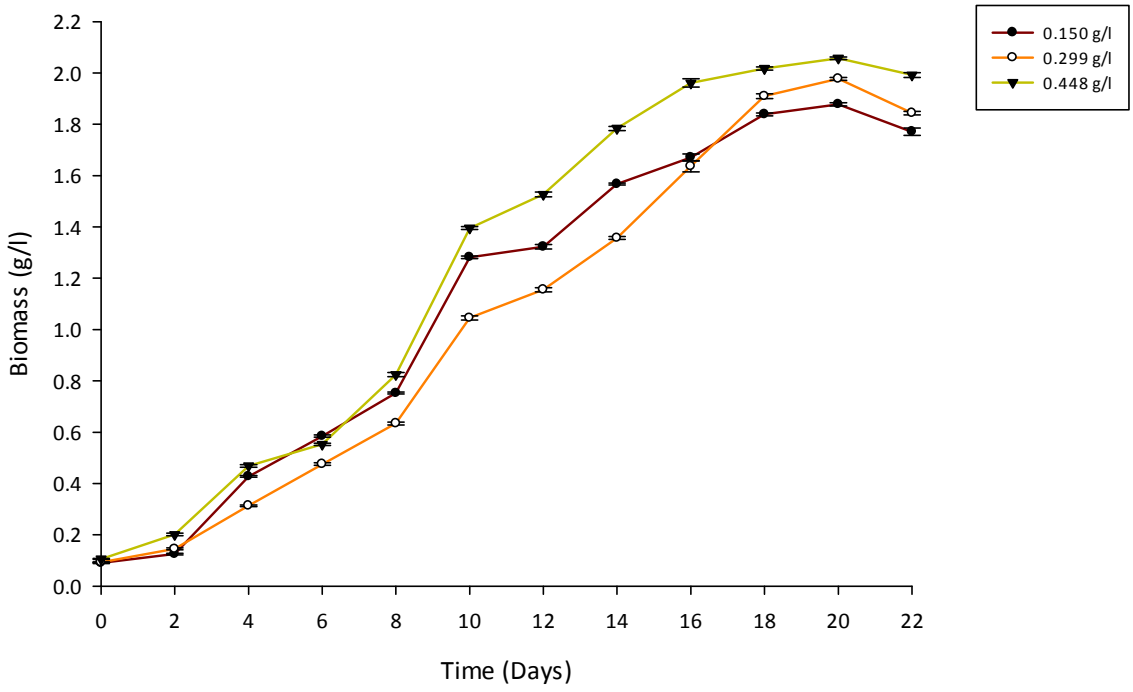

Figure 18: Effects of varying $NaNO_3$ concentrations (in g/l) on the growth of the *Chlorella* sp. over a 22 day duration. Each value is the mean value of three trials. Error bars indicate standard deviations.

From Figure 19, it can be observed that a gradual increase in NaH_2PO_4 concentration (0.013-0.09 g/l) encouraged the growth of the *Chlorella* sp. It was noted that at all NaH_2PO_4 concentrations, the microalga entered the stationary phase of growth around day 14, and

maintained this state up to day 20, thereafter leading to a decline in growth. A NaH_2PO_4 concentration of 0.09 g/l proved most effective in promoting growth of the *Chlorella* sp., generating a biomass concentration of 2.076 g/l on day 20 (Figure 19). This was a 9.55% increase in growth when compared to the lowest NaH_2PO_4 concentration (0.013 g/l) which produced 1.895 g/l biomass on day 20.

Like nitrate, phosphate is a major nutrient that is required for substantial microalgal growth. Phosphate is essential for almost all cellular processes i.e. nucleic acid synthesis as well as high energy generation and transfer within cells (Kulshreshtha and Singh, 2013). Tolerance to phosphate and optimum concentrations vary amongst microalgal species. The average range of NaH_2PO_4 tolerance for most microalgae is 50 µg/l - 20 mg/l) (Becker, 1995).

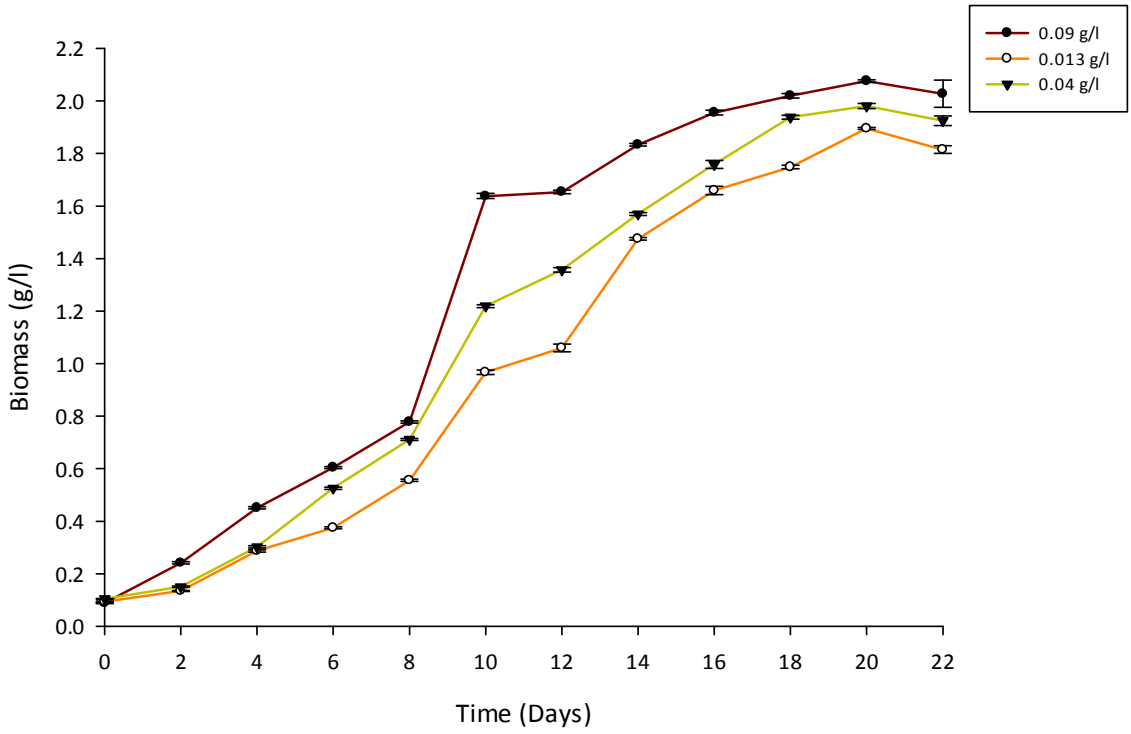

Figure 19: Growth of the *Chlorella* sp. in response to different NaH_2PO_4 concentrations (in g/l) over a 22 day period. Each value is the mean value of three trials. Error bars indicate standard deviations.

Microalgae differ in their ability to tolerate conditions of high salinity. In the present study, growth of the *Chlorella* sp. at different salt concentrations were investigated (30, 60 and 90 g/l). It was important to ascertain the influence of salinity on biomass production as this strain was originally isolated from a marine environment (44 g/l NaCl). Results obtained showed that the biomass yield at the different salt concentrations were comparable and differences between biomass concentrations were not significant. The highest biomass value (1.937 g/l) was recorded on day 20 at 30 g/l NaCl (Figure 20). Cultivation at 60 and 90 g/l NaCl produced 1.764 and 1.876 g/l biomass respectively on day 20. In a study by Barghbani *et al.* (2012),

Chlorella vulgaris was unable tolerate NaCl concentrations above 30 g/l and therefore no algal growth was observed. In another study, Fathi and Asem (2013), monitored the growth of a *Chlorella* sp. when subjected to three different salinities (10, 30 and 50 g/l). Results from their study showed that on day 15 the highest biomass was produced at 30 g/l NaCl. This biomass value was higher when compared to growth at the other salt concentrations (10 and 50 g/l), however there was no significant difference in growth at the different salinities (Fathi and Asem, 2013).

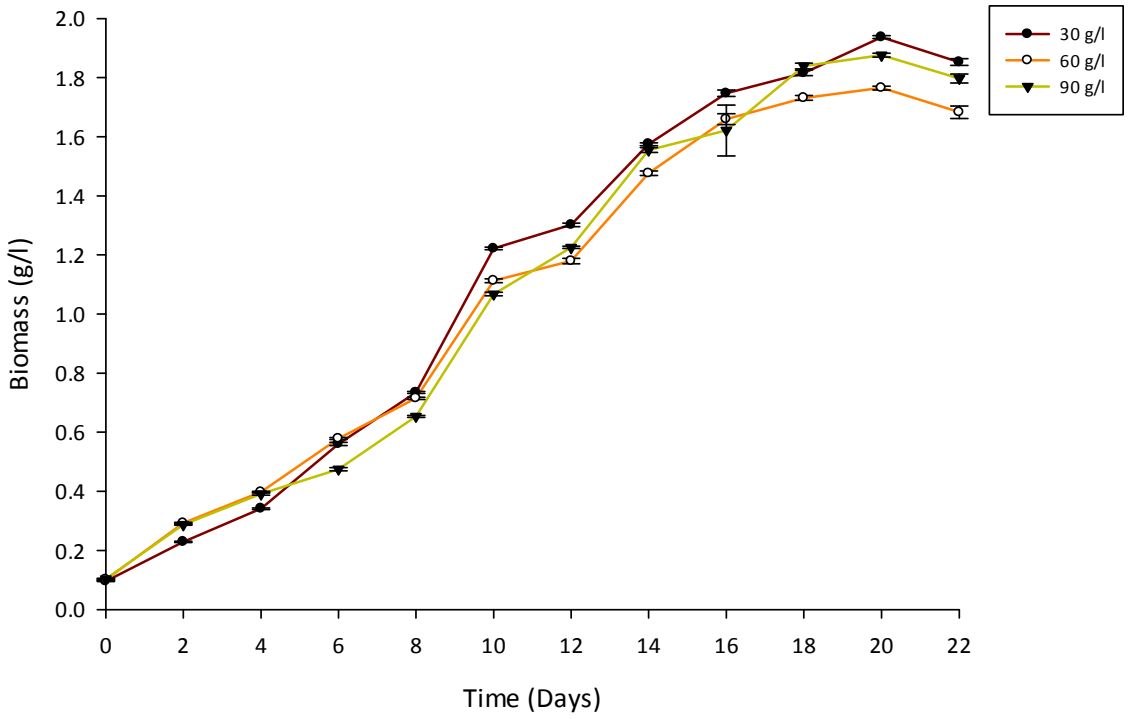

Figure 20: Effects of varying NaCl concentrations (in g/l) on the growth of the *Chlorella* sp. over a 22 day duration. Each value is the mean value of three trials. Error bars indicate standard deviations.

Apart from the macro elements (such as N, P and C), growth and biomass production of microalgae can also be affected by trace elements. This is due to the fact that trace elements are indispensable components of the enzyme active centre of algal cells and therefore, essential for the growing process of microalgae as they are linked to cell division (Dou *et al*., 2013). Hence, the effect of trace elements on the growth of the *Chlorella* sp. was determined. Trace metals are often prepared as a high concentration stock solution to allow for the accurate weighing of reasonably small amounts (Berges *et al*., 2001).

For the study, a trace metal stock solution was prepared using six components ($CuSO_4.5H_2O$, $ZnSO_4.7H_2O$, $CoCl_2.6H_2O$, $MnCl_2.4H_2O$, $Na_2MoO_4.2H_2O$, $Na_2EDTA.2H_2O$). Individual 200 ml stocks of the first five components were prepared (3.92 g/200ml $CuSO_4.5H_2O$; 8.8 g/200ml $ZnSO_4.7H_2O$; 4 g/200ml $CoCl_2.6H_2O$; 72 g/200ml $MnCl_2.4H_2O$; 2.52 g/200ml $Na_2MoO_4.2H_2O$). Thereafter, 250 µl of each individual stock was added to 200 ml water. Subsequently, 0.41 g $Na_2EDTA.2H_2O$ (the chelator) was added to this solution and boiled for 3 min. The solution was allowed to cool and adjusted to a pH of 7 and thereafter, a volume of 250 ml. The original ASW medium requires 0.5 ml/l of this trace metal stock solution.

The growth response of the *Chlorella* sp. to three different mixtures (0.5, 1 and 1.25 ml/l) of trace elements was observed. From Figure 21 it can be seen that the best biomass concentration (1.156 g/l) of the *Chlorella* sp. was achieved at a trace metal concentration of 0.5 ml/l on day 20. This was a 48.07% increase in biomass when compared to the highest trace metal concentration (1.25ml/l) which produced 0.786 g/l biomass on day 20. An intermediate trace metal concentration (1 ml/l) yielded 0.864 g/l biomass on day 20. This amount was very comparable to the amount produced at a 1.25 ml/l trace metal concentration. From this experiment it was evident that high trace metal concentrations (1 and 1.25 ml/l) were possibly toxic to the growth of the *Chlorella* sp. yielding considerably lower biomass values when compared to a lower trace metal concentration of 0.5 ml/l. In 1998, Boyer and Brand stated that trace elements could result in the abnormal cultivation of microalgae. Ilavarasi *et al*. (2011) also reported that even though trace metals induce growth of microalgae, high concentrations of these micronutrients leads to a decline in growth. This could possibly explain the lower biomass values obtained in the present study at high trace metal concentrations.

A few studies about the effects of trace elements and their components on the growth of microalgae have been reported. Studies by Jeffrey and Millton (1999), and Alexander and Markus (2006) showed that Mn ($MnCl_2.4H_2O$) is imperative for the growth of microalgae. This is owing to the fact that Mn is an important catalyst of photosynthesis as well as the activator of certain enzymes in microalgae. In another study by Yamochi (1984), it was found that the addition of EDTA ($Na_2EDTA.2H_2O$) formed a complex with several kinds of metal ions. The formation of this complex promoted absorption of metal ions by the microalgae which in turn stimulated growth.

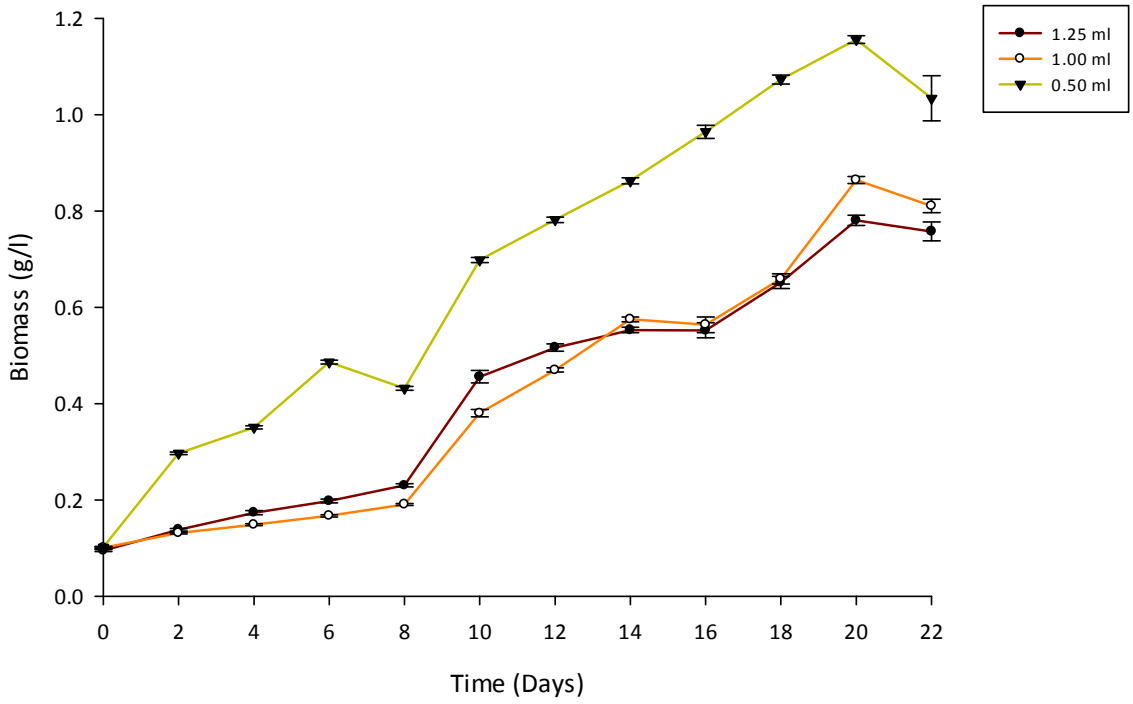

Figure 21: Time-course profiles of cell growth acquired under varying concentrations of trace metals (in ml/l). Each value is the mean value of three trials. Error bars indicate standard deviations.

A stock solution of Fe-EDTA was prepared using 5.71 g/l $FeC_6H_5O_7$ and 17.35 g/l $Na_2EDTA.2H_2O$. The original ASW medium requires 0.5 ml/l of this stock solution. Although Fe is usually only required in trace amounts, it acts as a versatile biochemical catalyst that is integral to the proper functioning of the elementary enzymatic reactions of PSI and PSII. This is probably due to the fact that Fe^{3+} is the assistant factor of several enzymes and is also essential for the formation of ferredoxin, cytochrome and Mo-Fe protein. Photosynthesis of algae is therefore dependent on Fe^{3+}. And efficient functioning of the photosynthetic apparatus is imperative for obtaining high biomass yields (Baky *et al*., 2012; Liu *et al*., 2008). In the

current experiment the *Chlorella* sp. was subjected to three different Fe-EDTA concentrations (0.5, 1 and1.25 ml/l) (Figure 22). The highest Fe-EDTA concentration (1.25 ml/l) produced greater biomass values during days 0-12 of cultivation when compared to cultivation at the other concentrations (0.5 and 1 ml/l Fe-EDTA). However, it was observed that from day 12, a 0.5 ml Fe-EDTA concentration yielded significantly higher biomass values ($p < 0.05$). The highest biomass concentration (1.823 g/l) was obtained on day on day 20 at a 0.5 ml Fe-EDTA concentration.

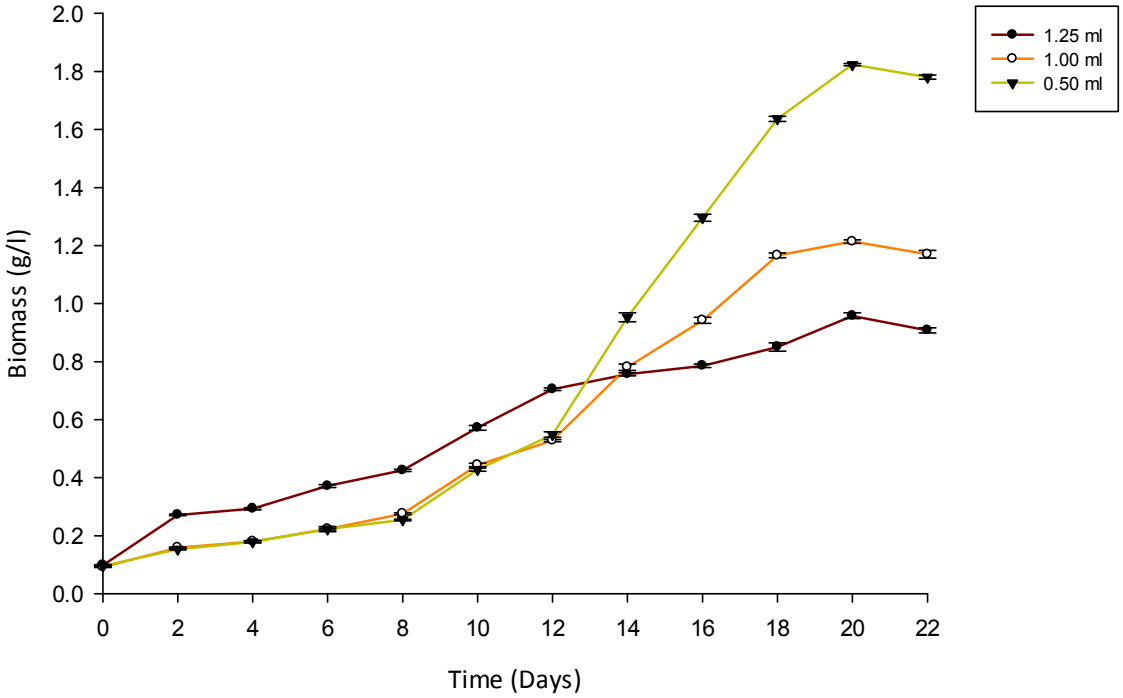

Figure 22: Growth of the *Chlorella* sp. in response to different Fe-EDTA concentrations (in ml/l) over a 22 day period. Each value is the mean value of three trials. Error bars indicate standard deviations.

Anhydrous salt stock solution was prepared using 0.39 g/l KCl, 0.2 g/l $NaHCO_3$ and 0.06 g/l H_3BO_3. The original ASW medium requires 33 ml/l of this stock solution. From Figure 23, it can be seen that the normal amount of anhydrous salt solution required for the original ASW medium was not sufficient to promote growth of the selected *Chlorella* sp, yielding 2.180 g/l biomass on day 20. When the anhydrous salt solution was doubled to 66 ml/l it was observed that the highest biomass of 2.250 g/l was achieved. This was a 3.22% increase in biomass when compared to the value obtained at the original anhydrous stock solution. It was further observed that 'too high' a concentration of anhydrous salt solution (99 ml/l) was possibly toxic to the *Chlorella* sp., as this concentration produced the lowest biomass value (1.971 g/l).

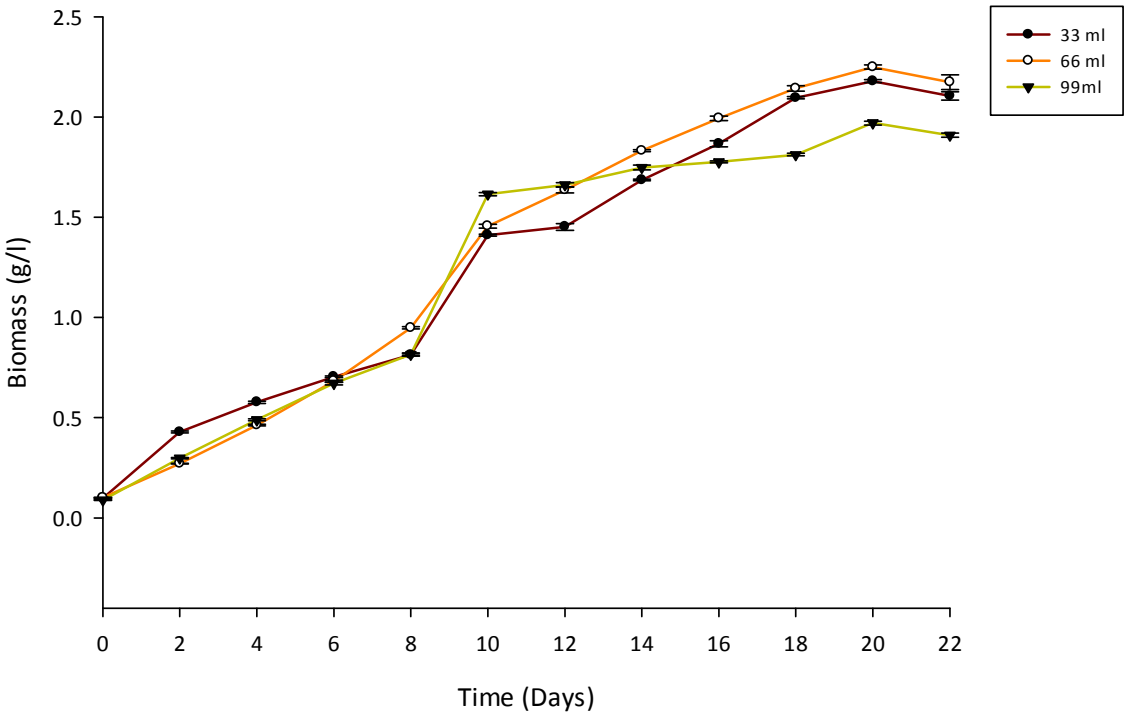

Figure 23: Effects of varying anhydrous salt concentrations (in ml/l) on the growth of the *Chlorella* sp. over a 22 day duration. Each value is the mean value of three trials. Error bars indicate standard deviations.

Hydrous salt stock solution was made up using 2.6 g/l $MgCl_2.6H_2O$, 3.56 g/l $MgSO_4.7H_2O$ and 0.77 g/l $CaCl_2.2H_2O$. The original ASW medium requires 133 ml/l of this stock solution. Growth of the *Chlorella* sp. at three different concentrations of hydrous salt solution were investigated. Results (Figure 24) suggest that 133 ml/l (which is the concentration required for the original ASW medium), was adequate for the cultivation of the *Chlorella* sp., producing the highest biomass (1.583 g/l) on day 20. This was a 26.01 and 45.19% increase in biomass when compared to cultivation at 266 and 399 ml/l hydrous stock solution respectively. It was therefore, concluded that further increases in concentration of the hydrous stock solution (266 and 399 ml/l) led to a decline in biomass (yielding 1.256 and 1.090 g/l biomass respectively).

Magnesium is a predominant component of hydrous salt stock solution as two different sources of Mg ($MgCl_2.6H_2O$ and $MgSO_4.7H_2O$) are required for preparing this solution. All microalgal species have an absolute requirement for Mg owing to the fact that this element is the central atom of the chlorophyll molecule and therefore occupies a strategic position in the photosynthetic apparatus of microalgal cells. Magnesium also plays a key role in the aggregation of ribosomes into functional units and in the formation of the enzyme catalase (Kulshreshtha and Singh, 2013).

Calcium ($CaCl_2.2H_2O$), which is the second major component of this solution, plays an important role in stress-tolerance, pathogenic resistance and growth and development (Gorain *et al*., 2013). This element has been found to be imperative for the growth of *Chlorella* spp. as it participates in nearly all aspects of growth and development (Gorain *et al*., 2013).

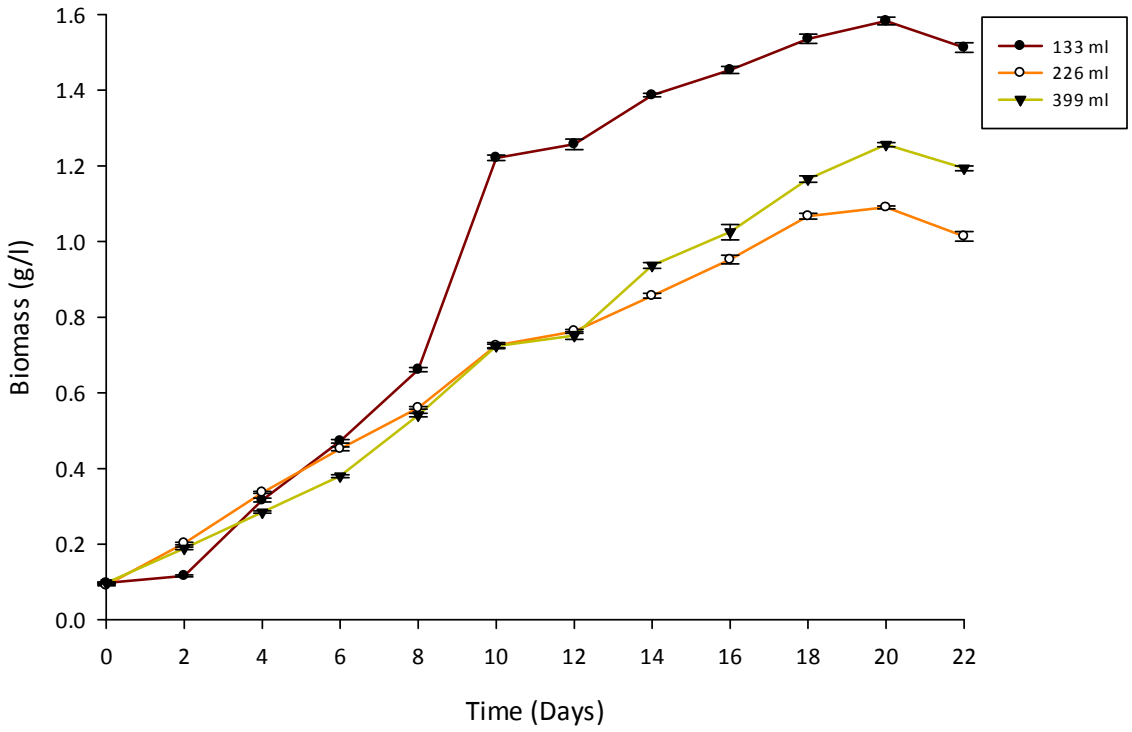

Figure 24: Effects of varying hydrous salt concentrations (in ml/l) on the growth of the *Chlorella* sp. over a 22 day duration. Each value is the mean value of three trials. Error bars indicate standard deviations.

5.3.3 Fractional Factorial Design

The first part of optimisation (discussed above) entailed ascertaining concentrations of the media components that had a substantial effect on the growth of the selected *Chlorella* sp. However, factorial design, which is one class of experimental designs, uses relatively few experiments to identify the important nutrients as well as any interactions between two or more nutrients. In a FFD, the number of experiments can be reduced without loss of information on

the major effects of each variable. If *N* factors were to be investigated, then the full factorial design would require 2^N experiments (Jeong *et al*., 2008).

$$\begin{aligned}\text{Biomass (g/l)} = {} & 2.758095238 + 0.015625 \times X_1 + 0.015625 \times X_5 - 0.113125 \\ & \times X_4 + 0.194375 \times X_6 + 0.063125 \times X_2 + 0.059375 \times X_3 \\ & + 0.051875 \times X_1X_5 - 0.125625 \times X_1X_2 + 0.065625 \times X_6X2_2 \\ & + 0.0856 \times X_2X_3\end{aligned} \quad \text{(Eq. 11)}$$

The mathematical model equation (Eq. 11**)** obtained from the experimental design in the present study was used to calculate the predicted values. The residue represents the difference between the actual and the predicted value. From Table 15, it can be seen that actual and predicted values did not vary greatly. The *Chlorella* sp. produced the highest biomass of 2.99 g/l (run 4) when grown in medium containing 0.61 g/l $Na_2SiO_3.9H_2O$; 0.6 g/l $NaNO_3$; 0.09 g/l NaH_2PO_4; 30 g/l NaCl; 0.5 ml/l trace metals; 0.5 ml/l Fe-EDTA; 33 ml/l anhydrous salts and 66.5 ml/l hydrous salts. The lowest biomass of 2.33 g/l was obtained at run 7. During run 7 the medium contained 0.61 g/l $Na_2SiO_3.9H_2O$; 0.6 g/l $NaNO_3$; 0.04 g/l NaH_2PO_4; 60 g/l NaCl; 0.5 ml/l trace metals; 0.15 ml/l Fe-EDTA; 66 ml/l anhydrous salts and 66.5 ml/l hydrous salts. Standards 17-21 (runs 2, 21, 15, 10 and 19) were the center points of the FFD, which represented five replications of an experiment at a central point. Biomass yield obtained for these runs were very similar thus validating the data of this experimental design.

Table 15: Fractional factorial experimental design for FFD0821 with the coded values of the variables tested showing actual, predicted and residual values

Std	Run	Factors								Actual	Predicted	Residual
		X_1	X_2	X_3	X_4	X_5	X_6	X_7	X_8			
1	6	-1	-1	-1	-1	-1	-1	-1	-1	2.58	2.56	0.023125
2	11	1	-1	1	-1	-1	1	-1	1	2.93	2.94	-0.01062
3	12	-1	1	-1	-1	-1	1	1	1	2.31	2.36	-0.05188
4	13	1	1	1	-1	-1	-1	1	-1	2.61	2.60	0.011875
5	4	-1	1	1	-1	1	1	-1	-1	2.99	3.01	0.020625
6	18	1	1	-1	-1	1	-1	-1	1	2.43	2.44	-0.01313
7	9	-1	-1	1	-1	1	-1	1	1	2.41	2.43	-0.02188
8	14	1	-1	-1	-1	1	1	1	-1	2.52	2.49	0.031875
9	20	-1	1	1	1	-1	-1	-1	1	2.70	2.70	0.004375
10	17	1	1	-1	1	-1	1	-1	-1	2.64	2.60	0.038125
11	16	-1	-1	1	1	-1	1	1	-1	2.53	2.53	-0.00563
12	5	1	-1	-1	1	-1	-1	1	1	2.47	2.51	-0.03938
13	1	-1	-1	-1	1	1	1	-1	1	2.52	2.52	0.004375
14	3	1	-1	1	1	1	-1	-1	-1	2.63	2.60	0.038125
15	7	-1	1	-1	1	1	-1	1	-1	2.33	2.33	-0.00312
16	8	1	1	1	1	1	1	1	1	2.93	2.95	-0.02688
17	2	0	0	0	0	0	0	0	0	2.89	2.90	-0.008
18	21	0	0	0	0	0	0	0	0	2.91	2.90	0.012
19	15	0	0	0	0	0	0	0	0	2.91	2.90	0.012
20	10	0	0	0	0	0	0	0	0	2.87	2.90	-0.028
21	19	0	0	0	0	0	0	0	0	2.91	2.90	0.012

Figure 25 shows the half-normal probability plot. After completion of the experiment this plot uses the ordered estimate to select which factors are significant and which are negligible. Both single and two-factor interactions were selected. The remaining unselected factors were subjected to a Shapiro-Wilk test to determine whether they were normally distributed. The w-value of the Shapiro-Wilk test was 0.887. All effects that lie along the line are considered negligible. Large effects were far-off from the probability line and were therefore selected to be included in the mathematical model.

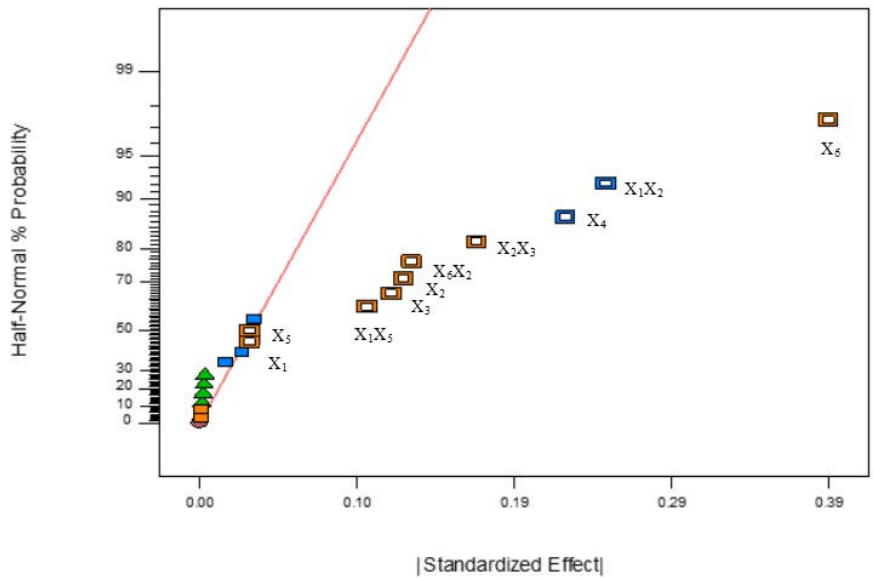

Figure 25: The half-normal probability plot for biomass produced by the *Chlorella* sp. Blue squares represent negative effects, while orange squares symbolise positive effects. Green triangle points are pure errors.

A Box Cox plot is necessary to ascertain the power of transformation required. If the residuals are a function of the magnitude of the predicted values, then a transformation is necessary. The blue line indicates the current transformation (if any), the green line illustrates the best model fit and the red line represents the confidence intervals surrounding it. From Figure 26, it can be seen that no transformation was required, as there was a lambda value of 1. This means that if the blue line falls within the two lines, then no transformation is required. Provided the data are positive, the power transformation allows transformation to any power in the range -3 to +3 (Sakia, 1992).

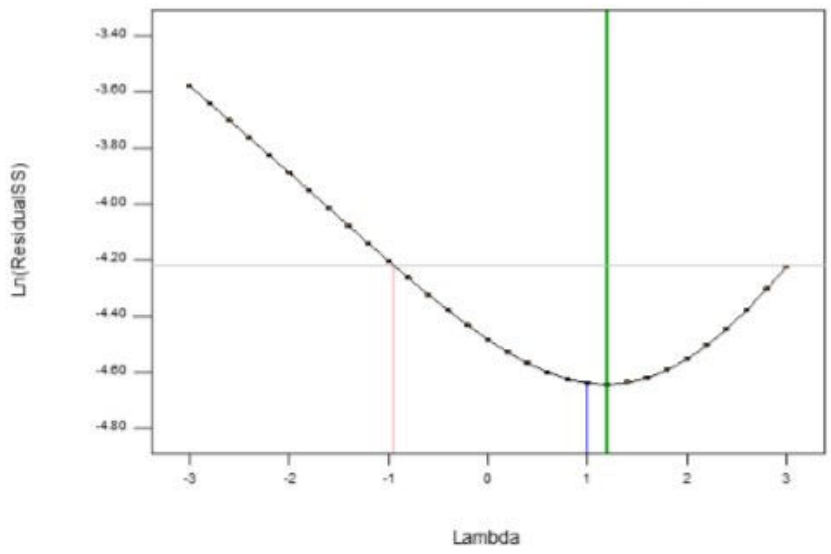

Figure 26: Box-Cox plot for FFD0821 indicating the position of lambda. This plot indicates whether a mathematical transformation is required for data to fit a higher-than linear model.

Figure 27 (the pareto chart), indicated the most significant factors and ranked them according to the greatest effect on biomass production. This chart was used to gain information on the effects of individual nutrient components as well as the interaction between the components. Factors above the Bonferroni limit are most certainly significant and should be included, while factors above the *t*-limit are possibly significant (Anderson and Whitcomb, 2005). Effects are ranked according to the greatest effect on biomass production. The largest positive responses (favourable effects on biomass production) were observed for individual factors X_2 ($NaNO_3$), X_3 (NaH_2PO_4) and X_6 (Fe-EDTA). This indicated that $NaNO_3$, NaH_2PO_4 and Fe-EDTA concentrations had similar synergistic effects.

Iron, which is provided in the form of Fe-EDTA, is one of the most important trace metals as it is directly involved in enzymatic reactions of photosynthesis (within PS I and II) (Singh *et*

al., 2015). It can be seen that X_6 (Fe-EDTA) displayed the largest positive response. This could be owing to the fact that a sufficient concentration of iron is required for proficient photosynthetic performance which directly affects biomass production and CO_2 fixation (Crofcheck *et al*., 2012). In 2008, Liu *et al*. reported that an increase in the iron concentration within the medium led to a considerable increase in the biomass production of *Chlorella vulgaris*. Similar findings were reported by Baky *et al*. (2012) using S. *obliquus*.

The second largest individual positive response was observed for X_2 ($NaNO_3$). Nitrate is essential for cell division and growth of microalgae as it is an indispensable constituent of protein synthesis. A sufficient supply of nitrate is necessary to maintain the metabolic balance between rate of nitrogen assimilation and the rate of carbon fixation. This balance is imperative for cellular metabolism (Adams *et al*., 2013; Singh *et al*., 2015).

X_3 (NaH_2PO_4) exhibited the third largest positive response. After nitrate, phosphate is the second most important macronutrient that is essential for microalgal growth as it plays a significant role in cellular metabolic processes (Singh *et al*., 2015; Solovchenko *et al*., 2016). Phosphate is required by microalgal cells for numerous purposes. Upon entry into a cell, a substantial amount of phosphate is used for the biosynthesis of cellular functional building blocks, while a small amount is stored away for possible phosphate shortages. Phosphates are an indispensable part of the polymer structure of nucleic acids. Nucleic acids, which are functional structures are primarily responsible for containing and transferring biological information (Solovchenko *et al*., 2016). The most abundant nucleic acid molecules in the cell are ribosomal RNAs. Ribosomal RNAs play a vital role in protein biosynthesis and therefore require adequate amounts of phosphate (Solovchenko *et al*., 2016). Intracellular phosphate has a crucial regulatory role as it is involved in the phosphorylation and de-phosphorylation of

proteins (Solovchenko *et al*., 2016; Wang *et al*., 2014). Other uses of phosphate include, phosphatidyl inositol which is involved in signaling and is present in the plasma membrane of microalgae and phospholipids which are important structural elements of biological membranes (Solovchenko *et al*., 2016).

Furthermore, phosphate is indispensable for energy storage and transduction. Triphosphate bonds of ATP which is the primary product of photosynthesis play a central role in algae as they are responsible for short-term energy storage. A considerable amount of intracellular phosphate is linked to numerous phosphate metabolites; principally sugar phosphates which are formed by direct or indirect participation of ATP as well as other energy rich phosphorylated compounds. Phosphate therefore plays a crucial role in the growth cycle of microalgal cells and this would explain why this nutrient was among the individual factors that displayed a large positive response.

Even though individual factors X_1 ($Na_2SiO_3.H_2O$) and X_5 (trace metals) were positive, they did not fall above the *t*-value limit. Interactions between X_2X_3 ($NaNO_3$ and NaH_2PO_4), X_2X_6 ($NaNO_3$ and Fe-EDTA) and X_1X_5 ($Na_2SiO_3.H_2O$ and trace metals) were positive and appeared above the Bonferroni limit, thus indicating that these interactions were definitely significant. On the other hand, the interaction between X_1 ($Na_2SiO_3.H_2O$) and X_6 (Fe-EDTA) indicated unfavorable or antagonistic effects on the biomass production.

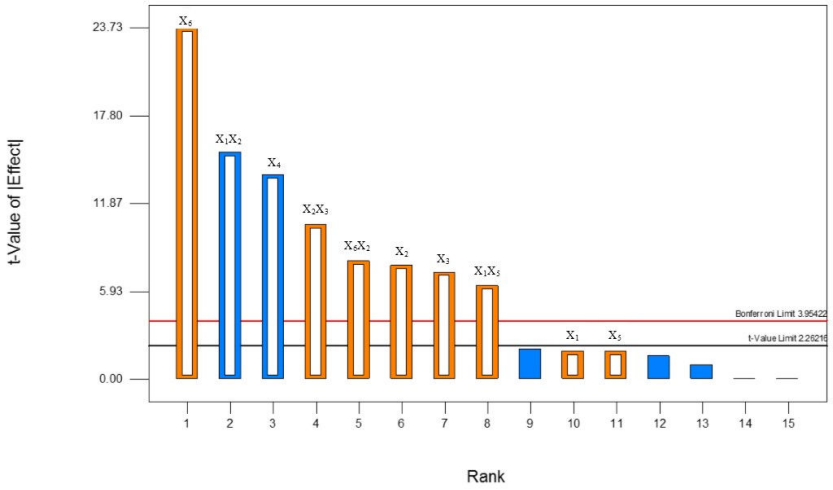

Figure 27: Pareto chart indicating the magnitudes of positive (orange) and negative (blue) effects on biomass production of the *Chlorella* sp. in the eight-factor design. Bars above the Bonferroni limit of 3.95 are certainly significant, while those above and *t*-value limit of 2.3 are possibly significant.

Once the experimental data in Table 15 was fitted to the polynomial equation (Eq. 11), ANOVA was able to generate the sum of squares, degrees of freedom (df), mean squares, F values and *p* values (Matos *et al*., 2015). Analysis of variance examines variations in a response and is able to ascertain which of the factors significantly affected the dependent variable. If the means of the variables are normally distributed, then ANOVA is able to compare the hypothesis of a difference in means of two or more factors. A p value < 0.05 and below suggests that there exists a significant difference in the means of the selected factors (95% confidence). This statistical tool is useful in determining if all the data points fit the model, thus indicating if the model used to predict the biomass yield was significant or not (Boddy and Smith, 2009; Jeong *et al*., 2008).

The F-test compares variance of individuals within the specific treatments to that of the variance among the means of the factors. Hence, the F distribution is a probability used to compare variances by examining their ratio. An F-value of 1 indicates that they are equal, or have no effect. A large F-value implies a large ratio and this often infers that the variance contributed by the model is significantly larger than the error. High F-values are also indicative of the fact that one or more of the factors differ from another (Jeong *et al*., 2008).

Table 16: Analysis of variance for the eight factor factorial model

Source	Sum of squares	Df	Mean Square	F value	p-value Prob>F	Significance
Model	1.42E+00	10	1.42E-01	10.274	0.0005	significant
X_1	3.91E-03	1	3.91E-03	0.283	0.6065	
X_5	3.91E-03	1	3.91E-03	0.283	0.6065	
X_4	2.05E-01	1	2.05E-01	14.825	0.0032	significant
X_6	6.05E-01	1	6.05E-01	43.769	< 0.0001	significant
X_2	6.38E-02	1	6.38E-02	4.616	0.0572	
X_3	5.64E-02	1	5.64E-02	4.084	0.0709	
X_1X_5	4.31E-02	1	4.31E-02	3.118	0.1079	
X_1X_2	2.53E-01	1	2.53E-01	18.283	0.0016	significant
X_2X_6	6.89E-02	1	6.89E-02	4.989	0.0495	significant
X_2X_3	1.17E-01	1	1.17E-01	8.494	0.0154	significant
Residual	1.38E-01	10	1.38E-02			
Lack of fit	1.37E-01	6	2.28E-02	71.266	0.0005	significant
Pure error	1.28E-03	4	3.20E-04			
Cor Total	1.56E+00	20				

According to the ANOVA table (Table 16), the main effects of X_4, X_6 and the combination X_1X_2, X_2X_6 and X_2X_3 were the only terms with *p* values less than 0.05 indicating that they were significant at the probability level of 95%. A model F-value of 10.27 implied that the model was significant. There was only a 0.05% chance that a 'Model F-value' this large could occur due to noise. Owing to the fact that the variation in the mean of the replicates were less than that of the design points, the lack of fit ($p < 0.05$) was significant. A 'Curvature F-value' of

1.20E+02 indicated that there was significant curvature in the design space. Curvature can be defined as the difference between the average of the center points and the average of the factorial points. Curvature suggested that a point of optimisation could be reached based on the model. From the results, the coefficient of determination (R^2) was 0.911. This value implied that this response model could explain 91.1% of the variability. Furthermore, the accuracy with which the calculations were compared was determined by the coefficient of variation % (CV). A high CV value usually implies low reliability of the experiment (Hao *et al*., 2012; Matos *et al*., 2015). In the present study, the low value obtained (CV = 4.26%) indicated a small residual variability in the data and good reliability of the experiments performed.

5.3.4 Central Composite Design

Based on the FFD results, variables of $NaNO_3$, NaH_2PO_4 and Fe-EDTA were subsequently employed to determine the independent significance on biomass production. Response Surface Methodology based on CCD aids in evaluating the relationship between the dependent variable (biomass production) and independent variable (medium components). The CCD experimental design comprised of twenty experiments and proved useful in acquiring data to fit a 2^{nd} order polynomial. From Table 17 it can be seen that the predicted and actual response for each individual experiment are close to each other as demonstrated by small residual values. Biomass production (g/l) corresponding to the combined effect of three components in the specified ranges are shown. Analysis of the response surface contour and surface plots as well as solving of the regression equation allowed for determination of optimum levels of the selected variables (Singh *et al*., 2009). The regression equation which is obtained after analysis of variance allowed for an estimation of the level of biomass concentration.

Table 17: Central composite experimental design showing the actual and predicted biomass values

Std	Run	Factors			Actual	Predicted	Residual
		X_2	X_3	X_6			
1	12	-1	-1	-1	2.836	2.767	0.069
2	10	1	-1	-1	2.701	2.746	-0.046
3	17	-1	1	-1	2.339	2.317	0.022
4	9	1	1	-1	3.051	3.027	0.024
5	14	-1	-1	1	2.661	2.652	0.009
6	1	1	-1	1	2.606	2.596	0.011
7	19	-1	1	1	2.094	2.016	0.079
8	11	1	1	1	2.656	2.692	-0.036
9	13	-α	0	0	2.173	2.263	-0.090
10	7	+α	0	0	2.858	2.814	0.044
11	18	0	-α	0	2.773	2.782	-0.009
12	15	0	+α	0	2.446	2.484	-0.037
13	3	0	0	-α	2.858	2.883	-0.025
14	6	0	0	+α	2.482	2.503	-0.021
15	4	0	0	0	2.880	2.949	-0.069
16	16	0	0	0	3.035	2.949	0.086
17	8	0	0	0	2.946	2.949	-0.003
18	20	0	0	0	2.936	2.949	-0.013
19	5	0	0	0	2.936	2.949	-0.013
20	2	0	0	0	2.968	2.949	0.019

$$\text{Biomass (g/l)} = 2.948799 + 0.163705 \times X_2 - 0.08876 \times X_3 - 0.11291 \times X_6 + 0.1829 \times X_2X_3 - 0.0087 \times X_2X_6 - 0.0463 \times X_3X_6 - 0.14505 \times X_2^2 - 0.11168 \times X_3^2 - 0.09046 \times X_6^2$$

(Eq. 12)

Analysis of variance values for biomass production of the *Chlorella* sp. for the CCD are shown in Table 18. The model F-value of 38.97 implies that this model was significant ($p < 0.0001$). This suggests that the fit for the model was good. There was only a 0.01% chance that a 'Model F-value' this large could occur due to noise (Jeong *et al*., 2008). The squares of the individual factors were included, as CCDs have a quadratic mathematical model. From the coefficient estimates and their corresponding *p* values it can be concluded that all the variables were significant ($p < 0.05$). Coefficients having small *p*-values are significantly greater than zero; i.e., they detect effects that appear to be truly important. For example, $p < 0.1$ implies significance at the 0.10 level ($\alpha = 0.10$). This corresponds to a 90% confidence level for a test of the hypothesis that the coefficient in question is equal to zero. Small *p*-values are therefore linked with large t-values since they imply that the coefficient is much greater than its standard error (SE) (Jeong *et al*., 2008). The 'Lack of fit' F-value of 2.18 suggests that the lack of fit is not significant relative to the pure error. The coefficient of determination R^2 controlled the fit of the models. From the ANOVA results, a high R^2 (0.972) and an Adj-R^2 (0.947) value was reported for the models. Both the R^2 and Adj-R^2 were close to 1.0, which implies high correlation between the experimental values and the predicted values.

Table 18: Analysis of variance for the central composite model

Source	Sum of squares	Df	Mean Square	F value	*p*-value Prob>F	Significance
Model	1.44E+00	9	1.60E-01	38.971	< 0.0001	significant
X_2	3.66E-01	1	3.66E-01	89.120	< 0.0001	significant
X_3	1.08E-01	1	1.08E-01	26.197	0.0005	significant
X_6	1.74E-01	1	1.74E-01	42.393	< 0.0001	significant
X_2X_3	2.68E-01	1	2.68E-01	65.166	< 0.0001	significant
X_2X_6	6.06E-04	1	6.06E-04	0.147	0.7090	
X_3X_6	1.71E-02	1	1.71E-02	4.176	0.0682	
X_2^2	3.03E-01	1	3.03E-01	73.834	< 0.0001	significant
X_3^2	1.80E-01	1	1.80E-01	43.766	< 0.0001	significant
X_6^2	1.18E-01	1	1.18E-01	28.718	0.0003	significant
Residual	4.11E-02	10	4.11E-03			
Lack of Fit	2.82E-02	5	5.63E-03	2.185	0.2056	not significant
Pure Error	1.29E-02	5	2.58E-03			
Cor Total	1.48E+00	19				

Analysis of the experimental data of the CCD generated response surface plots. These figures were built to elucidate individual and interactive effects of the experimental variables on the response. The response surface plot representing the biomass was obtained as a function of the concentrations of two medium components with the third nutrient being at the zero level. Response surface plots of $NaNO_3$, NaH_2PO_4 and Fe-EDTA against the biomass concentration can further explain the results of the statistical and mathematical analyses by understanding the interactions of the factors and finding the optimum concentration ranges of components required for maximum biomass production. Equation 9 was used to predict the contours converging on a point i.e the red region. For the maximal biomass production of 3.051 g/l (standard 4, run 9), which was predicted by the mathematical model, the regression equation revealed the following optimal coded units for the test variables: $X_2 = 1.20$ g/l, $X_3 = 0.09$ g/l and $X_6 = 0.50$ ml/l, which correspond to the concentrations of $NaNO_3$, NaH_2PO_4 and Fe-EDTA, respectively.

The contour plot (Figure 28) illustrates that the highest biomass yield would be generated if Fe-EDTA was kept at a constant of 0.63 ml/l and, if $NaNO_3$ and H_2PO_4 were increased (from 0.60 g/l $NaNO_3$ to 1.20 g/l and from 0.06 g/l H_2PO_4 to 0.09 g/l).

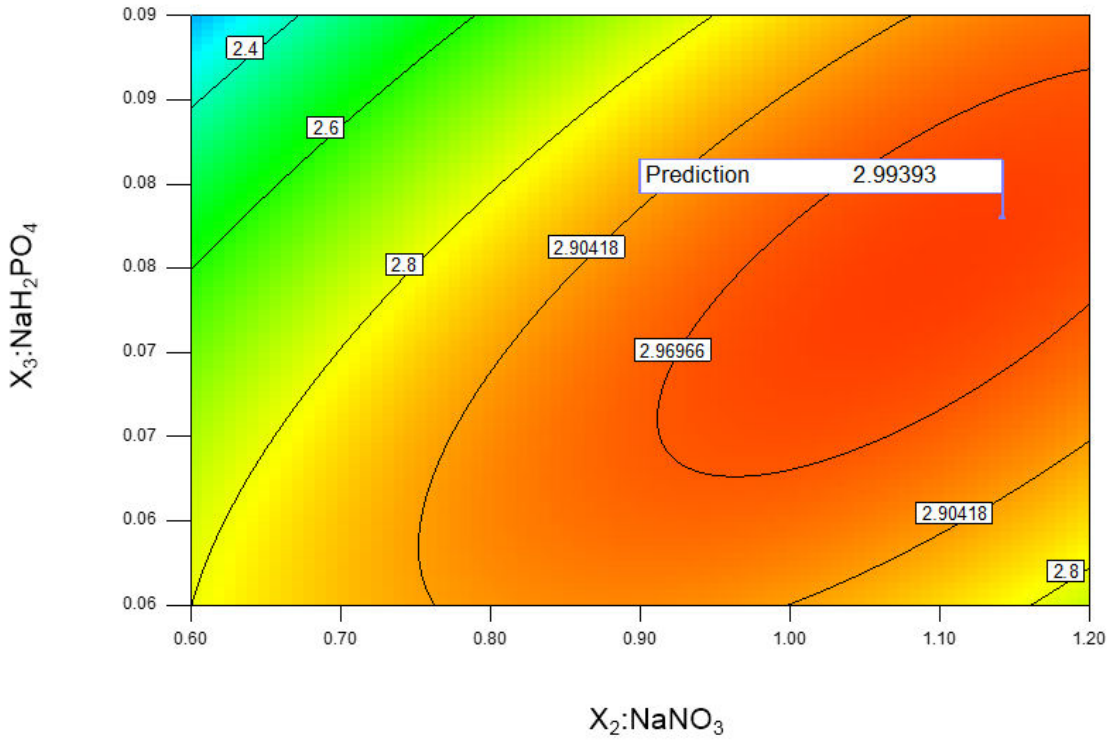

Figure 28: Contour plot of biomass production by *Chlorella* sp. showing the effects of two factors, $NaNO_3$ and NaH_2PO_4.

From the contour plot (Figure 29) depicting the interaction of Fe-EDTA and $NaNO_3$, it was noted that the maximum biomass will be produced if NaH_2PO_4 was kept at a constant (0.08 g/l), with a low Fe-EDTA concentration (0.56 g/l) as well as a high $NaNO_3$ concentration (1.2 g/l) was used.

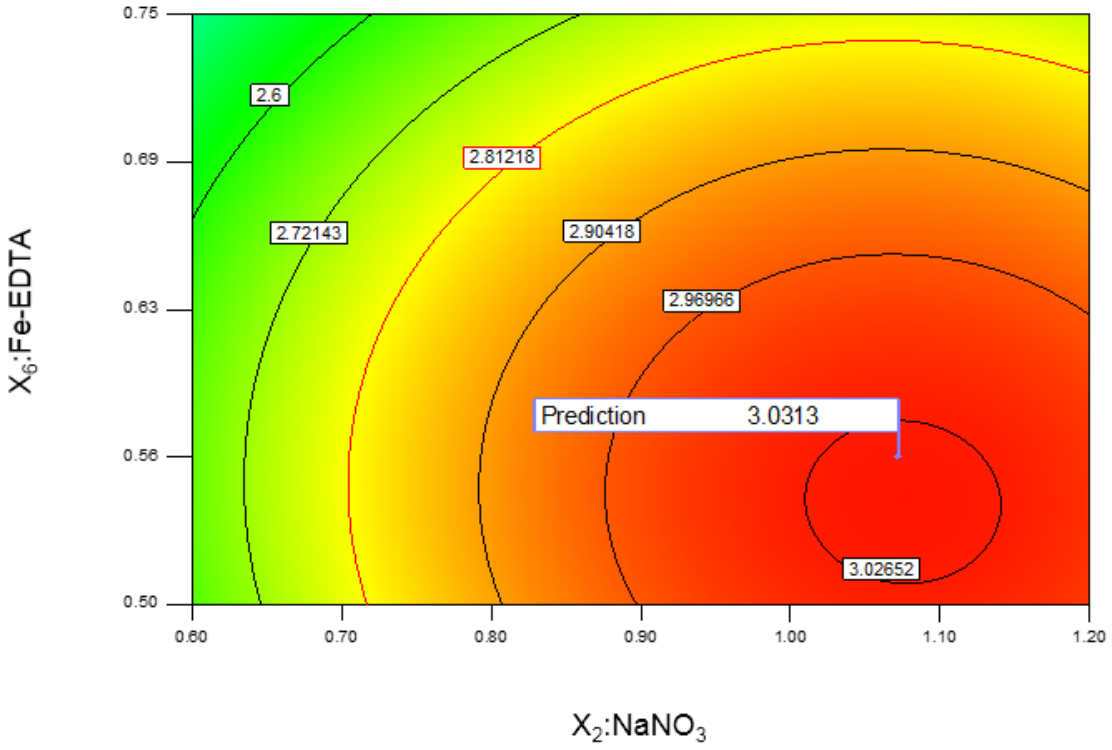

Figure 29: Contour plot of biomass production by *Chlorella* sp. showing the effects of two factors, $NaNO_3$ and Fe-EDTA.

From the contour plot below (Figure 30) (interaction of Fe-EDTA and H_2PO_4), it was observed that the maximum biomass will be produced if $NaNO_3$ were kept at a constant of 0.90 g/l and Fe-EDTA was at a concentration of 0.56 g/l with NaH_2PO_4 at a concentration of 0.07 g/l.

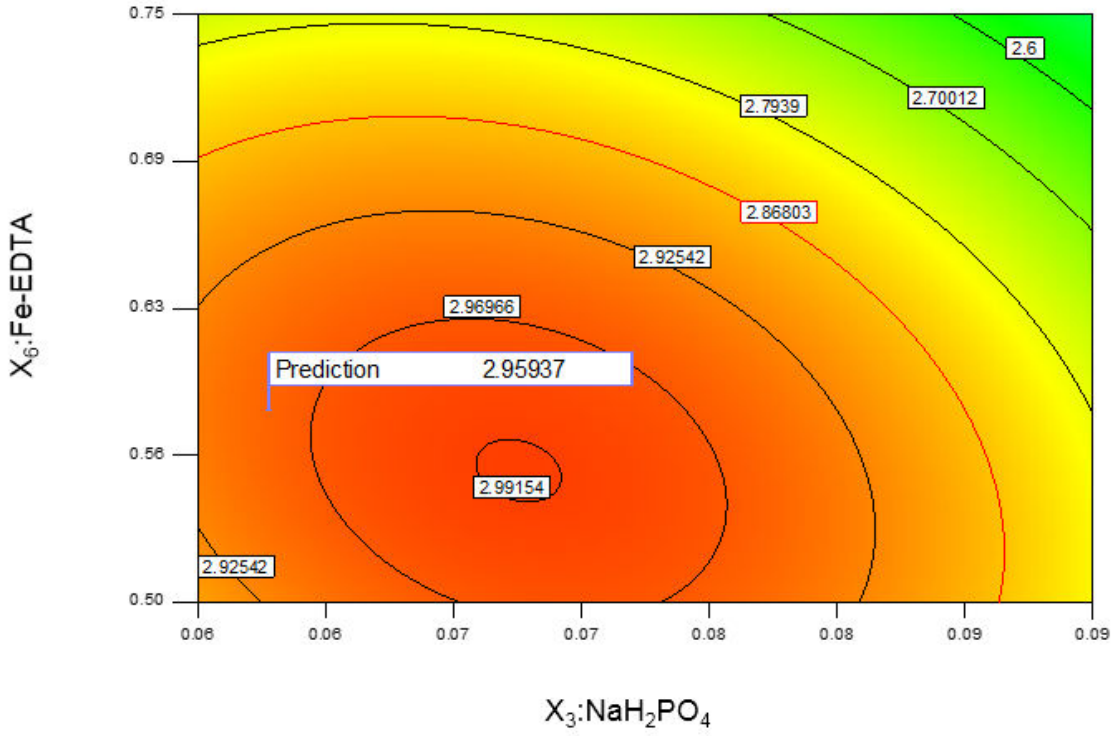

Figure 30: Contour plot of biomass production by *Chlorella* sp. showing the effects of two factors, NaH_2PO_4 and Fe-EDTA.

From the overall CCD results, it was noted that an increase in Fe-EDTA from ± 0.56 ml/l to ± 0.67 ml/l would lead to a decline in biomass. Furthermore, a drop in biomass production will also occur if the $NaNO_3$ and NaH_2PO_4 concentration is decreased below 0.9 g/l and 0.07 g/l, respectively.

The three factors represented in the cube plot had a significant impact on the biomass production of the *Chlorella* sp. A high biomass yield of 3.02736 g/l (Figure 31), was predicted if the components are used at the following concentrations viz, X_2: $NaNO_3$ at a high (1.20 g/l), X_3: NaH_2PO_4 at a high (0.09 g/l) and X_6: Fe-EDTA at a low (0.5 ml/l). Alternatively, a considerably lower biomass yield (2.01574 g/l) was predicted if the nutrient components were

at the following concentrations: X_2: $NaNO_3$ at a low (0.60 g/l), X_3: NaH_2PO_4 at a high (0.09 g/l) and X_6: Fe-EDTA at a high (0.75 ml/l).

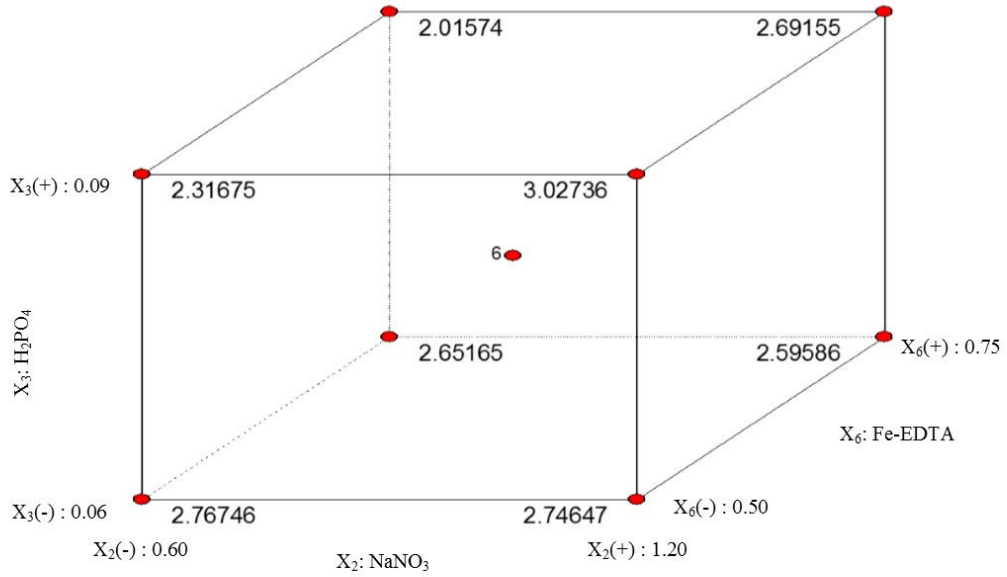

Figure 31: Cube plot illustrating the interactions between X_2: $NaNO_3$, X_3: NaH_2PO_4 and X_6: Fe-EDTA.

5.3.5 Validation Experiment

In order to test the prediction ability of the model, an additional set of experiments (verification experiment) that were different from CCD data was conducted. Only one solution for the confirmatory experiment was generated by the programme (Table 19). Under the optimal nutrient concentrations, the predicted response for biomass production was in the range of 2.0944 - 3.0512 g/l. The three replicate experiments yielded an average maximum concentration of 3.0010 g/l, which was 134.65% higher than the biomass yield (1.290 g/l) from

the original ASW medium. The agreement between the observed and predicted values confirms the validity and precision of the model.

Table 19: The optimised solution from the model, generated for the three factors to maximise biomass production of the *Chlorella* sp.

Solution	$NaNO_3$	NaH_2PO_4	Fe-EDTA	Biomass predicted	Standard error of mean	95% CI low	95% CI high
1	1.17	0.083	0.520	3.027	0.036	2.967	3.125

From Figure 32 it can be observed that there was a significant ($p < 0.05$) increase in biomass production by the *Chlorella* sp. when cultivated in the optimised modified medium (3.051 g/l) as compared to the yield produced when the microalgal strain was cultivated in the original ASW medium (1.290 g/l).

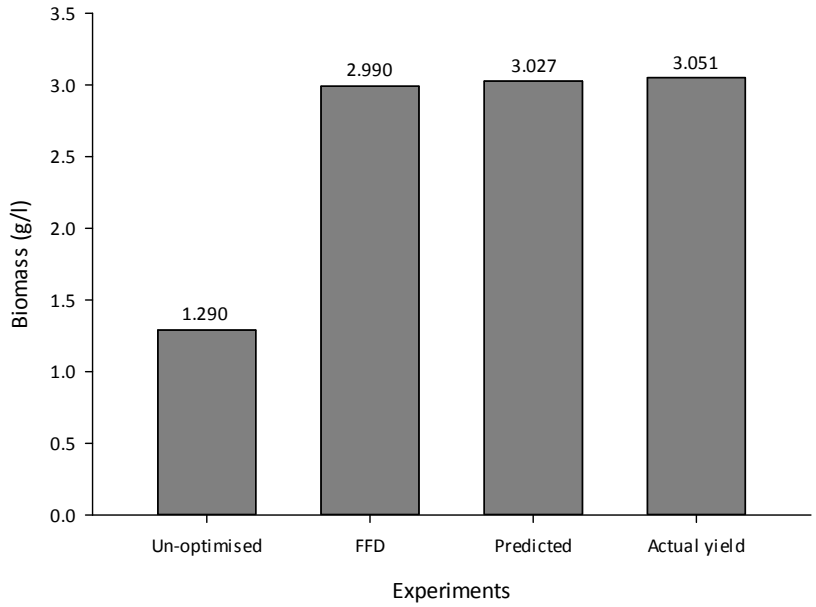

Figure 32: Biomass obtained when *Chlorella* sp. was grown in un-optimised and optimised ASW medium.

CHAPTER SIX: UTILISATION OF FLUE GAS FOR CULTIVATION OF THE SELECTED *CHLORELLA* SP. IN A PHOTOBIOREACTOR

6.1 INTRODUCTION

Over the years there has been global increases in GHGs emissions. Carbon dioxide is the main GHGs discharged, contributing up to 68% of total emissions (Ho *et al*., 2011; Kumar *et al*., 2011-a, b). The increase in GHG emissions can be attributed to anthropogenic activities such as intensive industrialisation, excessive fossil fuel usage and deforestation (Yadav *et al*., 2015). Research efforts using biological, physical and chemical techniques have led to the development of a few post-combustion CO_2-capture processes (Yadav *et al*., 2015). Biological CO_2 fixation which can be achieved through the photosynthesis by terrestrial plants and photosynthetic microorganisms (such as microalgae) as it is the only economical and environmentally viable technology of the future (Ho *et al*., 2011; Kumar *et al*., 2011-a, b).

Carbon dioxide sequestration from flue gases using biological systems presents a cost effective as well as an eco-friendly strategy (Ji *et al*., 2015; Jiang *et al*., 2011). When compared to terrestrial plants, microalgae have higher photosynthetic rates, faster growth rates and greater CO_2-fixation efficiency (10 - 50 times better) (Cheah *et al*., 2015; Ho *et al*., 2011). Microalgae also adapt easily to new environments, are simple and straightforward to work with and most importantly, their biomass can be utilised as a source of renewable energy or in the production of high value products (Duarte *et al*., 2016; Lam *et al*., 2012).

Microalgal biomass is rich in carbohydrates, proteins and lipids. Following cultivation with flue gas, the microalgal biomass could be exploited to extract useful by-products. This biorefinery concept could assist with the overall application becoming economically feasible

(Duarte *et al*., 2016). Carbohydrates derived from microalgal biomass can be used for bioethanol production. Proteins offer much potential as food and feed additives and also could be utilised in the pharmaceutical industry. Lipids can be used for biodiesel production or as edible oils since their essential fatty acids are beneficial to human health (Duarte *et al*., 2016; Vanthoor-Koopmansa *et al*., 2013).

Dried microalgal biomass contained roughly 50% carbon and is the main element required for microalgal nutrition. Most of this carbon was derived from CO_2 (Lam *et al*., 2012; Yadav *et al*., 2015). Theoretically, every 1 kg of microalgal biomass can fix approximately 1.83 kg of CO_2 (Jiang *et al*., 2013). Therefore, microalgae show much potential as valuable biomass for CO_2 biosequestration.

This work entailed the design, construction and use of a pilot scale PBR to demonstrate the viability of utilising a synthetic flue gas mixture for the growth of microalgae. A PBR configuration was used as opposed to a raceway system as PBRs permit the culture of a single species of microalgae for prolonged durations with lower risk of contamination (Brennan and Owende, 2010). Carbon dioxide is also utilised more effectively in PBRs (Brennan and Owende, 2010; Chisti, 2007; Vasumathi *et al*., 2012).The novelty of this aspect of the study lies in the fact that a very high CO_2 concentration (30%) formed part of the synthetic flue gas mixture.

6.2 MATERIALS AND METHODS

6.2.1 Microalgal Strain, Growth Medium and Culture Conditions

The *Chlorella* strain was grown and maintained in a modified version of ASW (suitable nutrient concentrations were determined from the optimisation study in the previous chapter), and was exposed to a light intensity of 175 μmol m^{-2} s^{-1}, a light/dark-cycle of 16:8 h and a temperature of 25±1°C on an orbital shaker at 90 rpm.The optimised medium contained: 0.61 g/l $Na_2SiO_3.9H_2O$, 1.17 g/l $NaNO_3$, 0.08 g/l NaH_2PO_4, 30 g/l NaCl, 0.15 ml/l trace metal stock solution (consisting of 3.920 g/200 ml $CuSO_4.5H_2O$ + 8.8 g/200 ml $ZnSO_4.7H_2O$ + 4 g/200 ml $CoCl_2.6H_2O$ + 72 g/200 ml $MnCl_2.4H_2O$ + 2.52 g/200 ml $Na_2MoO_4.2H_2O$ + 0.41 g/200 ml $Na_2EDTA.2H_2O$), 0.53 ml/l Fe-EDTA stock solution (consisting of 5.710 g/l $FeC_6H_5O_7$ + 17.350 g/l $Na_2EDTA.2H_2O$), 33 ml/l anhydrous salt stock solution (consisting of 0.780 g/l KCl + 0.40 g/l $NaHCO_3$ + 0.120 g/l H_3BO_3), and 66.5 ml/l hydrous salt stock solution (consisting of 5.200 g/l $MgCl_2.6H_2O$ + 7.120 g/l $MgSO_4.7H_2O$ + 1.540 g/l $CaCl_2.2H_2O$). During culture growth and maintenance the inoculums were adapted to elevated levels of CO_2 (up to 15% CO_2).

6.2.2 The Photobioreactor System

6.2.2.1 The flat panel photobioreactor experimental system

The pilot scale flat panel PBR that was designed and constructed for this study had a working volume of 3.5 l. Design considerations included the following requirements: effective photoreceptive surface area, pH monitoring, continuous agitation, effective and uniform flue gas delivery, accumulated O_2 release and allowance for gas and culture sampling. A gas flow meter (Flowstar) allowed for the gas flow rate to be adjustable. The culture chamber (Figure

34) was designed with a photo receptive surface area of 0.0726 m^2 and a surface area to volume ratio of 20 m^{-1}. The width of 0.05 m resulted in a lower area to volume ratio, however this compromise was necessary to create a 'dark zone' within the chamber to allow for cell recovery after exposure to the synthetic flue gas. The lighting source utilised were Sylvania Gro Lux t12" T5 8W fluorescent tubes (Osram Sylvania, Germany), which were placed on either side of the culture chamber. These fluorescent tubes irradiated the surface area with a light intensity of 175 µmol m^{-2} s^{-1}. Fluorescent lamps have been found to distribute light more or less uniformly along the length of the lamp (Kemka *et al.,* 2007). A sufficient supply of light energy was necessary for efficient CO_2 uptake and maximum biomass production (Chen *et al*., 2010). The optimum light intensity for the selected *Chlorella* sp. was ±175 µmol m^{-2} s^{-1}. A closed reactor with artificial lighting therefore, provided the ideal set up for cultivation of this organism, as conditions were controlled, keeping the light intensity at ±175 µmol m^{-2} $s^{-1.}$ Furthermore, according to Chen *et al*. (2010), as the concentrations of both cell and product increase, the light intensity would decrease exponentially with distance from the reactor wall. Hence, the light intensity is likely to decrease rapidly due to light shading effects arising from increases in cell concentrations or from formation of microalgal biofilm on the inner surface of the reactor walls. Microalgal cellular metabolism mode will switch in the absence of sufficient light energy, and thus both the productivity and biochemical composition of the microalgal cells are affected by the availability of light (Chen *et al*., 2010). To ensure maximum productivity, the distance of light to the reactor walls was decreased with an increase in cell density.

Agitation and aeration of the culture suspension was achieved by propelling air through two cylindrical 0.005 m diameter PVC tubes that bubbled the air at a depth of 0.25 m within the chamber. These PVC tubes were placed 0.05 m from their respective horizontal sides of the

reactor and ensured that the culture cells regularly migrated between the illuminated and dark zones.

A synthetic flue gas blend was obtained from AFROX (African Oxygen Limited). The concentrations of CO_2, O_2, NO_2, SO_2 and N_2 in the flue gas were 30%, 10%, 3.45%, 0.35% and 56.2%, respectively. The synthetic flue gas mixture was delivered *via* teflon tubing to a 0.2 m aquarium sparger located at the bottom of the reactor. This sparger effervesced the gas into the media. An exit port was installed at the bottom of the chamber for sampling purposes. It also allowed for the flushing, cleaning and sterilising of the reactor after the end of each run. Gas composition was analyzed by GC (Agilent 7820) using a thermal conductivity detector with N_2 as a carrier gas. Areas obtained after GC analysis was compared with reference curves to determine gas concentrations (Basu *et al*., 2013). This synthetic flue gas composition was formulated to mimic the flue gas composition released by cement manufacturing companies. The flue gas blend was fed into the reactor during different runs to ascertain whether the selected microalgal strain could grow under these adverse conditions.

6.2.2.2 Reactor operation

The PBR was operated under ambient temperatures (25$\pm$1°C) with a starting pH of 8 ± 01. Light intensity was maintained at 175 µmol m^{-2} s^{-1} with a photoperiod of 16:8 h using artificial light sources. Air was continuously bubbled through the chamber to ensure sufficient mixing and uniform exposure of the microalgae to the light sources. The synthetic flue gas mixture was delivered each day at periodic intervals into the culture chamber at a flow rate of 0.01m^3/min (flow rate range: 10 - 1200 l/h/r with a least count of 10 l/h/r) until the pH of the mixture dropped to 6. The airtight lid contained three septa for headspace gas analysis, three

gas input apertures, a one way gas release valve to periodically release oxygen-rich gas (produced during photosynthesis) and a pH probe to monitor acidity levels of the algae mixture.

The sample pH was directly determined using a Hanna model pH 211 meter. The lid of the reactor contained a port into which the pH probe was inserted. Once inside, the probe was permanently secured and sealed. This allowed for continuous pH monitoring. At the start of each PBR run, the pH meter was calibrated using standard solutions of pH 4 and 7 (Chiu *et al*., 2011).

Light intensity was measured adjacent to the surface of the PBR using a digital lux meter (Major Tech, South Africa). Overhead gas samples were taken on a daily basis from each of the three septa for GC analysis. At the end of each run, the microalgal culture within the culture chamber was evacuated and all reactor components were cleaned and sterilised.

6.2.3 Biochemical Composition Determination

The carbohydrate, protein and lipid composition of the microalgal biomass were determined during each reactor run.

6.2.3.1 Carbohydrate analysis (phenol-sulfuric acid method)

Polysaccharides present in the microalgal biomass were reduced to sugars by hydrolysis using H_2SO_4 and autoclaving (Dubois *et al*., 1956). Fifty millilitres of H_2SO_4 (2% v/v) was transferred to a 100 ml conical flask. Five hundred milligrams of dried algal biomass was then added to the acid solution. Hydrolysis of the mixture was achieved by autoclaving for 30 min at 121°C. After autoclaving flasks were removed and allowed to cool to room temperature and thereafter filtered to separate the dried biomass and the carbohydrate-rich solvent (Dubois *et*

al., 1956). Thereafter, 1 ml of 5% aqueous phenol was mixed with 2 ml of the carbohydrate solvent. Five millilitres of concentrated H_2SO_4 was rapidly added to this mixture. The mixture was allowed to stand for 10 min, vortexed for 30 s and then placed in a water bath at room temperature for 20 min to allow for colour development. Light absorption was measured at 490 nm using a spectrophotometer (SpectroquantR Pharo 300, Merck USA) (Albalasmeh *et al*., 2013; DuBois *et al*., 1956). Glucose solutions of different concentrations were used as a standard to construct a calibration curve (Fu *et al*., 2010).

6.2.3.2 Protein analysis

Protein extraction from the microalgal biomass was achieved using a modification of the Lowry method (Ansari *et al*., 2015; Lopez *et al*., 2010-b; Lowry *et al*., 1951). Reagents were prepared by following the procedure described by Lopez *et al*. (2010-b). Twenty five millilitres of lysis buffer solution was transferred to a mortar. Two hundred milligrams of dried microalgal biomass was then added to the lysis buffer solution. This mixture was adequately ground for approximately 5 min using a pestle, and thereafter vortexed for 2 min. To achieve separation the mixture was centrifuged for 10 min at 3000 rpm, and the supernatant was subsequently decanted into a clean tube. The remaining pellet was placed in the mortar and 25 ml of lysis buffer was added. The mixture was ground, vortexed, and centrifuged once more. Once the second lot of supernatant was obtained, both supernatants were pooled together and 0.5 ml of SDS solution was added. This mixture was then vortexed. To this mixture 5 ml of reagent-C was added and thereafter vortexed. Prior to the addition of 0.5 ml Folin reagent, the solution was left to rest for 10 min. Following the addition of the Folin reagent, the solution was mixed and allowed to stand for 30 min. Absorbance was subsequently measured at 750 nm using a spectrophotometer (SpectroquantR Pharo 300, Merck USA). To develop a calibration curve for protein quantification, bovine serum albumin (BSA) was dissolved in lysis buffer. Protein

yields (% w/w) were then established using the standard curve (Ansari *et al*., 2015; Lopez *et al*., 2010).

6.2.3.3 Lipid analysis

Cell disruption and extraction was achieved by a modification to the methods described by Guldhe *et al.* (2014) and Lee *et al*. (2010). Dried *Chlorella* sp. biomass was added to a 20 ml mixture of chloroform:methanol (2:1, v/v). This mixture was then subjected to the microwave technique to achieve cell disruption (Milestone S.R.L., Italy, output power 1200 W) at 100 °C for 10 min at 1000 W. The mixture was thereafter filtered to separate the cell debris and solvent mixture. The solvent was evaporated in an oven at 70°C. Five millilitres of hexane were added to the dried solvent and transferred to pre-weighed eppendorf tubes. The tubes were placed in an oven at 70°C to allow for the hexane to evaporate. The amount of crude lipid was quantified gravimetrically and the lipid yield (%) was calculated by the equation proposed by Guldhe *et al.* (2014):

$$Lipid\ yield\ (\%) = \frac{weight\ of\ extracted\ lipid}{amount\ of\ biomass}\ X\ 100 \qquad \text{(Eq.13)}$$

6.2.4 Analytical Methods

6.2.4.1 Growth profile and the logistic model

Biomass was determined daily by DCW measurements. A 50 ml sample was centrifuged (Heraeus multifuge centrifuge 4KR, USA) at 1509 x g for 15 min at 4^{o}C. The supernatant was

discarded and the pellet was washed with 0.05 M HCl and distilled water to remove non-biological adhering materials such as mineral precipitates, and dried at 60^{o}C for 24 h.

A plot of biomass (B) vs time (t) gives a sigmoid variation of biomass as a function of time, displaying lag, exponential and stationary phase of the culture (Kumar and Das, 2012). The growth profile can be explained by the logistic equation as formulated in Eq. 9. The growth kinetic values were determined by creating M-file for a genetic algorithm in MATLAB. The validation procedure was carried out using the correlation coefficient (r^2).

$$\frac{dB}{dt} = \mu_{\max} B\left(1 - \frac{B}{B_{\max}}\right) \qquad \text{(Eq. 9)}$$

Where:

B is the dry cell mass (g/l), B_{max} is the maximum dry cell mass (g/l) and μ_{max} is the apparent specific growth rate (d^{-1}).

6.2.5 Statistical Analysis

The responses were assessed using an analysis of variance followed by Tukey's test at a 95% confidence level.

6.2.6 CO_2 Uptake Rate

The CO_2 uptake rate (Q_{CO2}) in g/day was estimated for the first 19 days of cultivation by using the biomass productivity, the carbon content and the molar masses of CO_2 and carbon:

$$Q_{CO_2} = \frac{(X_1 - X_2)}{(t_1 - t_2)} \times X_c \times \frac{M_{CO_2}}{M_c} \times V$$

(Eq. 10)

Where:

X = cell concentration (g/l)

t = time (days)

X_C = the average mass fraction of carbon

M_{CO2} = 44 g/mol

M_C = 12 g/mol

V = working volume of incubation vessel (3 l)

6.2.7 Gas Chromatography

The respective head space CO_2 concentrations were verified using gas chromatography (GC). The GC system (Agilent 7820) was equipped with a thermal conductivity detector and contained a GS-Gaspro (30 m x 0.32 mm I.D) packed column. Nitrogen was used as the carrier gas. The operational conditions were as follows: injector temperature of 120°C, oven temperature of 80°C and detector temperature of 250°C. Areas under curves obtained after GC analysis was compared with reference curves to determine CO_2 concentrations (Basu *et al*., 2013).

6.2.8 Fluorescence Measurements

Effects of flue gas on the physiology of the isolated microalgal strains were determined using non-invasive fluorescence measurements. A Dual-PAM 100 Chlorophyll Fluorometer (Heinz Walz Gmbh, Effeltrich, Germany) was used for the fluorescence measurements of PSI and PSII. Photon irradiance (400 to 700 nm) incident on the sample surface was measured using a PAR micro-sensor (Spherical MicroQuantum Sensor US-SqS/W, Waltz) connected to the PAM fluorometer control unit. The Dual-PAM software v 1.19 was used to record and analyse all data. Relative electron transport rate was calculated by the Dual PAM software using the formula (Eq. 6) (Ramanna *et al*., 2014; White *et al*., 2011).

$$rETR = \frac{F'_q}{F'_m} \times PPFD$$

(Eq. 6)

Where: $F'q$ is a representation of the PSII operating efficiency and can be calculated from Eq. 6 (chapter 3); $F'm$ is the maximum fluorescence in a light adapted sample; $PPFD$ is the photoactive photon flux density.

6.2.9 Morphological Observation by Scanning Electron Microscopy (SEM)

The sample was mounted on a grid and then subjected to critical point drying in order to retain the fine microstructure of the algae samples. The sample was then fixed for 24h using 4% glutaraldehyde (w/v), and thereafter rinsed thrice in distilled water and dehydrated in a graded series of ethanol (30, 50, 75, 85, 95 and 100%) for 3 min. Th air dried film was made electrically

conductive by adding a gold palladium coating at a sputter current of 3 mA for 60 sec, using a Quorum (Q 150R ES) and images were viewed using a ZEISS Ultra plus FEG SEM (Basu *et al*., 2013; Hu *et al*., 2016; Tripathi *et al*., 2015).

6.3 RESULTS AND DISCUSSION

6.3.1 The Photobioreactor System

The design of this particular flat panel reactor system placed high emphasis on efficient CO_2 utilisation as well as practicality. A key design requirement for a PBR is the illumination S/V ratio. An efficient PBR is one that has a high S/V ratio (Ugwu *et al*., 2008). Flat panel reactors are characterised by a high S/V ratio (Kumar *et al*., 2011-b). A flat panel configuration was therefore employed, allowing the microalgae to be more efficiently and uniformly exposed to the light source (Sierra *et al*., 2008). Dimensions (0.33 m height X 0.22 m length X 0.05 m width) and components of PBR are shown in Figure 34. The PBR was constructed using transparent polyvinyl chloride (PVC) which had of an airtight lid (Figure 33) and a 3.5 l culture chamber (Figure 34). The type of material selected is of fundamental importance as it must lack toxicity, possess high mechanical strength, have high transparency, high durability, chemical stability and low cost (Molina *et al.,* 2001). The use of transparent PVC tubes provided the system with an effective yet durable option as it is permeable to light, non-toxic to algal cells and has a high strength-to-weight ratio. The culture chamber contained the microalgae mixture in a vertical orientation with Sylvania Gro Lux t12" T5 8W fluorescent tubes on either side running parallel to the reactor.

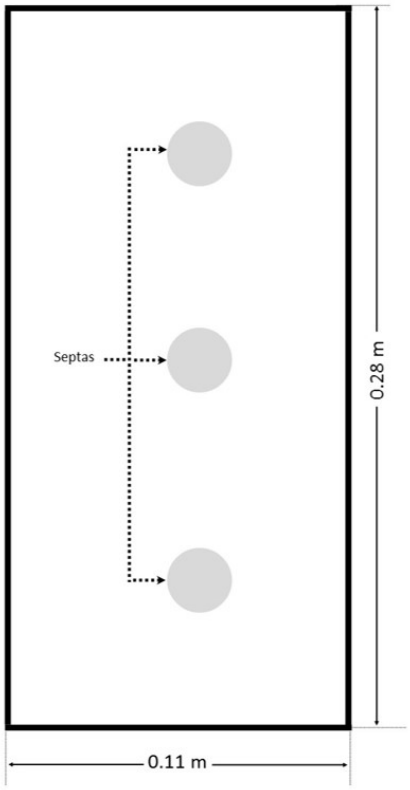

Figure 33: Schematic diagram depicting the photobioreactor lid.

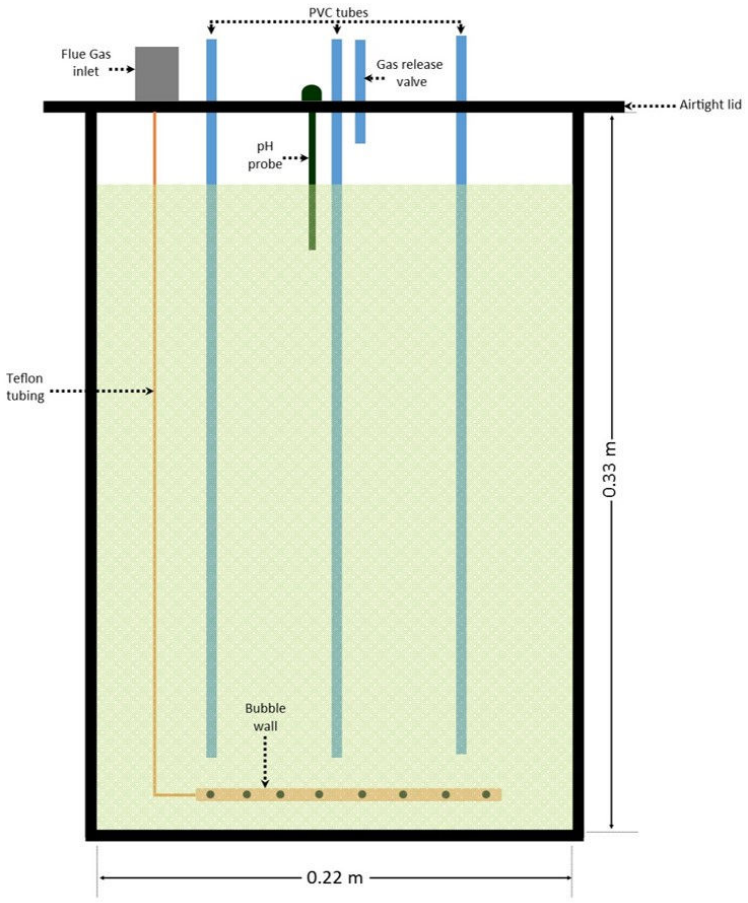

Figure 34: Schematic diagram depicting flat panel photobioreactor system.

The inclusion of an outlet for O_2-rich gas was critical to ensure that O_2 liberated during photosynthesis did not reach inhibitory levels. A one-way relief valve, fitted onto the reactor lid, allowed for air to flow outward while preventing contaminants from entering the PBR. Accumulation of O_2 within the reactor would have posed a serious problem. Oxygen rich headspace gas was therefore released periodically via the one-way gas relief valve. During photosynthesis O_2 is released due to the water splitting activity of PSII. Excessive accumulation of O_2 within a closed system would promote processes like photorespiration and photoinhibition that would ultimately lead to a reduction in the photosynthetic efficiency

causing a drastic decrease in the growth rate and yield of the microalgal culture (Kumar *et al*., 2011-b; Sousa *et al*., 2013). Photorespiration occurs due to the oxygenase activity of the RuBisCO enzyme. Inhibitory levels of O_2 would cause a change in the local O_2/CO_2 ratios and hence inhibit the carboxylase activity of the RuBisCO enzyme resulting in an increase in the oxygenase activity (Sousa *et al*., 2013). The oxygenase activity of RuBisCO can hinder approximately 50% of biomass formation (Giordano *et al*., 2005; Kumar *et al*., 2011-b). It is therefore imperative that PBRs are equipped with an efficient degassing system to remove large amounts of O_2 (Kumar *et al*., 2011-b).

6.3.2 Microalgae Growth Profile Using Synthetic Flue Gas

When using flue gas as a carbon source, two of the most critical factors impacting the growth performance would be the type of microalgal strain selected and the culture conditions. Characteristics of the selected microalgal strain directly affect both the carbon uptake rate and biomass production (Kao *et al*., 2014; Zhao and Su, 2014). In comparison to other microalgal candidates that have been researched for flue gas utilisation, *Chlorella* spp. usually exhibit better adaptation to the culture conditions and performance in terms of growth (Chiu *et al*., 2008; Kao *et al*., 2014; Yeh and Chang, 2012).

Figure 35 shows representative growth curves for the *Chlorella* strain during three different PBR runs (A, B and C). All experiments were performed in triplicate. During run A, the *Chlorella* strain was grown under optimised conditions of light intensity, photoperiod and nutrients (see previous chapters) and was also continuously aerated (flow regulated with gas rotameter) with the flue gas blend as described in section 6.2.2.1. Carbonic acid is produced when CO_2 dissolves in water. This weak acid dissociates into steps based on the temperature.

The energy imparted on the water can be directly related to the pKa of the respective reaction. The initial pH of the cultivation medium was adjusted to 8 ± 01. The negative impact of a major pH drop was diminished by the buffering action of MES. In 2012, Pires *et al*. reported that toxicity occurring at high CO_2 concentrations could be attributed to the reduced pH of the culture medium or by direct inhibition. Batch run C served as a control run: the *Chlorella* strain was periodically exposed to the flue gas mixture under un-optimised conditions of light intensity, photoperiod and nutrients. During the course of batch run B, the *Chlorella* strain was grown under optimised conditions of light intensity, photoperiod and nutrients and intermittently exposed to the flue gas mixture at a flow rate of $1m^3/s$ until the pH of the mixture dropped to 6 ± 01. During no flue gas aeration, the pH gradually increased back to 8 ± 01 owing to O_2 production during photosynthesis (Lara-Gil *et al*., 2016). At the start of each PBR run, a 10% v/v mid-log exponentially growing culture (from a predetermined growth curve) was used as seed inoculum.

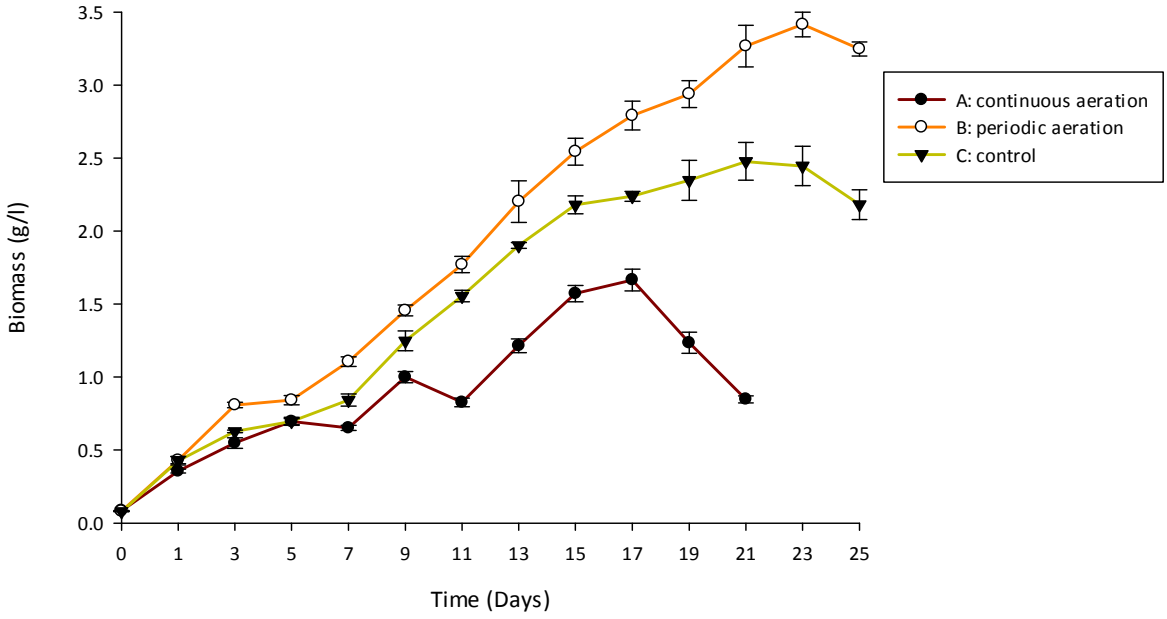

Figure 35: Growth profiles of the selected *Chlorella* sp. (A) cultured in a flat panel reactor aerated continuously with flue gas under optimised conditions of light intensity, photoperiod and nutrients, (B) grown under optimised conditions of light intensity, photoperiod and nutrients and periodic exposure to the flue gas mixture, (C) control run: periodic exposure to the flue gas mixture under un-optimised conditions of light intensity, photoperiod and nutrients.

From Figure 35, five well defined growth phases could be seen for PBR runs B and C: lag phase (days 0 - 3); exponential growth phase (days 3 - 5); linear growth phase (days 5 - 13); stationary growth phase (days 13 - 23); and a death phase which started from day 23. On the contrary, an erratic growth curve was observed under continuous gas supply (run A). It should also be noted that during run A the microalgae reached stationary phase much later (day 15) and entered the death phase much sooner (from day 17) in comparison to the other PBR runs.

Overall results obtained showed (Figure 35) that the *Chlorella* sp. was not adversely affected by the flue gas constituents as growth occurred at all PBR cycles, giving variable biomass

growth. Photobioreactor run B facilitated maximum growth, enabling the microalga to reach a biomass value of 3.415 g/l on day 23. This was a 37.87% increase in growth when compared to the control run (C), which produced 2.477 g/l biomass on day 23. During run A, the highest yield of 1.665 g/l was recorded on day 17, thereafter the culture entered the death phase. It was therefore concluded that continuous aeration of flue gas eventually inhibited growth even though the pH was maintained at 8 ± 01. This could be attributed to the fact that the microalgae was unable to fully adapt to rapid changes caused by continuous gas supply (Lara-Gil *et al*., 2016). Lara-Gil *et al*. (2016) conducted a study whereby two flue gas (simulated gas components found in a modern cement plant, in v/v: 25% CO_2, 800 ppm NO, 200 ppm SO_2 and 150 ppm cement kiln dust) aeration strategies (continuous supply and aeration cycles) were evaluated to cultivate *D. abundans*. They observed that during continuous gas supply the microalgae reached the stationary phase after 60 h of growth and thereafter entered the death phase. The culture pH was maintained above 5 during continuous aeration. Conversely, when the flue gas was supplied in cycles, exponential growth was present throughout the experimental period. They were able to conclude that when the flue gas was supplied in cycles, the growth of *D. abundans* was not drastically affected, yet even at a constant pH, continuous aeration of flue gas eventually inhibited growth.

Depending on the characteristics of the microalgal strain, the presence of NO_2 and SO_2 in flue gas could either prove toxic, inhibiting microalgal growth or they could serve as additional nitrogen and sulphur sources (Kao *et al*., 2014). Sulphur dioxide usually inhibits microalgal growth by lowering the pH of the culture medium due to hydrolysis of SO_2 which results in the release of H^+ ions (Jiang *et al*., 2013; Kao *et al*., 2014). Hydrolysis of SO_2 also produces SO_4^{2-} and HSO_4^- ions which can further impede microalgal growth (Chiu *et al*., 2011; Kao *et al*., 2014). In the present study, the pH of the medium was regularly determined to prevent any

adverse effects that could arise if the pH were to drop considerably. During runs B and C, a slight decrease (±2 units) in pH was allowed when the culture was aerated with the flue gas blend. Flue gas aeration was then halted, allowing the pH of the culture medium to gradually increase back to ±8. Thus, the minor pH changes did not significantly hinder microalgal growth. Studies suggest that by closely monitoring and controlling culture pH, the growth of microalgal strains during flue gas aeration is similar to those of microalgal cultures cultivated without the presence of flue gas compounds (Duarte *et al*., 2016; Yue *et al*., 2005). During this study the lowest pH recorded in the culture medium was approximately 6 ± 01. This pH decrease could likely be attributed to the high concentration of CO_2 as well as the presence of SO_2 in the flue gas.

Microalgae are able to utilise nitrogen in several forms, including NO, N_2, NO_2^-, NH_4^+ and NO_3^-. Nitrogen dioxide usually consists of 95% NO and 5% NO_2. Nitrogen oxide does not easily dissolve in H_2O, whereas NO_2 has a 6000-times higher solubility than NO. Nitric acid (HNO_3) or nitrous acid (HNO_2) is formed when any of the NO_x compounds dissolve in H_2O (Kao *et al*., 2014). In 2014, Kao *et al*., therefore proposed that NO_X present in flue gases could possibly dissolve in the microalgal culture broth and serve as an additional N-source for the microalgae, thereby contributing to increases in growth rate and biomass concentration.

Overall, results demonstrated that the selected *Chlorella* sp. was able to grow well in a closed flat panel PBR under conditions of flue gas aeration. Biomass yield, however, was greatly dependent on culture conditions and the mode of flue gas supply. In comparison to the other runs, run B yielded the maximum biomass value (3.415 g/l). During this run, not only was the *Chlorella* strain grown under optimised nutrient and environmental conditions, but the culture was also intermittently exposed to the flue gas mixture. The statistical significance in biomass

production values among the different PBR runs was determined by applying the Tukey's post hoc test (Appendix I). This test revealed that there was a significant difference in biomass yield between runs A and B and between runs A and C ($p < 0.05$). However, there was no significant difference in biomass values between runs B and C. In a study by Jiang *et al*. (2013), the maximum biomass yield (3.63 g/l) of S. *dimorphus* was obtained during intermittent sparging of simulated flue gas (15% (v/v) CO_2, 400 mg/l SO_2, 300 mg/l NO, balance N_2). An intermittent supply of flue gas during an experiment leads to a slight drop in pH and prevents an accumulation of H^+ ions in the medium. A build-up of H^+ ions would lead to a drastic reduction in pH and consequently inhibit cell growth (Jiang *et al*., 2013; Kao *et al*., 2014).

The logistic model was used to describe the microalgal growth profile by identifying μ_{max} and B_{max} of the culture during the different PBR runs (Table 20). The correlation between simulated results from the logistic equation and the actual data was determined by the r^2-value (Table 20). The logistic model tracked the experimental data in good agreement with a correlation determination (r^2) of 0.726 - 0.957. High r^2-values indicated that the logistic model accurately described microalgal growth at the different runs with minimal error. Values of μ_{max} and B_{max} varied among the runs. The μ_{max} of runs B and C had similar values of 0.361 d^{-1} and 0.388 d^{-1}, respectively. Although the highest μ_{max} of 0.443 d^{-1} was recorded for run A, this run displayed the lowest B_{max} of 1.261 g/l. Run B recorded the highest B_{max} of 3.187 g/l, exhibiting the best growth performance. This was in agreement with the biomass results discussed above (run B yielded the maximum biomass 3.415 g/l). The B_{max} value represents the maximum microalgal biomass concentration that can be supported at particular experimental conditions without any significant negative impact on the microalgal population.

Table 20: Estimated logistic model parameters (μ_{max} and B_{max}) at the different runs within the photobioreactor

	μ_{max} (d^{-1})	B_{max} (g/l)	r^2
Run A	0.4431	1.2613	0.7259
Run B	0.3615	3.1873	0.9571
Run C	0.3879	2.3511	0.9658

6.3.3 CO_2 Uptake Rate

Carbon dioxide uptake rates of the *Chlorella* sp. during the different PBR runs are depicted in Figure 36. Results obtained correlate with the biomass yield (Figure 35). As mentioned above, PBR run B facilitated maximum growth, enabling the microalga to reach a biomass value of 3.415 g/l on day 23. Similarly, the highest uptake rate (0.7971 g/day) was recorded during run B. Run B had a 55.87 and 39.21% higher CO_2 uptake rate when compared to the rates calculated for runs A and C, respectively. From all three PBR runs, run A produced the lowest biomass yield of 1.665 g/l. Likewise, the lowest uptake rate (0.5114 g/day) was observed during continuous flue gas aeration (PBR run A). Even though the control run (run C) had a slightly higher uptake rate (0.5726 g/day) when compared to that of run A, there was no significant difference ($p > 0.05$) between these two runs. This implies that continuous flue gas aeration as well as growth under un-optimised conditions hindered the CO_2 uptake rate of the microalgal strain. It can be further be deduced that biomass yield directly influenced uptake rate.

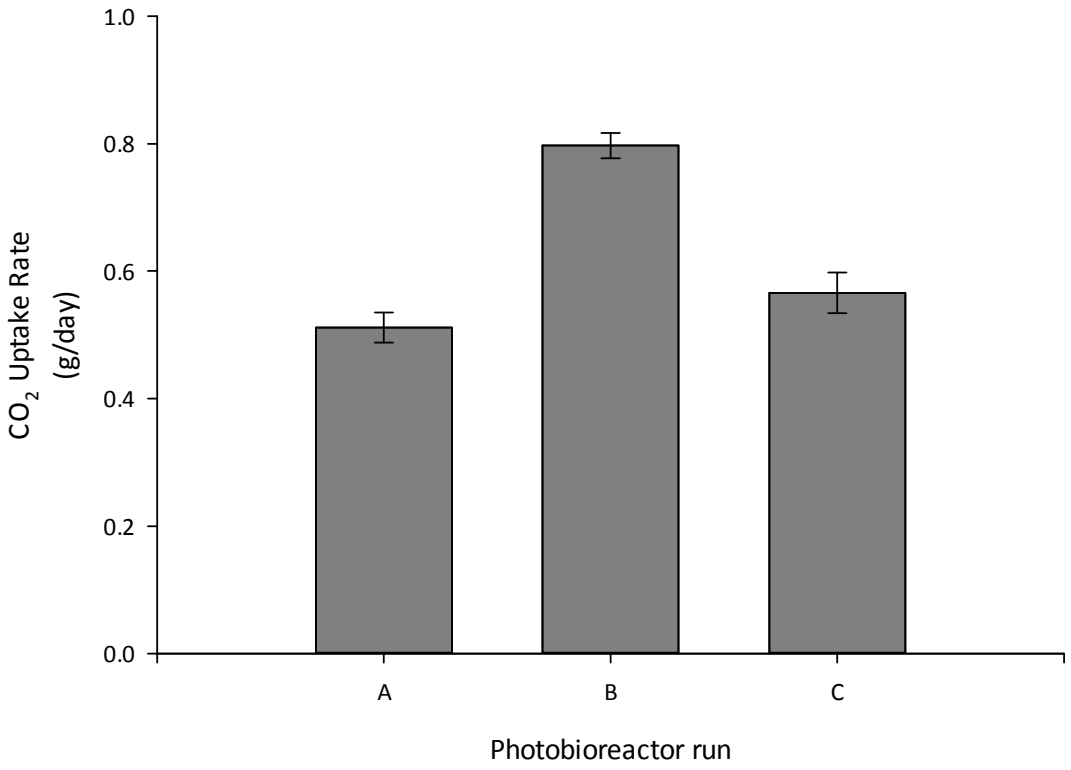

Figure 36: CO_2 uptake rate of the *Chlorella* sp. during the different photobioreactor runs (A) aerated continuously with flue gas under optimised conditions of light intensity, photoperiod and nutrients, (B) grown under optimised conditions of light intensity, photoperiod and nutrients and periodic exposure to the flue gas mixture, (C) control run: periodic exposure to the flue gas mixture under un-optimised conditions of light intensity, photoperiod and nutrients.

6.3.4 Fluorescence Measurements

The overall photosynthetic performance of a microalgal strain can be determined by the rETR, which is a measure of the rate of linear electron transport through PSII (Ramanna *et al*., 2014; White *et al*., 2011).

An increase in rETR within the first six days was observed for the strain in all the PBR runs. (Figure 37). Ramanna *et al*. (2014), proposed that an increase in rETR at the start of an experiment could be attributed to the acclimatisation of the culture to the new environmental conditions. Runs B and C showed a steady state in rETR up to day 18 before decreasing. This implies that PSII-dependent electron transport during these runs was not completely inhibited (Ramanna *et al*., 2014; White *et al*., 2011). Contrary to runs B and C, the rETR values recorded during PBR run A were inconsistent. The highest rETR reached by the culture during run A was 18.73 on day 15. While, run B displayed the maximum rETR value of 23.28 on day 15. Overall results showed that the lowest rETR values were seen for run A, whereas run B maintained a higher rETR when compared to the other runs. During both these runs (A and B) the culture was grown under optimised conditions of light intensity, photoperiod and nutrients however, there was a considerable difference in the physiological data obtained from PAM fluorometry. Results therefore suggested that the mode of flue gas supply played an important part as less physiological stress was evident in cells that were intermittently exposed to the flue gas blend (runs B and C) as opposed to cells that were cultured under conditions of continuous flue gas exposure (run A). An eventual decline to a rETR value of 0 suggests that the culture had entered/or was entering the death phase (Ramanna *et al*., 2014). From Figure 37 it can be seen that run A approached the death phase much earlier (day 21) when compared to the other 2 runs (B and C), that only advanced towards the death phase three days later (day 24).

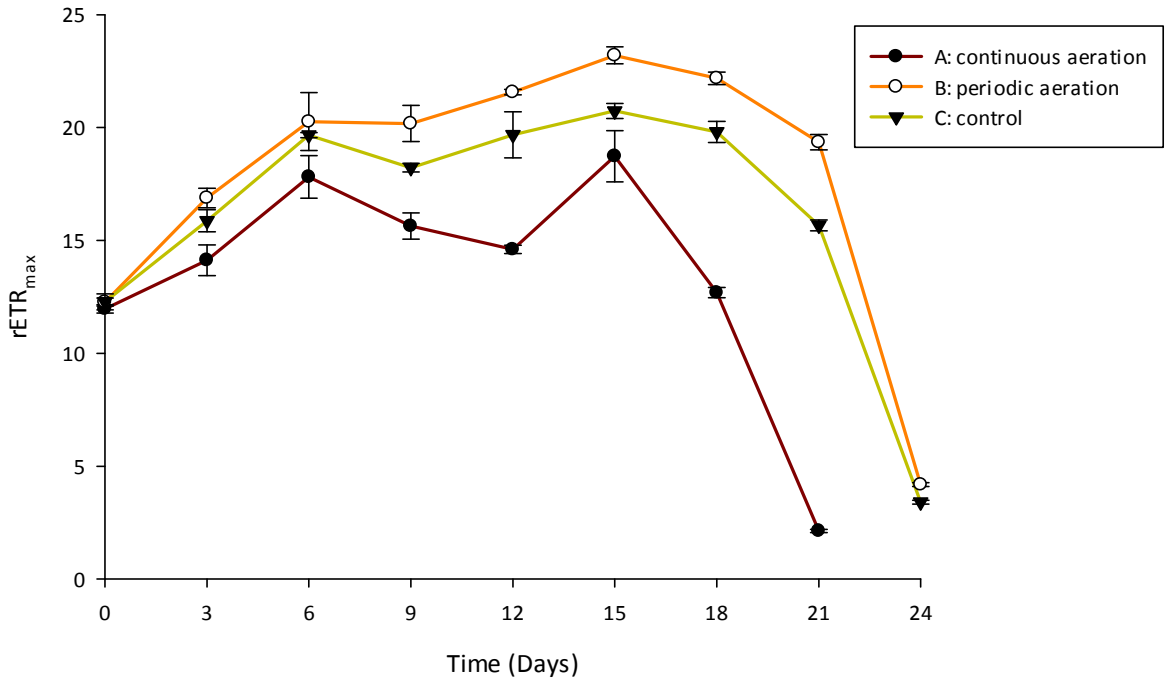

Figure 37: Maximum relative electron transport (rETR) at the different runs within the photobioreactor.

In 2011, White *et al.* used rETR measurements to assess microalgal nutrient stress. They observed a significant change in the physiological parameters of the microalgae during conditions of nitrogen depletion. Our findings showed that a continuous supply of flue gas (run A) led to significant physiological stress (erratic and lower rETR values). This was possibly due to toxicity (caused by nonstop exposure to high concentrations of CO_2 as well as the presence of SO_2 and NO_2). Continuous aeration with flue gas could have the normal production of ATP in the cells. This was evident by the lower and irregular rETR values. These conditions possibly reduced the efficiency of PSII which resulted in a decrease in the rate of photosynthesis (rETR), respiration and some enzyme activities ultimately leading to early microalgal death (Ramanna *et al.*, 2014; White *et al.*, 2011).

A polynomnial model was fitted to the data which yielded quadratic equations (Figures 38 ans 39) that showed maxima for rETR and uptake rate during most of the PBR runs (5 out of 6 of the equations). The quadratic model in most instances fitted the data well ($r^2 > 0.7$). Inferences drawn from the calculated values can be used for comparative purposes. The highest rETR (21.72) was obtained during an intermittent feeding of flue gas under optimised conditions at an optimum biomass concentration of 1.95 g/l (run B). This was greater than the control (run C) and the run where flue gas was continuously fed to the reactor (run A). Carbon dioxide uptake results mirrored the rETR and established a correlation between the two parameters, however the peak biomass for uptake was higher than the peak biomass for optimum rETR (refer to Figure 35). The maximum biomass concentration (1.95 g/l) at the optimal rETR is indiciative of a mid log culture, while the maximum uptake rate is at the early stationary phase. Photobioreactors need to be optimised for CO_2 uptake. The biomass production curves may yield an indication of the optimum during stationary phase. Relative electron transport rate peaks earlier than CO_2 uptake rate. This could be due to the fact that biomass has to establish vitality before it has the ability to take up CO_2. Theriotically, if a similar flat panel PBR were to be scaled-up to approximately 100 l and operated under optimal conditions (run B) using the *Chlorella* sp. in this study, then a potential CO_2 uptake of 26.570 g/day could be achieved.

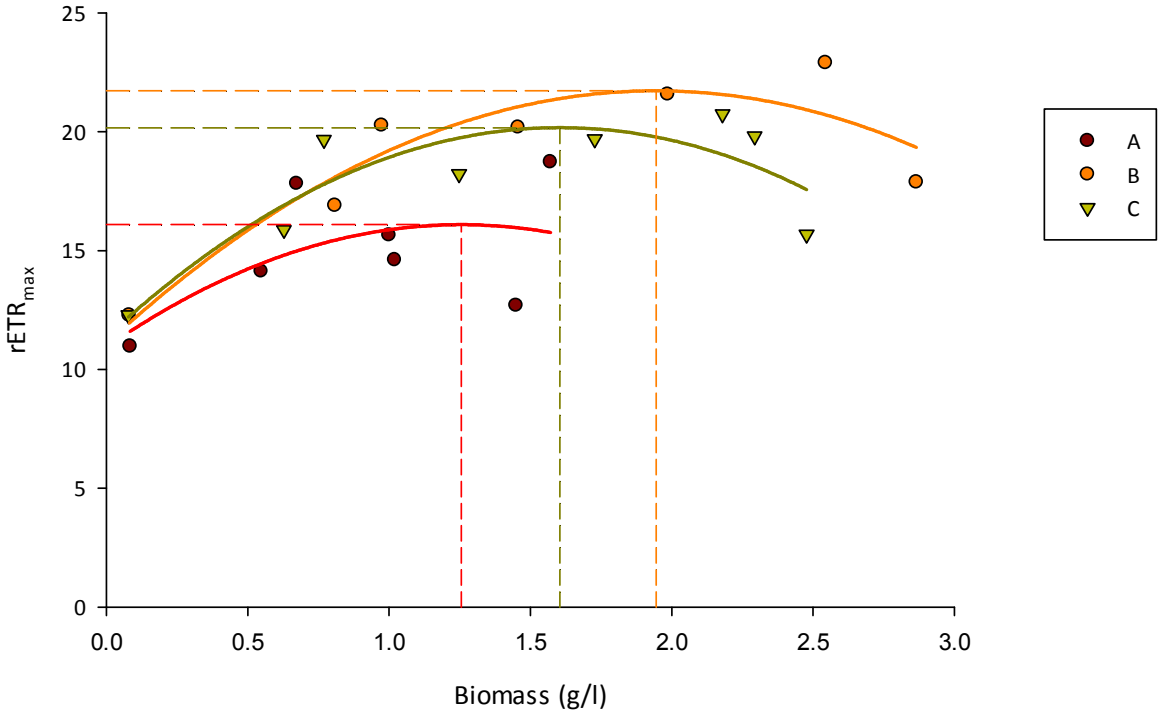

Figure 38: Relationship between rETR and biomass production during the different photobioreactor runs.

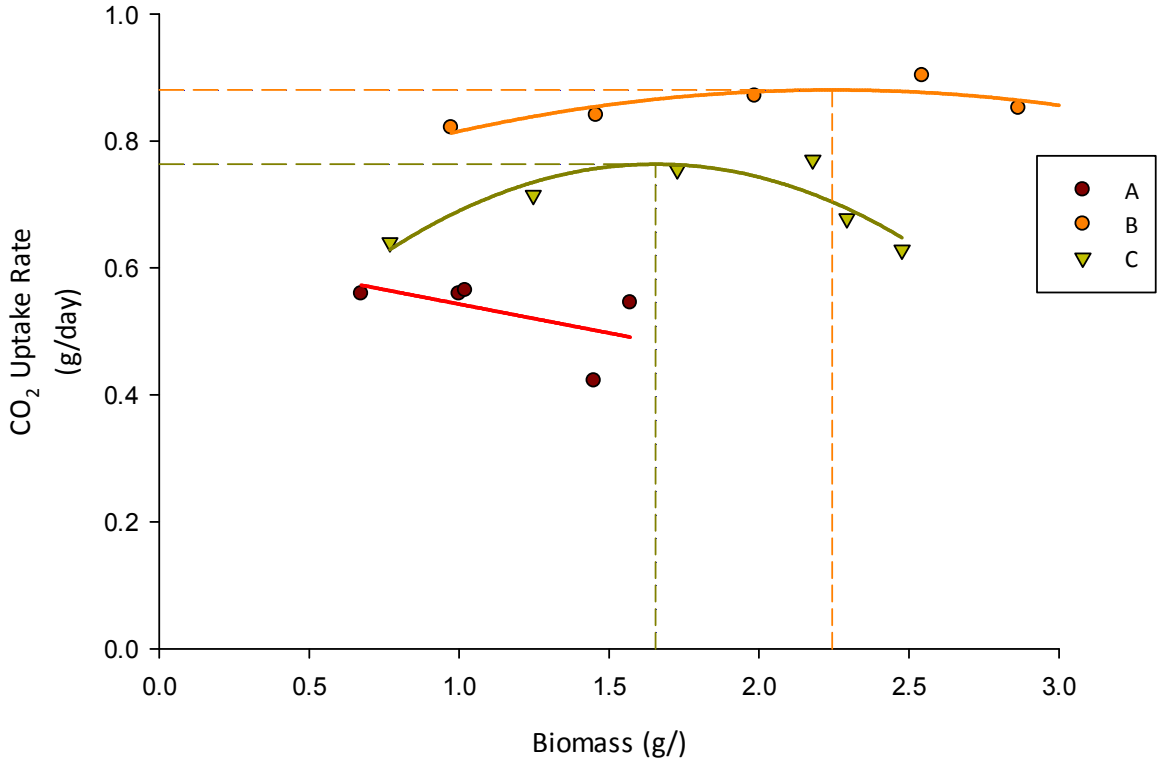

Figure 39: Relationship between CO_2 uptake rate and biomass production during the different photobioreactor runs.

6.3.5 Biochemical Composition

The impact of flue gas exposure on the synthesis of major metabolites (carbohydrates, proteins and lipids) was assessed.

According to Duarte *et al*. (2016), microalgal strains can suffer cell stress during unfavourable conditions, causing them to produce higher quantities of carbohydrate and lipid. This was evident in the current study (Table 21): carbohydrate and lipid concentrations in the *Chlorella* biomass on day 16 were considerably higher during adverse conditions of continuous flue gas exposure (run A). In 2008, Chiu *et al*., stated that exposure to CO_2 concentrations above 10% could possibly cause cellular stress and inhibition of microalgal growth. During these conditions, the microalgal cells yield higher amounts of lipid macromolecules. As seen in Table 21, only a slight increase was observed in carbohydrate and lipid concentrations on day 16 for run B. This therefore suggests that the growth conditions during run B were not stressful to the microalgal cells (Duarte *et al*., 2016). In 2013, Anjos *et al*., exposed a *Chlorella* sp. to 6% CO_2 and obtained a lipid concentration of approximately 10%. The authors of this study concluded that exposure to 6% CO_2 was not high enough to cause cellular stress in this microalga, therefore leading to the relatively low yield of this macromolecule (lipid) in the biomass. In a study by Kao *et al*. (2014), maximum lipid of 33.8% was obtained from a *Chlorella* sp. when the strain was cultivated with flue gas that contained approximately 24% CO_2, 15 - 20 ppm SO_2 and 25 - 30 ppm NO_2.

Table 21: Carbohydrate, protein and lipid production of *Chlorella* sp. during flue gas exposure at different runs

Metabolites (% w/w)	Run A				Run B				Run C			
	Day 0		Day 16		Day 0		Day 16		Day 0		Day 16	
	Ave	Std Err	Ave	Std Err	Ave	Std Err	Ave	Std Err	Ave	Std Err	Ave	Std Err
Carbohydrate	32.3	1.1	32.6	3.6	31.4	1.5	29.5	3.6	31.9	1.2	31.0	3.5
Protein	47.6	1.3	42.0	3.2	48.3	0.9	49.9	4.1	47.4	1.3	43.8	4.5
Lipid	19.9	1.0	24.9	2.7	19.8	1.1	19.9	1.0	19.9	0.9	24.0	1.3

Unlike the trend observed for carbohydrate and lipid accumulation, the protein content of the microalgal culture during this study decreased during run A (continuous flue gas exposure) and increased during conditions of intermittent flue gas exposure (run B) (Table 21). This could be explained by the fact that an enhancement in cell multiplication leads to increased protein production by microalgal cells, which were synthesised from CO_2 biofixation in the Calvin cycle (Duarte *et al*., 2016). In this study, run B yielded the most biomass and displayed the highest CO_2 uptake rate, thereby producing the most protein (57.6%). The presence of NO_2 and SO_2 in the flue gas could have also served as an additional nitrogen and sulfur sources for protein biosynthesis (Li *et al*., 2015). Proteins are macromolecules that have multiple functions in microalgal cells. They are not only involved in growth and maintenance but are also responsible for regulation of cellular activities (Duarte *et al*., 2016). In a study by Duarte *et al*. (2016), it was observed that the highest protein concentrations (50.8 - 52.3%) of C. *fusca* LEB 111 were obtained in experiments that displayed high growth rates and CO_2 biofixation efficiencies.

6.3.6 Morphological Observation by SEM

Figure 40 (images a - d) depicts SEM images of the *Chlorella* strain after 16 days of cultivation. Normal morphology was observed for cells not aerated with flue gas (Figure 40a). From Figure 40 it can also be seen that the surfaces of the algal cells were smoother when compared to alga cells exposed to flue gas. Cells were partially broken during intermittent flue gas exposure (images b and c). Continuous exposure to flue gas proved very toxic as cells were severely broken as seen in image d.

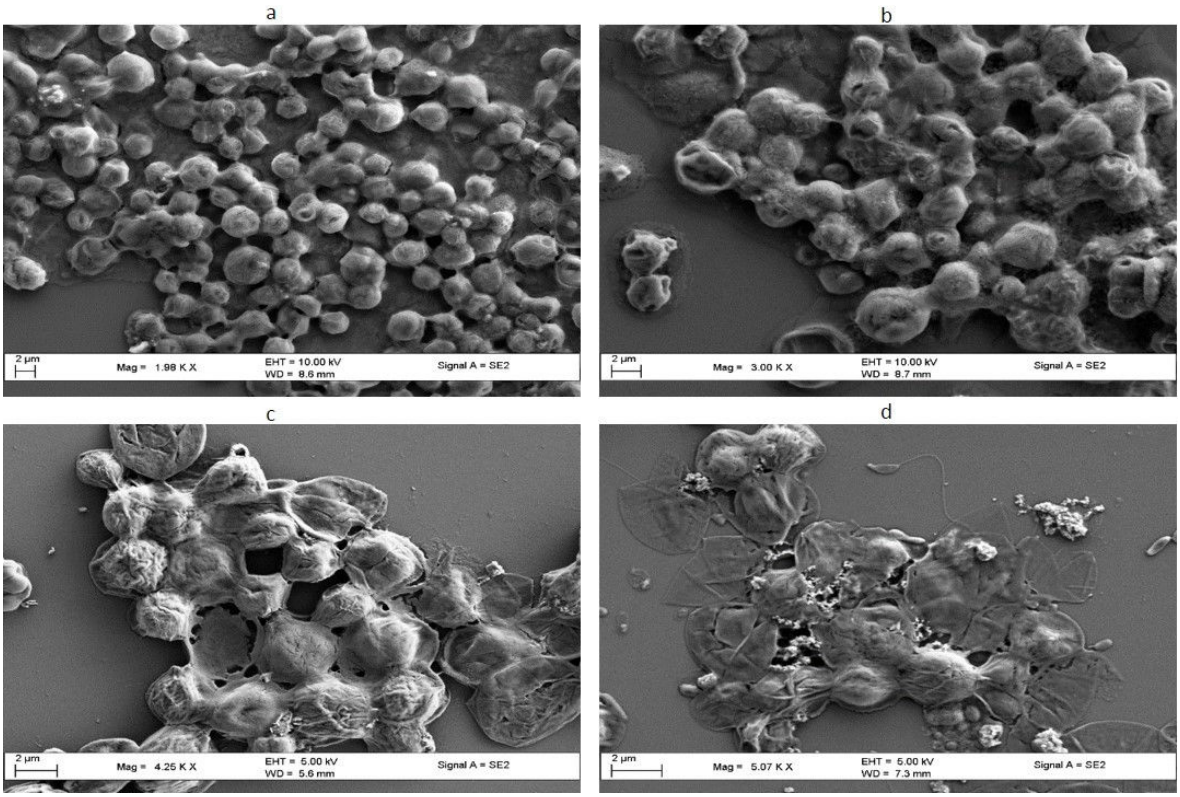

Figure 40: Scanning electron microscopic images of *Chlorella* sp. on day 16 of cultivation: (a) no flue gas aeration, (b) grown under optimised conditions of light intensity, photoperiod and nutrients and intermittently exposed to the flue gas mixture, (c) control run: periodic exposure to the flue gas mixture under un-optimised conditions of light intensity, photoperiod and

nutrients and (d) aerated continuously with flue gas under optimised conditions of light intensity, photoperiod and nutrients.

CHAPTER SEVEN: CONCLUSION AND RECOMMENDATIONS

7.1 CONCLUSIONS

Based on the research conducted, the following can be concluded:

- A novel indigenous *Chlorella* strain capable of growth in extremely high CO_2 concentrations (> 30%) was isolated. This strain displayed the most potential as a carbon sequester when compared to the other isolated microalgal strains. At high $NaHCO_3$ (2 g/l) and CO_2 (10 and 15%), concentrations, biomass production and CO_2 uptake by the *Chlorella* strain was the only culture comparable to that of the reference strain (*Coccolithus pelagicus* 913/3). This highlights the potential of utilising indigenous strains that have acclimatised to high CO_2 environments (strain was isolated from an aquatic sample close to high CO_2-producing industries).

- When comparing CO_2 and $NaHCO_3$ as carbon sources, the latter induced an overall slower microalgal growth rate and lower biomass production.

- *Coccolithus pelagicus* 913/3 and the isolated *Chlorella* strain displayed the highest $rETR_{max}$ during 15% CO_2, equivalent to values of 20.07 and 18.10, respectively. This was the first time a system for CO_2 fixation was assessed for its fitness for purpse using algal phyisological responses. These results were in accordance with the highest B_{max} recorded during 15% CO_2, demonstrating a lower degree of stress at higher CO_2 concentrations.

- Abiotic factors have an influence on the biomass production. The optimised abiotic conditions for higher biomass yield of the *Chlorella* strain were at 175 µmol m^{-2} s^{-1} and a light:dark cycle of 16:8, yielding B_{max} values of 1.762 and 2.514 g/l, respectively. Sunlight provides a light intensity of ± 5027 µmol m^{-2} s^{-1}. A closed reactor with artificial lighting therefore, provided the ideal set up for cultivation of this organism. These parameters have not been previously elucidated by a high-CO_2 sequestering *Chlorella* sp.

- Fractional factorial and CCDs were useful to determine the optimum concentration levels of medium components that significantly influence the biomass yield of the *Chlorella* sp. The experimental design predicted a maximum biomass production of 3.051 g/l, which was 134.65% higher when compared to cultivation using the original ASW medium (1.290 g/l). The optimised biomass yield was one of the highest recorded *Chlorella* sp. biomass concentrations recorded in literature to date.

- The design of the photobioreactor system proved to be both durable and practical. Furthermore, the bubble stone delivery system proved to be highly efficient in uniformly supplying the culture suspension with the CO_2 rich gas mixture.

- Overall results demonstrated that the *Chlorella* sp. was able to grow well in a closed flat panel reactor under conditions of flue gas aeration. Biomass yield, however, was dependent on culture conditions and the mode of flue gas supply. Run B facilitated maximum growth, enabling the microalga to reach a biomass value of 3.415 g/l on day 23. This was a 37.87% increase in growth when compared to the control run (C), which produced 2.477 g/l biomass on day 23.

- Less physiological stress ($rETR_{max}$) was evident in cells that were intermittently exposed to the flue gas blend (runs B and C) as opposed to cells that were cultured under conditions of continuous flue gas exposure (run A). Run B displayed the maximum rETR value of 23.28 on day 15.

- Morphological studies showed that the surfaces of the algal cells not exposed to flue gas were smoother when compared to the cells exposed to flue gas. Cells were partially broken during intermittent flue gas exposure, while continuous exposure to flue gas proved very toxic leading to severely broken cells.

7.2 RECOMMENDATIONS

Global warming and climate change has been attributed largely to increased CO_2 emissions. Flue gases from polluting industries are known to contribute to increases in CO_2 in the atmosphere. Therefore, applying on site treatment for flue gases has substantial potential to reduce harmful carbon emissions. Recommendations for future research are as follows:

- The isolated *Chlorella* strain proved to be a promising candidate for CO_2 sequestration. Further research could focus on the genetic manipulation of this strain in an attempt to further increase biomass yields and CO_2 uptake rates.

- Closed systems for microalgal-mediated CO_2 fixation require substantial amounts of capital for their sustained operation. Thus more efforts are required to improve photobioreactor technologies to increase their cost effectiveness and efficiency.

- Microalgal-mediated CO_2 fixation coupled with the production of biofuels/valuable by-products and wastewater treatment could present a promising alternative to existing CO_2 mitigation strategies. This will aid in improving the economics of the technology and assist in increasing the potential for large scale application.

REFERENCES

Adams, C., Godfrey, V., Wahlen, B., Seefeldt, L. and Bugbee, B. 2013. Understanding precision nitrogen stress to optimize the growth and lipid content trade off in oleaginous green microalgae. *Bioresource Technology*. **131**: 188-194.

Al-Hothaly, K., Taha, M., May, B., Stylianou, S., Ball, A. and Adetutu, E. 2015. The effect of nutrients and environmental conditions on biomass and oil production in *Botryococcus braunii* Race B strains. *European Journal of Phycology*. DOI: 10.1080/09670262.2015.1071875.

Alabi, A. O., Tampier, M. and Bibeau, E. 2009. Microalgae technologies and processes for biofuels/bioenergy production in British Columbia. The British Columbia Innovation Council, Winnipeg.

Albalasmeh, A. A., Berhe, A. A. and Ghezzehei, T. A. 2013. A new method for rapid determination of carbohydrate and total carbon concentrations using UV spectrophotometry. *Carbohydrate Polymers*. **97:** 253-261.

Alexander, P. and Markus, H. 2006. Effects of manganese on chlorophyll fluorescence in epiphytic cyano- and chlorolichens, *Flora-Morphology, Distribution, Functional Ecology of Plants*. **201:** 451-460.

Allen, M. B. and Arnon, D. I. 1955. Studies on nitrogen fixing blue green algae II. The sodium requirement of *Anabaena cylindrica*. *Plant Physiology*. **8**: 653-660.

Anderson, M. J. and Whitcomb, P. J. 2005. RSM simplified: Optimizing processes using response surface methods for design of experiments. New York, USA: Productivity Press. ISBN-13: 978-1563272974.

Anjos, M., Fernandes, B., Vicente, A., Teixeira, J. and Dragone, G. 2013. Optimization of CO_2 biomitigation by *Chlorella vulgaris*. *Bioresource Technology*. **139**: 149-154.

Ansari, F. A., Shriwastav, A., Gupta, S. K., Rawat, R., Guldhe, A. and Bux, F. 2015. Lipid extracted algae as a source for protein and reduced sugar: A step closer to the biorefinery. *Bioresource Technology*. **179:** 559-564.

Aresta, M., Dibenedetto, A. and Barberio, G. 2005. Utilization of macroalgae for enhanced CO_2 fixation and biofuels production: development of a computing software for an LCA study. *Fuel Process Technology*. **86:** 1679-1693.

Baker, N. 2008. Chlorophyll Fluorescence: A Probe of Photosynthesis in Vivo. *Annual Review of Plant Biology*. **59**: 89-113.

Baky, H. H. A. E., El-Baroty, G. S., Bouaid, A., Martinez, M. and Aracil, J. 2012. Enhancement of lipid accumulation in *Scenedesmus obliquus* by optimizing CO_2 and Fe^{3+} levels for biodiesel production. *Bioresource Technology*. **119:** 429-432.

Barghbani, R., Rezaei, K. and Javanshir, A. 2012. Investigating the effects of several parameters on the growth of *Chlorella vulgaris* using Taguchi's experimental approach. *International Journal of Biotechnology for Wellness Industries*. **1**: 128-133.

Basu, S., Roy, A. S., Mohanty, K. and Ghoshal, A. K. 2013. Enhanced CO_2 sequestration by a novel microalga: *Scenedesmus obliquus* SA1 isolated from bio-diversity hotspot region of Assam, India. *Bioresource Technology*. **143:** 369-377.

Basu, S., Roy, A. S., Mohanty, K. and Ghoshal, A. K. 2014. CO_2 biofixation and carbonic anhydrase activity in *Scenedesmus obliquus* SA1 cultivated in large scale open system. *Bioresource Technology*. **164:** 323-330.

Becker, E. W. 1995. Chapter 3: Culture media. Microalgae: Biotechnology and microbiology. Cambridge University Press.

Belay, A., Ota, Y., Miyakawa, K. and Shimamatsu, H. 1993. Current knowledge on potential health benefits of *Spirulina*. *Journal of Applied Phycology*. **5:** 235-41.

Benemann, J. R. 1993. Utilization of carbon dioxide from fossil fuel-burning power plants with biological system. *Energy Conversion Management*. **34:** 100-999.

Benemann, J. R., Koopman, B. L., Weissman, J. C., Eisenberg, D. M. and Oswald, W. J. 1977. Species control in large scale microalgae biomass production. Report to University of California Berkeley. SERL 77-5, SAN/740-77/1.

Benemann, J. R. and Oswald, W. J. 1996. Systems and economic analysis of microalgae ponds for conversion of CO_2 to biomass. Final report US DOE. http://www.osti.gov/bridge/servlets/purl/493389-FXQyZ2/webviewable/493389.pdf.

Berges, J. A., Franklin, D. J. and Harrison, P. J. 2001. Evolution of an artificial seawater medium: improvements in enriched seawater, artificial water over the last two decades. *Journal of Phycology*. **37:** 1138-45.

Boddy, R. and Smith, G. 2009. Statistical methods in practice for scientist and technologists. United Kingdom: John Wiley & Sons. ISBN: 9780470746646.

Borkenstein, C. G., Knoblechner, J., Fru¨hwirth, H. and Schagerl, M. 2011. Cultivation of *Chlorella emersonii* with flue gas derived from a cement plant. *Journal of Applied Phycology*. **23:** 131-135.

Borowitzka, M. A. 1999. Commercial production of microalgae: ponds, tanks, tubes and fermenters. *Journal of Biotechnology*. **70:** 313-321.

Box, G.E.P. 2005. Statistics for Experimenters - Second Edition. Hoboken, N.J, Wiley-Interscience. ISBN: 0-471-09315-7.

Boyer, G. L. and Brand, L. E. 1998. Trace elements and harmful algal blooms. *Physiological Ecology of Harmful Algal Blooms*. Springer, Berlin, Germany. pp. 489-508.

Brennan, L. and Owende, P. 2010. Biofuels from microalgae-a review of technologies for production, processing, and extractions of biofuels and co-products. *Renewable Sustainable Energy Reviews*. **14:** 557-577.

Burrows, E., Chaplen, F. and Ely, R. 2008. Optimization of media nutrient composition for increased photofermentative hydrogen production by *Synechocystis* sp. PCC 6803. *International Journal of Hydrogen Energy*. **33**: 6092-6099.

Calvin, M. 1989. 40 years of photosynthesis and related activities. *Photosynthetic Research*. **21:** 3-16.

Campbell, P. K., Beer, T. and Batten, D. 2011. Life cycle assessment of biodiesel production from microalgae in ponds. *Bioresource Technology*. **102:** 50-56.

Carroll, J. J. and Mather, A. E. 1992. The system carbon dioxide-water and the Krichevsky-Kasarnovsky equation. *Journal of Solution Chemistry*. **21:** 1201-1209.

Carvalho, P. J., Pereira, L. M. C., Goncalves, N. P. F., Queimada, A. J. and Coutinho, J. A. P. 2010. Carbon dioxide solubility in aqueous solutions of NaCl: Measurements and modeling with electrolyte equations of state. *Fluid Phase Equilibria*. **388:** 100-106.

Cerveny, J., Setlik, I., Trtilek, M. and Nedbal, L. 2009. Photobioreactor for cultivation and real-time, in situ measurement of O_2 and CO_2 exchange rates, growth dynamics, and of chlorophyll fluorescence emission of photoautotrophic microorganisms. *Engineering in Life Sciences*. **9:** 247-253.

Chang, H. X., Huang, Y., Fu, Q., Liao, Q. and Zhu, X. 2016. Kinetic characteristics and modeling of microalgae *Chlorella vulgaris* growth and CO_2 biofixation considering the coupled effects of light intensity and dissolved inorganic carbon. *Bioresource Technology*. **206**: 231-238.

Chang, E. H. and Yang, S. S. 2003. Some characteristics of microalgae isolated in Taiwan for biofixation of carbon dioxide. *Botanical Bulletin of Academia Sinica*. **44**: 43-52.

Changdong, S. and Azevedo, J. L. T. 2005. Estimating the higher heating value of biomass fuels from basic analysis data. *Biomass Bioenergy*. **28**: 499-507.

Cheah, W., McMinn, A., Griffiths, F. B., Westwood, K. J., Wright, S. W. and Clementson, L. A. 2013. Response of phytoplankton photophysiology to varying environmental conditions in the Sub-Antarctic and Polar Frontal Zone. *PLoS One*. DOI: 10.1371/journal.pone.0072165.

Cheah, W. Y., Show, P. L., Chang, J. S., Ling, T. C. and Juan, J. C. 2015. Biosequestration of atmospheric CO_2 and flue gas-containing CO_2 by microalgae. *Bioresource Technology*. **184:** 190-201.

Chen, X. W. and Gao, K. S. 2003. Effect of CO_2 concentrations on the activity of photosynthetic CO_2 fixation and extracelluar carbonic anhydrase in the marine diatom *Skeletonema costatum*. *Chinese Science Bulletin*. **48**: 2616-2620.

Chen, C. Y., Yeh, K. L., Su, H. M., Lo, Y. C., Chen, W. M. and Chang, J. S. 2010. Strategies to enhance cell growth and achieve high-level oil production of a *Chlorella vulgaris* isolate. *Biotechnology Progresses*. **26:** 679-686.

Cheng, L. H., Zhang, L., Chen, H. L. and Gao, C. J. 2006. Carbon dioxide removal from air by microalgae cultured in a membrane photobioreactor. *Separation Purification Technology*. **50:** 324-329.

Cheirsilp, B. and Torpee, S. 2012. Enhanced growth and lipid production of microalgae under mixotrophic culture condition: Effect of light intensity, glucose concentration and fed-batch cultivation. *Bioresource Technology*. **110**: 510-516.

Chiang, C. L., Lee, C. M. and Chen, P. C. 2011. Utilization of the cyanobacteria *Anabaena* sp. CH1 in biological carbon dioxide mitigation processes. *Bioresource Technology*. **102:** 5400-5405.

Chinnasamy, S., Ramakrishnan, B., Bhatnagar, A. and Das, K. 2009. Biomass production potential of a wastewater alga *Chlorella vulgaris* ARC 1 under elevated levels of CO_2 and temperature. *International Journal of Molecular Sciences*. **10**: 518-532.

Chisti, Y. 2007. Biodiesel from microalgae. *Biotechnology Advances*. **25:** 294-306.

Chisti, Y. 2008. Biodiesel from microalgae beats bioethanol. *Trends in Biotechnology*. **26:** 126-131.

Chiu, S. Y., Kao, C. Y., Chen, C. H., Kuan, T. C., Ong, S. C. and Lin, C. S. 2008. Reduction of CO_2 by a high density culture of *Chlorella* sp. in a semi continuous photobioreactor. *Bioresource Technology*. **99:** 3389-3396.

Chiu, S. Y., Kao, C. Y., Huang, T. T., Lin, C. J., Ong, S. C., Chen, C. D., Chang, J. S. and Lin, C. S. 2011. Microalgal biomass production and on-site bioremediation of carbon dioxide, nitrogen oxide and sulfur dioxide from flue gas using *Chlorella* sp. cultures. *Bioresource Technology*. **102:** 9135-9142.

Chiu, S. Y., Kao, C. Y., Tsai, M. T., Ong, S. C., Chen, C. H. and Lin, C. S. 2009. Lipid accumulation and CO_2 utilization of *Nannochloropsis oculata* in response to CO_2 aeration. *Bioresource Technology*. **100:** 833-838.

Chung, I. K., Beardall, J., Mehta, S., Sahoo, D. and Stojkovic, S. 2011. Using marine macroalgae for carbon sequestration: a critical appraisal. *Journal of Applied Phycology*. **23:** 877-886.

Clarens, A. F., Resurreccion, E. P., White, M. A. and Colosi, L. M. 2010. Environmental life cycle comparison of algae to other bioenergy feedstocks. *Environmental Science Technology*. **44:** 1813-1819.

Costa, J., Alves, M. and Ferreira, E. 2009. Principal component analysis and quantitative image analysis to predict effects of toxins in anaerobic granular sludge. *Bioresource Technology*. **100**: 1180-1185.

Costa, J. A. V., Linde, G. A. and Atala, D. I. P. 2000. Modelling of growth conditions for cyanobacterium *Spirulina platensis* in microcosms. *World Journal of Microbiology and Biotechnology*. **16:** 15-18.

Crofcheck, C. E. X., Shea, A., Montross, M., Crocker, M. and Andrews, R. 2012. Influence of media composition on the growth rate of *Chlorella vulgaris* and *Scenedesmus acutus* utilized for CO_2 mitigation. *Journal of Biochemical Technology*. **4**: 589-594.

Dautania, G. and Singh, G. 2012. Growth and protein profiling by the cyanobacterium *Anacystis nidulans* strains at different temperature and photoperiod. *Open Access Scientific Reports*. 1(10) DOI:10.4172/scientificreports.482.

de Morais, M. G. and Costa, J. A. V. 2007. Biofixation of carbon dioxide by *Spirulina* sp. and *Scenedesmus obliquus* cultivated in a three stage serial tubular photobioreactor. *Journal of Biotechnology*. **129:** 439-445.

Del Campo, J. A., Garcia-Gonzalez, M. and Guerrero, M. G. 2007. Outdoor cultivation of microalgae for carotenoid production: current state and perspectives. *Applied Microbiology and Biotechnology*. **74:** 117-1163.

Demirbas, A. and Demirbas, M. F. 2011. Importance of algae oil as a source of biodiesel. *Energy Conversion Management*. **52:** 163-170.

Devgoswami, C., Kalita, M., Talukdar, J., Bora, R. and Sharma, P. 2011. Studies on the growth behavior of *Chlorella*, *Haematococcus* and *Scenedesmus* sp. in culture media with

different concentrations of sodium bicarbonate and carbon dioxide gas. *African Journal of Biotechnology*. **10**: 13128-13138.

Dobrev, G. T., Pishtiyski, I. G., Stanchev, V. S. and Mircheva, R. 2007. Optimization of nutrient medium containing agricultural wastes for xylanase production by *Aspergillus niger* B03 using optimal composite experimental design. *Bioresource technology*. **98:** 2671-2678.

Dou, X., Lu, X. H., Lu, M. Z., Yu, L. S., Xue, R. and Ji, J. B. 2013. The effects of trace elements on the lipid productivity and fatty acid composition of *Nannochloropis oculata*. *Journal of Renewable Energy*. http://dx.doi.org/10.1155/2013/671545.

Duarte, J. H., Fanka, L. S. and Costa, J. A. V. 2016. Utilization of simulated flue gas containing CO_2, SO_2, NO and ash for *Chlorella fusca* cultivation. *Bioresource Technology*. **214**: 159-165.

DuBois, M., Gilles, K., Hamilton, J., Rebers, P. and Smith, F. 1956. Colorimetric method for determination of sugars and related substances. *Analytical Chemistry*. **28:** 350-356.

Eggert, A., Raimund, S., Michalik, D., West, J. and Karsten, U. 2007. Ecophysiological performance of the primitive red alga *Dixoniella grisea* (Rhodellophyceae) to irradiance, temperature and salinity stress: growth responses and the osmotic role of mannitol. *Phycologia*. **46**: 22-28.

Ernst, A., Deicher, M., Herman, P. M. and Wollenzien, U. I. 2005. Nitrate and phosphate affect cultivability of cyanobacteria from environments with low nutrient levels. *Applied Environmental Microbiology*. **71:** 3379-3383.

Farrelly, D. J., Everard, C. D., Fagan, C. C. and McDonnell, K. P. 2013. Carbon sequestration and the role of biological carbon mitigation: a review. *Renewable Sustainable Energy Reviews*. **21:** 712-727.

Fathi, M. and Asem, A. 2013. Investigating the impact of NaCl salinity on growth, β-carotene, and chlorophyll *a* in the content life of halophytes of algae *Chlorella* sp. *Aquaculture, Aquarium, Conservation & Legislation International Journal of the Bioflux Society*. **6:** 241-245.

Feng, Y., Warner, M., Zhang, Y., Sun, J., Fu, F. X., Rose, J. and Hutchins, D. 2008. Interactive effects of increased pCO_2, temperature and irradiance on the marine *coccolithophore Emiliania huxleyi* (Prymnesiophyceae). *European Journal of Phycology*. **43**: 87-98.

Fields, M. W., Hise, A., Lohman, E. J., Bell, T., Gardner, R. D., Corredor, L., Moll, K., Peyton, B. M., Characklis, G. W. and Gerlach, R. 2014. Sources and resources: importance of nutrients, resource allocation, and ecology in microalgal cultivation for lipid accumulation. *Applied Microbiology and Biotechnology*. **98:** 4805-4816.

Fu, C. C., Hung, T. C., Chen, J. Y., Su, C. H. and Wu, W. T. 2010. Hydrolysis of microalgae cell walls for production of reducing sugar and lipid extraction. *Bioresource Technology*. **101:** 8750-8754.

Geckler, R. P., Sane, J. O. and Tew, R. W. 1962. Highly concentrated carbon dioxide as a carbon source for continuous algae cultures [Online]. http://contrails.iit.edu/DigitalCollection/1962/AMRLTDR6 [2013, 03/06].

Genty, B., Briantais, J. M. and Baker, N. R. 1989. The relationship between the quantum yield of photosynthetic electron transport and quenching of chlorophyll fluorescence. *Biochimica et Biophysica Acta*. **90**: 87-92.

George, B., Pancha, I., Desai, C., Chokshi, K., Paliwal, C., Ghosh, T. and Mishra, S. 2014. Effects of different media composition, light intensity and photoperiod on morphology and physiology of freshwater microalgae *Ankistrodesmus falcatus* - A potential strain for bio-fuel production. *Bioresource Technology*. **171**: 367-374.

Gibbin, E. M. and Davy, S. K. 2014. The photo-physiological response of a model cnidarian-dinoflagellate symbiosis to CO_2-induced acidification at the cellular level. *Journal of Experimental Marine Biology and Ecology*. **457**: 1-7.

Gimpel, J. A., Specht, E. A., Georgianna, D. R. and Mayfield, S. P. 2013. Advances in microalgae engineering and synthetic biology applications for biofuel production. *Current Opinion in Chemical Biology*. **17:** 1-7.

Giordano, M., Beardall, J. and Raven, J. A. 2005. Mechanisms in algae: mechanisms, environmental modulation, and evolution. *Annual Reviews in Plant Biology*. **56:** 99-131.

Gnansounou, E., Dauriat, A., Villegas, J. and Panichelli, L. 2009. Life cycle assessment of biofuels: energy and greenhouse gas balances. *Bioresource Technology*. **100:** 4919-4930.

Godhe, A., Anderson, D. M. and Rehnstam-Holm, A. S. 2001. PCR amplification of microalgal DNA for sequencing and species identification: studies on fixatives and algal growth stages. *Harmful Algae*. **1:** 375-382.

Goldman, J. and McCarthy, J. 1978. Steady-state growth and ammonium uptake of a fast growing marine diatom. *Limnology and Oceanography*. **23**: 695-703.

Gorain, P. C., Bagchi, S. K. and Mallick, N. 2013. Effects of calcium, magnesium and sodium chloride in enhancing lipid accumulation in two green microalgae. *Environmental Technology*. http://dx.doi.org/10.1080/09593330.2013.812668.

Gouveia, L., Veloso, V., Reis, A., Fernandes, H., Novais, J. and Empis, J. 1996. Evolution of pigment composition in *Chlorella vulgaris*. *Bioresource Technology*. **157:** 159-163.

Greenwell, H. C., Laurens, L. M. L., Shields, R. J., Lovitt, R. W. and Flynn, K. J. 2010. Placing microalgae on the biofuels priority list: a review of the technological challenges. *Journal of the Royal Society Interface*. **7:** 703-726.

Gressel, J., van der Vlugt, C. J. B. and Bergmans, H. E. N. 2013. Environmental risks of large scale cultivation of microalgae: Mitigation of spills. *Algal Research*. http://dx.doi.org/10.1016/j.algal.2013.04.002.

Grobbelaar, J. U., Nedbal, L. and Tichy, V. 1996. Influence of high frequency light/dark fluctuations on photosynthetic characteristics of microalgae photo-acclimated to different light intensities and implications for mass algal cultivation. *Journal of Applied Phycology*. **8:** 335-343.

Guillard, R. R. L. 1975. Culture of phytoplankton for feeding marine invertebrates. In Culture of marine invertebrate animals, pp. 29-60. Edited by W. L. Smith & M. H. Chanley. New York: Plenum. ISN 1464-3774.

Guillard, R. R. L. and Hargraves, P. E. 1993. *Stichochrysis immobilis* is a diatom, not a chrysophyte. *Phycologia*. **32**: 234-236.

Guillard, R. R. L. and Ryther, J. H. 1962. Studies of marine planktonic diatoms. I. *Cyclotella nana Hustedt* and *Detonula confervaceae* (Cleve) *gran*. *Canadian Journal of Microbiology*. **8**: 229-239.

Guldhe, A., Singh, B., Rawat, I., Ramluckan, K. and Bux, F. 2014. Efficacy of drying and cell disruption techniques on lipid recovery from microalgae for biodiesel production. *Fuel*. **128:** 46-52.

Gutierrez, R., Gutierrez-Sachaz, R. and Nafid, I. A. 2008. Trend analysis using nonhomogeneous stochastic diffusion processes. Emission of CO_2, Kyoto protocol in Spain. *Stochastic Environmental Research and Risk Assessment*. **22**: 57-66.

Hanagata, N., Takeuchi, T., Fukuju, Y., Barnes, D. J. and Karube, I. 1992. Tolerance of microalgae to high CO_2 and high-temperature. *Phytochemistry*. **31:** 3345-3348.

Hansen, J., Johnson, D., Lacis, A., Lebedeff, S., Lee, P., Rind, D. and Russell, G. 1981. Climate impact of increasing atmospheric carbon dioxide. *Science*. **213**: 957-966.

Hao, Z., Cai, Y., Liao, X., Zhang, X., Fang, Z. and Zhang, D. 2012. Optimization of nutrition factors on chitinase production from a newly isolated *Chitiolyticbacter meiyuanensis* SYBC-H1. *Brazilian Journal of Microbiology*. **43**: 177-186.

Heasman, M., Diemar, J., O'Connor, W., Sushames, T. and Foulkes, L. 2000. Development of extended shelf-life microalgae concentrate diets harvested by centrifugation for bivalve molluscs-a summary. *Aquaculture Research.* **31:** 637-659.

Hende, S. V. D., Vervaeren, H. and Boon, N. 2012. Flue gas compounds and microalgae: (Bio) chemical interactions leading to biotechnological opportunities. *Biotechnology Advances*. doi:10.1016/j.biotechadv. 2012.02.015.

Ho, S. H., Chen, W. M. and Chang, J. S. 2010. *Scenedesmus obliquus* CNW-N as a potential candidate for CO_2 mitigation and biodiesel production. *Bioresource Technology*. **101:** 8725-30.

Ho, S. H., Chen, C. Y., Lee, D. J. and Chang, J. S. 2011. Perspectives on microalgal CO_2 emission mitigation systems-a review. *Biotechnology Advances*. **29:** 189-198.

Housecroft, C. E. and Sharpe, A. G. 2005. Inorganic chemistry. 2nd Edition. Essex (Egland): Pearson Education Limited.

Hsueh, H. T., Li, W. J., Chen, H. H. and Chu, H. 2009. Carbon bio-fixation by photosynthesis of *Thermosynechococcus* sp. CL-1 and *Nannochloropsis oculta*. *Journal of Photochemistry and Photobiology*. **95:** 33-39.

Hu, Q., Kurano, N., Kawachi, M., Iwasaki, I. and Miyachi, S. 1998. Ultra high cell-density culture of a marine green alga *Chlorococcum littorale* in a flat-plate photobioreactor. *Applied Microbiology and Biotechnology*. **49:** 655-662.

Hu, X., Zhou, J., Liu, G. and Gui, B. 2016. Selection of microalgae for high CO_2 fixation efficiency and lipid accumulation from ten *Chlorella* strains using municipal wastewater. *Journal of Environmental Sciences*. http://dx.doi.org/10.1016/j.jes.2015.08.030.

Huang, G., Chen, F., Wei, D., Zhang, X. and Chen, G. 2010. Biodiesel production by microalgal biotechnology. *Applied Energy*. **87:** 38-46.

Huntley, M. and Redalje, D. 2007. CO_2 mitigation and renewable oil from photosynthetic microbes: a new appraisal. *Mitigation and Adaptation Strategies for Global Change.* **12**: 573-608.

IEA (International Energy Agency): World energy outlook. 2002. Head of Publications Service, OECD/IEA 2, rue André-Pascal, 75775 Paris Cedex 16, France.

Ilavarasi, A., Mubarakali, D., Praveenkumar, R., Baldev, E. and Thajuddin, N. 2011. Optimization of various growth media to freshwater microalgae for biomass production. *Biotechnology*. **10:** 540-545.

Iverson, T. M. 2006. Evolution and unique bio-energetic mechanisms in oxygenic photosynthesis. *Current Opinion in Chemical Biology*. **10:** 91-100.

Iwasaki, I., Kurano, N. and Miyachi, S. 1996. Effects of high-CO_2 stress on photosystem II in a green alga, *Chlorococcum littorale*, which has a tolerance to high CO_2. *Journal of Photochemistry and Photobiology.* **36:** 327-332.

Jacob, A., Xia, A. and Murphy, J. D. 2015. A perspective on gaseous biofuel production from micro-algae generated from CO_2 from a coal-fired power plant. *Applied Energy*. **148:** 396-402.

Jacob-Lopes, E., Lacerda, L. M. C. F. and Franco, T. T. 2008. Biomass production and carbon dioxide fixation by *Aphanothece microscopica Nageli* in a bubble column photobioreactor. *Biochemical Engineering Journal*. **40:** 27-34.

Jacob-Lopes, E., Revah, S., Hernandez, S., Shirai, K. and Franco, T. T. 2009. Development of operational strategies to remove carbon dioxide in photobioreactors. *Chemical Engineering Journal*. **153:** 120-126.

Jacob-Lopes, E., Scoparo, C. H. G., Queiroz, M. I. and Franco, T. T. 2010. Biotransformations of carbon dioxide in photobioreactors. *Energy Conversion Management*. **51:** 894-900.

Jeffrey, M. R. and Millton, R. S. 1999. Effect of manganese and nickel on growth of selected algae in pH buffered medium. *Water Research*. **33:** 2448-2454.

Jeong, Sung-Eun, Park, J. K., Kim, J. D., Chang I. J., Hong, S. J., Kang, S. H. and Lee, C. G. 2008. Statistical optimization of the growth factors for *Chaetoceros neogracile* using fractional factorial design and central composite design. *Journal of Microbiology and Biotechnology*. **18:** 1919-1926.

Ji, M. K., Yun, H. S., Park, Y. T., Kabra, A. N., Oh, I. H. and Choi, J. 2015. Mixotrophic cultivation of a microalga *Scenedesmus obliquus* in municipal wastewater supplemented with food wastewater and flue gas CO_2 for biomass production. *Journal of Environmental Management*. **159:** 115-120.

Jiang, L., Luo, S., Fan, X., Yang, Z. and Guo, R. 2011. Biomass and lipid production of marine microalgae using municipal wastewater and high concentration of CO_2. *Applied Energy*. **88:** 3336-3341.

Jiang, Y. L., Zhang, W., Wang, J. F., Chen, Y., Shen, S. H. and Liu, T. Z. 2013. Utilization of simulated flue gas for cultivation of *Scenedesmus dimorphus*. *Bioresource Technology*. **128:** 359-364.

Juneau, P., Green, B. and Harrison, P. 2005. Simulation of Pulse-Amplitude-Modulated (PAM) fluorescence. Limitations of some PAM-parameters in studying environmental stress effects. *Photosynthetica*. **43**: 75-83.

Kadam, K. L. 2001. Microalgae production from power plant flue gas: Environmental implications on a life cycle basis. Technical report, National Renewable Energy Laboratory Contract No. DE-AC36-99-GO10337.

Kanniche, M. and Bouallou, C. 2007. CO_2 capture study in advanced integrated gasification combined cycle. *Applied Thermal Engineering*. **27**: 2693-2702.

Kanth, B. K., Jun, S. Y., Kumari, S. and Pack, S. P. 2014. Highly thermostable carbonic anhydrase from *Persephonella marina* EX-H1: Its expression and characterization for CO_2-sequestration applications. *Process Biochemistry*. **49:** 2114-2121.

Kao, C. Y., Chen, T. Y., Chang, Y. B., Chiu, T. W., Lin, H. Y., Chen, C. D., Chang, J. S. and Lin, C. S. 2014. Utilization of carbon dioxide in industrial flue gases for the cultivation of microalga *Chlorella* sp. *Bioresource Technology*. **166:** 485-493.

Keffer, J. and Kleinheinz, G. 2002. Use of *Chlorella vulgaris* for CO_2 mitigation in a photobioreactor. *Journal of Industrial Microbiology and Biotechnology*. **29**: 275-280.

Kemka, H., Ogbonda, Rebecca, E., Aminigo, and Gideon, O. A. 2007. Influence of aeration and lighting on biomass production and protein biosynthesis in a *Spirulina* sp. isolated from an

oil-polluted brackish water marsh in the Niger Delta, Nigeria. *African Journal of Biotechnology* **6**: 2596-2600.

Khan, S. A., Rashmi, Hussain, M. Z., Prasad, S. and Banerjee, U. C. 2009. Prospects of biodiesel production from microalgae in India. *Renewable Sustainable Energy Reviews*. **13:** 2361-2372.

Khoo, H. H., Sharratt, P. N., Das, P., Balasubramanian, R. K., Naraharisetti, P. K. and Shaik, S. 2011. Life cycle energy and CO_2 analysis of microalgae-to-biodiesel: preliminary results and comparisons. *Bioresource Technology*. **102:** 5800-5807.

Kim, J. M., Lee, K., Shin, K., Kang, J. H., Lee, H. W., Kim, M. and Jang, M. C. 2006. The effect of seawater CO_2 concentration on growth of a natural phytoplankton assemblage in a controlled mesocosm experiment. *Limnology and Oceanography*. **51**: 1629-1636.

King, A. L., Sañudo-Wilhelmy, S. A., Leblanc, K., Hutchins, D. A. and Fu, F. X. 2011. CO_2 and vitamin B12 interactions determine bioactive trace metal requirements of a subarctic Pacific diatom. *The ISME Journal*. **5**: 1388-1396.

Kromkamp, J. and Peene, J. 1999. Estimation of phytoplankton photosynthesis and nutrient limitation in the Eastern Scheldt estuary using variable fluorescence. *Aquatic Ecology*. **33**: 101-104.

Kulshreshtha, J. and Singh, G. P. 2013. Evaluation of various inorganic media for growth and biopigments of *Dunaliella Salina*. *International Journal of Pharma and Bio Sciences*. **4:** 1083-1089.

Kupriyanova, E., Pronina, N. and Los, D. 2017. Carbonic anhydrase - a universal enzyme of the carbon-based life. *Photosynthetica*. **55**: 3-19.

Kumar, K., Banerjee, D. and Das, D. 2014. Carbon dioxide sequestration from industrial flue gas by *Chlorella sorokiniana*. *Bioresource Technology*. **152**: 225-233.

Kumar, K. and Das, D. 2012. Growth characteristics of *Chlorella sorokiniana* in airlift and bubble column photobioreactors. *Bioresource Technology*. **116**: 307-313.

Kumar, K., Dasgupta, C. N., Nayak, B., Lindblad, P. and Das, D. 2011-a. Development of suitable photobioreactors for CO_2 sequestration addressing global warming using green algae and cyanobacteria. *Bioresource Technology*. **102**: 4945-4953.

Kumar, A., Ergas, S., Yuan, X., Sahu, A., Zhang, Q., Dewulf, J., Malcata, F. X. and Langenhove, H. V. 2011-b. Enhanced CO_2 fixation and biofuels production via microalgae: recent developments and future directions. *Trends in Biotechnology*. **28:** 371-380.

Kumar, M., Kulshreshtha, J. and Singh, G. 2011-c. Growth and biopigment accumulation of cyanobacterium *Spirulina platensis* at different light intensities and temperature. *Brazilian Journal of Microbiology*. **42**: 1128-1135.

Kumar, M., Kumari, P., Gupta, V., Reddy, C. R. K. and Jha, B. 2012. Biochemical responses of red alga *Gracilaria corticata* (Gracilariales, Rhodophyta) to salinity induced oxidative stress, *Journal of Experimental Marine Biology and Ecology*. **391**: 27-34.

Kumar, S., Tamura, K. and Nei, M. 2004. MEGA3: Integrated software for molecular evolutionary genetics analysis and sequence alignment. *Brief in Bioinform*. **5**: 150-163.

Kuramochi, T., Ramirez, A., Turkenburg, W. and Faaij, A. 2012. Comparative assessment of CO_2 capture technologies for carbon intensive industrial processes. *Progress Energy Combustion*. **38:** 87-112.

Kurano, N., Ikemoto, H., Miyashita, H., Hasegawa, T., Hata, H. and Miyachi, S. 1995. Fixation and utilization of carbon dioxide by microalgal photosynthesis. *Energy Conversion Management*. **36:** 689-692.

Lam, M. K. and Lee, K. T. 2011. Renewable and sustainable bioenergies production from palm oil mill effluent (POME): win-win strategies toward better environmental protection. *Biotechnology Advances*. **29:** 124-141.

Lam, M. and Lee, K. 2013. Effect of carbon source towards the growth of *Chlorella vulgaris* for CO_2 bio-mitigation and biodiesel production. *International Journal of Greenhouse Gas Control*. **14**: 169-176.

Lam, M. K., Lee, K. T. and Mohamed, A. R. 2012. Current status and challenges on microalgae-based carbon capture. *International Journal of Greenhouse Gas Control*. **10:** 456-469.

Langley, N. M., Harrison, S. T. L. and Van Hille, R. P. 2012. A critical evaluation of CO_2 supplementation to algal systems by direct injection. *Biochemical Engineering Journal*. **68:** 70-75.

Lara-Gil, J. A., Senes-Guerrero, C. and Pacheco, A. 2016. Cement flue gas as a potential source of nutrients during CO_2 mitigation by microalgae. *Algal Research*. **17:** 285-292.

Lee, Y. K. 2001. Microalgal mass culture systems and methods: their limitation and potential. *Journal of Applied Phycology*. **13:** 307-315.

Lee, J. S., Kim, D. K., Lee, J. P., Park, S. C., Koh, J. H., Cho, H. S. and Kim, S. W. 2002. Effects of SO_2 and NO_2 on growth of *Chlorella* sp. KR-1. *Bioresource Technology*. **8:** 1-4.

Lee, J. S. and Lee, J. P. 2003. Review of advances in biological CO_2 mitigation technology. *Biotechnology Bioprocess Engineering*. **8:** 354-359.

Lee, J. Y., Yoo, C., Jun, S. Y., Ahn, C. Y. and Oh, H. M. 2010. Comparison of several methods for effective lipid extraction from microalgae. *Bioresource Technology*. **101:** 575-577.

Lenaers, G., Maroteaux, L., Michot, B. and Herzog. 1989. Dinoflagellates in evolution: a molecular phylogenetic analysis of large subunit ribosomal RNA. *Journal of Molecular Evolution*. **29**: 40-51.

Li, Y., Horsman, M., Wang, B., Wu, N. and Lan, C. 2008. Effects of nitrogen sources on cell growth and lipid accumulation of green alga *Neochloris oleoabundans*. *Applied Microbiology and Biotechnology*. **81**: 629-636.

Li, X. K., Xu, J. L., Guo, Y., Zhou, W. Z. and Yuan, Z. H. 2015. Effects of simulated flue gas on components of *Scenedesmus raciborskii* WZKMT. *Bioresource Technology*. **190**: 339-344.

Lipinsky, E. S. 1992. R&D status of technologies for utilization of carbon dioxide. *Energy Conversion Management*. **33:** 505-512.

Liu, Q. and Liu, Z. 2011. Carbon supported vanadia for multi-pollutants removal from flue gas. *Fuel*. doi:10.1016/j.fuel.2011.05.015.

Liu, Z. Y., Wang, G. C. and Zhou, B. C. 2008. Effect of iron on growth and lipid accumulation in *Chlorella vulgaris*. *Bioresource Technology*. **99:** 4717-4722.

Logothetis, K., Dakanali, S., Ioannidis, N. and Kotzabasis, K. 2004. The impact of high CO_2 concentrations on the structure and function of the photosynthetic apparatus and the role of polyamines. *Journal of Plant Physiology*. **161**: 715-724.

Long, S., Humphries, S. and Falkowski, P. 1994. Photoinhibition of photosynthesis in nature. *Annual Reviews of Plant Biology*. **45**: 633-662.

Lopez, C. V. G., Fernandez, F. G. A., Sevilla, J. M. F., Fernandez, J. F. S., Garcı´a, M. C. C. and Grima, E. M. 2010-a. Utilization of the cyanobacteria *Anabaena* sp. ATCC 33047 in CO_2 removal processes. *Bioresource Technology*. **100:** 5904-5910.

Lopez, C. V. G., Garcia, M. D. C. C., Fernandez, F. G. A., Bustos, C. S., Chisti, Y. and Sevilla, J. M. F. 2010-b. Protein measurements of microalgal and cyanobacterial biomass. *Bioresource Technology*. **101:** 7587-7591.

Low-DÉCarie, E., Fussmann, G. F. and Bell, G. 2011. The effect of elevated CO_2 on growth and competition in experimental phytoplankton communities. *Global Change Biology*. **17**: 2525-2535.

Lowry, O. H., Rosebrough, N. J., Farr, A. L. and Randall, R. J. 1951. Protein measurement with the folin phenol reagent. *Journal of Biological Chemistry*. **193:** 265-275.

Maeda, K., Owada, M., Kimura, N., Omata, K. and Karube, I. 1995. CO_2 fixation from flue gas on coal fired thermal power plant by microalgae. *Energy Conversion Management*. **36:** 717-720.

Markle, H. 1977. CO_2 transport and photosynthetic productivity of a continuous culture of algae. *Biotechnology Bioengineering*. **19:** 1851-62.

Martin-Jezequel, V., Hildebrand, M. and Brzezinski, M. A. 2000. Silicon metabolism in diatoms: implications for growth. *Journal of Phycology*. **36**: 821-840.

Mata, T. M., Martins, A. A. and Caetano, N. S. 2010. Microalgae for biodiesel production and other applications: a review. *Renewable Sustainable Energy Reviews*. **14:** 217-232.

Matos, A. P., Ferreira, W. B., de Oliveira Torres, R. C., Morioka, L. R. I., Canella, M. H. M., Rotta, J., da Silva, T., Moecke, E. H. S. and Anna, E. S. S. 2015. Optimization of biomass production of *Chlorella vulgaris* grown in desalination concentrate. *Journal of Applied Phycology*. **27:** 1473-1483.

Matsumoto, H., Shioji, N., Hamasaki, A., Ikuta, Y., Fukuda, Y., Sato, M., Endo, N. and Tsukamoto, T. 1995. Carbon dioxide fixation by microalgae photosynthesis using actual flue gas discharged from a boiler. *Applied Biochemical Biotechnology*. **51:** 681-692.

Mehta, J., Sharma, P., Jakhetia, M., Syedy, M., Makhijani, K. and Khamora, N. 2012. Impact of different physical and chemical environment for mass production of *Spirulina pletensis*- an immunity promoter. *International Research Journal of Biological Sciences*. **1:** 49-56.

Metting, F. B. 1996. Biodiversity and application of microalgae. *Journal of Industrial Microbiology and Biotechnology*. **17:** 477-89.

Miyairi, S. 1995. CO_2 assimilation in a thermophilic cyanobacterium. *Energy Conversion Management*. **36:** 763-766.

Mohan, S. V., Modestra, J. A., Amulya, K., Butti, S. K. and Velvizhi, G. 2016. A circular bioeconomy with biobased products from CO_2 sequestration. *Trends in Biotechnology*. **34**: 506-519.

Moheimani, N., Webb, J. and Borowitzka, M. 2012. Bioremediation and other potential applications of coccolithophorid algae: A review. *Algal Research*. **1**: 120-133.

Molina, G. E., Belarbi, E. H., Fernandez, F. G., Medina, A. R. and Chisti, Y. 2001. Tubular photobioreactor design for algal cultures. *Journal of Biotechnology*. **92:** 113-131.

Molina-Grima, E., Belarbi, E. H., Fernandez, A. F. G., Robles, M. A. and Chisti, Y. 2003. Recovery of microalgal biomass and metabolites: process options and economics. *Biotechnology Advances*. **20:** 491-515.

Montgomery, D.C. 2005. Design and Analysis of Experiments, Sixth Edition. John Wiley and Sons Inc, USA. ISBN-13: 978-0471316497.

Murugesan, A., Umarani, C., Chinnusamy, T. R., Krishan, M., Subramanian, R. and Neduzchezhain, N. 2008. Production and analysis of bio-diesel from non-edible oils - A review. *Renewable and Sustainable Energy Reviews*. **111**: 800-813.

Mutanda, T., Ramesh, D., Karthikeyan, S., Kumari, S., Anandraj, A. and Bux, F. 2011. Bioprospecting for hyper-lipid producing microalgal strains for sustainable biofuel production. *Bioresource Technology*. **102:** 57-70.

Nagase, H., Eguchi, K., Yoshihara, K., Hirata, K. and Miyamoto, K. 1998. Improvement of microalgal NO_x removal in bubble column and airlift reactors. *Journal of Fermentation Bioengineering*. **86:** 421-423.

Nakajima, Y. and Ueda, R. 2000. The effect of reducing light-harvesting pigment on marine microalgal productivity. *Journal of Applied Phycology*. **12:** 285-290.

Negoro, M., Hamasaki, A., Ikuta, Y., Makita, T., Hirayama, K. and Suzuki, S. 1993. Carbon dioxide fixation by microalgae photosynthesis using actual flue gas discharged from a boiler. *Applied Biochemistry and Biotechnology*. **39:** 643-653.

Olaizola, M. 2003. Commercial development of microalgal biotechnology: from the test tube to the marketplace. *Bimolecular Engineering*. **20:** 459-466.

Ono, E. and Cuello, J. L. 2006. Feasibility assessment of microalgal carbon dioxide sequestration technology with photobioreactor and solar collector. *Biosystem Engineering*. **95:** 597-606.

Ono, E. and Cuello, J. L. 2007. Carbon dioxide mitigation using thermophilic cyanobacteria. *Biosystem Engineering*. **96:** 129-134.

Ota, M., Kato, Y., Watanabe, H., Watanabe, M., Sato, Y. and Smith, R. L. 2009. Fatty acid production from a highly CO_2 tolerant alga, *Chlorocuccum littorale*, in the presence of inorganic carbon and nitrate. *Bioresource Technology*. **100:** 5237-5242.

Packer, M. 2009. Algal capture of carbon dioxide; biomass generation as a tool for greenhouse gas mitigation with reference to New Zealand energy strategy and policy. *Energy Policy*. **37:** 3428-3437.

Pedroni, P., Davison, J., Beckert, H., Bergman, P. and Benemann, J. 2001. A proposal to establish an international network on biofixation of CO_2 and greenhouse gas abatement with microalgae. *Journal of Energy Environmental Technology*. **1:** 136-150.

Pires, J. C. M., Alvim-Ferraz, M. C. M., Martins, F. G. and Simoes, M. 2012. Carbon dioxide capture from flue gases using microalgae: engineering aspects and biorefinery concept. *Renewable Sustainable Energy Reviews*. **16:** 3043-3053.

Power, M. 1998. Introduction recovery in aquatic ecosystems: Considerations for definition and measurement. *Journal of Aquatic Ecosystem Stress and Recovery*. **6**: 179-180.

Pradhan, L., Bhattacharjee, V., Mitra, R., Bhattacharya, I. and Chowdhury, R. 2015. Biosequestration of CO_2 using power plant algae (*Rhizoclonium hieroglyphicum* JUCHE2) in a flat plate photobio-bubble-reactor - Experimental and modeling. *Chemical Engineering Journal*. **275**: 381-390.

Pujari, V. and Chandra, T. S. 2000. Statistical optimization of medium components for improved synthesis of riboflavin by *Eremothecium ashbyii*. *Bioprocess Engineering*. **23:** 303-307.

Radakovits, R., Jinkerson, R. E., Darzins, A. L. and Posewitz, M. C. 2010. Genetic engineering of algae for enhanced biofuel production. *Eukaryotic Cell*. **9:** 486-501.

Radmann, E. M., Camerini, F. V., Santos, T. D. and Costa, J. A. V. 2012. Isolation and application of SO_X and NO_X resistant microalgae in biofixation of CO_2 from thermoelectricity plants. *Energy Conversion and Management.* **52:** 3132-3136.

Raeesossadati, M., Ahmadzadeh, H., McHenry, M. and Moheimani, N. 2014. CO_2 bioremediation by microalgae in photobioreactors: Impacts of biomass and CO_2 concentrations, light, and temperature. *Algal Research*. **6**: 78-85.

Raja, R., Hemaiswarya, S., Kumar, N. A., Sridhar, S. and Rengasamy, R. 2008. A perspective on the biotechnological potential of microalgae. *Critical Reviews in Microbiology*. **34:** 77-88.

Ralph, P. J. and Gademann, R. 2003. Rapid light curves: a powerful tool to assess photosynthetic activity. *Aquatic Biology*. **82:** 222-237.

Ramanna, L., Guldhe, A., Rawat, I. and Bux, F. 2014. The optimization of biomass and lipid yields of *Chlorella sorokiniana* when using wastewater supplemented with different nitrogen sources. *Bioresource Technology*. **168**: 127-135.

Ramanan, R., Kannan, K., Deshkar, A., Yadav, R. and Chakrabarti, T. 2010. Enhanced algal CO_2 sequestration through calcite deposition by *Chlorella* sp. and *Spirulina platensis* in a mini-raceway pond. *Bioresource Technology*. **101:** 2616-2622.

Raveonandro, P. H., Ratianarivo, D. H., Joannis-Cassan, C., Isambert, A. and Rahermandimby, M. 2008. Influence of light quality and intensity in the cultivation of *Spirulina platensis* from Toliara (Madagascar) in a closed system. *Journal of Chemical Technology and Biotechnology*. **83:** 842-848.

Rebolloso-Fuentes, M. M., Navarro-Perez, A., García-Camacho, F., Ramos-Miras, J. J. and Guil-Guerrero, J. L. 2001. Biomass nutrient profiles of the microalga *Nannochloropsis*. *Journal of Agricultural and Food Chemistry*. **49**: 2966-2972.

Rogelj, J., Meinshausen, M. and collegues. 2010. Copanenhagen accord pledges are paltry, current national emissions targets can't limit global warming to 2ºC, calculated-they might even lock the world into exceeding 3ºC warming. *Nature Opinion*. **464**: 1126-1129.

Rosgaard, L., de Porcellinis, A. J., Jacobsen, J. H., Frigaard, N. U. and Sakuragi, Y. 2012. Bioengineering of carbon fixation, biofuels, and biochemistry in cyanobacteria and plants. *Journal of Biotechnology*. **162:** 134-147.

Ryu, H., Oh, K. and Kim, Y. 2009. Optimization of the influential factors for the improvement of CO_2 utilization efficiency and CO_2 mass transfer rate. *Journal of Industrial and Engineering Chemistry*. **15**: 471-475.

Saitou, N. and Nei, M. 1987. The neighbor-joining method: A new method for reconstructing phylogenetic trees. *Molecular Biology and Evolution*. **4**: 406-425.

Sakia, R. M. 1992. The Box-Cox transformation technique: a review. *The Statistician*. **41**: 169-178.

Satoh, A., Kurano, N. and Miyachi, S. 2001. Inhibition of photosynthesis by intracellular carbonic anhydrase in microalgae under excess concentrations of CO_2. *Photosynthetic Research*. **68:** 215-224.

Sayre, R. 2010. Microalgae: The potential for carbon capture. *BioScience*. **60:** 722-727.

Schanz, F. and Zahler, U. 1981. Prediction of algal growth in batch cultures. *Schweizerische Zeitschrift für Hydrologie*. **43**: 103-113.

Scragg, A. H., Illman, A. M., Carden, A. and Shales, S. W. 2002. Growth of microalgae with increased calorific values in a tubular bioreactor. *Biomass Bioenergy*. **23:** 67-73.

Seckbach, J. and Libby, W. F. 1970. Vegetative life on Venus? Or investigations with algae which grow under pure CO_2 in hot acid media at elevated pressures. *Origins in Life Evolution Biology*. **2:** 121-143.

Sharma, Y. C., Singh, B. and Korstad, J. 2011. A critical review on recent methods used for economically viable and eco-friendly development of microalgae as a potential feedstock for synthesis of biodiesel (critical review). *Green Chemistry*. **13:** 2993-3006.

Sheehan, J., Dunahay, T., Benemann, J. and Roessler, P. 1998. A look back at the U. S. Department of Energy's aquatic species program - biodiesel from algae. NREL/TP-580-24190. US Department of Energy's Office of Fuels Development.

Sierra, E., Acien, F. G., Fernandez, J. M., Garcia, J. L., Gonzalez, C. and Molina, E. 2008. Characterization of a flat plate photobioreactor for the production of microalgae. *Chemical Engineering Journal*. **138**: 136-147.

Silveira, S. T., Burkert, J. F., Costa, J. A., Burkert, C. A. and Kalil, S. J. 2007. Optimization of phycocyanin extraction from *Spirulina platensis* using factorial design. *Bioresource Technology*. **98:** 1629-1634.

Singh, U. B. and Ahluwalia, A. 2013. Microalgae: a promising tool for carbon sequestration. *Mitigation and Adaptation Strategies for Global Change*. **18**: 73-95.

Singh, P., Guldhe, A., Kumari, S., Rawat, I. and Bux, F. 2015. Investigation of combined effect of nitrogen, phosphorus and iron on lipid productivity of microalgae *Ankistrodesmus falcatus* KJ671624 using response surface methodology. *Biochemical Engineering Journal*. **94:** 22-29.

Singh, N. K., Parmar, A. and Madamwar, D. 2009. Optimization of medium components for increased production of C-phycocyanin from *Phormidium ceylanicum* and its purification by single step process. *Bioresource Technology*. **100:** 1663-1669.

Skjanes, K., Lindblad, P. and Muller, J. 2007. BioCO_2-a multidisciplinary, biological approach using solar energy to capture CO_2 while producing H_2 and high value products. *Biomolecular Engineering*. **24**: 405-413.

Slade, R. and Bauen, A. 2013. Micro-algae cultivation for biofuels: Cost, energy balance, environmental impacts and future prospects. *Biomass and Bioenergy*. **53**: 29-38

Solovchenko, A., Gorelova, O., Selyakh, I., Pogosyan, S., Baulina, O., Semenova, L., Chivkunova, O., Voronova, E., Konyukhov, I., Scherbakov, P. and Lobakova, E. 2015. A novel CO_2-tolerant symbiotic *Desmodesmus* (Chlorophyceae, Desmodesmaceae): Acclimation to and performance at a high carbon dioxide level. *Algal Research*. **11**: 399-410.

Solovchenko, A., Verschoor, A. M., Jablonowski, N. D. and Nedbal, L. 2016. Phosphorus from wastewater to crops: An alternative path involving microalgae. *Biotechnology Advances*. **34:** 550-564.

Somnath, D. S. and Smita, S. L. 2010. Statistical media optimization for lutein production from microalgae *Auxenochlorella protothecoides* SAG 211-7A. *International Journal of Advanced Biotechnology and Research*. **1**: 104-114.

Sorensen, B. H., Nyholm, N. and Baun, A. 1996. Algal toxicity tests with volatile and hazardous compounds in air-tight test flasks with CO_2 enriched headspace. *Chemosphere.* **32**: 1513-1521.

Sousa, C., Compadre, A., Vermue, M. H. and Wijffels, R. H. 2013. Effect of oxygen at low and high light intensities on the growth of *Neochloris oleoabundans*. *Algal Research.* **2**: 122-126.

Spolaore, P., Joannis-Cassan, C., Duran, E. and Isambert, A. 2006. Commercial applications of microalgae. *Journal of Bioscience and Bioengineering*. **101:** 87-96.

Stewart, C. and Hessami, M. A. 2005. A study of methods of carbon dioxide capture and sequestration-the sustainability of a photosynthetic bioreactor approach. *Energy Conversion Management*. **46:** 403-420.

Suh, I. S. and Lee, C. G. 2003. Photobioreactor engineering: design and performance. *Biotechnology Bioprocess Engineering*. **8:** 313-321.

Sung, K. D., Lee, J. S., Shin, C. S., Park, S. C. and Choi, M. J. 1999. CO_2 fixation by *Chlorella* sp. KR-1 and its cultural characteristics. *Bioresource Technology*. **68:** 269-273.

Sutherland, D. L., Howard-Williams, C., Turnbull, M. H., Broady, P. A. and Craggs, R. J. 2015. The effects of CO_2 addition along a pH gradient on wastewater microalgal photo-physiology, biomass production and nutrient removal. *Water Research*. **70**: 9-26.

Suzuki, G. T., Fleuri, L. and Macedo, G. A. 2009. Influence of nitrogen and carbon sources on riboflavin production by wild strain of *candida* sp. *Food Bioprocess Technology*. DOI 10.1007/s11947-009-0262-3.

Swarnalatha, G. V., Hegde, N. S., Chauhan, V. S. and Sarada, R. 2015. The effect of carbon dioxide rich environment on carbonic anhydrase activity, growth and metabolite production in indigenous freshwater microalgae. *Algal Research*. **9:** 151-159.

Sydney, E., Sturm, W., de Carvalho, J., Thomaz-Soccol, V., Larroche, S. and Pandey, C. 2010. Potential carbon dioxide fixation by industrially important microalgae. *Bioresource Technology*. **101**: 5892-5896.

Tamura, K., Peterson, D., Peterson, N., Stecher, G., Nei, M. and Kumar, S. 2011. MEGA5: molecular evolutionary genetics analysis using maximum likelihood, evolutionary distance, and maximum parsimony methods. *Molecular Biology and Evolution*. **28**: 2731-2739.

Tasharrofia, N., Adrangie, S., Khoshayandd, M. R., Fazelia, M., Rastegarc, H. and Faramarzia, M. A. 2011**.** Optimization of chitinase production by *Bacillus pumilus* using Plackett-Burman design and response surface methodology. *Pharmaceucal Research*. **10**: 759-768.

Thiruvenkatachari, R., Su, S., An, H. and Yu, X. X. 2009. Post combustion CO_2 capture by carbon fibre monolithic adsorbents. *Progress in Energy and Combustion*. **35**: 438-455.

Tripathi, R., Singh, J. and Thakur, I. S. 2015. Characterization of microalga *Scenedesmus* sp. ISTGA1 for potential CO_2 sequestration and biodiesel production. *Renewable Energy*. **74**: 774-781.

Tsoutsos, T., Kouloumpis, V., Zafiris, T. and Foteinis, S. 2010. Life cycle assessment for biodiesel production under Greek climate conditions. *Journal of Clean Production*. **18:** 328-335.

Ugwu, C. U., Aoyagi, H. and Uchiyama, H. 2008. Photobioreactors for mass cultivation of algae. *Bioresource Technology*. **99:** 4021-4028.

Vanthoor-Koopmansa, M., Wijffelsa, R. H., Barbosac, M. J. and Eppinka, M. H. M. 2013. Biorefinery of microalgae for food and fuel. *Bioresource Technology*. **135**: 142-149.

Vasumathi, K. K., Premalatha, M. and Subramanian, P. 2012. Parameters influencing the design of photobioreactors for the growth of microalgae. *Renewable Sustainable Energy Reviews*. **16:** 5443-5450.

Viskari, P. J. and Colyer, C. L. 2003. Rapid extraction of phycobiliproteins from cultured cyanobacteria samples. *Analytical Biochemistry*. **319:** 263-71.

Wang, H., Gau, B., Slade, W. O., Juergens, M., Li, P. and Hicks, L. M. 2014. The global phosphoproteome of *Chlamydomonas reinhardtii* reveals complex organellar phosphorylation in the flagella and thylakoid membrane. *Molecular Cellular Proteomics*. **13:** 2337-2353.

Wang, B., Li, Y. Q., Wu, N. and Lan, C. Q. 2008. CO_2 bio-mitigation using microalgae. *Applied Microbiology and Biotechnology*. **79:** 707-718.

Wang, H. M., Pan, J. L., Chen, C. Y., Chiu, C. C., Yang, M. H., Chang, H. W. and Chang, J. S. 2010. Identification of anti-lung cancer extract from *Chlorella vulgaris* C-C by antioxidant property using supercritical carbon dioxide extraction. *Process Biochemistry*. **45:** 1865-72.

Watanabe, M. M., Kawachi, M., Hiroki, M. and Kasai, F. 2000. NIES collection list of strains, microalgae and protozoa. Microbial culture collections (ed) National Institute for Environmental Studies, Tsukuba, Japan.

Watanabe, Y., Ohmura, N. and Saiki, H. 1992. Isolation and determination of cultural characteristics of microalgae which functions under CO_2 enriched atmosphere. *Energy Conversion and Management*. **33**: 545-552.

White, S., Anandraj, A. and Bux, F. 2011. PAM fluorometry as a tool to assess microalgal nutrient stress and monitor cellular neutral lipids. *Bioresource Technology*. **102**: 1675-1682.

White, S., Anandraj, A. and Trois, C. 2013. The effect of landfill leachate on hydrogen production in *Chlamydomonas reinhardtii* as monitored by PAM Fluorometry. *International Journal of Hydrogen Energy*. **38**: 14214-14222.

Wu, Y. P., Gao, K. S. and Riebesell, U. 2010. CO_2-induced seawater acidification affects physiological performance of the marine diatom *Phaeodactylum tricornutum*. *Biogeosciences*. **7**: 2915-2923.

Yadav, G., Karemore, A., Dash, S. K. and Sen, R. 2015. Performance evaluation of a green process for microalgal CO_2 sequestration in closed photobioreactor using flue gas generated in-situ. *Bioresource Technology*. **191:** 399-406.

Yamochi, S. 1984. Nutrient factors involved in controlling the growth of red tide flagellates *Prorocentrum micans*, *Eutreptiella* sp. and *Chattonella mirina* in Osaka Bay. *Bulletin of the Plankton Society of Japan*. **32:** 97-106.

Yang, Y. and Gao, K. 2003. Effects of CO_2 concentrations on the freshwater microalgae, *Chlamydomonas reinhardtii*, *Chlorella pyrenoidosa* and *Scenedesmus obliquus* (Chlorophyta). *Journal of Applied Phycology*. **5**: 379-389.

Yang, C., Hua, Q. and Shimizu, K. 2000. Energetics and carbon metabolism during growth of microalgal cells under photoautotrophic, mixotrophic and cyclic light-autotrophic/dark-heterotrophic conditions. *Biochemical Engineering Journal*. **6:** 87-102.

Yeh, K. L. and Chang, J. S. 2012. Effects of cultivation conditions and media composition on cell growth and lipid productivity of indigenous microalga *Chlorella vulgaris* ESP-31. *Bioresource Technology*. **105:** 120-7.

You, T. and Barnett, S. M. 2004. Effect of light quality on production of extracellular polysaccharides and growth rate of *Porphyridium cruentum*. *Biochemical Engineering Journal*. **19:** 251-258.

Yue, L. and Chen, W. 2005. Isolation and determination of cultural characteristics of a new highly CO_2 tolerant fresh water microalgae. *Energy Conversion and Management*. **46**: 1868-1876.

Yue, L. H., Chen, W. G., Li, J. G. and Jin, J. Y. 2005. *Chlorella* ZY1 cultivation and its CO_2 fixation in the environmental condition of flue gases. *Journal of Qingdao University of Science and Technology*. **26:** 15-19.

Yun, Y., Lee, S., Park, J., Lee, C. and Yang, J. 1997. Carbon dioxide fixation by algal cultivation using wastewater nutrients. *Journal of Chemical Technology and Biotechnology*. **69**: 451-545.

Zeng, X., Danquah, M. K., Chen, X. D. and Lu, Y. 2011. Microalgae bioengineering: from CO_2 fixation to biofuel production. *Renewable Sustainable Energy Reviews*. **15:** 3252-3260.

Zhang, L., Happe, T. and Melis, A. 2002. Biochemical and morphological characterization of sulfur-deprived and H_2-producing *Chlamydomonas reinhardtii* (green alga). *Planta*. **214:** 552-561.

Zhao, B. and Su, Y. 2014. Process effect of microalgal-carbon dioxide fixation and biomass production: a review. *Renewable and Sustainable Energy Reviews*. **31:** 121-132.

Zhao, B., Zhang, Y., Xiong, K., Zhang, Z., Hao, X. and Liu, T. 2011. Effect of cultivation mode on microalgal growth and CO_2 fixation. *Chemical Engineering Research Design*. **9:** 1758-1762.

Zijffers, J. W. F., Schippers, K. J., Zheng, K., Janssen, M., Tramper, J. and Wijffels, R. H. 2010. Maximum photosynthetic yield of green microalgae in photobioreactors. *Marine Biotechnology*. **12:** 708-718.

Zittelli, G. C., Lavista, F., Bastianini, A., Rodolfi, L., Vincenzini, M. and Tredici, M. R. 1999. Production of eicosapentaenoic acid by *Nannochloropsis* sp. cultures in outdoor tubular photobioreactors. *Journal of Biotechnology*. **70:** 299-312.

APPENDICES

Appendix A: Data obtained for Tukey's post hoc test (Chapter Three)

Table 22: Data obtained for Tukey's post hoc test for the different strains when grown at 15% CO_2

Tukey's Multiple Comparison Test	Mean Diff.	q	Significant? p < 0.05?	Summary	95% CI of Diff
I-0 vs I-1	0.2983	12.56	Yes	***	0.1990 to 0.3975
I-0 vs I-2	0.2929	12.33	Yes	***	0.1936 to 0.3921
I-0 vs I-3	0.008111	0.3415	No	ns	-0.09117 to 0.1074
I-0 vs I-4	0.1946	8.195	Yes	***	0.09536 to 0.2939
I-0 vs I-5	0.2612	11.00	Yes	***	0.1619 to 0.3605
I-1 vs I-2	-0.005389	0.2269	No	ns	-0.1047 to 0.09389
I-1 vs I-3	-0.2901	12.22	Yes	***	-0.3894 to -0.1909
I-1 vs I-4	-0.1036	4.363	Yes	*	-0.2029 to -0.004329
I-1 vs I-5	-0.03706	1.560	No	ns	-0.1363 to 0.06223
I-2 vs I-3	-0.2848	11.99	Yes	***	-0.3840 to -0.1855
I-2 vs I-4	-0.09822	4.136	No	ns	-0.1975 to 0.001060
I-2 vs I-5	-0.03167	1.333	No	ns	-0.1309 to 0.06762
I-3 vs I-4	0.1865	7.854	Yes	***	0.08725 to 0.2858
I-3 vs I-5	0.2531	10.66	Yes	***	0.1538 to 0.3524
I-4 vs I-5	0.06656	2.802	No	ns	-0.03273 to 0.1658

Table 23: Data obtained for Tukey's post hoc test for the different strains when grown at 10% CO_2

Tukey's Multiple Comparison Test	Mean Diff.	q	Significant? p < 0.05?	Summary	95% CI of Diff
I-0 vs I-1	0.2090	11.10	Yes	***	0.1303 to 0.2877
I-0 vs I-2	0.2376	12.62	Yes	***	0.1589 to 0.3164
I-0 vs I-3	0.002194	0.1165	No	ns	-0.07652 to 0.08091
I-0 vs I-4	0.1913	10.16	Yes	***	0.1125 to 0.2700
I-0 vs I-5	0.2365	12.56	Yes	***	0.1578 to 0.3152
I-1 vs I-2	0.02864	1.521	No	ns	-0.05008 to 0.1074
I-1 vs I-3	-0.2068	10.98	Yes	***	-0.2855 to -0.1281
I-1 vs I-4	-0.01775	0.9426	No	ns	-0.09647 to 0.06097
I-1 vs I-5	0.0275	1.460	No	ns	-0.05122 to 0.1062
I-2 vs I-3	-0.2354	12.50	Yes	***	-0.3142 to -0.1567
I-2 vs I-4	-0.04639	2.463	No	ns	-0.1251 to 0.03233
I-2 vs I-5	-0.001139	0.06048	No	ns	-0.07986 to 0.07758
I-3 vs I-4	0.1891	10.04	Yes	***	0.1103 to 0.2678
I-3 vs I-5	0.2343	12.44	Yes	***	0.1556 to 0.3130
I-4 vs I-5	0.04525	2.403	No	ns	-0.03347 to 0.1240

Table 24: Data obtained for Tukey's post hoc test for the different strains when grown at 5% CO_2

Tukey's Multiple Comparison Test	Mean Diff.	q	Significant? p < 0.05?	Summary	95% CI of Diff
I-0 vs I-1	0.05361	5.394	Yes	**	0.01207 to 0.09516
I-0 vs I-2	0.03075	3.094	No	ns	-0.01080 to 0.07230
I-0 vs I-3	0.003472	0.3494	No	ns	-0.03807 to 0.04502
I-0 vs I-4	0.02592	2.608	No	ns	-0.01563 to 0.06746
I-0 vs I-5	0.07461	7.507	Yes	***	0.03307 to 0.1162
I-1 vs I-2	-0.02286	2.300	No	ns	-0.06441 to 0.01868
I-1 vs I-3	-0.05014	5.045	Yes	**	-0.09168 to -0.008594
I-1 vs I-4	-0.02769	2.787	No	ns	-0.06924 to 0.01385
I-1 vs I-5	0.02100	2.113	No	ns	-0.02055 to 0.06255
I-2 vs I-3	-0.02728	2.745	No	ns	-0.06882 to 0.01427
I-2 vs I-4	-0.004833	0.4863	No	ns	-0.04638 to 0.03671
I-2 vs I-5	0.04386	4.413	Yes	*	0.002316 to 0.08541
I-3 vs I-4	0.02244	2.258	No	ns	-0.01910 to 0.06399
I-3 vs I-5	0.07114	7.158	Yes	***	0.02959 to 0.1127
I-4 vs I-5	0.04869	4.900	Yes	*	0.007149 to 0.09024

Table 25: Data obtained for Tukey's post hoc test for the different strains when grown at 0.5% CO_2

Tukey's Multiple Comparison Test	Mean Diff.	q	Significant? p < 0.05?	Summary	95% CI of Diff
I-0 vs I-1	0.05361	5.394	Yes	**	0.01207 to 0.09516
I-0 vs I-2	0.03075	3.094	No	ns	-0.01080 to 0.07230
I-0 vs I-3	0.003472	0.3494	No	ns	-0.03807 to 0.04502
I-0 vs I-4	0.02592	2.608	No	ns	-0.01563 to 0.06746
I-0 vs I-5	0.07461	7.507	Yes	***	0.03307 to 0.1162
I-1 vs I-2	-0.02286	2.300	No	ns	-0.06441 to 0.01868
I-1 vs I-3	-0.05014	5.045	Yes	**	-0.09168 to -0.008594
I-1 vs I-4	-0.02769	2.787	No	ns	-0.06924 to 0.01385
I-1 vs I-5	0.02100	2.113	No	ns	-0.02055 to 0.06255
I-2 vs I-3	-0.02728	2.745	No	ns	-0.06882 to 0.01427
I-2 vs I-4	-0.004833	0.4863	No	ns	-0.04638 to 0.03671
I-2 vs I-5	0.04386	4.413	Yes	*	0.002316 to 0.08541
I-3 vs I-4	0.02244	2.258	No	ns	-0.01910 to 0.06399
I-3 vs I-5	0.07114	7.158	Yes	***	0.02959 to 0.1127
I-4 vs I-5	0.04869	4.900	Yes	*	0.007149 to 0.09024

Table 26: Data obtained for Tukey's post hoc test for the different strains when grown at 0.03% CO_2

Tukey's Multiple Comparison Test	Mean Diff.	q	Significant? p < 0.05?	Summary	95% CI of Diff
I-0 vs I-1	0.04775	4.633	Yes	*	0.004667 to 0.09083
I-0 vs I-2	0.03472	3.369	No	ns	-0.008361 to 0.07781
I-0 vs I-3	-0.01439	1.396	No	ns	-0.05747 to 0.02869
I-0 vs I-4	0.01186	1.151	No	ns	-0.03122 to 0.05494
I-0 vs I-5	0.06339	6.150	Yes	***	0.02031 to 0.1065
I-1 vs I-2	-0.01303	1.264	No	ns	-0.05611 to 0.03006
I-1 vs I-3	-0.06214	6.029	Yes	**	-0.1052 to -0.01906
I-1 vs I-4	-0.03589	3.482	No	ns	-0.07897 to 0.007194
I-1 vs I-5	0.01564	1.517	No	ns	-0.02744 to 0.05872
I-2 vs I-3	-0.04911	4.765	Yes	*	-0.09219 to -0.006028
I-2 vs I-4	-0.02286	2.218	No	ns	-0.06594 to 0.02022
I-2 vs I-5	0.02867	2.781	No	ns	-0.01442 to 0.07175
I-3 vs I-4	0.02625	2.547	No	ns	-0.01683 to 0.06933
I-3 vs I-5	0.07778	7.547	Yes	***	0.03469 to 0.1209
I-4 vs I-5	0.05153	5.000	Yes	*	0.008445 to 0.09461

Table 27: Data obtained for Tukey's post hoc test for the different strains when grown at 2 g/l $NaHCO_3$

Tukey's Multiple Comparison Test	Mean Diff.	q	Significant? p < 0.05?	Summary	95% CI of Diff
I-0 vs I-1	0.2909	12.20	Yes	***	0.1912 to 0.3906
I-0 vs I-2	0.2462	10.32	Yes	***	0.1465 to 0.3459
I-0 vs I-3	0.002944	0.1235	No	ns	-0.09675 to 0.1026
I-0 vs I-4	0.1871	7.846	Yes	***	0.08742 to 0.2868
I-0 vs I-5	0.2989	12.53	Yes	***	0.1992 to 0.3986
I-1 vs I-2	-0.04472	1.875	No	ns	-0.1444 to 0.05497
I-1 vs I-3	-0.2879	12.07	Yes	***	-0.3876 to -0.1883
I-1 vs I-4	-0.1038	4.352	Yes	*	-0.2035 to -0.004085
I-1 vs I-5	0.007972	0.3343	No	ns	-0.09172 to 0.1077
I-2 vs I-3	-0.2432	10.20	Yes	***	-0.3429 to -0.1435
I-2 vs I-4	-0.05906	2.476	No	ns	-0.1587 to 0.04064
I-2 vs I-5	0.05269	2.210	No	ns	-0.04700 to 0.1524
I-3 vs I-4	0.1842	7.722	Yes	***	0.08447 to 0.2839
I-3 vs I-5	0.2959	12.41	Yes	***	0.1962 to 0.3956
I-4 vs I-5	0.1118	4.686	Yes	*	0.01206 to 0.2114

Table 28: Data obtained for Tukey's post hoc test for the different strains when grown at 1 g/l $NaHCO_3$

Tukey's Multiple Comparison Test	Mean Diff.	q	Significant? p < 0.05?	Summary	95% CI of Diff
I-0 vs I-1	0.1553	8.016	Yes	***	0.07429 to 0.2362
I-0 vs I-2	0.1072	5.536	Yes	**	0.02626 to 0.1882
I-0 vs I-3	-0.1321	6.819	Yes	***	-0.2130 to -0.05110
I-0 vs I-4	0.04664	2.408	No	ns	-0.03432 to 0.1276
I-0 vs I-5	0.1617	8.348	Yes	***	0.08071 to 0.2426
I-1 vs I-2	-0.04803	2.480	No	ns	-0.1290 to 0.03293
I-1 vs I-3	-0.2873	14.83	Yes	***	-0.3683 to -0.2063
I-1 vs I-4	-0.1086	5.608	Yes	**	-0.1896 to -0.02765
I-1 vs I-5	0.006417	0.3313	No	ns	-0.07454 to 0.08738
I-2 vs I-3	-0.2393	12.35	Yes	***	-0.3202 to -0.1583
I-2 vs I-4	-0.06058	3.128	No	ns	-0.1415 to 0.02038
I-2 vs I-5	0.05444	2.811	No	ns	-0.02651 to 0.1354
I-3 vs I-4	0.1787	9.227	Yes	***	0.09774 to 0.2597
I-3 vs I-5	0.2937	15.17	Yes	***	0.2128 to 0.3747
I-4 vs I-5	0.1150	5.939	Yes	**	0.03407 to 0.1960

Table 29: Data obtained for Tukey's post hoc test for the different strains when grown at 0.6 g/l $NaHCO_3$

Tukey's Multiple Comparison Test	Mean Diff.	q	Significant? p < 0.05?	Summary	95% CI of Diff
I-0 vs I-1	0.1242	9.908	Yes	***	0.07180 to 0.1766
I-0 vs I-2	0.08419	6.717	Yes	***	0.03180 to 0.1366
I-0 vs I-3	-0.03664	2.923	No	ns	-0.08904 to 0.01576
I-0 vs I-4	0.04181	3.335	No	ns	-0.01059 to 0.09420
I-0 vs I-5	0.1247	9.948	Yes	***	0.07230 to 0.1771
I-1 vs I-2	-0.04000	3.191	No	ns	-0.09240 to 0.01240
I-1 vs I-3	-0.1608	12.83	Yes	***	-0.2132 to -0.1084
I-1 vs I-4	-0.08239	6.573	Yes	***	-0.1348 to -0.02999
I-1 vs I-5	0.0005000	0.03989	No	ns	-0.05190 to 0.05290
I-2 vs I-3	-0.1208	9.640	Yes	***	-0.1732 to -0.06843
I-2 vs I-4	-0.04239	3.382	No	ns	-0.09479 to 0.01001
I-2 vs I-5	0.0405	3.231	No	ns	-0.01190 to 0.09290
I-3 vs I-4	0.07844	6.258	Yes	***	0.02605 to 0.1308
I-3 vs I-5	0.1613	12.87	Yes	***	0.1089 to 0.2137
I-4 vs I-5	0.08289	6.613	Yes	***	0.03049 to 0.1353

Table 30: Data obtained for Tukey's post hoc test for the different strains when grown at 0.2 g/l $NaHCO_3$

Tukey's Multiple Comparison Test	Mean Diff.	q	Significant? p < 0.05?	Summary	95% CI of Diff
I-0 vs I-1	0.01989	4.684	Yes	*	0.002138 to 0.03764
I-0 vs I-2	0.01125	2.649	No	ns	-0.006501 to 0.02900
I-0 vs I-3	-0.02164	5.096	Yes	**	-0.03939 to -0.003888
I-0 vs I-4	0.03344	7.876	Yes	***	0.01569 to 0.05120
I-0 vs I-5	0.03169	7.464	Yes	***	0.01394 to 0.04945
I-1 vs I-2	-0.008639	2.034	No	ns	-0.02639 to 0.009112
I-1 vs I-3	-0.04153	9.779	Yes	***	-0.05928 to -0.02378
I-1 vs I-4	0.01356	3.192	No	ns	-0.004196 to 0.03131
I-1 vs I-5	0.01181	2.780	No	ns	-0.005946 to 0.02956
I-2 vs I-3	-0.03289	7.745	Yes	***	-0.05064 to -0.01514
I-2 vs I-4	0.02219	5.227	Yes	**	0.004443 to 0.03995
I-2 vs I-5	0.02044	4.814	Yes	*	0.002693 to 0.03820
I-3 vs I-4	0.05508	12.97	Yes	***	0.03733 to 0.07283
I-3 vs I-5	0.05333	12.56	Yes	***	0.03558 to 0.07108
I-4 vs I-5	-0.00175	0.4121	No	ns	-0.01950 to 0.01600

Table 31: Data obtained for Tukey's post hoc test for the different strains when grown at 0.05 g/l $NaHCO_3$

Tukey's Multiple Comparison Test	Mean Diff.	q	Significant? p < 0.05?	Summary	95% CI of Diff
I-0 vs I-1	0.01139	4.673	Yes	*	0.001201 to 0.02158
I-0 vs I-2	0.01681	6.896	Yes	***	0.006618 to 0.02699
I-0 vs I-3	-0.008389	3.442	No	ns	-0.01858 to 0.001799
I-0 vs I-4	0.01628	6.679	Yes	***	0.006090 to 0.02647
I-0 vs I-5	0.02172	8.913	Yes	***	0.01153 to 0.03191
I-1 vs I-2	0.005417	2.223	No	ns	-0.004771 to 0.01560
I-1 vs I-3	-0.01978	8.115	Yes	***	-0.02997 to -0.009590
I-1 vs I-4	0.004889	2.006	No	ns	-0.005299 to 0.01508
I-1 vs I-5	0.01033	4.240	Yes	*	0.0001458 to 0.02052
I-2 vs I-3	-0.02519	10.34	Yes	***	-0.03538 to -0.01501
I-2 vs I-4	-0.0005278	0.2166	No	ns	-0.01072 to 0.009660
I-2 vs I-5	0.004917	2.017	No	ns	-0.005271 to 0.01510
I-3 vs I-4	0.02467	10.12	Yes	***	0.01448 to 0.03485
I-3 vs I-5	0.03011	12.36	Yes	***	0.01992 to 0.04030
I-4 vs I-5	0.005444	2.234	No	ns	-0.004743 to 0.01563

Appendix B: Recipe for ASW media (Watanabe *et al.*, 1992; Watanabe *et al.*, 2000)

	1 liter stock solution g/l	Quantity (per liter medium)
Anhydrous salts		
NaCl		100.00 g
KCl		0.78 g
$NaHCO_3$		0.40 g
H_3BO_3		0.12 g
Hydrous Salts		
$MgCl_2.6H_2O$		5.2 g
$CaCl_2 \cdot 2H_2O$		1.54 g
$MgSO_4.7H_2O$		7.12 g
Major Nutrients		
$NaNO_3$	8149	5.0 ml
NaH_2PO_4	8.8	1.0 ml
$Na_2SiO_3.9H_2O$	60.82	0.5 ml
Minor Nutrients		
Ferric ammonium citrate	0.06	10.0 ml
EDTA (disodium salt)	0.01	10.0 ml
$NaCO_3$	0.2	10.0 ml
Trace metal solution		1.0 ml

Anhydrous salts were added individually and dissolved completely by continuously mixing with a magnetic stirrer. Thereafter the hydrous salts were added and dissolved in the solution. The pH of the medium was adjusted to 7.2 using 1M HCl to avoid excessive precipitation of salts. Medium was sterilised for 20 minutes at 121ºC and 100 kPa pressure.

Trace metal:

Components	g/200 ml
$CuSO_4.5H_2O$	3.92
$MnCl_2 \cdot 4H_2O$	72.0
$ZnSO_4 \cdot 7H_2O$	8.80
$NaMoO_4 \cdot 2H_2O$	2.52
$CoCl_2.6H_2O$	4.00
$Na_2EDTA.2H_2O$	0.14

Trace metal stock solution was added after sterilisation to avoid degradation of the components.

Appendix C: Recipe for BG11 media (Watanabe *et al.*, 2000)

Compound	g/l
$NaNO_3$	1.5
$K_2HPO_4.3H_2O$	0.04
$MgSO_4.7H_2O$	0.075
$CaCl_2.2H_2O$	0.036
Citric acid	0.006
$FeCl_3.\ 6H_2O$	0.006
EDTA	0.001
Na_2CO_3	0.2
Trace metal solution	1 ml

Trace metal mix

Compound	g/l
H_3BO_3	2.86
$MnCl_2.4H_2O$	1.81
$FeCl_3.6H_2O$	97.0
$Na_2MoO_4.2H_2O$	0.390
$CuSO_4.\ 5H_2O$	0.079
$CO(NO_3)_2.6H_2O$	0.049

Add the indicated quantity of compounds and bring the final volume to 1L using distilled water. Autoclave for 15 min at 121 °C at 1 atm. pH should be 7.5 at room temperature after autoclaving.

Appendix D: Recipe for NSW (natural seawater) media (Watanabe *et al*., 2000)

Medium

Filter natural seawater through GF/C filters and autoclave at 15 min at 121 °C at 1 atm.

Appendix E: Recipe for L1 media (Guillard and Hargraves, 1993)

(1) Trace elements stock solution (per liter)

Quantity	Compound	Stock Solution
3.15 g	$FeCl_3 \cdot 6H_2O$	-
4.36 g	$Na_2EDTA \cdot 2H_2O$	-
0.25 mL	$CuSO_4 \cdot 5H_2O$	2.45 g/l dH_2O
3 mL	$Na_2MoO_4 \cdot 2H_2O$	19.9 g/l dH_2O
1 mL	$ZnSO_4 \cdot 7H_2O$	22 g/l dH_2O
1 mL	$CoCl_2 \cdot 6H_2O$	10 g/l dH_2O
1 mL	$MnCl_2 \cdot 4\ H_2O$	180 g/l dH_2O
1 mL	H_2SeO_3	1.3 g/l dH_2O
1 mL	$NiSO_4 \cdot 6H_2O$	2.7 g/l dH_2O
1 mL	Na_3VO_4	1.84 g/l dH_2O
1 mL	K_2CrO_4	1.94 g/l dH_2O

(2) Vitamin mix stock solution

Compound	g/l
Vitamin B12	0.0005
Vitamin B1	0.1
Biotin	0.0005

Medium

Compound	per litre
$NaNo_3$	0.075 g
$NaH_2PO_4.2H_2O$	0.00565 g
Trace elements stock (1)	1 ml
Vitamin mix stock (2)	1 ml

Make up to 1 litre with filtered natural seawater. Adjust pH to 8.0 with 1M NaOH or HCl. Sterilise by autoclaving for 15 min at 121 ℃ at 1 atm, and use when cooled to room temperature.

Appendix F: Recipe for ATCC 1142 media (Allen and Arnon, 1955)

Compound	Quantity
NaCl	100.0 g
KNO_3	0.253 g
$NaNO_3$	0.212 g
K_2HPO_2 (56 g/l)	6.25 ml
Solution A	25.0 ml

Each of the above is added to 969.0 ml of filtered seawater. K_2HPO_2 solution was aseptically added after sterilisation.

Solution A:

Components	g/l	Per litre solution (ml)
4% $MgSO_4 \cdot 7H_2O$		500.0
1.2% $CaCl_2 \cdot 2H_2O$		500.0
Microelements stock		500.0
$MnCl_2 \cdot 4H_2O$	0.36	
MoO_3	0.036	
$ZnSO_2 \cdot 7H_2O$	0.044	
$CuSO_2 \cdot 5H_2O$	0.0158	
H_3BO_3	0.572	
NH_4VO_3	0.0046	
$CoCl_2 \cdot 6H_2O$	0.008	
FeEDTA solution**	160.0 ml	

** Firstly 5.2 g KOH is dissolved in 186 ml dH_2O, thereafter 20.4 g $Na_2EDTA \cdot 2H_2O$ is added to this solution. $FeSO_4 \cdot 7H_2O$ (13.7 g) is added to 364 ml of dH_2O. Finally both solutions are mixed. Filtered air is bubbled through solution until colour change. Final pH ~3.5.

Appendix G: Recipe for f/2 media (Guillard and Ryther, 1962)

(1) Trace elements stock solution

Compound	g/l
Na_2 EDTA	4.16
$FeCl_3.6H_2O$	3.15
$CuSO_4.5H_2O$	0.01
$ZnSO_4.7H_2O$	0.022
$CoCl_2.6H_2O$	0.01
$MnCl_2.4H_2O$	0.18
$Na_2MoO_4.2H_2O$	0.006

(2) Vitamin mix stock solution

Compound	g/l
Cyanocobalamin (Vitamin B_{12})	0.0005
Thiamine HCl (Vitamin B_1)	0.1
Biotin	0.0005

Medium

Compound	Quantity per litre
$NaNo_3$	0.075 g
$NaH_2PO_4.2H_2O$	0.00565 g
Trace elements stock solution (1)	1 ml
Vitamin mix stock solution (2)	1 ml

Make up to 1 litre with filtered natural seawater. Adjust pH to 8.0 with 1M NaOH or HCl. Sterilise by autoclaving for 15 min at 121 °C at 1 atm and use when cooled to room temperature.

Appendix H: Recipe for f/2 + Si media (Guillard, 1975)

(1) Trace elements stock solution

Compound	g/l
Na_2 EDTA	4.36
$FeCl_3.6H_2O$	3.15
$CuSO_4.5H_2O$	0.01
$ZnSO_4.7H_2O$	0.022
$CoCl_2.6H_2O$	0.01
$MnCl_2.4H_2O$	0.18
$Na_2MoO_4.2H_2O$	0.06

(2) Vitamin mix stock solution

Compound	g/l
Cyanocobalamin (Vitamin B_{12})	0.0005
Thiamine HCl (Vitamin B_1)	0.1
Biotin	0.0005

(3) Sodium metasilicate stock solution

Compound	g/l
$Na_2SiO_3.9H_2O$	30

Medium

Compound	Quantity per litre
$NaNO_3$	0.075 g
$NaH_2PO_4.2H_2O$	0.00565 g
Trace elements stock solution (1)	1.0 ml
Vitamin mix stock solution (2)	1.0 ml
Sodium metasilicate stock solution (3) *	1.0 ml

* Add while stirring

Make up to 1 litre with filtered natural seawater. Adjust pH to 8.0 with 1M NaOH or HCl. Sterilise by autoclaving for 15 min at 121 °C at 1 atm and use when cooled to room temperature.

Appendix I: Data obtained for Tukey's post hoc test (Chapter Six)

Table 32: Data obtained for Tukey's post hoc test for the different photobioreactor runs

Tukey's Multiple Comparison Test	Mean Diff.	q	Significant? P < 0.05?	Summary	95% CI of diff
Run A vs Run C	-0.4963	4.609	Yes	**	-0.8791 to -0.1135
Run A vs Run B	-0.7982	7.413	Yes	***	-1.181 to -0.4154
Run B vs Run C	-0.3020	2.804	No	ns	-0.6848 to 0.08085

PhD Thesis

ORIGINALITY REPORT

%13	%10	%5	%2
SIMILARITY INDEX	INTERNET SOURCES	PUBLICATIONS	STUDENT PAPERS

PRIMARY SOURCES

1	Ho, S.H.. "Perspectives on microalgal CO"2-emission mitigation systems - A review", Biotechnology Advances, 201103/04 Publication	%1
2	www.researchgate.net Internet Source	%1
3	Entregado a Durban University of Technology el 2012-06-30 Student Paper	<%1
4	Cheah, Wai Yan, Pau Loke Show, Jo-Shu Chang, Tau Chuan Ling, and Joon Ching Juan. "Biosequestration of atmospheric CO2 and flue gas-containing CO2 by microalgae", Bioresource Technology, 2015. Publication	<%1
5	www.ros.hw.ac.uk Internet Source	<%1
6	Submitted to Indian Institute of Technology, Bombay Student Paper	<%1